université PARIS-SACLAY

Effets d'une contamination diffuse des sols sur leurs émissions de gaz à effet de serre : cas du cuivre pour la prise en compte d'une contamination dans les modèles de surface continentale et l'évolution des risques en contexte de changement climatique

Thèse de doctorat de l'université Paris-Saclay

École doctorale n° 581, agriculture, alimentation, biologie, environnement et santé (ABIES)
Spécialité de doctorat : sciences de l'environnement
Unité de recherche : Université Paris-Saclay, INRAE, AgroParisTech, UMR ECOSYS, 78850, Thiverval-Grignon, France.
Référent : AgroParisTech

Thèse présentée et soutenue à Paris-Saclay, le 30/11/2021, par

Laura SERENI

Composition du Jury

Benoit GABRIELLE Professeur, AgroParisTech (Université Paris-Saclay)	Président
Gwenaël IMFELD Directeur de recherche, CNRS (Université de Strasbourg)	Rapporteur & Examinateur
Thierry LEBEAU Professeur, Université de Nantes	Rapporteur & Examinateur
Samuel ABIVEN Professeur, ENS Paris	Examinateur
Florence MAUNOURY-DANGER Maitresse de conférences, Université de Lorraine	Examinatrice
Nicolas VUICHARD Ingénieur, CEA (Université Paris-Saclay)	Examinateur

Direction de la thèse

Isabelle LAMY Directrice de recherche, INRAE centre IDF Versailles-Grignon	Directrice de thèse
Bertrand GUENET Chargé de recherche, CNRS (ENS Paris)	Co-Directeur & Examinateur

Thèse de doctorat

NNT : 2021UPASB066

Remerciements :

Du début à la fin, je ne pourrais assez remercier Isabelle et Bertrand pour m'avoir laissé le temps de finir d'apprendre à voir, faire et penser, pour votre confiance et vos attentions. A Bertrand de m'avoir proposé cette thèse et à Isabelle de m'y avoir acceptée, puis poussée dans encore d'autres projets. Merci pour tous les échanges, d'avoir toujours écouté et discuté, sans chercher à imposer.

Merci également, à Jean-Christophe, Nathalie et Olivier pour les discussions enrichissantes et les coups de pouces dans les derniers articles.

Evidemment, merci à Pierre et Lauric (et Bertrand) de m'avoir embarquée dans l'étude des sols. Puis pour les discussions, conseils &co ; et à Julie-Mai pour sa ténacité.

Sans originalité, cette thèse doit beaucoup à Alexandra Assanovna Elbakyan, mais aussi aux différentes équipes rendant publiques leurs bases de données (JRC, TRENDY, GIMMPS, ISIMIP…) et à Philippe pour m'avoir aidé à y accéder.

Je suis aussi profondément reconnaissante envers tous ceux avec qui j'ai pu travailler avant cette thèse, à l'ENS, à l'IPGP ou au CIRAD ; à l'ENS pour l'attribution d'une bourse de thèse.

Merci également aux écotox, pour leurs explications faune, sol ou dosage, leurs mots d'attention entre 2 tasses de café. Merci aussi à ROMENS pour les discussions libres et variées et d'apporter à chaque quinzaine sa question. Et bien avant cela déjà à V.Dubroca.

Une pensée pour Lucie et Antoine, dans l'aventure commune ; des mercis pour Maylis pour les aprèms découpe ou ping-pong ; à Elisa, pour les conversations entre 2 portes, manèges, composts ou verres; à Nico et Anthony pour les soirées 50 missions, babyfoot, chaises à moutons, rose en point de croix, kilos de pommes et d'artichauts et merci à Willy pour les doubles doses piscine, les conseils diplomatiques et les $\vec{M}$; à Zoé et Nils pour les questions -à moins que ce ne soit des remarques ?- aux plus agé.e.s pour leur moral support, d'avoir relu, et de ne l'avoir pas fait, et bien sûr, à ce.ux.elles qui manquent.
Et il y a aussi toutes celles-zéceux que je n'ai vu que sporadiquement pendant ces 3 ans, mais avec qui les échanges restent précieux (Laura, Manu, Sarah, Marie, Marion…).

Et j'en oublie encore certainement dans cette liste, qui m'aurait apporté une idée, une formulation ou un pansement.

Publications

- Laura Sereni, Bertrand Guenet, and Isabelle Lamy. Does copper contamination affect soil co2 emissions? a literature review. *Frontiers in Environmental Science*, 9:29, 2021.
- Isabelle Lamy, Laura Sereni, and Bertrand Guenet. Sols contaminés, carbone organique des sols et dérèglement climatique : quelles relations ? In Christian Mougin, Francis Douay, Marine Canavese, Thierry Lebeau, and Elisabeth E. Rémy, editors, *Les sols urbains sont ils cultivables ?*, chapter 11. QUAE, October 2020.
- Laura Sereni, Bertrand Guenet, Olivier Crouzet, Charlotte Blasi*, and Isabelle Lamy. Responses of soil nitrification activities to copper after a moisture stress *Environmental Science an pollution research* Submitted
- Laura Sereni, Bertrand Guenet, Charlotte Blasi*, Olivier Crouzet, Jean-Christophe Lata and Isabelle Lamy. To what extend a soil contamination can affect greenhouse gas emissions? An attempt to calibrate a nitrification/denitrification model. *Biogeosciences*, Submitted
- Laura Sereni, Bertrand Guenet, and Isabelle Lamy. Mapping risks associated with soil copper contamination using availability and bio-availability proxies at the European scale *Environmental science and pollution research*, Submitted.

Communications

2021 **Goldschmidt** Copper contaminated soils at the European scale: comparing hazards and risks using the three complementary metrics of total soil contents and total and free contents in solution
2021 **Journées du département de géosciences ENS** Impact d'un double stress sur les émissions azotées d'un sol : calibration et utilisation du modèle dndc
2020 **EGU,** Soil copper contamination effect on carbon mineralisation: evidence of a soil CO2 emission decrease from litterature review
2019 **Ecoscience Ecosys** : Implémentation de l'effet de la contamination au Cu d'un sol soumis à différentes pressions hydriques dans un modèle de nitrification-dénitrification (DNDC)
2019 **Rencontres Sites et Sols Pollués**, *ADEME*, Poster presentation in session Comprehension des mécanismes et transfert des polluants (knowledge of mechanisms and transfert of pollutants).
2019 **Ecoscience Ecosys** : « Interactions entre pollution au Cu des sols et leurs émissions de CO2 en contexte de changement climatique : résultats d'une revue bibliographique sur la mise en évidence de l'effet du cuivre sur la minéralisation du carbone »
2018 **Journée ABIES** Soil copper contamination effect on carbon mineralisation: evidence of general basal respiration decrease from literature review

Enseignement et encadrement :

2021 : Encadrement Stage L3 Julie Mai Paris
2019-2020 : TD C L1-S1 Université Versailles Saint Quentin en Yvelines (24h)
2019 : tp-td faune 1ere année AgroParisTech (3h)

Résumé :

Dans le contexte du changement climatique la compréhension des facteurs modulant les émissions de gaz à effet de serre (GES) des sols est essentielle. Parmi ceux-ci, les facteurs pédo-climatiques sont majoritairement étudiés. La contamination des sols n'est en revanche pas considérée malgré les grandes surfaces déjà concernées. Pourtant, il est connu qu'une contamination peut affecter les activités des organismes des sols à l'origine des émissions de GES mais la résultante sur les émissions à l'échelle globale reste peu renseignée. Pour répondre à cette question, nous avons étudié le cuivre (Cu) du fait de ses nombreuses utilisations agricoles et de sa réactivité vis-à-vis des constituants du sol et avons travaillé selon deux axes : i) associer, à l'échelle continentale, une contamination des sols en Cu à ses différentes formes et à leur risque pour l'environnement ; ii) intégrer des fonctions réponses au Cu pour les émissions de GES liées aux cycles de C et N dans les modèles de surfaces continentales.

Une première partie étudiant la (bio)disponibilité du Cu à l'échelle de l'Europe et les effets d'un double stress (humidité et contamination) sur la nitrification des sols a pu montrer que les conditions pédo-climatiques historiques, présentes et futures influençaient l'ampleur de l'impact d'une contamination. Dans la deuxième partie nous avons confirmé la nécessité de prendre la contamination en compte dans les estimations de flux de GES des sols par les modèles de surface continentales. Nous avons établi des fonctions reliant la concentration en Cu des sols à leurs émissions de CO2 puis à leurs émissions d'espèces azotées en re-paramétrant le modèle biogéochimique DNDC en un nouveau modèle DNDC-Cu. Ce modèle DNDC-Cu a ensuite été utilisé pour estimer les émissions azotées de sols contaminés sous diférentes humidités du sol.

In the context of climate change, it is essential to understand the factors modulating greenhouse gas (GHG) emissions from soils (CO2, N2O, NOx...). Among these, pedo-climatic factors are mainly studied. However, soil contamination is not considered despite the large surface areas already concerned. However, it is known that contamination can affect the activities of soil organisms at the origin of the greenhouse gases emissions, but the result on global emissions remains poorly understood. To answer this question, we studied copper (Cu) because of its numerous uses for instance in agriculture and its reactivity with soil constituents and worked along two axes: i) to associate at the continental scale a Cu contamination of soils with the different forms of Cu and their risk for the environment; ii) to integrate response functions to Cu for GHG emissions related to C and N cycles in land surface models.

A first part studying the (bio)availability of Cu at the European scale and the effects of a double stress (moisture and contamination) on soil nitrification showed that historical, present and future soil-climatic conditions influence the magnitude of the impact of a contamination. In the second part, we confirmed the need to take contamination into account in the estimation of soil GHG fluxes by land surface models to estimate soil heterotrophic respiration. We established functions relating soil Cu concentration to soil CO2 emissions and soil N species emissions for different soil moisture and re-parameterized the DNDC biogeochemical model into a DNDC-Cu version. Then, we used our DNDC-Cu to estimate N species emissions for contaminated soils under different soil moistures.

Table des matières

Contexte et Objectifs

Les sols constituent un grand stock de carbone (C) et d'azote (N), respectivement de l'ordre de 1950 à 3050 PgC (1500 à 2400 PgC pour les sols hors climat donnant lieu aux permafrost) et 450 à 650 PgC pour la végétation (Ipcc, 2013)) et 95-140 PgN (Schlesinger and Bernhard, 2013). Ces stocks très importants s'accompagnent de flux majeurs dans les sols ainsi qu'entre les sols et l'atmosphère. On estime par exemple les flux de C entre les sols et l'atmosphère à environ 100 $PgC.an^{-1}$ pour la photosynthèse contre 75 (Schlesinger and Andrews, 2000) à 98 (Hashimoto et al., 2015) $PgC.an^{-1}$ pour la respiration du sol ; 44 % de cette respiration étant due à la respiration autotrophe des racines et 56 % à la respiration hétérotrophe (Rh) des bactéries et champignons du sol. Les émissions d'N des sols sont quant à elles estimées aux alentours de 10.7 $TgN.an^{-1}$ (Ipcc, 2013).

Depuis le milieu du XVII^{e} siècle les activités anthropiques ont provoqué une augmentation des concentrations atmosphériques en de nombreux gaz tels que le CO_2, les N_2O ou les NO_x que ce soit par des émissions directes ou via la perturbation des cycles biogéochimiques de ces éléments. Le CO_2 atmosphérique a ainsi augmenté de 40 % (829 contre 589 PgC en 1750, (Prather et al., 2012; Joos et al., 2013)) avec une augmentation annuelle de l'ordre de 4 $PgC.an^{-1}$. Les émissions de N_2O ont quant à elles augmenté de 20 % (+ 3.6 $TgN\text{-}N_2O.an^{-1}$ (Ciais et al., 2013)) entre autre du fait de la consommation d'engrais azotés. L'augmentation de la concentration atmosphérique de ces gaz à effet de serre provoque i) des modifications du climat (température, fréquence et intensité des précipitations…) ; ii) des perturbations des cycles biogéochimiques du C et de l'N. Dans ce contexte, du fait de l'importance des flux de C et N entre les sols et l'atmosphère (10 fois les émissions annuelles anthropiques de C et N), ceux-ci sont de prime importance.

Différents facteurs environnementaux contrôlent les cycles de C et N, comme la disponibilité de la matière organique, celle des nutriments, les faunes et flores locales ou le climat. A l'échelle de la Terre, les simulations de cycles biogéochimiques continentaux (qui cherchent entre autres à prédire les évolutions des concentrations dans le sol et les flux d'émissions vers l'atmosphère d'espèces carbonées et azotées selon différentes conditions environnementales) incluent principalement les effets de la température, de l'humidité et de la texture du sol.

En parallèle de l'augmentation des émissions de gaz à effet de serre, les révolutions industrielle et agricole se sont faites avec celle de l'utilisation de métaux et minéraux ou engrais. Parmi ceux-ci, le cuivre (Cu) est largement présent dans les sols du fait de ses utilisations variées et anciennes (industrie pour la conductance de chaleur et d'électricité, essences diesel, supplémentation des alimentations porcines et bovines que l'on retrouve dans les épandages ou fongicide). La consommation mondiale de Cu est estimée à environ 10 000 t/an jusqu'aux année 1850 (Hong et al., 1996) pour atteindre près de 20 millions de tonnes par an en 2016 (Pietrzyk and Tora, 2018). Les émissions d'usines et dépôts industriels ou émissions de pots catalytiques peuvent ainsi induire de fortes concentrations locales en Cu dans les sols (jusqu'à quelques milliers de mg $Cu.kg^{-1}$ de sol alors que la concentration moyenne endogénique des sols est de 20 à 50 mg $Cu.kg^{-1}$ selon le type de roche mère ayant présidé à la formation du sol (Thornton and Webb, 1980; Sauvé et al., 1997; Smorkalov and Vorobeichik, 2011)). Dans les parcelles agricoles en particulier dans les vignes, l'usage répété d'amendements organiques ou de fongicides enrichis en Cu (sulfate de cuivre) et sa forte affinité pour la matière organique des sols le rendant peu labile amènent à mesurer des concentrations en Cu en moyenne 3 fois plus élevées que dans les autres sols (Ballabio et al., 2018a). La contamination diffuse ou ponctuelle en Cu peut

ainsi toucher de larges surfaces, les surfaces agricoles représentant par exemple 5 milliards d'ha sur Terre et la moitié des surfaces continentales en l'Europe (FAO, 2015, 2020).

Pour autant, malgré l'importante part de sols contaminés (près de 30% en Europe (Tòth et al., 2016)), l'impact d'une contamination sur les populations bactériennes ou sur les fonctions des sols a principalement été étudiée d'une part à l'échelle locale et d'autre part très peu au regard de fonctions globales comme les émissions de gaz à effet de serre. Des disparités dans les effets de la contamination sur la faune selon les propriétés du sol ou les conditions de contamination (Moreno et al., 2009; Fernández-Calviño and Bååth, 2016) ont pu être mises en évidence et la généricité d'un effet de la contamination n'est pas établie.

Par ailleurs, le changement climatique est connu comme pouvant affecter les processus biologiques des sols, mais les effets conjoints du changement climatique et de la contamination des sols sur leurs fonctions restent mal connus. En effet, les effets des doubles stress sont contrastés selon les types et intensités de stress. Dans certains cas les premiers stress augmentent la résistance de l'écosystème par la sélection de communautés plus résistantes, l'adaptation ou des changements physiologiques (Beddington and May, 1977; Odum et al., 1979). D'autre part, les modifications du climat peuvent aussi affecter la disponibilité des contaminants et restent mal connus. Certaines études ont ainsi pu montrer l'importance de la température (Ma et al., 2006a; Xing et al., 2011) ou des alternances de cycle d'assèchement/réhumectation sur l'association du Cu à la matière organique (MO), mais les résultats sont contrastés (Han et al., 2001; Zheng and Zhang, 2011; Xu et al., 2013).

Dans ce contexte, l'objectif générale de la thèse est d'estimer les effets d'une contamination en Cu sur les émissions de C et N des sols en contexte de changement climatique. La figure 1 schématise les relations qui seront abordées ainsi que les chapitres qui en traiteront.

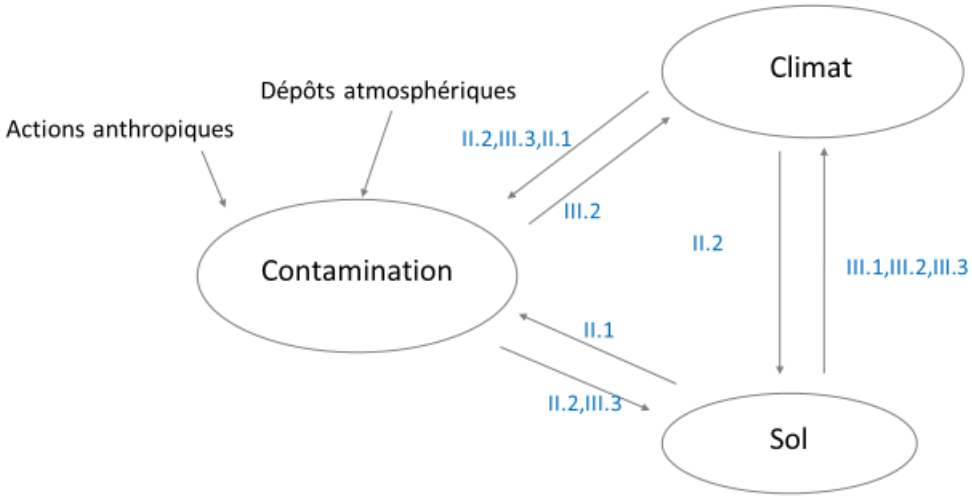

Fig. 1 : Schéma résumant les principales interactions reliant sol, climat, et contamination. En bleu sont indiqués les points de focus des différents chapitres de la thèse, le premier chapitre étant une introduction générale.

Le changement climatique sera abordé sous l'angle des modifications des précipitations. Celles-ci sont en effet moins bien renseignées en termes d'effet que les températures mais on sait que des variations importantes de précipitations (sècheresse ou inondations) peuvent affecter le fonctionnement biologique et la structure des sols, et donc à la fois les fonctions de minéralisation du C (dans notre cas respiration hétérotrophe Rh) ou la nitrification ainsi que la disponibilité des contaminants via la solution du sol. Dans ce document, une première partie d'introduction permettra d'expliciter i) les principaux mécanismes et les régulations environnementales des cycles du C et de l'N dans les sols ainsi que leur intégration dans les modèles de biogéochimie continentale ii) certains enjeux autour de la (bio)disponibilité des contaminants et iii) les mécanismes et conséquences des stress climatiques ou de contamination connus sur les sols. Ensuite, une seconde partie se concentrera sur l'analyse de la pertinence des notions de (bio)disponibilité à l'échelle de l'Europe et au regard des modifications de précipitations à venir tels que donnés selon différents scénarios prédictifs. La question de la sensibilité des fonctions du sol à la disponibilité des contaminants en contexte de changement climatique sera également abordée. La troisième partie visera à introduire l'effet de la contamination en Cu dans les modèles mécanistiques de prévisions d'émissions de gaz à effet de serre. Pour cela nous évaluerons les biais d'estimation de Rh de modèles de surface continentale face à la contamination en Cu et proposerons une relation générale entre la contamination en Cu et Rh. Nous aborderons ensuite en termes de finalité l'introduction des stress de contamination et de précipitation dans un modèle d'émissions azotées, supposées plus sensibles aux variations d'humidité que les émissions carbonées.

s

Partie I. : Origine des émissions de gaz à effet de serre des sols liées aux cycles de C et N et importance des pressions de contamination chimique et climatique

A. Cycles du carbone et de l'azote dans les sols et leurs contrôles

A.1. Cycle du carbone

Les sols sont un milieu hétérogène constitué schématiquement de phases liquides (eau et solutés dissous comme des ions minéraux, métalliques ou de la matière organique pour 25%), gazeuses (25%) et solides (phases minérales pour environ 45% ou organiques pour 5%). Parmi les constituants organiques on distingue deux fractions l'une vivante, l'autre constituée de débris végétaux ou animaux ou de molécules organiques plus ou moins polymérisées. On estime que la partie souterraine des plantes est de taille équivalente à la partie aérienne tandis que la biomasse microbienne est estimée à 10^9 cellules par gramme de sol (Raynaud and Nunan, 2014).

L'énergie utilisée par le vivant étant véhiculée par les formes réduites du C, le transfert de C au long de la chaine trophique est un des paramètres les plus intégrateurs des écosystèmes. La dégradation de la MO, source du C des sols, est un processus très général accompli par de nombreux organismes en conditions aérobies suivant l'équation I.1. :

(I.1) $CH_2O + O_2 \rightarrow CO_2 + H_2O$,

CH_2O étant une brique élémentaire de la MO

En revanche, les temps de résidence (durée des transformations) dans le sol de la MO et l'intensité des flux de respiration associés peuvent grandement varier. Par exemple, on estime que le temps de résidence du carbone est d'environ 1306 ans dans les forêts tropicales contre plus de 5600 ans dans les toundras (Luo et al., 2019).

Le climat (température, précipitations, cycles de gel…) peut affecter la production primaire et donc les apports de matière fraîche ainsi que les vitesses de dégradation. A ceci s'ajoutent différents mécanismes de persistance de la matière organique dans les sols qui restent très débattus, entre récalcitrance chimique de la matière organique à la dégradation et /ou protection physique de celle-ci par les composés du sol (Lützow et al., 2006). Nous apporterons plus de détails sur ces différents facteurs aux paragraphes A.3 et B.

A.2. Cycle de l'azote

L'azote (N) est un des composants principaux des protéines et des enzymes mais est difficilement assimilable par les plantes ou micro-organismes sous sa forme prépondérante N_2. La plupart (80-85% (Schlesinger and Bernhardt, 2013, chap 12)) de N utilisé par les plantes vient de la minéralisation de N provenant de tissus morts ou ajoutés artificiellement sous la forme d'engrais composés de NH_4 ou NO_3. La transformation de N dans le sol peut être résumée en 4 étapes principales (Schlesinger and Bernhardt, 2013, chap 12), voir fig I.1 :

i) La décomposition de la MO relargue des acides aminés utilisés directement.

ii) La nitrification réduit le NH_4^+ en NO_3^- et NO_2 avec émission de NO_2 et N_2O (eq. I.2, I.3, I.4).

iii) NO_3^- est converti en NH_4^+ par les DNRA (dissimilatory nitrate reduction to ammonium).

iv) La dénitrification transforme NO_3^- en NO_2, N_2 et N_2O.

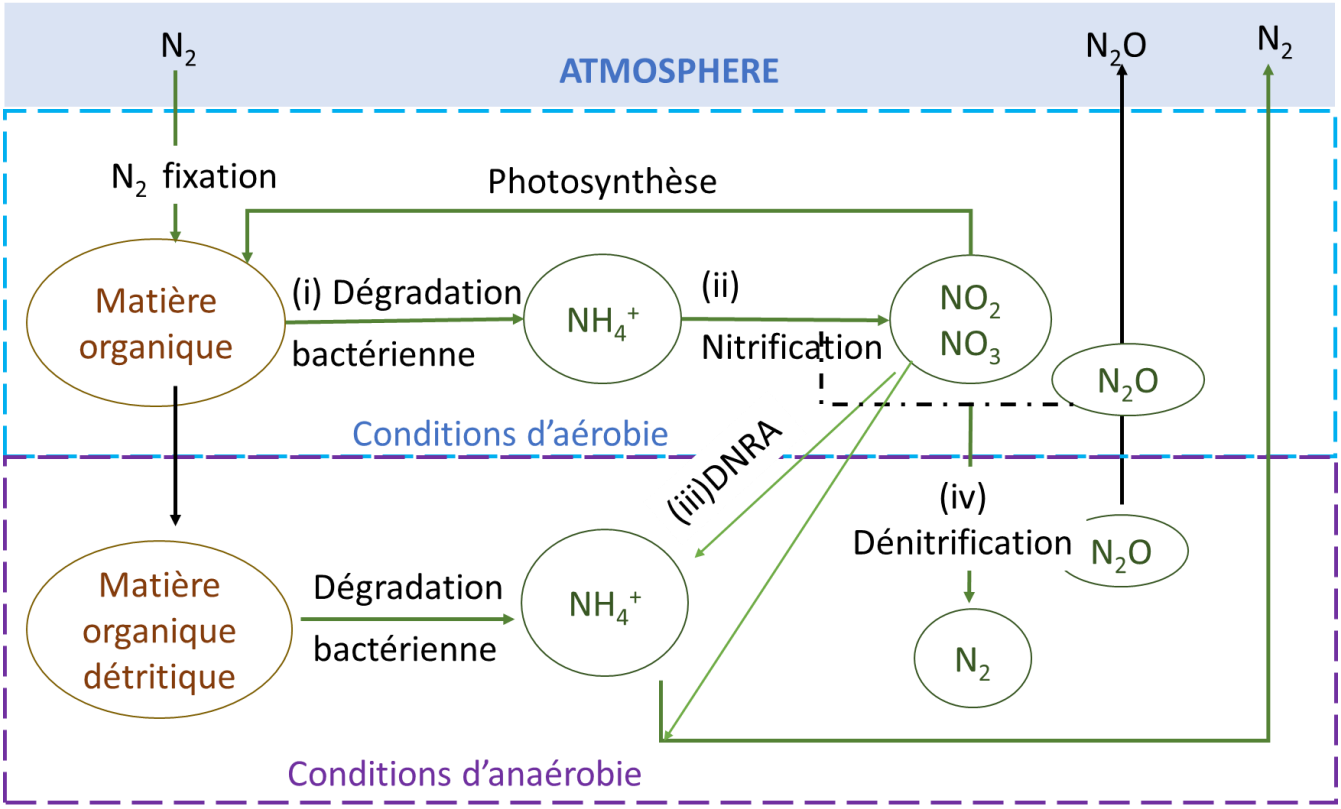

Fig. I.1.: Représentation schématique des différentes transformations de l'azote dans les sols, adapté de (Schlesinger and Bernhardt, 2013a, chap 12). En noir sont représentés les flux de diffusion, en vert les réactions de transformations. La matière organique détritique correspond à la matière organique partiellement dégradée en milieu aérobie et pour laquelle certaines réactions de dégradation ne s'effectuent qu'en anaérobie.

Au cours de chacune de ces transformations les espèces produites peuvent être utilisées par les plantes ou les micro-organismes. Les plantes utilisent préférentiellement NO_3^-, mobile dans la solution du sol, même si dans certains écosystèmes NH_4^+ est favorisé (Paul, 2015, chap 14). Chacune de ces étapes est constituée de différentes réactions accomplies par différents groupes de micro-organismes plus ou moins spécialistes.

La nitrification (ii) est principalement effectuée par des bactéries chimio-autotrophes des genres *Nitrosomonas* et *Nitrobacter* ainsi que dans une moindre mesure, certains procaryotes et archées (Schimel et al., 1984; Duggin et al., 1991).

Les réactions générales de nitrification autotrophes sont du type I.2, I.3a, I.3b :

(I.2) $NH_4^+ \rightarrow NH_3 + H^+$

(I.3a) $NH_3 + O_2 + 2e^- \rightarrow NH_2OH + H_2O$

(I.3b) $NH_2OH + H_2O \rightarrow NO_2^- + 5H^+ + 4e^-$

NO_2^- étant peu stable dans la solution du sol viennent alors les étapes I.4a et I.4b :

(I.4a) $3\ NO_2^- + 3H^+ \rightarrow 3\ HNO_2$

(I.4b) $3\ HNO_2 \rightarrow HNO_3 + 2\ NO + H_2O$.

En parallèle NH_2OH se décompose suivant l'Eq. I.4c

(I.4c) $NH_2OH + HNO_2 \rightarrow N_2O + 2\ H_2O$

Des bactéries et champignons hétérotrophes peuvent également contribuer à la nitrification suivant la réaction I.5.

(I.5) $NH_4^+ + NO_2^- \rightarrow N_2 + 2H_2O$

Il n'est pas clairement établi si la nitrification hétérotrophe est un processus générique ou si elle n'a lieu que dans des micro environnements où l'autotrophe est inhibée. La dénitrification, réduction de NO_3^- en NO, N_2O et N_2 (iv, fig. I.1), est en revanche un processus générique accompli par quasi toutes les bactéries hétérotrophes (Schlesinger and Bernhardt, 2013, chap 12). Les différentes réactions de la dénitrification (eq I.6a-d) produisent des espèces azotées gazeuses émises dans l'atmosphère :

(I.6a): $2NO_3^- + 4H^+ + 4e^- \rightarrow 2NO_2 + 2H_2O$

(I.6b) $2NO_2^- + 4H^+ + 2e^- \rightarrow 2NO + 2H_2O$

(I.6c) $2NO + 2H^+ + 2e^- \rightarrow 2N_2O + H_2O$

(I.6d) $N_2O + 2H^+ + 2e^- \rightarrow N_2 + H_2O$

Dans la dénitrification, NO_3 est utilisé comme accepteur final des électrons, là où O_2 est utilisé dans la nitrification. NO_3 étant un accepteur d'électrons moins efficace qu'O_2, la dénitrification a tendance à n'avoir lieu qu'en environnement anaérobie (Paul, 2015, chap. 14). La quantité d'O_2 dans le sol contrôle ainsi les proportions des différentes réactions.

D'autres réactions additionnelles (DNRA, fig. I.2) peuvent transformer l'N des sols mais elles sont quantitativement bien moins importantes que la minéralisation, la nitrification et la dénitrification.

Le cycle de l'N englobe donc différentes réactions en compétition les unes avec les autres et toutes émettrices de gaz à effet de serre.

Si certaines dégradations participant au cycle du C sont privilégiées par les conditions environnementales ou spécialisées du fait de la nature de la MO, quasiment tous les micro-organismes du sol y participent. En revanche, les différentes étapes du cycle de l'N sont effectuées par des groupes assez spécifiques. Différents paramètres environnementaux tels que le degré d'aérobie (et à l'inverse d'humidité) des sols, la température ou le pH peuvent jouer sur les proportions de chaque branche du cycle et seront détaillés au paragraphe suivant.

A.3. Contrôles environnementaux des cycles du C et de l'N

La minéralisation du C et de l'N a lieu par des processus biotiques directs ainsi que par l'action d'exo-enzymes. Tous les facteurs environnementaux susceptibles d'affecter les processus biologiques ou les réactions chimiques catalysées par les exo-enzymes peuvent donc modifier les taux des réactions. Parmi les mieux étudiés et représentés se trouvent les effets de la température et des précipitations. Les effets de la nature de la matière à décomposer ou de la structure du sol sont notables mais moins bien renseignés du fait de la diversité et de la complexité des molécules impliquées.

On considère généralement que dans la gamme de température mésophile (20-45°C) l'activité microbienne double tous les 10° (Paul, 2015 chap. 2) mais les effets à long terme du réchauffement climatique sur les activités enzymatiques sont difficiles à prévoir car une adaptation à la température des communautés en place pourrait limiter l'augmentation des activités dues à celle des températures (Oechel et al., 2000; Davidson and Janssens, 2006). Tous les mécanismes en lien avec les effets des variations de température sur les fonctions des sols ou sur les contaminants ne seront pas détaillés ici et nous nous limiterons à expliciter ceux en lien avec la composition du sol et de la MO et ceux des variations de précipitations.

i. Accessibilité de la MO et stœchiométrie des réactions

Les importances relatives de la constitution de la MO ou de son accessibilité dans les vitesses de dégradation sont mal connues. On estime cependant généralement que de forts contenus en lignines limitent la dégradation des MO et les composés aux structures complexes comme la lignine ne sont souvent dégradés que par des groupes d'organismes spécifiques. Les rapports C:N étant plus élevés dans la MO que dans la biomasse microbienne (C:N dans l'humus= 160 et C:N biomasse =12 (Schlesinger and Bernhardt, 2013, chap 12)), l'N est souvent limitant pour la croissance microbienne et le cycle du C des sols restreint par la quantité d'azote disponible.

En parallèle, la texture du sol peut affecter la capacité des micro-organismes à dégrader la MO. Six et al., (2000) résument ainsi les principaux mécanismes permettant aux argiles d'agir sur la biomasse microbienne grâce à leur surface de réaction : i) les argiles peuvent promouvoir la croissance microbienne en maintenant le pH dans une gamme optimale (Bitton et al., 1976) ; ii) Les argiles peuvent adsorber certains métabolites inhibant la croissance microbienne (Stotzky, 1966; Martin and Haider, 2015) ou iii) les interactions argiles-microbes peuvent protéger les organismes de la dessiccation. La stabilité de la MO peut également augmenter (donc sa dégradation et la respiration associée diminuer) par la formation de complexes avec les argiles ou avec les oxydes amorphes (Allison

et al., 1949; Hayes and Clapp, 2001). Les oxydes de fer, ou de métaux comme l'aluminium, le zinc ou le cuivre peuvent ainsi interagir avec les colloïdes pour former des micelles stabilisées ou avec des polysaccharides et de la MO pour former des complexes plus stables (Martin et al., 1966; Brynhildsen and Rosswall, 1997).

Les taux de respiration associés aux vitesses de décomposition de la MO dépendent donc en partie de la présence de micro-organismes capables d'effectuer certaines transformations spécifiques ainsi que de la composition du sol qui peut à la fois protéger certaines MO de la dégradation et certains micro-organismes de conditions néfastes pour eux (pH, sécheresse…).

ii. Effets des précipitations

Les réactions de minéralisation de C et de N décrites plus haut (A.1 et A.2.) consomment de l'O_2 et produisent de l'H_2O (eq. I.1, I.3a, I.4b, I.5, I.6a-d) ou entrent en compétition avec des réactions impliquant de l'O_2 (nitrate dénitrification, eq. I.6). Les précipitations peuvent ainsi affecter les cycles de C et N par leur effet direct sur le contenu en eau du sol ainsi que par la quantité d'air dans le sol (c'est-à-dire par la porosité non remplie d'eau).

Les précipitations peuvent varier largement d'une région à l'autre mais aussi au sein d'une même région (par ex. le Brésil ou l'est de l'Amérique peuvent recevoir 6-10 mm par jour certains mois de l'année et moins d' 1mm par jour pendant d'autres mois (Adler et al., 2017)). Les prévisions de changement climatique prévoient des augmentations, diminutions ou intensifications des périodes sèches et humides selon les régions. Les effets des précipitations sur les cycles du C et N seront donc décrits sous 2 angles : i) les effets directs du contenu en eau sur les émissions de C et N et ii) les effets des variations de précipitations telles qu'ayant lieu lors de succession de sécheresse ou pluies intenses.

La minéralisation du C est un processus principalement aérobie (eq. I.1). La quantité d'eau dans le sol déterminant l'O_2 rémanent, la minéralisation a tendance à diminuer avec la saturation en eau du sol. On considère qu'à partir de 60% de pores saturés en eau les activités anaérobies dominent. De l'autre côté du spectre, quand les sols s'assèchent les pores sont disconnectées et la diffusion des substrats dans la solution du sol diminue alors que la concentration en sels augmente (Paul, 2015, chap 2). De trop faibles niveaux en eau ont donc aussi tendance à limiter l'activité microbienne, principalement du fait de la limitation en substrat (Schimel, 2018). La fig. I.2 décrit la courbe conceptuelle de la respiration microbienne face à la quantité d'eau des sols.

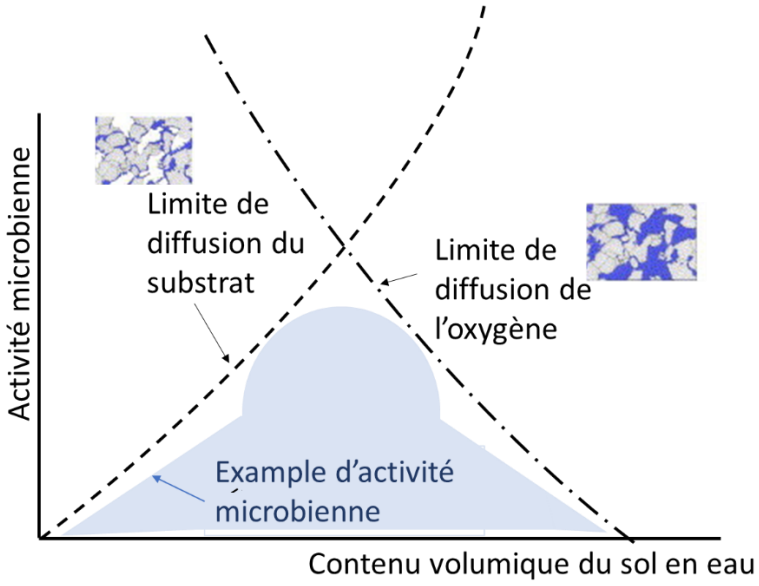

Fig. I.2: Schéma conceptuel des relations entre l'activité microbienne macroscopique et le contenu en eau du sol, issu de Or et al., (2007)

D'autre part, comme vu au paragraphe A.2., le cycle de l'N est en équilibre entre les processus de nitrification (eq. I.2, I.3, I.4a et I.4b) qui produisent de NO_3 et requièrent de l'O_2 et la dénitrification qui transforme NO_3 en N_2 (eq I.6a-d).

Les proportions relatives de NO,N_2O et N_2 issues de la dénitrifications dépendent donc entre autre du contenu en eau du sol (Wolf and Russow, 2000; Khalil et al., 2004a). Schlesinger and Bernhardt, 2013 (chap 6) décrivent un pattern général d'augmentation des émissions de NO issues de la nitrification quand le contenu en eau est faible, suivi par une diminution des émissions de NO et une augmentation de celles de N_2O quand le contenu en eau du sol est modéré. Proche de la saturation, toutes les émissions seraient du N_2 issu de la dénitrification (fig. I.3).

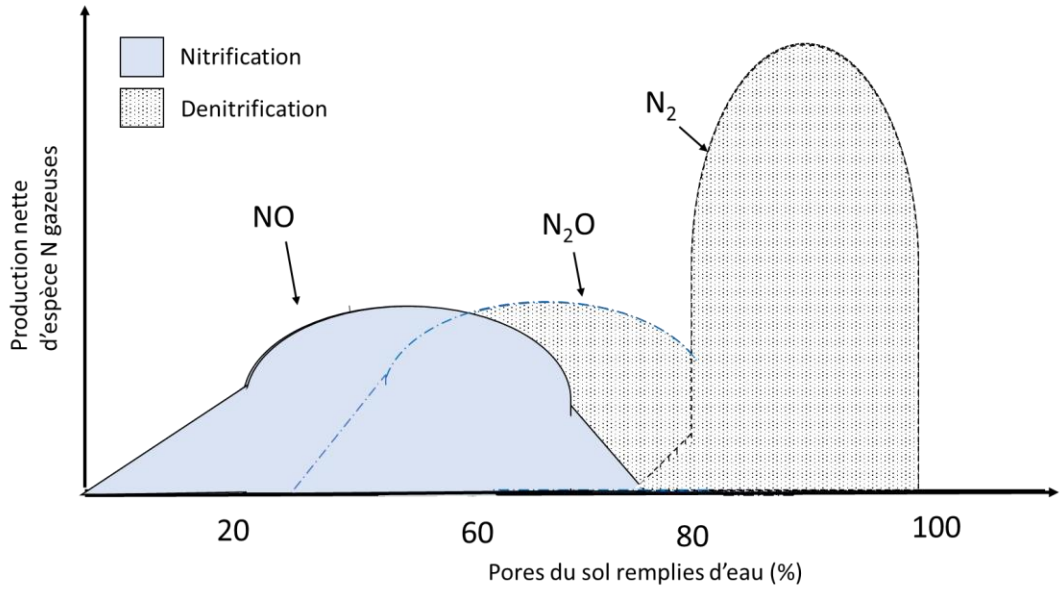

Fig. I.3: Parts relatives des émissions de NO, N_2O et N_2 issues de la nitrification et de la denitrification en fonction du contenu en eau des sols. D'après (Davidson et al., 2000).

Les variations d'humidité du sol régulières permettent aux communautés microbiennes de s'adapter par différents mécanismes comme l'accumulation d'osmolytes, la synthèse de polysaccharides retenant l'eau, la dormance, le remplacement des communautés actives etc…… (Schimel, 2018).

Les facteurs environnementaux tels que les précipitations ou la composition du sol et de la MO peuvent donc modifier l'intensité des différents flux de C et N du sol et les variations environnementales peuvent induire adaptations ou complémentarités des communautés. Des variations trop abruptes ou prolongées dans un extrême ou l'autre de précipitations comme dans la composition du sol peuvent en revanche affecter plus notablement les communautés microbiennes. Dans le paragraphe suivant nous détaillerons deux exemples de stress et de leurs interactions sur les fonctions de minéralisation du C et de l'N : l'un climatique via l'exemple des cycles assèchement-ré-humectations et l'autre chimique via l'exemple d'une contamination en élément trace métallique comme le Cu.

B. Impact des stress externes sur les cycles du C et de l'N des sols : exemple des modifications de l'intensité des précipitations associées au changement climatique et de la contamination au Cu.

Dans cette partie nous détaillerons les effets d'un type de stress induit par les cycles de dessiccation-humectation étant amenés à se multiplier avec le changement climatique, avant d'aborder les effets d'un autre type de stress qu'est celui de la contamination au Cu, contaminant particulièrement présent du fait de la multiplicité de ses usages. Puis, nous examinerons les effets conjoints que peuvent avoir changement climatique et pression de contamination sur les fonctions des sols.

B.1. Assèchement et ré-humectation des sols : un exemple de phénomène climatique exacerbé par le changement climatique.

L'alternance de périodes de sécheresses et de périodes de fortes pluies (variations plus importantes que celles subies actuellement) peut induire un stress sur les écosystèmes. Or, on s'attend à ce que les régimes de précipitations extrêmes varient en fréquence et en intensité au cours des prochaines années (Christensen and Christensen, 2003; Ruosteenoja et al., 2018), pouvant affecter drastiquement le fonctionnement des écosystèmes (Hueso et al., 2012; Otkin et al., 2018; Schimel, 2018). On considère généralement que les stress au niveau de l'écosystème se traduisent par une réduction des cycles internes et une diminution de l'efficacité dans l'utilisation des ressources (Odum, 1985). Lors des évènements dessiccation -humectations, 3 processus majeurs détaillés ci-dessous affectent les cycles de C et N : i) un flush de nutriments ; ii) un impact sur la structure du sol ; iii) une perturbation des communautés microbiennes.

i) Un effet général des cycles de dessiccation-humectation est l'augmentation plus ou moins brutale du taux de minéralisation de C à la suite de la ré humectation suivie par une diminution plus ou moins rapide avec l'assèchement. Cette augmentation est connue sous le nom de

l'effet Birch et est vue comme la libération dans la solution du sol de composés facilement décomposables préalablement retenus dans la structure des argiles et ainsi préservés des communautés microbiennes (Birch, 1958). La nature de ce carbone, entre ancien carbone stable et osmolytes issus de cellules mortes, est en revanche moins claire (Schimel, 2018).

ii) Un deuxième effet est la modification de la structure du sol. Par exemple, l'immersion d'agrégats de sol peut favoriser leur craquellement à l'assèchement, exposant alors la MO. De plus, les agrégats peuvent augmenter localement les concentrations en O_2 et favoriser les processus aérobies comme la nitrification. Le craquellement des agrégats peut alors modifier ces processus (Denef et al., 2001a, 2001b; Khalil et al., 2004b; Kremen et al., 2005). Enfin, la structure globale des sols ou le type d'argile peuvent être modifiés, avec des augmentations de la surface spécifique de sorption (Oades, 1984; Walworth, 1992; Sánchez-García et al., 2020), des diminutions et/ou augmentation de la force ionique de la solution du sol, ou des altérations liée aux parties hydrophobes de la MO (Kleber et al., 2007).

iii) Enfin, lors d'alternance de sécheresse et de fortes pluies, certaines adaptations des micro-organismes à la sécheresse comme à l'accumulation de solutés peuvent être néfastes. En effet, avec la réhumectation rapide les microbes doivent relarguer rapidement les solutés accumulés afin d'être en équilibre osmotique avec la solution du sol (Killham and Firestone, 1984; Csonka, 1989; Harris, 2015). La succession rapide dans les conditions hydriques du sol impose donc un stress intense aux micro-organismes qui alternent rapidement les adaptations antagonistes (Wood, 2015). Plusieurs études ont ainsi pu montrer que l'alternance de périodes de sécheresse et de fortes humidités peut significativement réduire la biomasse microbienne, affecter sa composition, ou induire les micro-organismes à entrer en dormance (Manzoni et al., 2012; Schimel, 2018).

B.2. Effet du Cu sur les fonctions des sols.

i. Effets généraux du Cu sur les fonctions des sols

Les stress métalliques ont été beaucoup étudiés mais la plupart des études se concentrent sur la définition de doses de contaminants tolérables par les écosystèmes locaux via la mesure de biomasse microbienne ou de réactions enzymatiques considérées représentatives (car intégratives) de l'état de l'écosystème. Une diminution générale de la biomasse microbienne sous l'effet de contamination aux métaux lourds a pu être mise en évidence à travers la revue de Bååth (1989). Cependant, les différents micro-organismes montrent des sensibilités différentes à la contamination. Par exemple, les champignons tolèreraient de plus fortes doses de contaminants que les bactéries tandis que certaines communautés de bactéries nitrifiantes seraient particulièrement sensibles (Pancholy et al., 1975; Maliszewska et al., 1985). Certains auteurs ont aussi pu montrer des pertes de fonctions dans les premiers jours suivant une contamination suivies d'une restauration de ces fonctions au cours du temps (Holtan-Hartwig et al., 2002). D'autres études ont pu constater une diminution de la minéralisation du C avec la contamination au Cu lors d'incubations réalisées avec de la litière fraîche, mais aucune variation dans la minéralisation du C lorsqu'il n'y avait pas d'apport de matière fraîche (Soler-Rovira et al., 2013). Enfin, outre les effets directs sur les micro-organismes qui peuvent ou non s'adapter au stress induit par le Cu et la production de radicaux libres, le Cu peut s'associer avec la MO du sol et diminuer sa dégradabilité (voire paragraphe A.3.i), donc les émissions de CO_2 associées. La résultante de cette contamination sur les fonctions de minéralisation de C et N des sols est alors

difficile à estimer. De plus, outre les variations dues aux sensibilités des organismes, la disponibilité du Cu dans le sol affecte également ses effets.

ii. Spéciation et disponibilité du Cu

Dans les sols, le Cu existe sous différentes formes: i) inclus dans la structure primaire et secondaire des minéraux ; ii) inclus dans des carbonates ou oxides ; iii) adsorbé à la MO solide ou aux argiles ; iv) complexé dans la solution du sol (Cu-OH, Cu-CO_3, Cu$(CO_3)_2^{2-}$ …) ; v) sous forme de cation Cu^{2+} libre dans la solution du sol (Reed and Florida, 1996).

Le Cu inclus dans les minéraux primaires ou secondaires est lié par des structures covalentes et est non labile, considéré inerte vis-à-vis des plantes ou des micro-organismes (West et al., 1981). Ces formes de Cu ne peuvent pas se dissocier facilement dans la solution du sol, mais sont en équilibre à long terme (années) avec une portion plus labile de Cu (par exemple à travers l'altération et l'érosion du sol)(Reed and Florida, 1996).

Le plus gros pool de Cu labile est constitué de Cu adsorbé à la surface d'argiles et de matières organiques chargées négativement (West et al., 1981). Ce pool de Cu est en équilibre avec la solution du sol, les ions Cu adsorbés pouvant s'échanger avec des ions positivement chargés comme H^+ ou d'autres cations.

Enfin, un petit pool de Cu se trouve dans la solution du sol sous forme de Cu libre ou complexées (en général de l'ordre de 10^{-7} à 10^{-8} mol.L^{-1}) .

On considère traditionnellement que le Cu inclus dans les minéraux ou adsorbé aux composés du sol représente les réserves (on parle de facteur de quantité). Le Cu en solution est considéré comme le facteur d'intensité qui peut affecter les plantes ou les organismes (West et al., 1981; Reed and Florida, 1996). La figure I.4 représente schématiquement ces différents pools et les temps d'échange caractéristiques entre chacun d'entre eux.

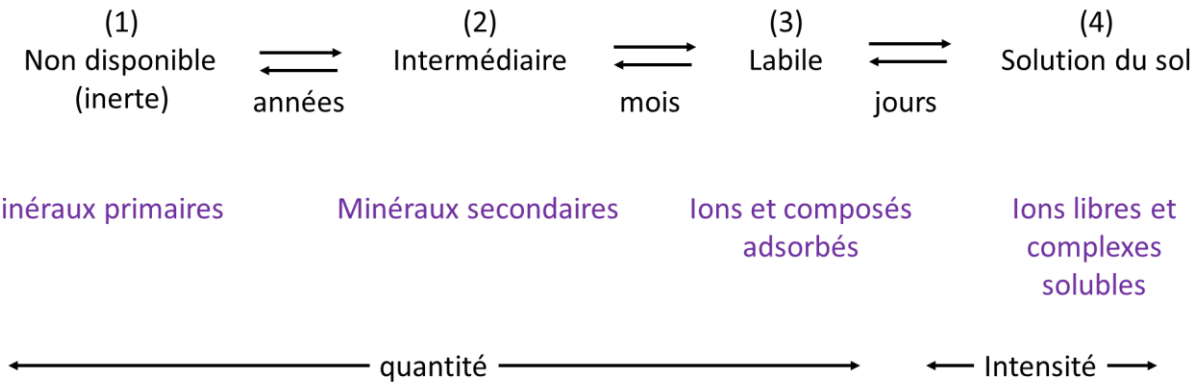

Fig. I.4 : Représentation schématique des différents pools de Cu du sol et de leurs dynamiques de transfert, tiré de (West et al., 1981).

La répartition du Cu entre les phases solides et la solution du sol est gouvernée par des processus de sorptions impliquant des substances telles que les humus, les phyllosilicates, les carbonates, les minéraux de charges variables selon le pH ((oxy-hydroxydes de fer, manganèse, aluminium, ou phyllosilicates recouverts de ces hydroxydes) (Jackson, 1998; Sparks, 2003; Violante et al., 2005, 2007a). Les substances humiques contiennent de nombreux groupes fonctionnels pouvant complexer des cations comme les éléments traces métalliques donc le Cu. Cette formation de

complexes a plusieurs conséquences : i) ils modifient les équilibres dans le sens d'un empêchement de la précipitation des métaux ; ii) ils peuvent véhiculer les éléments traces dans la solution du sol ; iii) ils réduisent la toxicité lorsque la forme libre est considérée comme la plus impactante (organismes exposés via la solution du sol). Pour des raisons géométriques, le Cu est préférentiellement lié à la MO mais plus faiblement aux minéraux que d'autres éléments traces (Violante et al., 2007b; Manceau and Matynia, 2010).

Le pH du sol, en modifiant le nombre de sites disponibles affecte largement la spéciation du Cu. Temminghoff et al., (1997) ont par exemple observé 30% de Cu en solution lié au carbone organique dissous à pH=3.9 contre près de 99% à pH=6.6.
La quantité de Cu disponible vis-à-vis de la faune et flore du sol et donc ses effets dépend donc largement des propriétés du sol : matière organique, pH, argile…

Outre les caractéristiques des sols certaines études ont pu montrer que le climat affectait également la disponibilité du Cu. Xing et al., (2011), et Sangiumsak and Punrattanasin, (2014) ont ainsi pu montrer une augmentation de la sorption du Cu avec une augmentation de la température tandis que Ma et al. (2006) ont pu montrer que le temps nécessaire pour atteindre l'équilibre de sorption du Cu augmentait avec la température. D'autres études se sont focalisées sur les évènements d'inondations ou périodes de sécheresse avec des résultats contrastés : Xu et al. (2013) ont montré un plus grand pool de Cu labile avec alternance de dessiccation-humectation tandis que Zheng and Zhang, (2011) l'ont montré sous inondation constante. De même Han et al. (2001) ont trouvé une augmentation de la proportion de Cu lié à la MO avec des cycles dessiccation-humectation, tandis que Xu et al., (2013) ont montré un relargage du Cu lié à la MO, suite à la minéralisation de celle-ci lors des cycles de dessiccation-humectation.

Les effets du changement climatique et en particulier celui du changement de précipitations sur la disponibilité du Cu (directement ou via des effets sur d'autres facteurs pédologiques) restent donc encore mal établis. D'autre part, les réactions des écosystèmes aux doubles stress sont souvent plus complexes et fortes que celles à chacun des stress. Quelques exemples de réactions des écosystèmes aux double stress et leurs limites sont présentés en B.3

B.3. Effets de double stress sur les fonctions des sols

Les réponses des fonctions des sols à des doubles stress dépendent de la nature et intensité de ces derniers. Dans certains cas les premiers stress augmentent la résistance de l'écosystème par la sélection de communautés plus résistantes, par l'adaptation ou par des changements physiologiques (Beddington and May, 1977; Odum et al., 1979). Par exemple, une pollution métallique de longue durée induirait une modification des communautés microbiennes leur permettant de mieux résister à un stress métallique secondaire, c'est le principe du PICT, pollution induced community tolerance (Diaz-Ravina et al., 1994; Blanck, 2002).

Dans d'autres cas, les écosystèmes sans stress (subissant des variations environnementales dans leurs gammes habituelles) sont supposés plus stables, car pouvant accéder à un vaste panel de ressources leur permettant de maintenir leurs fonctions face aux stress.

Pour autant, les réactions face aux stress de différentes natures sont variées : Tobor-Kapłon et al., (2006) ont pu montrer qu'une exposition longue au Cu augmentait la résistance à la chaleur ou à l'alternance dessiccation-humectation tandis que Li et al., (2016) montrent une moindre résistance de

la respiration induite à l'alternance dessiccation-humectation dans des sols initialement contaminés au Cu.

En A et B.1, B.2., nous avons pu voir que les fonctions de minéralisation du C et de l'N dépendaient également de paramètres environnementaux comme les facteurs pédologiques ou les conditions climatiques. La MO et le contenu en azote du sol et les émissions de gaz à effet de serre des sols présentant de grands intérêts agronomiques et climatiques, les démarches pour les prédire en fonction des paramètres environnementaux existent depuis longtemps. Ces modèles sont présentés dans le paragraphe C.

C. Les modèles de décomposition de la MO du sol : une méthode pour prédire les émissions de gaz à effet de serre des sols en fonction de facteurs environnementaux.

Les premiers modèles de décomposition de la MO en fonction de la température, de la structure du sol et des précipitations ont été développés dès les années 40 (Jenny, 1941). La dynamique globale du C des sols est régit par les apports en MO fraiche, les transformations de celle-ci et les pertes de C par la respiration hétérotrophe (Schlesinger and Bernhardt, 2013). La première formulation mathématique globale proposée par Henin et Dupuis (Henin and Dupuis, 1945; Luo et al., 2016) est une décroissance de premier ordre de la masse de C suivant l'équation I.7a:

Eq.I.7a : $\frac{dX(t)}{dt} = u(t) - kX(t)$

Où X(t) est la masse de C restant au temps t et k un coefficient de décomposition.

Les différences de temps de résidence du C dues à la variabilité physico-chimique sont généralement prises en compte en utilisant la forme matricielle de l'équation I.7b :

Eq. I.7b: $\begin{cases} \frac{dX(t)}{dt} = Bu(t) - A\xi(t)KX(t) \\ X(t=0) = X_0 \end{cases}$

Où X(t) est un vecteur représentant les tailles des différents pools de C, B est un vecteur de coefficients de partition entre les pools de plantes, A est une matrice carrée de coefficients de transfert, ξ(t) est une matrice diagonale de scalaires des paramètres environnementaux, K est une matrice diagonale de taux de décomposition, X_0 est un vecteur représentant les tailles des pool initiaux. Avec cette formulation, les émissions de CO_2 (la respiration de chaque pool) correspondent à la somme des éléments de chaque ligne de la matrice A multipliés par -1.

La formulation des équations de décomposition de la MO varie peu depuis les premiers modèles et ces structures sont utilisées par la plupart des modèles régionaux comme Century, RothC ou CN. La prise en compte des paramètres environnementaux par ces modèles est souvent limitée, par exemple aux simples contenus en lignine pour déterminer les proportions de litière fraiche allant dans chaque pool ou au contenu en argile et limon dans la prise en compte de la structure du sol (Parton et al., 1987; Campbell and Paustian, 2015).

Un exemple de ces modèles compartimentaux est le modèle CENTURY, dont le schéma en fig. I.5 indique les fonctions de partage de la MO (plant residue) en 2 pools de litière (structural et metabolic C) et 3 pools de C du sol (active, slow, passive) définis selon le temps de résidence du C. Cette structure est commune avec de nombreux autres modèles tel que RothC.

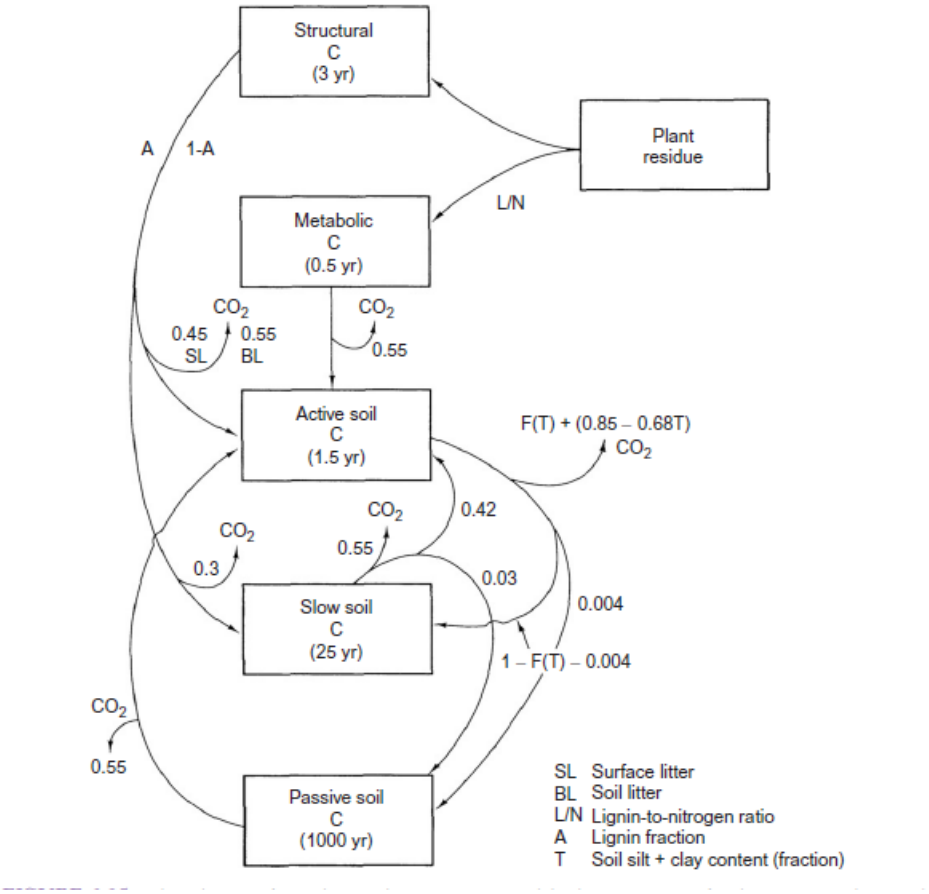

Fig I.5. : Représentation schématique du modèle CENTURY, d'après (Parton et al., 1987).

Outre ces propriétés structurales, les modèles de dynamique de la matière organique peuvent prendre en compte des facteurs environnementaux tels que la température, l'humidité du sol ou la disponibilité du substrat qui peuvent alors moduler la fonction de décomposition $\xi(t)$, voir fig. I.5 où sont indiqués par exemple les effets de la texture du sol (F(T)) et de la composition de la MO (L/N, A). Des modèles de dynamique d'N prennent également en compte la stœchiométrie et la compétition entre les réactions de nitrification et de dénitrification en fonction des paramètres environnementaux.

Les calibrations des fonctions $\xi(t)$ sont néanmoins difficiles et ont nécessité l'utilisation de grands jeux de données de décomposition et d'incubations de sol, éventuellement calibrés sur différentes gammes de paramètres du sol. Ces modèles restent encore maintenant largement utilisés (voire directement transposés) pour des prédictions régionales ou à plus grande échelle de flux d'émissions ou stocks des sols de C, voire N dans les modèles globaux à végétation dynamique (ou Dynamic global vegetation model, DGVM). Ces modèles à grandes échelles utilisent pour partie l'azote

comme simple contrainte stoechiométrique sur le cycle du C (voir A.3.i)), d'autres modèles ont une formulation plus explicite qui intègre les différentes réactions du cycle (A.2.2.)

Les DGVMs et les modèles de système Terre sont souvent utilisés pour prédire les variations de concentrations atmosphérique de C et N en fonction de l'usage des terres ou de scénarios climatiques (Friedlingstein et al., 2001; Lawrence et al., 2011; Wang et al., 2013). Devant leur usage prospectif ou en vue de l'application de législations, il reste primordial d'améliorer leurs capacités prédictives en réponse à ces scénarios. A l'heure actuelle, les principales améliorations envisagées sont la représentation explicite d'un pool microbien ou des pratiques agricoles en terme de fertilisation et d'amendements (Arneth et al., 2010; Schimel, 2013; Wieder et al., 2013), tandis qu'une des sources principales de variabilité entre les modèles vient des variables externes considérées (CEC pour RothC contre argile pour CENTURY par exemple).

La contamination des sols concerne de grandes surfaces (estimées autour de 28% en Europe (Tóth et al., 2016)) et les réglementations à l'échelle des territoires peuvent être à l'origine des différences observées sur l'ampleur des contaminations des sols. Il est donc d'intérêt majeur de déterminer si une contamination peut affecter les émissions de gaz à effet de serre des sols, sous quelles conditions et si oui de la prendre en compte dans les modèles utilisés à des fins prospectives sur des scénarios d'usage des terres. Dans ce contexte, la seconde partie de la thèse discutera les métriques de contamination à l'échelle continentale (Cu total, Cu en solution ou Cu libre) à prendre en compte dans le contexte d'un changement climatique. En effet, à la variabilité spatiale de la concentration en Cu des sols, s'ajoutant celle des variables pédo-climatiques qui affecte sa disponibilité, nous supposons que l'impact du Cu sur l'environnement à l'échelle de l'Europe varie plus que la seule concentration en Cu. Il s'agira de déterminer d'une part les zones à risque en Europe, d'autre part l'évolution de celles-ci avec le changement climatique et enfin la prise en compte du double stress, chimique et climatique, sur les fonctions des sols au regard des quantités de cuivre total ou en solution. Dans une troisième partie, nous chercherons à montrer la pertinence de la prise en compte d'une contamination en Cu dans les modèles de surface continentale en supposant qu'une part de l'erreur de modélisation de ces modèles s'explique par la non considération de la contamination du sol en Cu. Nous proposerons des fonctions de réponse génériques intégrant l'effet du Cu sur la minéralisation du C à partir d'une revue quantitative grâce aux nombreuses études ayant pu étudier cet effet localement. Enfin, nous proposerons des fonctions de réponses prenant en compte l'effet d'une contamination en Cu sur la minéralisation de l'azote. Cet effet étant, d'une part moins bien renseigné que celui sur la minéralisation du carbone, d'autre part plus sensible aux variations de précipitation, nous nous baserons sur des incubations de laboratoires effectuées à différentes humidités et seront ainsi en mesure de proposer des fonctions réponses intégrant le double stress de contamination au Cu et d'humidité dans un modèle biogéochimique.

Partie II : Pertinence de l'évaluation de la disponibilité des contaminants vis à vis des fonctions des sols en contexte de changement climatique

Cette partie II est divisée en deux chapitres, respectivement « représentation spatiale des risques liés au Cu en contexte de changement des précipitations à l'échelle» (Chapitre II.1) et à l'« Estimation de l'effet d'une contamination au Cu après un stress d'humidité sur l'inhibition d'activités nitrifiante du sol » (Chapitre II.2)

Le chapitre II.1 présente deux études ayant trait d'une part aux estimations de disponibilités du Cu, en particulier libre et en solution (sous chapitre II.1 A) et d'autre part à l'évolution des possibilités de pertes et d'accumulations en Cu en Europe à l'échelle du siècle selon différents scénarios de changement climatique (sous chapitre II.1.B). La première étude (II.1.A) a visé à établir les zones à risques en Europe vis-à-vis du Cu en solution et du Cu libre en se basant sur les caractéristiques pédologiques et les concentrations en Cu total disponibles à cette échelle. La deuxième étude (II.1.B) a permis de pointer les zones susceptibles d'exporter de fortes quantités de Cu en solution suites à de possibles importantes variations de précipitations dues au changement climatique.

Le chapitre II.2. présente également deux études, portant sur l'impact des stress conjugués de variations d'humidité des sols et de contamination sur les fonctions de nitrification du sol (II.2.A) ; complétée par une mise en évidence d'éventuelles modifications des propriétés de mise en solution du Cu sous l'influence de cycles d'humectation-dessiccation (II.2.B).

Les chapitre II.1 se rapporte aux interactions entre climat, contamination et sols telles que schématisées ci-dessous :

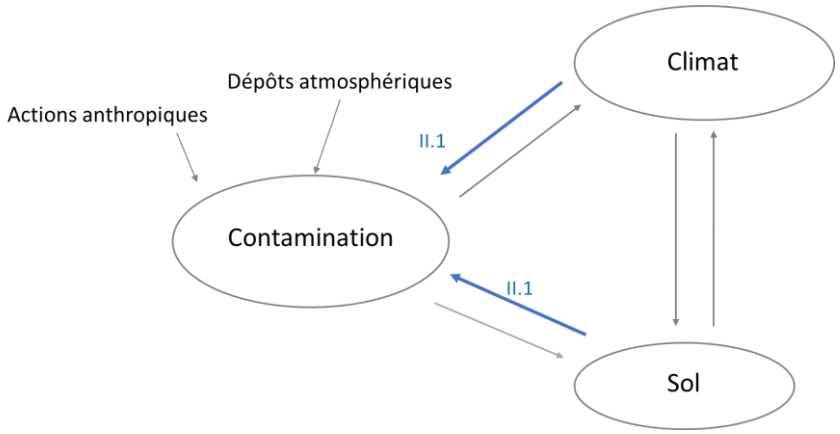

Chapitre II.1: Représentation des risques liés au Cu en contexte de changement de précipitation à l'échelle de l'Europe

II.1.A Représentation spatiale à l'échelle européenne des risques associés à une contamination en Cu via l'utilisation de proxies de disponibilité et bio-disponibilité

Résumé en français du papier soumis à science of the total environment :

La contamination des sols par des éléments trace métalliques comme le cuivre (Cu) peut affecter leur fonctionnement. Les politiques et normes environnementales comme les mesures effectuées lors de campagne d'étude des sols font toujours référence à la teneur totale en cuivre. Les teneurs en Cu dans la solution du sol ou les teneurs en Cu libre se sont pourtant avérées être de meilleurs indicateurs des risques de mobilité du Cu ou de sa (bio)disponibilité pour les organismes du sol. Plusieurs équations empiriques ont été définies à l'échelle locale pour prédire les quantités de Cu dans la solution du sol sur la base des teneurs totales en Cu du sol et des principaux paramètres du sol impliqués dans le partage entre sol et solution. Néanmoins, malgré leur pertinence dans l'évaluation des risques, ces équations ne sont pas appliquées à grande échelle spatiale en raison des difficultés à effectuer des changements du local au régional. Nous avons ainsi collecté les équations empiriques de la littérature et sélectionné celles permettant d'estimer la quantité de Cu en solution, (proxy du Cu disponible), à partir des teneurs totales en Cu et des paramètres du sol. Nous avons fait de même pour l'estimation du Cu libre en solution (proxy du Cu biodisponible). Ces équations ont été utilisées pour fournir des cartes européennes de Cu (bio-)disponible basées sur celle de Cu total en Europe. Les résultats ont permis de comparer les cartes de Cu disponible et biodisponible à l'échelle européenne. La comparaison de chaque forme de Cu à sa valeur médiane respective a permis d'identifier les zones spécifiques de risques liées à chacun de ces deux proxies. Des divergences plus importantes entre la carte du Cu biodisponible et la carte du Cu total qu'entre celle du Cu disponible et celle du Cu total sol ont pu être mises en évidence.

Conclusion intermédiaire (1) :

Suite à cette étude décrite dans le sous chapitre II.1.A, il était intéressant de pouvoir quantifier le risque d'export de Cu qui peut être approximé par la concentration de Cu en solution. Mais les quantités de Cu effectivement exportées dépendront à la fois de la quantité de Cu dans la solution du sol et de la quantité de solution de sol. A la variabilité spatiale du Cu en solution s'ajoute donc celle des précipitations. Or, on s'attend à des changements de précipitations dans les années à venir sous l'impact du changement climatique, certaines zones subiront alors des précipitations plus intenses, d'autres moins. De fait, la quantité de Cu exporté pourra être modifiée suite à des variations de débit. Ainsi, dans le sous chapitre II.1.B, nous avons identifié des zones à risque d'exports de Cu en solution en intégrant à la fois les aspects de spéciation du Cu et de quantité de solution du sol en climat actuel et futur. Le déploiement d'un modèle dynamique intégrant des apports en Cu ou en tenant compte du

fond pédogéochimique inaltérable en Cu n'a pas été possible dans le temps de la thèse. Ceci est lié au manque d'informations sur les apports et du fait des difficultés de représentations. On n'estimera donc pas directement les quantités de Cu exporté via la solution du sol comme dans cette partie, mais on comparera les quantités de débit de solution du sol à la proportion de Cu à même de passer en solution, définie par sa constante de dissociation K_f.

II.1.B. Evolution des possibilités des pertes et des accumulations en Cu en Europe à l'échelle du siècle selon différents scénarios de changement climatique*

Résumé en français du manuscrit en cours de soumission à science of the total environment:

L'utilisation anthropique d'éléments traces métalliques à des fins industrielles ou agricoles se traduit par des dépôts à la surface des sols. Parmi ces éléments traces, le cuivre (Cu) est largement utilisé notamment en agriculture pour ses propriétés fongicides. Dans les sols, seul le Cu en solution est mobile et peut être transféré pour atteindre les cours d'eau, les rivières ou les lacs. La répartition entre le Cu en solution et le Cu total est déterminée par les propriétés du sol. Ainsi, la mobilité du Cu peut varier en grande partie en raison des conditions locales du sol mais aussi en raison des changements dans l'hydrologie du sol. En effet, lorsque les ruissellements sont élevés et que le Cu est mobile, le Cu dans la solution du sol peut être lessivé, alors que de faibles écoulements et une partition limitée du Cu en phase liquide peuvent conduire à une accumulation du Cu dans les sols. Par conséquent, la connaissance du ruissellement du sol (et de sa dynamique) ainsi que de la partition du Cu entre les phases solides du sol et la solution du sol permet d'identifier les zones d'accumulation potentielle ou de lixiviation potentielle du Cu. Or, en raison du changement climatique, on s'attend à ce que les écoulements du sol changent au cours du siècle suite à la modification de régime des précipitations. Dans cette étude, nous avons utilisé les coefficients de partage (Kf) entre le cuivre total et dissous et les résultats des simulations de ruissellement pour le climat actuel et futur afin d'estimer les zones de lixiviation (LP) ou d'accumulation potentielle (AP) à l'échelle européenne. Les scénarii de changement climatique étant incertains, nous avons mené notre étude pour 2 types de concentration représentatives : RCP 2.6 et RCP 6.0. Les zones de LP et AP ont été définis en comparant Kf et les écoulements à leur médiane respective sur l'Europe. Nos résultats montrent que, à l'heure actuelle, 5,9 ±1,34 % (médiane, écart médian) et 4,9 ±1,4 % des points de grille sont concernés respectivement par le LP et le AP. Les surfaces de LP et le AP augmentent au cours du siècle, le pourcentage de l'Europe concerné par le LP étant de 7,8 ±1,5 % et par le AP de 6,1 ±2,8 % pour le RCP 2.6 en 2090, et de 8,9 ±2,3 % pour le LP et 9,1 ±1,3 % pour le AP avec le RCP 6.0.

* Basé sur le rapport de stage Paris J-M. 2021. Evolution of soils copper loss to aquatic systems under different scenarios of climate change in EuropeL3 Géosciences ENS Encadrement L. Sereni , B. Guenet et I.Lamy

II.1.A. Mapping risks associated with soil copper contamination using availability and bio-availability proxies at the European scale

Laura Sereni[1*], Bertrand Guenet[2], Isabelle Lamy[1]

[1] Université Paris-Saclay, INRAE, AgroParisTech, UMR 1402 ECOSYS, Ecotoxicology Team, 78026, Versailles, France
[2] Laboratoire de Géologie de l'ENS, PSL Research University, CNRS, UMR 8538, IPSL, Paris, France

***Correspondence:** Laura Sereni laura.sereni@inrae.fr

Submitted in Sciences of the Total Environment, October 15th 2021

Abstract

Soil contamination by trace elements like copper (Cu) can affect soil functioning. Environmental policies with guidelines and soil survey measurements still refer to the total contents of Cu in soils. However, Cu contents in soil solution or free Cu contents have been shown to be better proxies of risks of Cu mobility or (bio)availability for soil organisms. Several empirical equations have been defined at the local scale to predict the amounts of Cu in soil solution based on both total soil Cu contents and main soil parameters involved in the soil/solution partitioning. Nevertheless, despite the relevance for risk assessment, these equations are not applied at a large spatial scale due to difficulties to perform changes from local to regional. To progress in this challenge, we collected several empirical equations from literature and selected those allowing estimation of the amount of Cu in solution, used as a proxy of available Cu, from the knowledge of both total soil Cu contents and soil parameters. We did the same for the estimation of free Cu in solution, used as a proxy of bioavailable Cu These equations were used to provide European maps of (bio-)available Cu based on the one of total soil Cu over Europe. Results allowed comparing the maps of available and bio-available Cu at the European scale. This was done with respective median values of each form of Cu to identify specific areas of risks linked to these two proxies. Higher discrepancies were highlighted between the map of bioavailable Cu and the map of soil total Cu compared to the Cu available map. Such results can be used to assess environmental-related issues for land use planning.

Highlights:

- Mapping of risks due to soil copper contamination was made at the European scale
- We used soil Cu maps and partitioning equations to derive risk assessment maps
- We provided maps of available and bio available risks
- Risk estimation for available Cu and total Cu differs in 26% of the grid points
- Risk estimation for bio-available Cu and total Cu differs in 69% of the grid points

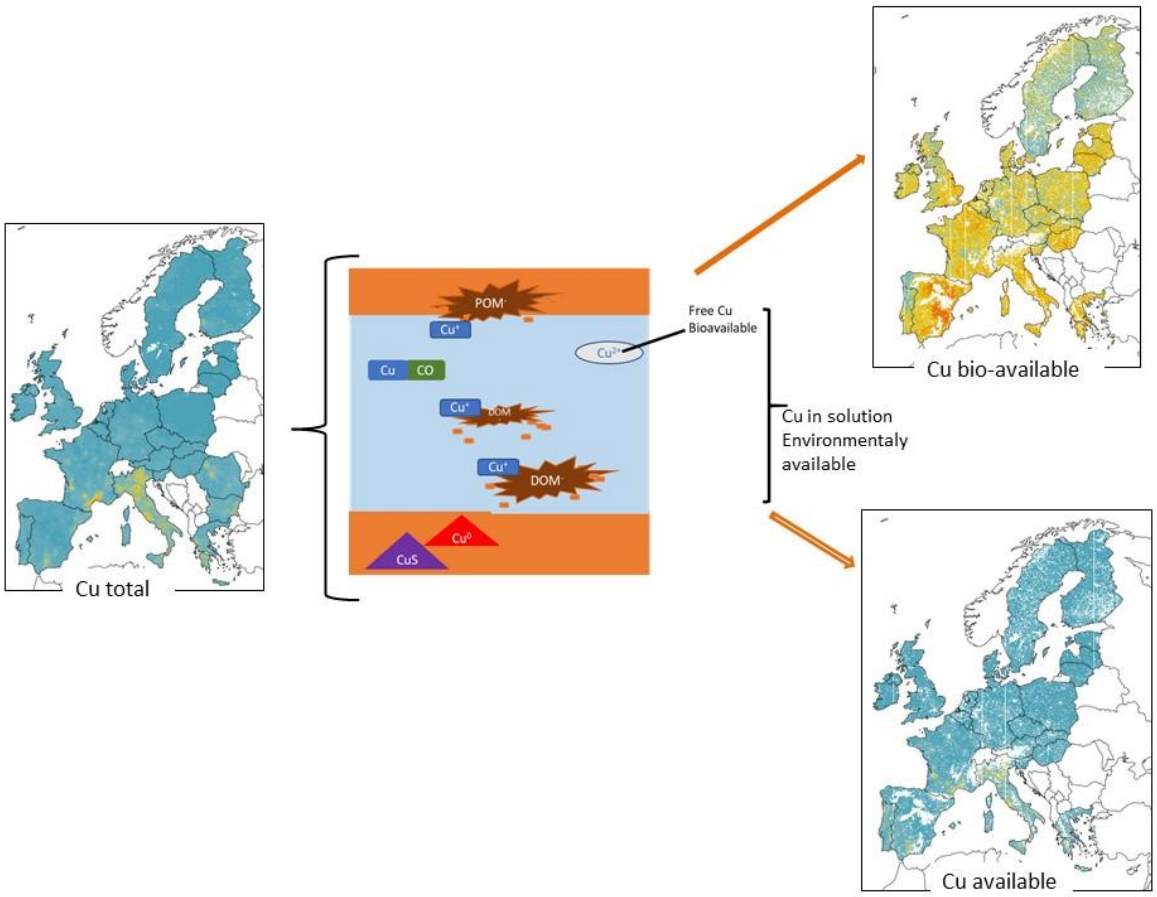

Keyword: Trace element, mobility, transfer function, risk assessment, diffuse contamination, regional assessment

1. Introduction

From a spatial point of view, native indigenous trace elements in soils largely vary around the world due to bedrock. In addition, atmospheric deposition, agriculture, mine tailing or industrial activities can be important exogenous sources of soil trace element contamination (Hong et al., 1996; Nicholson et al., 2003). Fluxes of trace elements in ecosystems include their accumulation in surface soil horizons and their release to the soil solution, to the organisms or until the aquifers. While trace elements are often required for biological systems, large amounts may have toxic effects (Flemming and Trevors, 1989; Shabbir et al., 2020). Among the trace elements, copper (Cu) is widely used in industrial and agricultural sectors. In the absence of contamination, Cu is found as a native trace element at various total concentrations in soils, typically from 5 until 50 mgCu kg^{-1} depending on the bedrock, but concentrations above 100 mgCu kg^{-1} can be observed in Australia or in Baltic shield (Salminen and Gregorauskiene, 2000). Additionally, inputs from different sources like manure, pesticides or fertilizers are regularly added, leading at a spatial scale to various total soil contents at least in the surface soil horizon. The annual amounts of Cu deposited on soils through atmospheric contamination or for agronomical purposes were estimated around 3900 gCu km^{-2} $year^{-1}$ (~0.01mgCu kg^{-1}) for atmospheric deposition and between 100 and 800 gCu km^{-2} $year^{-1}$ (respectively 0.003 and 0.025 mgCu kg^{-1}) for agricultural inputs depending on the fertilizers and crop type (Azimi et al., 2004). Outputs by crops or leaching waters are more difficult to estimate (Romkens et al., 2004), but globally general pattern leads to Cu accumulation in surface horizons. Thus, most of the environmental quality standard are defined on the basis of the total soil metal content in the surface horizon, while the relevance of such a value in terms of risks for metal mobility or bio-availability had been questioned (Kördel et al., 2013).

Indeed, total soil Cu content can be schematically divided into a pool of sorbed Cu on the solid phase and a pool of Cu present in the liquid phase, both in equilibrium. Cu in solution can also be divided into a pool of Cu complexed to either organic or mineral species and a pool of Cu in the free Cu^{2+} form (e.g. Cu in solution not bound to organic nor to mineral anions, see fig II.1.A.1). Concerning this later pool, the free ion activity model (FIAM) argues that the free form of a trace metal (M) element as M^{n+} is the most biologically impacting form (Parker et al., 2001). Thus, the small and labile fraction of free Cu can be used to advantage as a proxy of bio-available Cu (Lanno et al., 2004; Thakali et al., 2006). But the knowledge of the total amount of Cu in solution is also important because it's the most likely total pool of Cu that can easily exchange and be available for organisms or for exportation through runoff. Total contents of Cu in solution are therefore assimilated to a pool of environmentally available Cu. But when the total trace element content in soil is the only available data, this value is used by default to express the risks even if overestimated (Ministry of the Environment, 2007; Oorts et al., 2006b; Smolders et al., 2009). Several studies have underlined the importance of the knowledge of soil parameters (organic matter content, pH, ionic strength or dissolved organic carbon) to calculate the Cu speciation, i.e. the repartition of Cu in its different forms (Degryse et al., 2009; Mondaca et al., 2015; Sauvé et al., 2000b). In the literature, three main ways can be identified to calculate total Cu in solution and/or free Cu^{2+} forms from the knowledge of total soil Cu contents, two of them being based on empirical statistical relationships and one of them on thermodynamic mechanistic models.

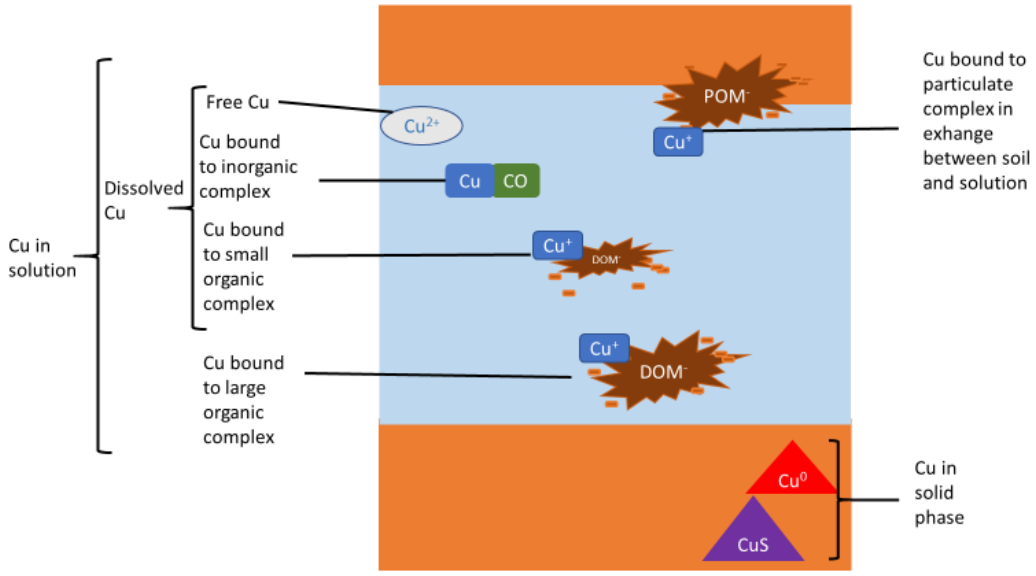

Fig II.1.A.1 Schematic view of the different forms of Cu in soil systems, POM being particulate organic matter in the solid phase to which Cu can be sorbed, DOM being dissolved organic matter in the soil solution, which binds Cu.

From a mechanistic point of view, thermodynamic models allow the calculation of the speciation of Cu in solution using the total soil Cu content and a detailed composition of the soil solution with organic and inorganic compounds as input data. This is currently made with models such as WHAM or Vminteq (Kinniburgh et al., 1996; Tipping, 1998) which iteratively compute total Cu concentration under its different chemical forms providing the knowledge of the equilibrium constants of all the potential species. Many hypotheses have to be made to take into account the polyelectrolytic nature of organic matter, the surface geometry and the electrostatic interactions for complexation and adsorption processes. If such modellings allow a detailed and precise estimation of the different forms of Cu in solution, their use at large scale is complex and challenged due to the number of input data needed. For that, empirical equations can be advantageously used compared to thermodynamic modelling when all the different data are not available.

Empirical relationships result from statistics regression based on large field-data sets. One approach is to estimate coefficients of partition between solid and solution phases or between solid and free Cu, at the other to estimate directly either Cu in solution or free Cu as a sum of several soil parameters. For our purpose, the use of coefficient of partition is few robust because based on the assumption that the different forms of Cu are at the equilibrium. Hence, we rather focused on the direct expression of Cu in solution or of free Cu. Numerous empirical equations have been developed

to estimate Cu in solution or free Cu based on local measurements or data collections, and variables are traditionally log transformed with a generic expression as following:

(1) $$\log_{10} Cu_f = c_0 + c_1 \log_{10}(Cu_{total}) + \sum c_i \log_{10}(X_i)$$ (Groenenberg et al., 2010),

where X_i are the different soil parameters and f the form of Cu (free or in solution) considered.

Recent soil survey from the Joint Research Center (JRC) were performed and maps of total metal soil contents at the European union scale were produced. These maps underlined large diffuse soil Cu contamination with some hot spots of high total soil Cu concentrations (Ballabio et al., 2018). Applied to Cu, the application of the previous equation could fill the gap of the absence of knowledge of the large-scale distribution of Cu availability, using Cu in solution as a proxy, and the absence of knowledge of the large-scale distribution of Cu bio-availability, using free Cu^{2+} as a proxy. Indeed, availability or bio-availability are data still not documented despite their importance for risk estimation and land management.

In this context, the aim of this work was threefold: 1) provide a literature review of statistical empirical relationships established for estimation of available Cu (Cu in solution) or bioavailable Cu (free Cu) 2) define, at the European scale, areas of potential risks e.g of Cu environmental availability or of Cu biological toxicity and 3) link, at the European scale, the risk due to the presence of a soil Cu contamination to the risk of Cu availability and of Cu bio-availability. We decided not to explore the use of mechanistic models but rather to focus on empirical equations easier to use at larger spatial scales. Based on the literature review, we choose the more appropriate relationships in the objective of application on a European database of total Cu measurements. We highlighted areas of risks of i) available Cu (Cu in solution) and ii) bio-available Cu (free Cu) with the comparison of the two values at each grid point with their respective median. This allowed us to define areas of risks without using debated threshold values (Carlon, 2007). Furthermore, the use of relative variations through comparisons with median limited misinterpretation due to intercept effects in the chosen empirical equation and allowed underlining the effects of pedological factors. Finally, we identified areas with conflicting or converging risk assessment of availability or of bio-availability compared to the total Cu risk assessment.

2. Material and Methods

2.1. Equation's review

In order to provide estimates of Cu forms relevant for risks assessment at the European scale, we collected empirical equations from the literature estimating Cu in solution or free Cu using a two steps approach. We first ran (at the date December 2020) bibliographic research on WOS looking for Cu AND (availab*) AND soil AND TOPIC function. We then completed this research using the references of the collected articles. This allowed gathering the relationships to estimate Cu in solution and free Cu on the basis of soil pedogeochemical characteristics. We only selected relationships using

pedogeochemical characteristics commonly measured such as soil organic matter (OM) or soil organic C, dissolved organic carbon (DOC), cationic exchange capacity (CEC), clay percentage and pH.

Statistical empirical equations mostly provided estimation of Cu contents in solution and free Cu concentrations based on total Cu contents and others soils parameters. Some empirical equations estimated so-called "dissolved" trace metal i.e. trace metal in solution after filtration at 0.45 µm. But contrarily to other heavy metals, few Cu is associated to large colloids removed with filtration (Jensen et al., 1999). Since our study focused on the application of transfer functions to estimate (bio-)available risks we focused on the application of equations for Cu in solution and for free Cu including both the calculation of Cu in solution or dissolved Cu that we considered equally.

To provide a generic guide to selecting empirical equations while reviewing, we listed the transfer functions together with: 1) measurement protocols to acquire Cu data, 2) the number of data used to establish the statistical relationship, 3) their associated R2, 4) the range of soil properties used to define the relationships, 5) the number of times they have been cited, and 6) the number of citations per year. Indeed, among papers, the protocols to acquire Cu data were not uniforms. Measurements of total soil Cu contents were made using different methods, i) after a total HF soil mineralization thus including Cu pedological background, or ii) after a "pseudo-total" soil digestion thanks to aqua regia or iii) after a 0.43 M HNO_3 extraction. It is recognized that the two last extractions approximate total Cu soil content (ISO, 2006; Sastre et al., 2002; USEPA, 2007). The dilute acid extraction has also been established as an ISO 17586:2016 norm to analyze potential environmental available trace elements. Similarly to determine Cu in solution, we found in the collected papers several methods to extract soil solution while various types of extraction are known to give different kinds of soil solution (Weihermüller et al., 2007). Finally, because the experimental free Cu measurement requires specific equipment's (a selective Cu electrode or a devise with Donnan membrane (Minnich and McBride, 1987; Pampura et al., 2006)) several studies used theoretical results from speciation modelling software rather than direct experimental measurements.

2.2. Estimation of (bio)-available Cu maps

In this study we used the European soil Cu survey from the LUCAS database provided by the JRC from which total Cu is based on the aqua regia protocol (Ballabio et al., 2018; Tóth et al., 2016). Hence, we selected from our provided generic guide the transfer functions issued from studies using aqua regia protocols to measure total Cu.

With these collected empirical equations, the estimations of Cu contents in solution and of free Cu contents in solution allowed building respectively maps of so-called available and bioavailable Cu based on pedological mapping provided by the JRC at a 0.5 km scale. The total Cu map was downloaded from https://esdac.jrc.ec.europa.eu/content/copper-distribution-topsoils (Ballabio et al., 2018), pH was downloaded from https://esdac.jrc.ec.europa.eu/content/chemical-properties-european-scale-based-lucas-topsoil-data (Ballabio et al., 2019), clay values were obtained from https://esdac.jrc.ec.europa.eu/content/topsoil-physical-properties-europe-based-lucas-topsoil-data (Ballabio et al., 2016), and total organic carbon (Corga) data were obtained from https://esdac.jrc.ec.europa.eu/content/topsoil-soil-organic-carbon-lucas-eu25 (de Brogniez et al., 2015). Soil OM values were converted to soil Corga content using Corga=OM/2 (Pribyl, 2010). For computational time purpose, we used the climate data operator software cdo (Schulzweida, 2017) to

remap at 0.01° the data originally at the 0.5km scale. Maps of available and bio-available Cu were computed at the 0.01° with previously chosen equations and R v3.5.

2.3. Risk assessment

For each proxy associated to Cu (available, bio-available, and total soil content), high-risk areas were identified by computing a risk indicator (RI) in % defined through a comparison with the median value (eq. II.1.A. 2).

Eq. II.1.A.2.: $RI_f = \frac{|Cu_{f,k}| - |Cu_{f,Med}|}{|Cu_{f,Med}|} \times 100$,

where f is the proxy of Cu risk (available, bio-available or total), $|Cu_{Med}|$ is the absolute value of its median value and $|Cu_{f,k}|$ is the absolute value of the form f of Cu for the grid point k.

We chose the median rather than the mean value as the reference because of the presence of very few points having high Cu values that pushed up the average (see results 3.2.1). Following Reimann et al. (2005), we also identified areas with concentrations of total Cu, available Cu and bio-available Cu smaller or higher than the median ± 2 times the median average deviations.

The relevance of total Cu to assess soil risk was checked by the comparison of RI_{total} with RI_f (with f=Cu available or bio-available). Three main classes were defined for total Cu with a Risk Index higher, lower, or similar to the risk index of the (bio)available forms, together with 5 subdivisions cases as following:

- 1) $RI_{total} >> RI_f$
    - A) $RI_{total} > 0$ and $RI_f < 0$
    - B) $RI_f < RI_{total}$ and $RI_{total} - RI_f >$ median $(RI_{total} - RI_f) + 2 \times$ mean average deviation $(RI_{total} - RI_f)$
- 2) $RI_{total} << RI_f$
    - A) $RI_{total} < 0$ and $RI_f > 0$
    - B) $RI_f > RI_{total}$ and $RI_f - RI_t >$ median $(RI_{total} - RI_f) + 2 \times$ mean average deviation $(RI_{total} - RI_f)$
- 3) $RI_{total} \sim RI_f$ defined as $|RI_{total} - RI_f| <$ median $(RI_{total} - RI_f) + 2 \times$ mean average deviation $(RI_{total} - RI_f)$

These classes and their subdivisions were defined to highlight the areas where risk assessment based on total Cu differs from those based on available Cu or on bio-available Cu.

The first class ($RI_{total} >> RI_f$) refers to cases where the calculations from the grid points indicated that soil may be considered at risk when considering total Cu measurements but not considering (bio)-available Cu (depending on the f Cu form). For 1 A) the soil may be considered at risk when considering total but not (bio)-available Cu. For 1B) the soil is considered at risk for the two indicators but the risk

may be largely underestimated considering (bio)-available Cu in comparison to total Cu. The second class (RI_{total} << RI_f) refers to cases where soil may be considered without risk when considering total Cu but at risk considering (bio)-available Cu. For 2A) the soil may be considered without risk when considering total Cu contents but at risk when considering (bio)-available Cu. For 2B) the soil is considered at risk for the two indicators but the risk may be largely underestimated considering total Cu in comparison to (bio)-available Cu. The third situation (RI_{total} ~ RI_f) refers to cases where the differences between total and (bio)-available Cu contents are rather small.

Maps and statistical analysis were calculated using R version 3.5 (R Core Team, 2018) .

3. Results

3.1. Literature Review of empirical equations

We collected 29 relationships aiming at estimating (bio-)available Cu using total Cu contents and soil parameters from 16 references compiled in table II.1.A.1. From those 16 references, 1 was produced as part of a report for the environmental research institute of Wageningen (Alterra)(Römkens et al., 2004) on a Dutch soil survey with rather low Cu concentrations close to the local diffuse agricultural contamination in Cu (maximal values around 321mgCu.kg^{-1} while other equations are built on contamination up to a few thousand mgCu.kg^{-1}) and with a significant number of data (416). However, the measurements of available Cu were made with a DTPA extraction rather than with dilute salts and the estimation of the total soil Cu content was based on a 0.43 M HNO_3 extraction. Although interesting, the data from Romkens et al were not further investigated in this paper

The oldest equation specifically applied to Cu was provided by Lexmond (1980) (see eq. II.1.A. 11 in table II.1.A.1) to estimate bio-available Cu (expressed as - log(Cu) = pCu) and the last equation we found was designed by Li et al. (2017) (see eq. II.1.A.10 in table II.1.A.1) to estimate bio-available Cu. Among these 29 relationships, we found 13 equations aiming at estimating specifically the available Cu (Cu in solution) and 16 estimating the bio-available Cu (free Cu). Assuming that yearly rate of citations is a proxy for a scientific consensus and/or the easy-to-use, we found that many studies used the Sauvé et al., (2000a) approach with 61 citations/year (see eq. II.1.A. 6 table II.1.A.1, II.1.A.2 and II.A.2.3), or the McBride et al., (1997) approach with 37 citations/year (see eq. II.1.A.3, table II.1.A.1,II.1.A.2 and II.1.A.3) followed by those of the Tipping et al., (2003) approach with 23 citations/year (see eq. II.1.A.14 table II.1.A.1 and II.1.A.3). Total soil Cu was the most frequent predictor to calculate available Cu with 11/13 equations using total Cu while pH was the most frequent predictor to calculate bioavailable Cu with 16/16 equations based on pH.

3.1.1 Selection of the empirical equation to build the available Cu map

Table II.1.A.2 provides the collected 15 equations of the literature estimating the amount of Cu in solution used here as a proxy for available Cu, and taken into account soil properties. The corresponding soil solution extraction and total Cu mineralization methods are reported in table II.1.A.1. Total soil Cu content is the most frequent explaining variable as a reliable predictor for all except one relationship. All the relationships showed that available Cu decreases when soil pH increases, so that there are more available Cu under acid soil conditions. DOC's partial slope is mostly found as non-significant or positive, indicating that dissolved organic carbon can bind Cu in solution through organic complexes On the other hand, the equation performed for Cu by Sauvé et al. (2000a)

was fitted on more than 350 data collected in the literature, and seem to be the most robust empirical equations in estimation of dissolved Cu. It is also the most cited equation preferentially used to convert a large range of soil Cu total contents into dissolved Cu values. The willing to include as much data point originating from various databases is coupled with the lack of information about the measurement techniques involved. In fact, "total" Cu is mentioned without specifying the soil digestion method. In complement, we also noted the empirical equation of Mondaca (2015) (table II.1.A.2. eq. II.1.A.9) which was fitted with data from Chili and can thus be more appropriate for semi-arid region and their typical pedological characteristics and climate compare to Europe (Garcia et al., 2017; Steven, 2017). Finally, among the collected equations, those from McBride et al., (1997) (table II.1.A.2 eq. II.1.A.3 a-c) are among the most commonly used with more than 36 citations/year. The authors provided two main regressions with exclusion or inclusion of data points (table II.1.A.2 eq. II.1.A.3a.) with highest (>100g.kg^{-1}) OM content (Table II.1.A.2 eq. II.1.A.3b.). The equations II.1.A.3 a,b were built on the basis of a 70 points dataset including a long term contamination due to sludge inputs or industrial activities deposition. For the eq. II.1.A.3a (table II.1.A.2) a maximal total soil Cu concentration around 3000 mg.kg^{-1} was achieved, whereas the equation 3c was based on a dataset with Cu contamination from 7 to 1000 mg.kg^{-1}. Total soil Cu concentrations were measured with acid micro-wave digestion providing values close to aqua regia extraction whereas available Cu values came from 0.01 M $CaCl_2$ extractions (eq. II.1.A.3a,b) or water extractions (II.1.A.3c). Moreover, all the variables of the equations are available in the LUCAS database we intend to use. We therefore selected the equation 3b that fitted more data points to calculate the available Cu at the European scale.

Table II.1.A.1: Sources of transfer functions, number of citations on 29.07.2021, measured variables, extraction procedure and n° of equation (for correspondence with tables 2 and 3) collected from the selected papers.Cu-ISE = copper ion-selective electrode, DPASV = differential pulse anodic stripping voltammetry

DOI	Authors	Year of publication	Times cited	Yearly citation rate	"Total" Cu measurement	Solution extraction	free Cu estimation	response variable	N° equation in the next tables
10.18174/njas.v28i3.17030	Lexmond et al.	1980	114	2.8	HNO_3, $HClO_4$ and H_2SO_4 in a ratio of 40:4:1	0.01M $CaCl_2$	resine extraction	pCu	11
10.1111/j.1365-2389.1997.tb00554.x	McBride et al.	1997	882	36.8	Nitric acid microwave digestion and H_2SO_4-HNO_3 (1:1 by volume), completing digestion with a few drops of HClO	Water extract and 0.01M $CaCl_2$	Cu-ISE	pCu; Cu solution	3a-e
10.1023/A:1018312109677	Sauvé et al.	1997	383	16	HNO_3 microwave	0.01M $CaCl_2$	Cu-ISE	pCu	5a,5b
10.1021/es9907764	Sauvé et al.	2000	1279	60.9	review of "total"	Water displacement, lysimeter, and water or neutral salt extractions		Cu solution	6

10.1021/es0000910	Vulkan et al.	2000	180	8.6	aqua regia	soil pore water	Cu-ISE	pCu	13
10.1016/S0269-7491(03)00058-7	Tipping et al.	2003	405	22.5	nitric and perchloric acids, followed by leaching of the residues with 5 mol l1 HCl, and analysis by ICP–AES.	2%HNO_3	WHAM	pCu	14a-b
10.1021/es030155h	Lofts et al.	2004	219	12.8	EDTA	0.02MCaCl2, +data from Tipping 2003 , Sauvé 1997	CU-ISE and WHAM	pCu	15
Alterra Report 305, May 2004 http://edepot.wur.nl/16988 .	Römkens et al.	2004	66	3.8	0.43 HNO_3	0.05 mol.L Ca-EDTA	CHARON model	Cu solution ; pCu	
10.1016/S1001-0742(06)60016-8	Luo et al.	2006	18	1.2	HF, $HClO_4$ and HNO_3 with a ratio of 3:1:1	0.01 Kcl	electrode (DPASV)	Cu solution; pCu	7a-b
10.1016/j.jhazmat.2005.09.033	Luo et al.	2006	84	5.6	HF, $HClO_4$ and HNO_3 with a ratio of 3:1:1	0.01 Kcl	electrode (DPASV)	Cu solution; pCu	8
10.1097/SS.0b013e3181bf2f52	Unanumo et al.	2009	12	0.8	aqua regia	0.01M $CaCl_2$	WHAM	pCu	12

10.1111/j.1365-2389.2009.01201.x	Groenenberg et al.	2010	102	9.3	0.43 HNO_3	0.01 ou 0.02 $CaCl_2$	WHAM-and Cu-ISE for partial data	pCu	16
10.1080/09064710.2013.785586	Ivezic et al.	2012	6	0.7	1:15 HNO_3	water 1:10	WHAM	Cu solution	4a
10.1002/jpln.201400349	Mondaca et al.	2015	15	2.5	were digested in boiling nitric acid followed by perchloric acid addition	0.1 $MKNO_3$	Cu-ISE	Cu solution; pCu	9a-c
10.1080/09542299.2017.1404437	Li et al.	2017	3	1	aqua regia	filtred pore water	Cu-ISE	Cu solution; pCu	10a-c

Table II.1.A.2: Transfer functions for Cu available reviewed from literature under the form $\log_{10}Cu_{solution} = a \log_{10}Cutot + b \log_{10}OM + c \log_{10}clay + d \log_{10}pH + e$..Cu is expressed in mg.kg $soil^{-1}$, OM is expressed in g.kg $soil^{-1}$ or in % of OM (specified in the row), DOC is expressed in mgC.L^{-1} and clay in %. hen parameters incertitude's were provided, they have been reported in the table.

a.

Source	N°	R.V	e	Log (Cu tot)	pH	Log (OM)	Log (DOC)	Log (clay)	R2	number of data	Range Cu tot ($mg.kg^{-1}$)	Range OM ($g.kg^{-1}$)	Range pH
(McBride et al., 1997)	II.1.A. 3a	Log ($Cu_{solution}$) ($\mu g.L^{-1}$)	0.699	0.86	-0.11				0.87	67	14-2600		3.3-6.6
	II.1.A. 3b	Log ($Cu_{solution}$) ($\mu g.L^{-1}$	1.42	0.94	-0.1	-0.68 ($g.kg^{-1}$)			0.85	70	14-2600		3.3-6.6
	II.1.A. 3c	Log ($Cu_{solution}$) ($\mu g.L^{-1}$)	0.05	0.76					0.86	31	7-1010	2.4-27.4	4.2-7.8
(Ivezić et al., 2012)	II.1.A. 4a	Log ($Cu_{solution}$)	-0.24	0.80	-0.02	-0.53 (%)	0.54		0.42	74	5.7-141	1.8-20.4	4.3-8.1
	II.1.A. 4b	Log ($Cu_{solution}$) ($\mu g.L^{-1}$)	-0.45	0.77		-0.62 (%)	0.65		0.42	74	5.7-141	1.8-20.4	4.3-8.1
(Sauvé et al., 1997)	II.1.A. 5a	Log ($Cu_{solution}$) ($\mu g.L^{-1}$)	13.2 (±7.9)	0.32 (±0.01)					0.89	66	14-3083	4.1-554.6	3.3-7.6

(Sauvé et al., 2000)	II.1.A. 6a	Log ($Cu_{solution}$)	1.37 (±0.14)	0.931 (±0.05)	-0.21 (±0.02)	-0.21[1] (±0.02)			0.611	353			2-9
(Luo et al., 2006b)	II.1.A. 7a	Log ($Cu_{solution}$) (µg.L-1)	1.21 (±0.45)	0.32 (±0.16)		1.08 (±0.33) (%)			0.32	39	280-1752		5.3-7.61
	II.1.A. 7b	Log ($Cu_{solution}$) (µg.L^{-1})	2.08 (±0.11)			1.33 (±0.32) (%)			0.38	39	280-1752		5.3-7.61
(Luo et al., 2006a)	II.1.A. 8a	Log ($Cu_{solution}$) (µg.L^{-1})	2.20 (±0.11)			0.88 (±0.28) (%)			0.205	40	280-1930	26-62	5.5-7.8
(Mondaca et al., 2015)	II.1.A. 9a	Log ($Cu_{solution}$) (µg.L^{-1})	0.69	0.5		0.73			0.36	86	56-4441	12.0-62	6.2-7.8
	II.1.A. 9b	Log ($Cu_{solution}$) (µg.L^{-1})	-1.01	0.75		0.95		1.23	0.70	86	56-4441	12.0-62	6.2-7.8
(Li et al., 2017)	II.1.A. 10a	Log ($Cu_{solution}$) (µmol.L^{-1})	-2.976	0.515				1.23	0.63	34			

[1.]Data expressed in percentage of C [2] Data expressed in mg Cu .kg soil

Table II.1.A.3. Transfer functions for (bio-)available Cu reviewed from literature for estimation of pCu (units in brackets). pCu = a $\log_{10}$Cutot + b $\log_{10}$OM + c $\log_{10}$clay + d $\log_{10}$pH +e. R.V is for response variable and e. for intercept. Total Cu is expressed in mg.kg^{-1}, OM in g.kg^{-1} or percentage (precision in the row), clay in percentage.

Source	Eq .	R.V	e	Log (Cu tot)	pH	Log (OM)	Log (CEC)	other	Log (clay)	R2	number of data	Range CuTot	Range OM g.kg	Range pH
(Lexmond, 1980)	11	pCu (mol L^{-1})	5.08	-2.38	1.07					0.989	16	10-400	16.8	3.9-6.2[b]
(McBride et al., 1997)	3d	pCu (µg L^{-1})	1.28	-1.95	1.37	1.95(g.kg^{-1})				0.897	70	17-2600		3.3-6.6
(McBride et al., 1997)	3e	pCu (µg L^{-1})	1.8	-1.1	1.6	1.8 (g kg-^{1})				0.91	10	6-1440	15-395	4.5-7.2
(Sauvé et al., 1997)	5b	pCu (µg L^{-1})	3.42 (±0.5)	-1.7 (±0.12)	1.4 (±0.08)					0.848	66	14-3083	4.1-554.6	3.3-7.6
(Unamuno et al., 2009)	12a	Log (Cu^{2+}) (mg.kg^{-1})	-2.1		0.085				0.005	29	18-10389			
(Unamuno et al., 2009)	12b	Log (Cu^{2+}) (mg.kg^{-1})	-2.079	0.593	-0.053				0.73					

(Unamuno et al., 2009)	12c	Log (Cu^{2+}) ($mg.kg^{-1}$)	-2.259	0.594	-0.058	0.09 ($g.kg^{-1}$)			0.732	29	18-10389			
(Vulkan et al., 2000)	13a	pCu ($\mu g.L^{-1}$)	-0.53	-1.47	1.79					0.89	22	19.4-8645	98-698	5.5-8
(Tipping et al., 2003)	14a	pCu ($\mu g.kg^{-1}$)	-1.34	-0.54 ($\mu mol.g^{-1}$)	1.15	0.40 (%)				0.94	98		100-1000	
(Tipping et al., 2003)	14b	pCu ($\mu g.kg^{-1}$)	-5.35	-1.09 ($\mu mol.g^{-1}$)	1.17	0.52 (%)				0.87	165			
(Lofts et al., 2004)	15	pCu(nM)	-4.99	-0.93	1.26	0.63(%)				0.9	151	0.96-637	0.41-97.8	3.35-8.27
(Luo et al., 2006b)	7b	pCu ($\mu g.L^{-1}$)	-2.24 (±0.96)		1.47 (±0.14)					0.76	39	280-1752		5.3-7.61
(Groenenberg et al., 2010)	16	pCu ($mol.L^{-1}$)	0.48	0.81	-1	-0.89 (%)			0.83	216	0.6-326	2-97.8		3.3-8.3
(Mondaca et al., 2015)	9c	pCu ($\mu g\ L^{-1}$)	5.54	-0.74	0.67	0.75(%)				0.58	86	56-4441	12.0-62	
(Li et al., 2017)	10b	pCu ($mol.L^{-1}$)	-4.303	-1.639	1.171					0.65	34			

(Li et al., 2017)	10c	pCu (mol.L^{-1})	-0.783	-1.6 (Cu solution, µg L^{-1})	1.3 log					0.65	34			

a. pH in the resin extraction ; b. pH in soil solution determined by $CaCl_2$; c. Al_{ox} and Fe_{ox} are respectively aluminum and iron oxydes

$^{0.85}$ with [Cu] in mol respectively per kg en per liters.

Table 4: Deciles of concentration for total soil Cu contents (mg.kg^{-1}), Cu in solution (µg L^{-1}) and free Cu (mg kg^{-1}), also expressed as pCu (-log(freeCu))

decile	0.00	0.01	0.05	0.10	0.15	0.20	0.25	0.40	0.50
total Cu	0.81	3.44	5.03	6.25	7.23	8.08	8.89	11.36	13.21
Cu solution	0.20	0.68	1.01	1.26	1.45	1.63	1.83	2.63	3.36
pCu	-2.01	-0.78	-0.45	-0.28	-0.15	-0.04	0.07	0.49	0.78
free Cu	9.48 E-05	0.001	0.003	0.006	0.010	0.017	0.028	0.085	0.165

decile	0.60	0.70	0.75	0.8	0.90	0.95	0.99	1.00
total Cu	15.35	17.94	19.56	21.65	28.38	36.8	28.38	129.95
Cu solution	4.17	5.08	5.64	6.33	8.49	10.71	15.60	45.05
pCu	1.07	1.38	1.56	1.77	2.25	2.58	3.14	4.02
free Cu	0.324	0.636	0.845	1.095	1.892	2.823	5.965	101.771

3.1.2. Selection of the empirical equation to build the bio-available Cu map

Considering that bio-available Cu can be approximated by the content of free Cu in solution, we gathered the equations predicting pCu (= - $\log_{10}[Cu^{2+}]$) from literature which are reported in table II.1.A.3. We took into account an important parameter when comparing the equations, specified in table II.1.A.1: the fact that bio-available Cu is experimentally measured or theoretically predicted by speciation software. Ten studies were based on measurements and six on modelling. In all the resulting empirical equations pCu is negatively correlated to total soil Cu content and positively correlated to pH and OM. This means that there are more bio-available Cu when the total soil Cu content is high and when the soil organic content is low. Interestingly, in almost all the empirical equations with pCu, the parameters associated to pH and total Cu coefficients are roughly of equal importance. On the contrary, the parameters associated to total Cu are from 4 to 40 times more important than that of pH in relationships to calculate available Cu.

McBride et al., (1997) and Tipping et al., (2003) reported the most commonly used equations to determine free Cu. Their regressions were based respectively on 70 (Table II.1.A.3 eq. II.1.A.3d, 3e) and 165 samples (Table II.1.A.3 eq. II.1.A.14a, 14b.) from long term contaminated soils with a large range of contamination going up to 3000 mgCu.kg soil $^{-1}$. It is important to note that the two studies used the same data set than that of Sauvé et al., (1997) for the eq. II.1.A.5b (Table II.1.A.3). McBride et al (1997) built their regression on the 70 data of Sauvé et al., (1997) with inclusion of pH, total Cu and OM. This last parameter was excluded by Sauvé et al., (1997) in the equation they proposed (eq. II.1.A.5b) because it was shown to be strongly related to soil Cu content. Tipping et al. (2003) proposed an equation using an extension of the Sauvé's dataset adding 98 points from moorland soils (table II.1.A.3, Eq. II.1.A.14b). They also provided an empirical equation restricted on the moorland soils

(table II.1.A.3 eq. II.1.A.14a) which can be particularly useful for soils with high OM contents, this parameter been found to significantly impact Cu availability and equation's parameter values. Finally, we chose to use the equation 14b from Tipping et al., (2003) since it was based on the largest dataset and the pCu data were measured and not estimated using a mechanistic model.

3.2. Application to Europe mapping

3.2.1. Selected regression and computed maps

The total Cu concentration in the LUCAS databased provided by the JRC varied from 1 to 130 mg Cu kg soil^{-1} with most (75%) of the values below 20 mg Cu kg soil^{-1} and 99.9% below 52mg Cu kg^{-1} (table II.1.A.4, fig. II.1.A.1). With the definition of geochemical baselines as values in the range of median ± two times the average deviation (Reimann et al., 2005), we considered that 1.5% of the soils are over-concentrated with a total soil Cu content >28mg.kg-^{1}, and none being depleted. The range of risk index for total Cu was RI $_{total}$ [-94% - 883%]. Roughly, 25 % of the grid points had RI $_{total}$ >50% meaning with a total soil Cu content higher than two times the median European value. Furthermore, less than 10% of the grid points had RI $_{total}$ >100% and around 10% of the grid points had RI $_{total}$ < -50% (suppl table II.1.A.2).

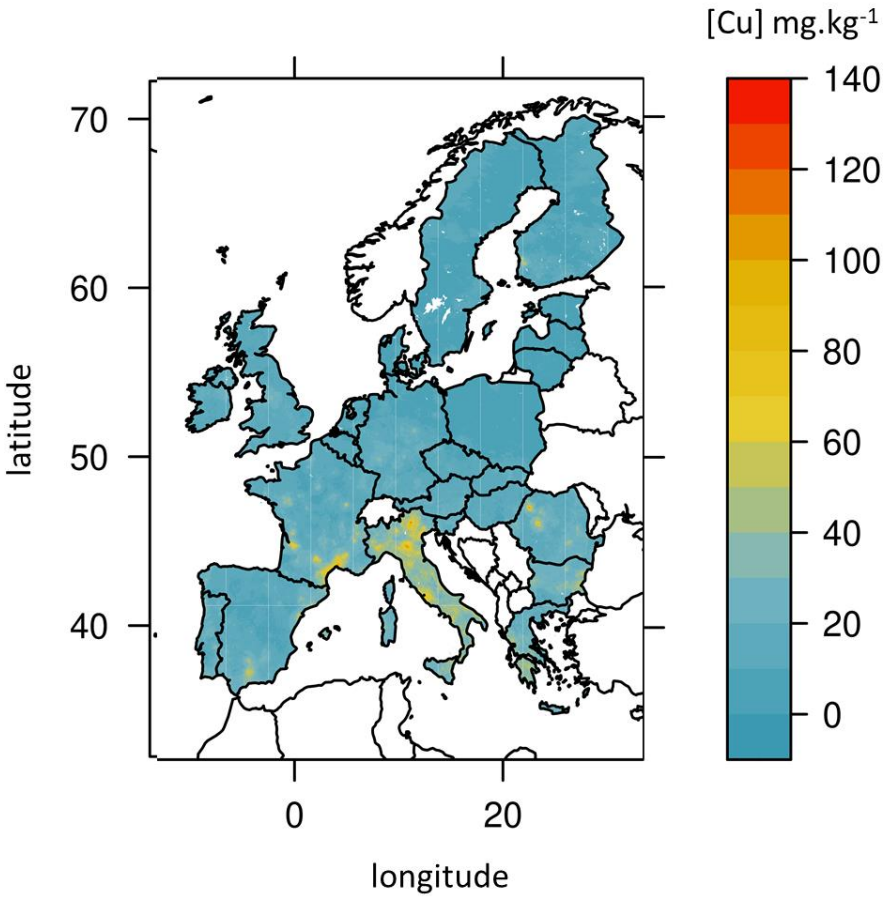

Fig II.1.A.2: European map of total Cu in soils (mg.Cu. kgsoil^{-1}) after conversion at 0.01°, using the data from the JRC, extracted from https://esdac.jrc.ec.europa.eu/content/copper-distribution-topsoils (Ballabio et al., 2018)

Based on the choice of transfer functions and the data provided by the JRC, we calculated and edited two different maps at the European union scale: one of the available Cu based on the McBride et al, (1997) estimation (eq. II.1.A.3b) to derive available Cu in solution (fig II.1.A.3) and one of the bio-available Cu based on the Tipping et al., (2003) regression to derive pCu (eq. II.1.A.n°14b) (fig II.1.A.4).

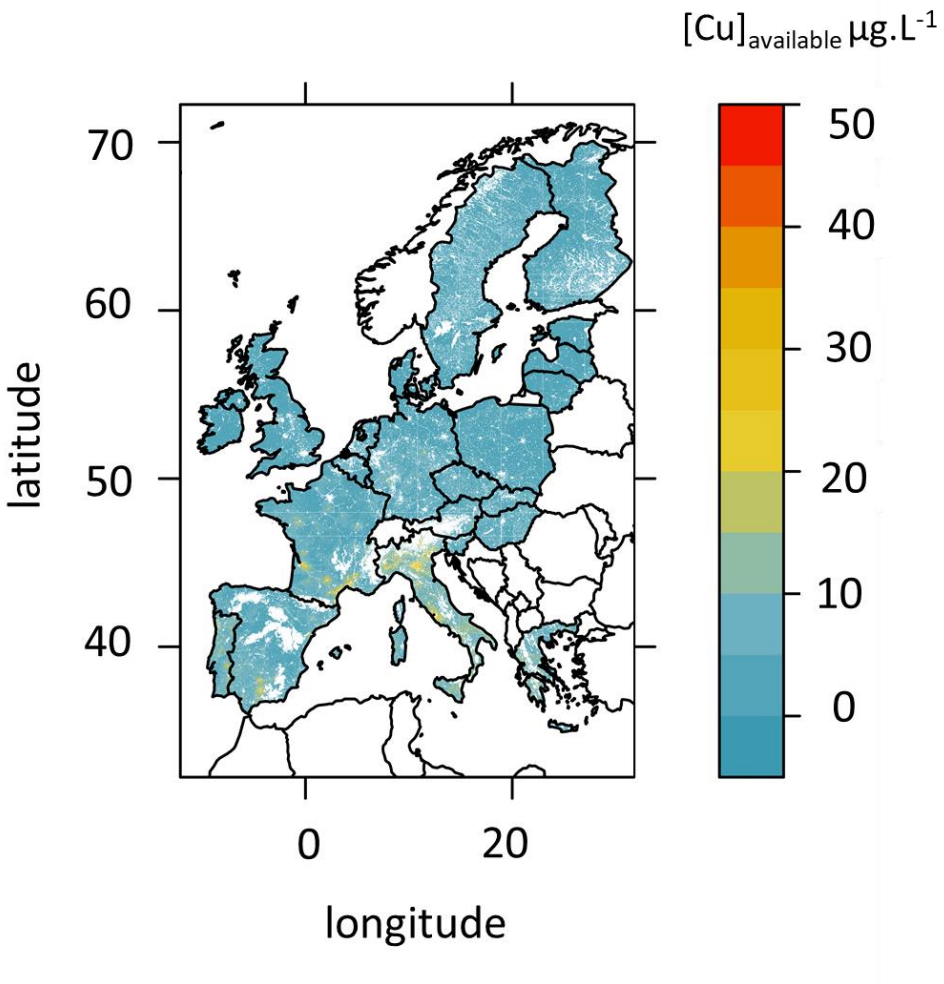

Fig II.1.A.3.: European map of available Cu (taken Cu contents in soil solution as a proxy in µg.L-1) at 0.01°estimated using the empirical equation of McBride et al (1997) (eq. II.1.A. 3b, table II.1.A.2) and the map of total Cu (fig II.1.A.2) with pH and Corga provided by the JRC. Lat and lon refers to latitude and longitude, while vertical color scale is for available Cu concentrations ($\mu g.L^{-1}$).

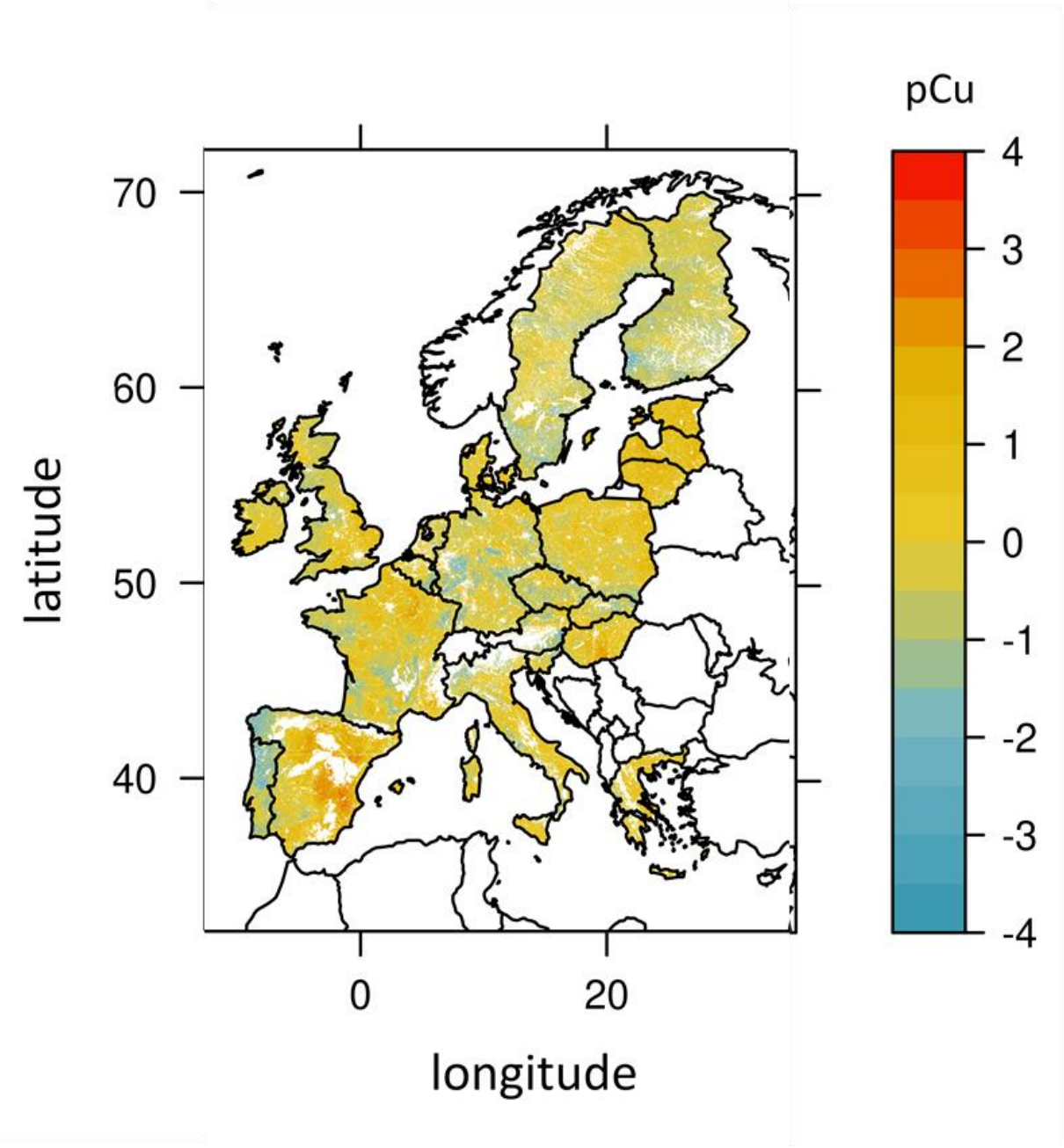

Fig. II.1.A.4. European map of bio-available Cu (taken free Cu contents in soil solution as a proxy expressed in term of pCu) at 0.01° based on Tipping's et al (2003) empirical equation (eq. II.1.A.14b, table II.1.A.3) and the map of total Cu, and with pH and Corga provided by the JRC. Lat and lon refers to latitude and longitude, while vertical scale is for bio-available Cu concentration expressed in pCu = -log[Cu^{2+}].

Due to the lack of Corga measurements in mountain soils, there is part of the European territory without estimation of available Cu. Estimation of available Cu varied from 0.2 to 45 µg Cu L^{-1} with 75% of the values below 5.6 µg Cu L^{-1} and 99% below 15 µg Cu L^{-1} (table II.1.A.4). With the definition of geochemical baselines as values in the range of median ± two times the average deviation (Reimann et al., 2005), 10.% of the soils are considerate as over-concentrated with available Cu > 8.5 µg Cu L^{-1} and none are considered as depleted.

Bio-available Cu varies from 1.79 *10^{-9} to 0.002 mg Cu kg^{-1} with 75% of the values below 2.80 10^{-5} mgCu.kg^{-1} and 99% below 1.80 10^{-4}mg Cu kg^{-1} (table II.1.A.4). 1.87% of the grid points have bio-available Cu defined as below the geochemical baseline and 0.01% above.

An area of high concentration for one form of Cu is not systematically highly concentrated if we considered another Cu form. For instance, the region with higher bio-available Cu (pCu <-0.4, 95% decile, in North West Spain or Austria) have total Cu ranging from 2.2 (<1% decile) to 90 mg Cu kg^{-1} soil (99% decile) and available Cu from 0.6 (1% decile) to 35.6 µg Cu L^{-1} (>99% decile) (suppl. table II.1.A.1). In this example, high bio-available Cu is linked to low total Cu or low available Cu, highlighting that the three proxies do not necessarily follow the same pattern.

3.2.2. Spatialization of available Cu risks and comparison of risk index with the total Cu map

The range of variations compared to the median values are similar between total Cu and available Cu (suppl. Table II.1.A.2 and II.A.3). For available Cu, the range of $RI_{available\ Cu}$ is [- 94% to 1241 %]. Roughly, 30% of the grid points had $RI_{available\ Cu}$ > 50%, 10% had $RI_{available\ Cu}$ > 150% , and 20% had $RI_{available\ Cu}$ < -50% (suppl table II.1.A.3). Total Cu and available Cu show similar pattern of highest/lowest concentrations (suppl. Fig. II.1.A.4 and II.1.A.5). Highest concentrations are mostly found in Eastern Europe, South of Spain, Portugal, parts of West France and of England but there are also some small areas in North West of Norway and South of Sweden (fig. II.1.A.2 and II.1.A.3).

The comparison between $RI_{available\ Cu}$ and RI_{total} is shown in fig II.1.A.5. This map highlights important differences in risk consideration. Only 6.0% of the grid points fitted with situation 1 as described in the material and method section, indicating that the risk assessment based on total Cu may be overestimated compared to the risk assessment based on available Cu. Indeed, we have $RI_{total} >> RI_{available\ Cu}$ for 5.3 % of the grid points (case 1A) and opposite signs with positive $RI_{total\ Cu}$ for 0.7% of the grid points (case 1B). This was mainly assessed for Ireland, North West of Norway, and South of Finland and for isolated points in Germany. More grid points (19.6 %) fitted the situation 2, indicating that risk assessment based on total Cu is underestimated compared to risk assessment based on available Cu. Indeed, we have $RI_{total} << RI_{available\ Cu}$ for 10.7% of the grid points (case 2A) and $RI_{total\ Cu}<0$ but $RI_{available\ Cu}>0$ for 8.9% of the grid points (case 2B). These situations mostly occurred in central Spain, central France and North East Germany, south Spain, Italy and central East Europe. Comparable RI for total and for available Cu (see situation 3 in paragraph 2.3) were mostly found in Scandinavia, Brittany (France), Germany, and central Italy. As a consequence, 25.6% of the grid points present discrepancies when risk assessment is based on total Cu or based on available Cu.

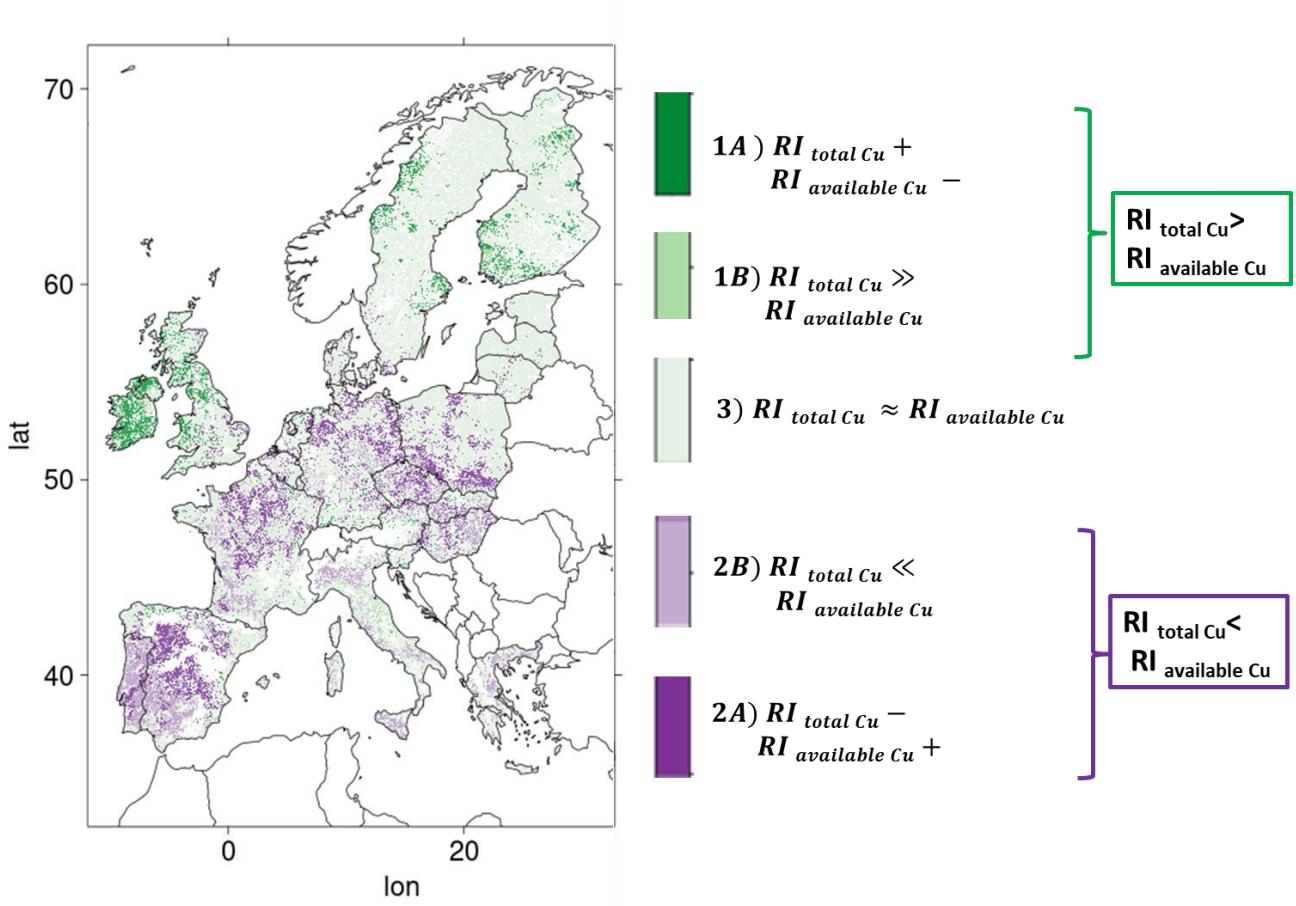

Fig. II.1.A.5: Map of risk assessment showing the comparison between total and available Cu at 0.01° based on the RI $_{\text{total Cu}}$ and RI $_{\text{available Cu}}$ following the 5 cases defined in the material and method section 2.3. from purple meaning an underestimation of risk based on total rather to available Cu to green meaning an overestimation of risk based on total rather than to available Cu

3.2.3. Spatialization of bio-available Cu risks and comparison of risk index with the total Cu map

The computed map of bio-available Cu expressed as pCu is given in fig II.1.A.4. This map differs from the map of total Cu (fig. II.1.A.2) and that of available Cu (fig. II.1.A.3) with hotspots in Galicia (North West of Spain), parts of West England, and Roma region but no other areas in Italy. Germany and West ex former Union present high bio-available Cu concentrations despite relatively low total Cu (figs II.1.A.2, II.1.A.4). High bio-available Cu contents observed in West Iberian, Germany, and South Scandinavia coincide with areas of low pH and emphasize the strong dependency of bio-available Cu to pH. Indeed, because pH is high in the Adriatic coast of Italy and Lombardy, there are low bio-available Cu contents despite relatively high soil total Cu contents (Fig. II.1.A.2, II.1.A.4 and suppl. Fig. II.1.A.2). The range of variations in bio-available Cu are largest than the variations in total or in available Cu with RI $_{\text{bio-available Cu}}$ varying from [-99.9% to 61679 %]. Moreover, numerous grid-points are far from the median. Indeed, RI $_{\text{bio-available Cu}}$ was < -58% for 40% of the grid points and RI $_{\text{bio-available Cu}}$>1000% for more than 10% of the grid points. For 1% of the grid points, mostly in West Iberia, RI $_{\text{bio-available Cu}}$ was > 3520% (suppl table II.1.A.4). Areas of RI $_{\text{bio-available Cu}}$ are much narrowed than those of RI $_{\text{available Cu}}$, so that central and East Spain, center West of France and North-East coast of Italy would be under- rather than over-concentrated in bio-available Cu. Besides, large parts of Scandinavia have high levels of bio-available Cu (suppl fig. II.1.A.4)

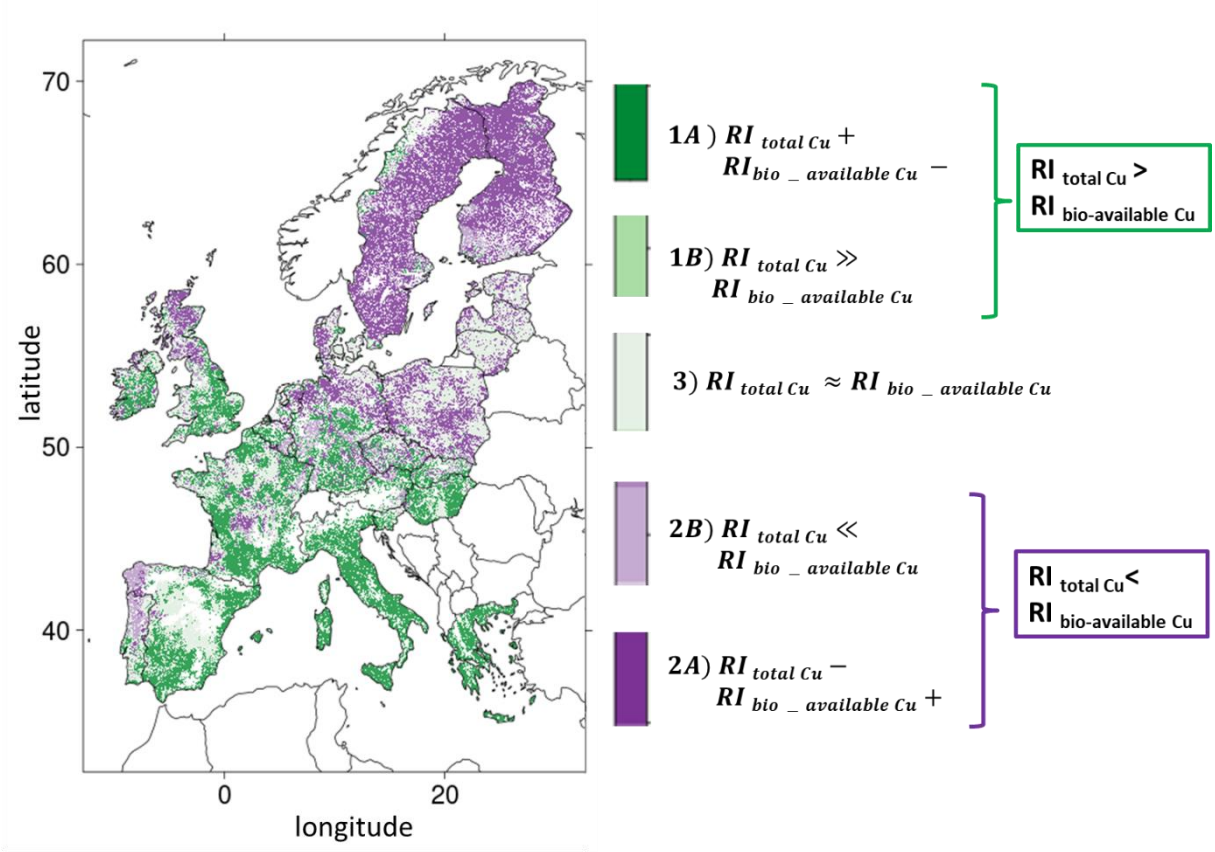

Fig. II.1.A.6: Map of risk assessment showing the comparison between the $RI_{total\ Cu}$ and $RI_{bio\text{-}available\ Cu}$ following the 5 cases defined in the material and method section 2.3, from purple meaning an underestimation of risk based on total rather to bio-available Cu to green meaning an overestimation of risk based on total rather than to bio-available Cu

The comparison of $RI_{bio\text{-}available\ Cu}$ with RI_{total} in fig II.1.A.6 shows important differences in risk consideration. 28.9% of the grid points fitted with situation 1, indicating that the risk assessment based on total Cu may be overestimated compared to the risk assessment based on bio-available Cu. Almost all of this 28.9% of the grid-points have $RI_{total\ Cu} > 0$ but $RI_{bio\text{-}available\ Cu} < 0$ (case 1A. in paragraph 2.3). On the contrary, 39.5 % of the grid points fitted with case 2 indicating that the risk assessment based on total Cu may be underestimated compared to the risk assessment based on bio-available Cu. In details, 34.3% of the grid points have $RI_{total\ Cu} < 0$ but $RI_{available\ Cu} > 0$ (case 2A in paragraph 2.3) and 5.2% $RI_{total} << RI_{available\ Cu}$ (case 2B). These situations mostly occur in Scandinavia, West Iberian Peninsula and North of Central Europe. Comparable RI for total and for bio-available Cu (situation 3 in paragraph 2.3) were mostly found in central Spain, Poland, Czech Republic or Slovakia. Therefore, 68.4% of the grid points present discrepancies when risk assessment is based on total Cu instead of bio-available Cu.

4. Discussion

4.1. Generic purpose of empirical equations

The present study was mostly focused on the determination of the available Cu pool (assimilated to the Cu content in solution) and of the bio-available Cu pool (assimilated to the free Cu content in

solution). We showed that the collected empirical equations were defined on measurements based on different extractions procedures for available Cu. Besides site-specific properties, the differences in experimental procedures can explain the differences in fitted coefficients. There is, however, a good agreement between studies in their selection of variables considering pH, total soil Cu, soil OM, DOC, or clay as key variables to predict (bio)available Cu. In fact, pH was found to be the most important predictor with 24 empirical equations involving all the forms of Cu (dissolved or free) using pH as a predictor followed by OM and total Cu, whereas CEC or clay were more rarely found as predictors of interest. The importance of pH in cation partitioning is well recognized (Buchter et al., 1989; Flemming and Trevors, 1989; Sauvé et al., 2000a) and the effect of pH can be explain with a semi mechanistic approach which assumes that free cation such as Cu^{2+} and H^{+} compete for adsorption on carbonates or OM (Basta et al., 1993; Harter and Naidu, 1995; (McBride et al., 1997; Bradl, 2004). The relative weight of OM, pH or total Cu in empirical equations were however different between equations for available Cu or for bio-available Cu (table II.1.A.2, 3). Indeed, the log of available Cu increases of roughly 1 unit per unit of increase in total Cu or per 5 units of decrease in pH while bio-available Cu (pCu) decreases of roughly 1 unit per unit of increase in log of total Cu or per unit of decrease in pH. Thus, due to the low pH in North Spain, Norway, Germany and West England, bio-available Cu is particularly high (i.e. with low pCu values) in these regions despite low total Cu contents (around 10 mg.kg soil $^{-1}$).

Our results are consistent with the competition between H^{+} and Cu^{2+} for sorption onto soil OM only in the case of available Cu, but for sorption onto both soil OM and DOC in the case of bio-available Cu. However, cation availability cannot be limited to a first order relationship of binding with organic matter because the decrease in available Cu in solution with the increase in pH involves different processes. For instance, above pH 7.7 most of Cu in solution is expected to be found as $Cu(OH)_2$ and is about to precipitate (Ma et al., 2006b) ; on the other hand studies found that between pH=4.5 and 7.7 Cu would be retained by ferric hydroxide coated sands (Al-Sewailem et al., 1999). The aim of the empirical equations we collected here was to provide generic equations valid over a wide range of parameters for application at a large scale (Cavallaro and McBride, 1978) despite these different processes. Thus, apart complete speciation models which require numerous parameters like dissolved organic matter form, some equations as those provided by Römkens et al., (2004) complete the classical parameters by Fe or Al oxydes content. In their study the improvement is however limited (r2 from 0.65 to 0.66 when adding Fe and Al oxydes) which suggests punctual outliers rather than generic predictor. On the contrary, the good fit of new coefficients of empirical equations based on restricted number of predictors (pH, total Cu, soil OM) selected by other studies (Lofts et al., 2004) confirm their genericity and suggest that they can be extrapolated to different sites and then used for upscaling to Europe maps.

4.2. What is the usefulness of using Cu in solution or free Cu to characterize risk assessment?

Our results show a large variability in Europe considering all the forms of Cu. For both available and bio-available Cu, we identified patterns of high concentrations at the regional scale. However, in both cases the 1% points that are more concentrated were isolated rather than regionally located, suggesting hot spots. For available Cu, these most concentrated grid points were mostly in North Italy and South East of France but we could not precisely delimitate an area of concern. For bio-available Cu these local hot spots were rather in Austria, North Spain and in South-West Finland. The total Cu survey performed by the JRC (Ballabio et al., 2018) identified that Nomenclature of Territorial Units 2 (NUTS 2, regional scale) was one of the most determinant factor to explain total Cu concentration at

the European scale. Thus, wine producing regions have globally high Cu concentration because of the use of “bouillie Bordelaise” for vineyards, but environmental guidelines of each local administration also limit total Cu concentration. In our study, we found that co-factors like soil OM and pH largely affect Cu availability even at a large scale, and that pH was in equal importance than total Cu to explain bio-available Cu variations. In addition, areas like Scandinavia with moderate total Cu but low pH exhibit high bio-available Cu values so that the associated risk is higher with this last proxy.

Besides, with the assumption that Cu in solution could be exported through runoff to downstream ecosystem, amount of rainfall would be of major importance to consider risk at both local and regional scale (Lefrancq et al., 2014; Xu et al., 2014). Most of the areas with high concentrations of available or bioavailable Cu are located around the Mediterranean Sea, where summer are usually dry with intense thunderstorms and cold and wet winters. Climatic scenario forecast a global decrease in precipitation in these regions, but also that rainfall events will be more intense (Christensen and Christensen, 2003; Giorgi and Lionello, 2008). Thus, if the average export could decrease with a decrease in rainfall, flushes of higher intensities coupled with erosion could arise (Imfeld et al., 2020; van der Knijff et al., 2000). Thus, a new question we may answer is the availability of Cu in the retention ponds where concentrations will increase due to upstream exports. In parallel, we found that bio-available Cu was particularly high in Portugal and Scandinavia where climatic prevision forecasts particularly a high temperature rise, drought for Portugal and higher rainfall patterns for Scandinavia (Christensen and Christensen, 2003). These modifications in climate may thus affect plants and soil micro-organisms to the Cu stress and affect their response to soil Cu (J. Li et al., 2017; Tobor-Kapłon et al., 2006). Here we highlighted that contamination assessment based on total Cu differs from the assessment based on (bio-)available Cu, even at the regional scale. Thus, it might help to take into account the expected climate change to gain in robustness when assessing the evolution of soil contamination.

4.3. Are contaminated soils at equilibrium?

The equations we reviewed here were mostly constructed on data from long term contaminated soils where Cu species were supposed to be in field at equilibrium. However, in this study, we used total Cu data acquired during field campaigns without precision on the temporality of the Cu inputs nor on the delay after Cu applications. But several studies show that extractability of Cu decreases with time after addition of Cu due to a so-called “ageing process” (Oorts et al., 2006a; Tom-Petersen et al., 2004). To take into account the time after contamination in Cu solubilization, kinetic descriptions of Cu availability have emerged (Ma et al., 2006a, 2006b; Zeng et al., 2017). These studies fishowed that not only the final distribution of Cu but also the kinetics of availability also depend on soil factors. Two different kinetics were identified. One concerns a rapid diffusion of Cu (from minutes to month) mostly controlled by diffusion processes and associated nucleation - precipitation –which will rather depend on soil structure (Ma et al., 2006a; Zeng et al., 2017). The second concerns a slow diffusion of Cu (months to decades) also controlled by the temperature, the pH and soil OM with a faster decrease in availability (e.g. less Cu in soil solution) at higher pH or higher OM (Ma et al., 2006b; Zeng et al., 2017). The soils with low OM contents or low pH are hence not only the more prone to exhibit the highest (bio)-available Cu, but they are also the more prone to exhibit it longer (months rather than days or week) after contamination. Thus, in the case of regular Cu input the (bio-)available Cu amounts might be higher than estimated in the present study due to non-equilibrium after contamination.

.

5. Conclusion

In this study, we reviewed the empirical equations to estimate available and bio-available Cu from soil total Cu and pedological factors currently measured. On the basis of 29 equations, our results emphasize the dependence of available Cu to pH but also that bio-available Cu is much more dependent on pH than available Cu. We highlighted similarities as well as differences between areas of risks regarding three different metrics. Areas with a high level of total Cu and high risks of available Cu were more similar than those with bio-available Cu. Indeed, around 74% of the grid points exhibited comparable risks in term of either total or available Cu against 31.5% of the grid points exhibiting comparable risks in term of either total or bio-available Cu. Besides, at the europen scale, some regions that classified without risk regarding their total Cu concentration may in turn be considered at risk considering available Cu or considering bio-available Cu. Our results show that about 20% of the grid points may be concerned by an underestimation of risk regarding total Cu against available Cu and 39% may be concerned by an underestimation of risk regarding total Cu against bio-available Cu. These areas are non-negligible and underlined the need to estimate with risks with regard to a specific effect, in our case biological or environmental availability.

Acknowledgments : the author thank the LabeX BASC for its funding through the CONNEXION project. Laura Sereni also thanks the ENS for her grant.

Ethical Approval: this paper has no ethical issue (not working on animal or human issues)

Consent to Participate: all authors consent to participate to this scientific publication done with the results of the study performed within the framework of the CONNEXION project funded by the Agence National de la Recherche

Funding: the study was found by the Agence Nationale de la Recherche with the LabEx BASC (ANR-11-LABX-0034) and the CONNEXION project.

The datasets generated and analyzed during the current study are available in the DataINRAe repository, https://data.inrae.fr/dataset.xhtml?persistentId=doi:10.15454/OWI8JR

References

Al-Sewailem, M.S., Khaled, E.M., Mashhady, A.S., 1999. Retention of copper by desert sands coated with ferric hydroxides. Geoderma. https://doi.org/10.1016/S0016-7061(98)00082-2

Azimi, S., Cambier, P., Lecuyer, I., Thevenot, D., 2004. Heavy metal determination in atmospheric deposition and other fluxes in northern France agrosystems. Water. Air. Soil Pollut. 157, 295–313. https://doi.org/10.1023/B:WATE.0000038903.25700.5a

Ballabio, C., Lugato, E., Fernández-Ugalde, O., Orgiazzi, A., Jones, A., Borrelli, P., Montanarella, L., Panagos, P., 2019. Mapping LUCAS topsoil chemical properties at European scale using Gaussian process regression. Geoderma. https://doi.org/10.1016/j.geoderma.2019.113912

Ballabio, C., Panagos, P., Lugato, E., Huang, J.H., Orgiazzi, A., Jones, A., Fernández-Ugalde, O., Borrelli, P., Montanarella, L., 2018. Copper distribution in European topsoils: An assessment based on LUCAS soil survey. Sci. Total Environ. 636, 282–298. https://doi.org/10.1016/j.scitotenv.2018.04.268

Ballabio, C., Panagos, P., Monatanarella, L., 2016. Mapping topsoil physical properties at European scale using the LUCAS database. Geoderma. https://doi.org/10.1016/j.geoderma.2015.07.006

Basta, N.T., Pantone, D.J., Tabatabai, M.A., 1993. Path analysis of heavy metal adsorption by soil. Agron. J. https://doi.org/10.2134/agronj1993.00021962008500050018x

Bradl, H.B., 2004. Adsorption of heavy metal ions on soils and soils constituents. J. Colloid Interface Sci. https://doi.org/10.1016/j.jcis.2004.04.005

Buchter, B., Davidoff, B., Amacher, M.C., Hinz, C., Iskandar, I.K., Selim, H.M., 1989. Correlation of Freundlich Kd and n retention parameters with soils and elements. Soil Sci. https://doi.org/10.1097/00010694-198911000-00008

Carlon, C., 2007. Derivation methods of soil screening values in europe. a review and evaluation of national procedures towards harmonisation, JRC Scientific and Technical Reports. https://doi.org/EUR 22805_EN

Cavallaro, N., McBride, M.B., 1978. Copper and Cadmium Adsorption Characteristics of Selected Acid and Calcareous Soils1. Soil Sci. Soc. Am. J. 42, 550. https://doi.org/10.2136/sssaj1978.03615995004200040003x

Christensen, J.H., Christensen, O.B., 2003. Severe summertime flooding in Europe. Nature 421, 805–806. https://doi.org/10.1038/421805a

de Brogniez, D., Ballabio, C., Stevens, A., Jones, R.J.A., Montanarella, L., van Wesemael, B., 2015. A map of the topsoil organic carbon content of Europe generated by a generalized additive model. Eur. J. Soil Sci. https://doi.org/10.1111/ejss.12193

Degryse, F., Smolders, E., Parker, D.R., 2009. Partitioning of metals (Cd, Co, Cu, Ni, Pb, Zn) in soils: concepts, methodologies, prediction and applications - a review. Eur. J. Soil Sci. 60, 590–612. https://doi.org/10.1111/j.1365-2389.2009.01142.x

Flemming, C.A., Trevors, J.T., 1989. Copper toxicity and chemistry in the environment: a review. Water. Air. Soil Pollut. 44, 143–158. https://doi.org/10.1007/BF00228784

Garcia, C., Moreno, J.L., Hernandez, T., Bastida, F., 2017. Soils in arid and semiarid environments: The importance of organic carbon and microbial populations. Facing the future. Biol. Arid Soils 15–29. https://doi.org/10.1515/9783110419047-002

Giorgi, F., Lionello, P., 2008. Climate change projections for the Mediterranean region. Glob. Planet. Change 63, 90–104. https://doi.org/10.1016/j.gloplacha.2007.09.005

Groenenberg, J.E., Römkens, P.F.A.M., Comans, R.N.J., Luster, J., Pampura, T., Shotbolt, L., Tipping, E., De Vries, W., 2010. Transfer functions for solid-solution partitioning of cadmium, copper, nickel, lead and zinc in soils: Derivation of relationships for free metal ion activities and validation with independent data. Eur. J. Soil Sci. 61, 58–73. https://doi.org/10.1111/j.1365-2389.2009.01201.x

Harter, R.D., Naidu, R., 1995. Role of Metal-Organic complexation in metal sorption by Soils. Adv. Agron. https://doi.org/10.1016/S0065-2113(08)60541-6

Hong, S., Candelone, J.P., Soutif, M., Boutron, C.F., 1996. A reconstruction of changes in copper production and copper emissions to the atmosphere during the past 7000 years. Sci. Total Environ. https://doi.org/10.1016/0048-9697(96)05171-6

Imfeld, G., Meite, F., Wiegert, C., Guyot, B., Masbou, J., Payraudeau, S., 2020. Do rainfall characteristics affect the export of copper, zinc and synthetic pesticides in surface runoff from headwater catchments? Sci. Total Environ. 741, 140437. https://doi.org/10.1016/j.scitotenv.2020.140437

ISO, 2006. Soil quality- Extraction of trace elements soluble in aqua regia. 61010-1 © Iec2001 2006, 13.

Jensen, D.Læ., Ledin, A., Christensen, T.H., 1999. Speciation of heavy metals in landfill-leachate polluted groundwater. Water Res. 33, 2642–2650. https://doi.org/10.1016/S0043-1354(98)00486-2

Kinniburgh, D.G., Milne, C.J., Benedetti, M.F., Pinheiro, J.P., Filius, J., Koopal, L.K., Van Riemsdijk, W.H., 1996. Metal ion binding by humic acid: Application of the NICA-Donnan model. Environ. Sci. Technol. https://doi.org/10.1021/es950695h

Kördel, W., Bernhardt, C., Derz, K., Hund-Rinke, K., Harmsen, J., Peijnenburg, W., Comans, R., Terytze, K., 2013. Incorporating availability/bioavailability in risk assessment and decision making of polluted sites, Using Germany as an example. J. Hazard. Mater. 261, 854–862. https://doi.org/10.1016/j.jhazmat.2013.05.017

Lanno, R., Wells, J., Conder, J., Bradham, K., Basta, N., 2004. The bioavailability of chemicals in soil for earthworms, in: Ecotoxicology and Environmental Safety. https://doi.org/10.1016/j.ecoenv.2003.08.014

Lefrancq, M., Payraudeau, S., García Verdú, A.J., Maillard, E., Millet, M., Imfeld, G., 2014. Fungicides transport in runoff from vineyard plot and catchment: Contribution of non-target areas. Environ. Sci. Pollut. Res. 21, 4871–4882. https://doi.org/10.1007/s11356-013-1866-8

Lexmond, T.M., 1980. The effect of soil pH on copper toxicity to forage maize grown under field conditions. Netherlands J. Agric. Sci. 28, 164–184. https://doi.org/10.18174/njas.v28i3.17030

Li, B., Ma, Y., Yang, J., 2017. Is the computed speciation of copper in a wide range of Chinese soils reliable? Chem. Speciat. Bioavailab. 29, 205–215. https://doi.org/10.1080/09542299.2017.1404437

Li, J., Liu, Y.R., Cui, L.J., Hu, H.W., Wang, J.T., He, J.Z., 2017. Copper Pollution Increases the Resistance of Soil Archaeal Community to Changes in Water Regime. Microb. Ecol. https://doi.org/10.1007/s00248-017-0992-0

Lofts, S., Spurgeon, D.J., Svendsen, C., Tipping, E., 2004. Deriving soil critical limits for Cu, Zn, Cd, and Ph: A method based on free ion concentrations. Environ. Sci. Technol. 38, 3623–3631. https://doi.org/10.1021/es030155h

Ma, Y., Lombi, E., Nolan, A.L., McLaughlin, M.J., 2006a. Short-term natural attenuation of copper in soils: Effects of time, temperature, and soil characteristics. Environ. Toxicol. Chem. 25, 652–658. https://doi.org/10.1897/04-601R.1

Ma, Y., Lombi, E., Oliver, I.W., Nolan, A.L., McLaughlin, M.J., 2006b. Long-term aging of copper added to soils. Environ. Sci. Technol. 40, 6310–6317. https://doi.org/10.1021/es060306r

McBride, M., Sauvé, S., Hendershot, W., 1997. Solubility control of Cu, Zn, Cd and Pb in contaminated soils. Eur. J. Soil Sci. 48, 337–346. https://doi.org/10.1111/j.1365-2389.1997.tb00554.x

Ministry of the Environment, F., 2007. Threshold and guideline values for harmful substances in soil. Gov. Decree Assess. Soil Contam. Remediat. Needs 6.

Minnich, M.M., McBride, M.B., 1987. Copper Activity in Soil Solution: I. Measurement by Ion-selective Electrode and Donnan Dialysis. Soil Sci. Soc. Am. J. https://doi.org/10.2136/sssaj1987.03615995005100030003x

Mondaca, P., Neaman, A., Sauvé, S., Salgado, E., Bravo, M., 2015. Solubility, partitioning, and activity of copper-contaminated soils in a semiarid region. J. Plant Nutr. Soil Sci. 178, 452–459. https://doi.org/10.1002/jpln.201400349

Nicholson, F.A., Smith, S.R., Alloway, B.J., Carlton-Smith, C., Chambers, B.J., 2003. An inventory of heavy metals inputs to agricultural soils in England and Wales. Sci. Total Environ. 311, 205–219. https://doi.org/10.1016/S0048-9697(03)00139-6

Oorts, K., Bronckaers, H., Smolders, E., 2006a. Discrepancy of the microbial response to elevated copper between freshly spiked and long-term contaminated soils, in: Environmental Toxicology and Chemistry. pp. 845–853. https://doi.org/10.1897/04-673R.1

Oorts, K., Ghesquiere, U., Swinnen, K., Smolders, E., 2006b. Soil properties affecting the toxicity of CuCl2 and NiCl 2 for soil microbial processes in freshly spiked soils, in: Environmental Toxicology and Chemistry. https://doi.org/10.1897/04-672R.1

Pampura, T., Groenenberg, J.E., Rietra, R.P.J.J., 2006. Comparison of methods for copper free ion activity determination in soil solutions of contaminated and background soils. For. Snow Landsc. Res. 80, 305–322.

Parker, D.R., Pedler, J.F., Ahnstrom, Z.A.S., Resketo, M., 2001. Reevaluating the free-ion activity model of trace metal toxicity toward higher plants: Experimental evidence with copper and zinc. Environ. Toxicol. Chem. https://doi.org/10.1002/etc.5620200426

Pribyl, D.W., 2010. A critical review of the conventional SOC to SOM conversion factor. Geoderma 156, 75–83. https://doi.org/10.1016/j.geoderma.2010.02.003

R Core Team, 2018. R software: Version 3.5.1. R Found. Stat. Comput. https://doi.org/10.1007/978-3-540-74686-7

Reimann, C., Filzmoser, P., Garrett, R.G., 2005. Background and threshold: Critical comparison of methods of determination. Sci. Total Environ. 346, 1–16. https://doi.org/10.1016/j.scitotenv.2004.11.023

Romkens, P.F.A.M., Bonten, L.T.C., Rietra, R.P.J.J., 2004. Copper leaching from soils: an inventory of available data and model concepts. Alterra 1–60.

Römkens, P.F.A.M., Groenenberg, J.E., Bonten, L.T.C., de Vries, W., Bril, J., 2004. Derivation of partition relationships to calculate Cd, Cu, Ni, Pb, Zn solubility and activity in soil solutions. Alterra 305, 75.

Salminen, R., Gregorauskiene, V., 2000. Considerations regarding the definition of a geochemical baseline of elements in the surficial materials in areas differing in basic geology. Appl. Geochemistry. https://doi.org/10.1016/S0883-2927(99)00077-3

Sastre, J., Sahuquillo, A., Vidal, M., Rauret, G., 2002. Determination of Cd, Cu, Pb and Zn in environmental samples: Microwave-assisted total digestion versus aqua regia and nitric acid extraction. Anal. Chim. Acta. https://doi.org/10.1016/S0003-2670(02)00307-0

Sauvé, S., Hendershot, W., Allen, H.E., 2000a. Solid-solution partitioning of metals in contaminated soils: Dependence on pH, total metal burden, and organic matter. Environ. Sci. Technol. 34, 1125–1131. https://doi.org/10.1021/es9907764

Sauvé, S., Hendershot, W., Herbert E., A., 2000b. Solid-Solution Partitioning of Metals in Contaminated Soils: Dependence on pH, Total Metal Burden, and Organic Matter. Am. Chem. Soc. 1125–1131. https://doi.org/10.1021/es9907764

Schulzweida, U., 2017. CDO User' s Guide. Guide 1–206.

Sébastien Sauvé, Murray B., M., Wendell A., N., William H., H., 1997. Copper Solubility and Speciation of In Situ Contaminated Soils: Effects of Copper Level, pH and Organic Matter. Water. Air. Soil Pollut. 100, 133–149.

Shabbir, Z., Sardar, A., Shabbir, A., Abbas, G., Shamshad, S., Khalid, S., Natasha, Murtaza, G., Dumat, C., Shahid, M., 2020. Copper uptake, essentiality, toxicity, detoxification and risk assessment in soil-plant environment. Chemosphere 259, 127436. https://doi.org/10.1016/j.chemosphere.2020.127436

Smolders, E., Oorts, K., Van Sprang, P., Schoeters, I., Janssen, C.R., McGrath, S.P., McLaughlin, M.J., 2009. Toxicity of trace metals in soil as affected by soil type and aging after contamination: Using calibrated bioavailability models to set ecological soil standards. Environ. Toxicol. Chem. https://doi.org/10.1897/08-592.1

Steven, B., 2017. An introduction to arid soils and their biology. Biol. Arid Soils 1–13. https://doi.org/10.1515/9783110419047-001

Thakali, S., Allen, H.E., Di Toro, D.M., Ponizovsky, A.A., Rooney, C.P., Zhao, F.J., McGrath, S.P., Criel, P., Van Eeckhout, H., Janssen, C.R., Oorts, K., Smolders, E., 2006. Terrestrial Biotic Ligand Model. 2. Application to Ni and Cu toxicities to plants, invertebrates, and microbes in soil. Environ. Sci. Technol. https://doi.org/10.1021/es061173c

Tipping, E., 1998. Humic ion-binding model VI: An improved description of the interactions of protons and metal ions with humic substances. Aquat. Geochemistry. https://doi.org/10.1023/A:1009627214459

Tipping, E., Rieuwerts, J., Pan, G., Ashmore, M.R., Lofts, S., Hill, M.T.R., Farago, M.E., Thornton, I., 2003. The solid-solution partitioning of heavy metals (Cu, Zn, Cd, Pb) in upland soils of England and Wales. Environ. Pollut. 125, 213–225. https://doi.org/10.1016/S0269-7491(03)00058-7

Tobor-Kapłon, M.A., Bloem, J., De Ruiter, P.C., 2006. Functional stability of microbial communities from long-term stressed soils to additional disturbance. Environ. Toxicol. Chem. https://doi.org/10.1897/05-398R1.1

Tom-Petersen, A., Hansen, H.C.B., Nybroe, O., 2004. Time and Moisture Effects on Total and Bioavailable Copper in Soil Water Extracts. J. Environ. Qual. https://doi.org/10.2134/jeq2004.5050

Tóth, G., Hermann, T., Szatmári, G., Pásztor, L., 2016. Maps of heavy metals in the soils of the European Union and proposed priority areas for detailed assessment. Sci. Total Environ. 565, 1054–1062. https://doi.org/10.1016/j.scitotenv.2016.05.115

USEPA, 2007. Microwave assisted acid digestion of sediments, sludges, soils, and oils. Method 3051a. In Test methods for evaluating solid waste. US Environ. Prot. Agency, Off. Solid Waste, Econ. Methods, Risk Anal. Div. Washington, DC, USA. http//www.epa.gov/waste/hazard/testmethods/sw846/online/3_series.htm 1–30.

van der Knijff, J.M., Jones, R.J.A., Montanarella, L., 2000. Soil erosion risk assessment in Europe, Luxembourg: Office for Official Publications of the European Communities.

Weihermüller, L., Siemens, J., Deurer, M., Knoblauch, S., Rupp, H., Göttlein, A., Pütz, T., 2007. In Situ Soil Water Extraction: A Review. J. Environ. Qual. 36, 1735–1748. https://doi.org/10.2134/jeq2007.0218

Xu, J., Wei, Q., Yu, Y., Peng, S., Yang, S., 2014. Leaching of heavy metals from rice fields with different irrigation management. Polish J. Environ. Stud. 23, 2279–2286.

Zeng, S., Li, J., Wei, D., Ma, Y., 2017. A new model integrating short- and long-term aging of copper added to soils. PLoS One 12, 19–24. https://doi.org/10.1371/journal.pone.0182944

Supplementary table II.1.A.1 : Deciles of concentration of total Cu (mg kg^{-1}), Cu in solution (µg L^{-1}) and pCu (-log(free Cu)) for the outliers of total Cu (total Cu>30mg kg^{-1}), Cu in solution (Cu in solution > 10.71µg L-1) and free Cu (pCu<(-0.45)).

	0%	1%	5%	10%	15%	20%	25%
Cu total >36.8 mg.kg-1							
Cu available	2.2	6.5	7.8	8.6	9.1	9.6	10.1
Cu bio-available	-1.6	-0.3	0.6	0.8	1.0	1.1	1.3
Cu available>10.71 µg.L-1							
Cu total	13.5	19.3	23.6	26.6	28.9	31.0	33.0
Cu bio-available	-1.7	-0.6	0.1	0.4	0.7	0.8	1.0
Cu bio-available (pCu)<-0.45							
Cu total	2.2	4.1	5.6	6.5	7.0	7.6	8.1
Cu bio-available	0.6	1.2	1.4	1.5	1.6	1.7	1.8

	40%	50%	60%	70%	75%	80%	85%	90%	95%	99%	100%
Cu total >36.8 mg.kg^{-1}											
Cu available	11.4	12.3	13.2	14.3	14.9	15.6	16.5	17.8	20.0	24.7	45.0
Cu bio-available	1.6	1.8	2.0	2.1	2.2	2.3	2.4	2.5	2.6	2.8	3.3
Cu available>10.71 µg.L^{-1}											
Cu total	37.8	40.7	43.6	47.0	49.0	51.3	54.0	57.8	64.4	79.2	128.2
Cu bio-available	1.5	1.7	1.9	2.1	2.2	2.3	2.4	2.5	2.6	2.8	3.1
Cu bio-available (pCu)<-0.45											
Cu total	9.5	10.5	11.7	13.5	14.6	15.9	17.7	20.3	24.2	35.3	90.3
Cu bio-available	2.1	2.3	2.7	3.5	4.0	4.6	5.2	6.1	7.8	12.3	35.6

Supplementary table II.1.A.2 : Percentiles for the difference to the median of total Cu (in % of the median value)

decile	0%	1%	5%	10%	15%	20%	25%	40%	50%
percentage of variation with median	-93.9	-74.0	-61.9	-52.7	-45.3	-38.8	-32.7	-14.1	0.0

decile	60%	70%	75%	80%	85%	90%	95%	99%	100%
percentage of variation with median	16.2	35.8	48.3	63.9	83.9	114.8	178.6	296.7	883.6

Supplementary table 3 : Percentiles for the difference to the median of Cu in solution (in % of the median value)

decile	0%	1%	5%	10%	15%	20%	25%	40%	50%
percentage of variation with median	-94.06	-79.87	-69.84	-62.64	-56.86	-51.39	-45.63	-21.69	0.00

decile	60%	70%	75%	80%	85%	90%	95%	99%	100%
percentage of variation with median	24.16	51.33	67.97	88.41	115.01	152.81	218.88	364.60	1241.25

Supplementary table II.1.A.4 : Percentiles for the difference to the median of free Cu (in % of the median value)

decile	60%	70%	75%	80%	85%	90%	95%	99%	100%
percentage of variation with median	96.87	286.23	413.11	564.47	759.43	1048.60	1613.57	3520.78	61678.97

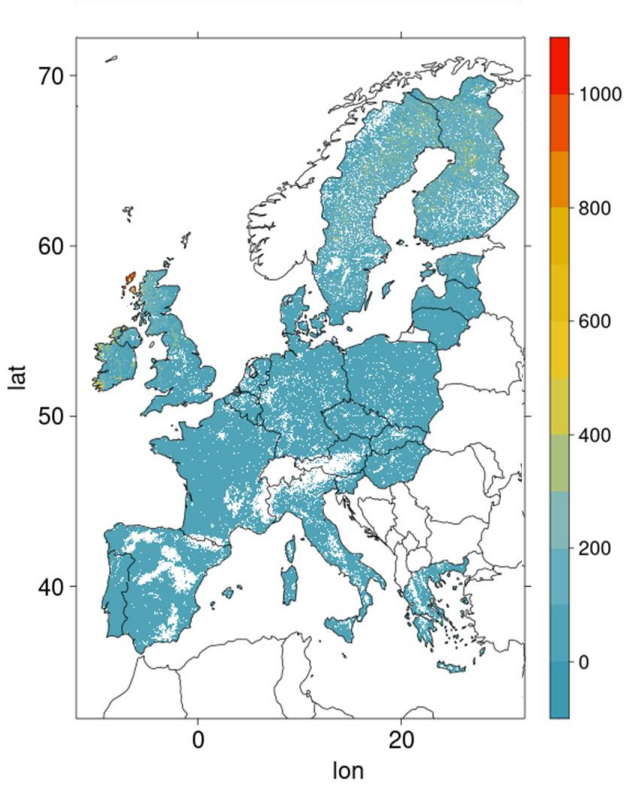

Supplementary Fig. II.1.A.1 : Corga map of Europe from https://esdac.jrc.ec.europa.eu/content/topsoil-soil-organic-carbon-lucas-eu25 (de Brogniez et al., 2015).

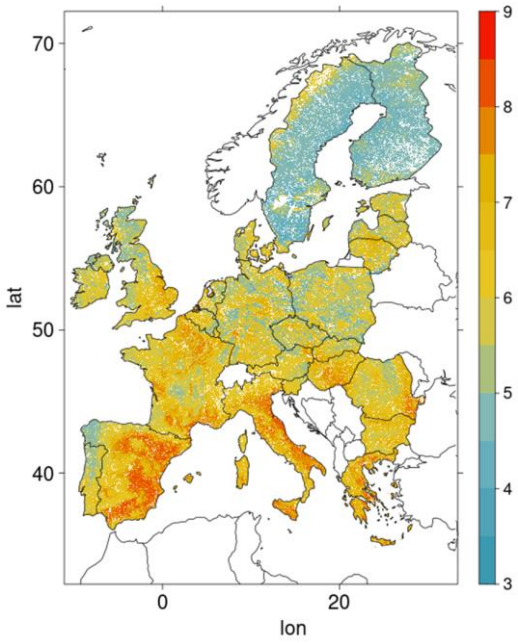

Supplementary Fig. II.1.A.2 : pH map of Europe from https://esdac.jrc.ec.europa.eu/content/chemical-properties-european-scale-based-lucas-topsoil-data (Ballabio et al., 2019)

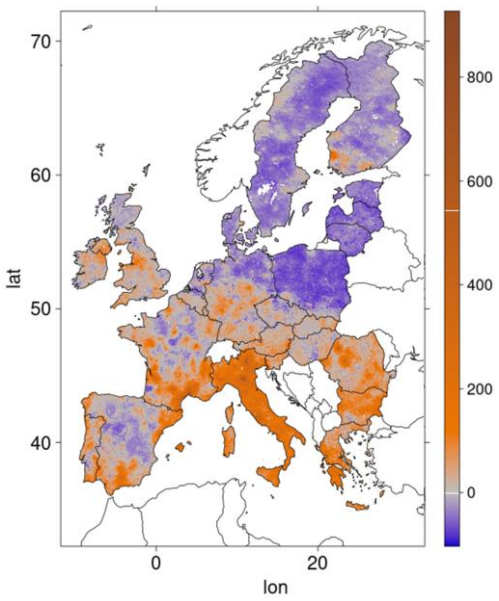

Supplementary Fig II.1.A.3. : Percentage of differences between total Cu and median total Cu value (13,2 mg.kg soil $^{-1}$) in Europe

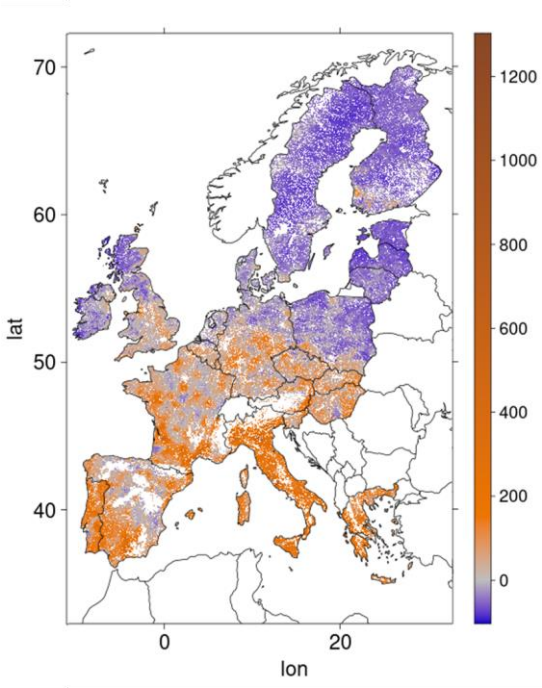

Supplementary Fig. II.1.A.4. : Percentage of differences between Cu in solution (estimated from eq 3b) and median Cu in solution (3.36 µg.L^{-1}) value in Europe

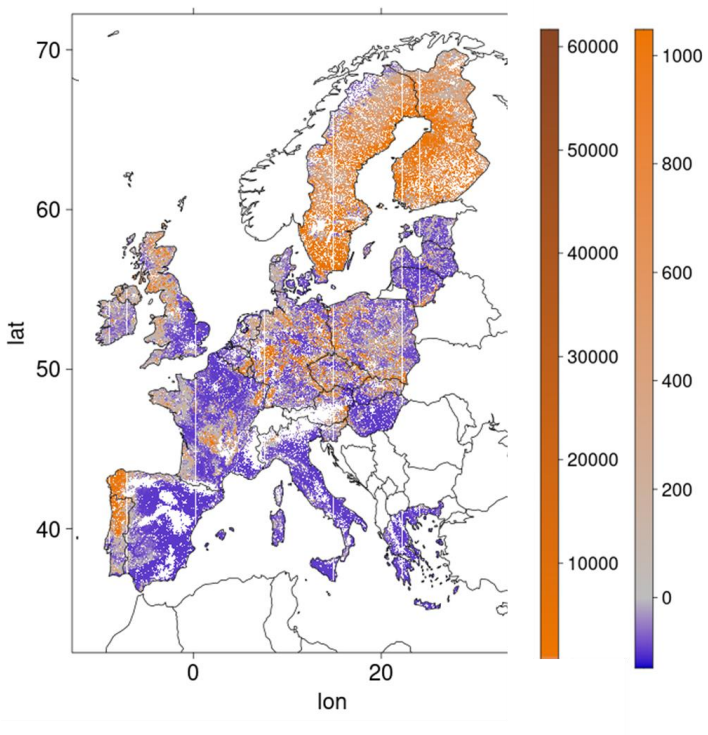

Supplementary Fig. II.1.A.5 : Percentage of differences between free Cu (estimated from eq 14b.) and median free Cu (0.165µg.L^{-1}) value in Europe

II.1.B. Evolution of soils copper leaching and accumulation potential under different scenarios of climate change in Europe -

SERENI Laura[1], PARIS Julie-Maï[2], GUENET Bertrand[2], LAMY Isabelle[1]

[1] Université Paris-Saclay, INRAE, AgroParisTech, UMR 1402 ECOSYS, Ecotoxicology Team, 78026, Versailles, France

[2] Laboratoire de Géologie de l'ENS, PSL Research University, CNRS, UMR 8538, IPSL, Paris, France

Expected journal for submission: Sciences of the total environment

Summary:

Anthropogenic use of trace elements for industrial or agricultural purpose induced their deposition on soil surfaces. Among trace elements, copper (Cu) is widely used especially in agriculture for its fungicide's properties. In soils, only the Cu in solution is mobile and can be horizontally transferred and may reach streams, rivers or lakes. The partition between Cu in solution and total Cu is driven by soil properties. Thus, Cu mobility may largely varies due to local soil conditions but also because of changes in soil hydrology. Indeed, when runoffs are high and Cu is mobile, Cu in soil solution may leach while low runoffs and reduced Cu partition may lead to Cu accumulation. Hence, the knowledge of soil runoff (and of its dynamic) and of Cu partitioning between soil solid phases and soil solution allows to identify area of potential accumulation or of potential leaching of Cu. Soils runoffs are expected to change during the century due to climate change because of precipitation regime modification. In this study, we used partition coefficients (K_f) between total and dissolved copper and runoffs simulation results for current and future climate to estimate area of leaching (LP) or of accumulation potential (AP) at the European scale. Because there are also uncertainties in climate change scenario, we conducted our study for 2 Representative Concentration Pathway: RCP 2.6 and RCP 6.0. LP and AP were defined with comparison of K_f and runoffs to their respective median over Europe. Our results show that, for present day 5.9 ±1.34 % (median, median deviation) and 4.9 ±1.4 % of the grid cells are concerned respectively by LP and AP. Both LP and AP are found to increase during the century with percentage of Europe concerned by LP of 7.8 ±1.5% and by AP of 6.1 ±2.8 % for RCP 2.6 in 2090 and of 8.9 ±2.3 % for LP and 9.1 ±1.3 % for AP with RCP 6.0.

1. INTRODUCTION

Soils trace element concentration is highly variable due to parental rocks or anthropogenic inputs from various nature (Flemming and Trevors, 1989; Salminen and Gregorauskiene, 2000; Noll, 2003). Due to their mobility they can further accumulated in deposition zones or be transported by surface runoff in association or not with soil particles in soil solution (Jacobson et al., 2005; Komárek et al., 2010). If trace elements are required for several biological mechanisms, when highly concentrated they may have toxic effects on organisms (Giller et al., 1998). Among heavy metals, copper (Cu) is widely used as pesticide, especially against downy mildew in vineyards (Komárek et al., 2010). Also, if Cu concentration in soils may largely varies depending on soil bedrock with typical baselines concentrations from 5 mgCu kg^{-1} to 20 mgCu kg^{-1} (Salminen and Gregorauskiene, 2000), concentrations larger than 100 mgCu kg^{-1} soil are current in agricultural and especially vineyards parcels (Ballabio et al., 2018). However, most of the soil Cu pool is included into minerals or sorbed on soils constituents and is not bioavailable but this fraction is key variable to measure to estimate the effect of Cu on living organisms (Rooney et al., 2006; Broos et al., 2007). Indeed, it is commonly accepted that the whole Cu stocks in soils, may be conceptually divided into different pools of Cu forms in close equilibrium. Schematically, these pools are governed by sorption processes, so that, local soil properties such as pH, cationic exchange capacities or organic carbon levels may affect the proportion of Cu in the different pools (Vidal et al., 2009). Any modifications in soil properties or soil solution composition may thus affect Cu amount in the different phases.

In parallel, climate change due to anthropogenic activities is expected to affect rainfall during the next decades with shifts in precipitations frequencies and intensities at the local and the regional scale (Christensen and Christensen, 2003). Consequently, water flows are about to be modified across the century because of climate change (Mimikou et al., 2000) with various intensities depending on the anthropogenic activities and associated climate change. In particular, surface runoffs can be affected by modification of rainfall intensity with higher surface runoffs fluxes when rainfall intensity increase because of water accumulation in the surface due to limited water infiltration (Chu et al., 2019). Changes in runoff do not only modify the water fluxes but also all the elements that are either in solution or particulate in the soil solution including Cu (Babcsányi et al., 2016). Accumulation or leaching risk of Cu are therefore due to the combined effect of local runoff amount and of local soil properties controlling the partition between total Cu and Cu in solution. As a consequence, we assume that climate change some regions may rather tend to accumulate Cu while other may tend to leach Cu. Thus, in this study, we aimed at estimating the Cu leaching (LP) or accumulation (AP) potential area in Europe. LP or AP area will be estimated through combination of coefficient of partitioning (K_f) at the equilibrium between solid phases and solution phases, and runoff. The use of K_f allows us to determine area with high potential of leaching even if current Cu concentration is low. We focused on the current climatic condition and on their evolution along the XXI century according to two climate change scenario (RCP 2.6 and RCP 6.0). To account for the difficulty in runoff predictions, and to dismiss between rainfall prediction uncertainty and land surface scheme runoff calculations, we will use a set of simulations provided by the ISIMIP project where different land surface models are driven by different climate forcing calculated by different climate models.

2. MATERIALS AND METHODS

2.1. Equations to estimate dissolution of copper in soils

K_f is defined under equilibrium assumption. Hence, both sorbed and soluble forms are under constant interactions and exchange. The rigorous definition of K_f is based on sorbed vs solution species. However, for practical reason of measurement and applicability K_f is commonly rather calculated considering total Cu (Degryse et al., 2009). Cu can be described with a general form of Cu partition coefficient between soil and solution– K_f – defined as Eq.II.1.B.1:

$$\text{(II.1.B.1)}\ K_f = \frac{Cu_{total}}{Cu_{dissolved}n}$$

With *n* representing the variation in bonding strength with metal loading (Groenenberg et al., 2010). By this, a low K_f indicates that a high part of Cu is in solution for a given total Cu amount. K_f may locally vary depending on different soil parameters (Elzinga et al., 1999; Degryse et al., 2009)$_i$. Thus, K_f can be estimated using eq. II.1.B.2:

$$\text{(II.1.B.2)}: log_{10}(K_f) = a_0 + \sum_i a_i log_{10}(X_i)$$

with X_i the different soil parameters and a_i correspond parameters.

In the literature several studies aimed at determining the equation (II.1.B.2) based on statistical relationships between soils data and Cu in solution and total measurement. The parameter X_i and their coefficient a_i may thus varies between studies and the data set used for regression. In this study, the estimation of K_f will be applied at the European scale, also the chosen equation has to:

i) Include only parameters that are measured in large soil surveys

ii) Been fitted on a large range of each soil parameter

iii) Focused on in situ long term contamination rather than fresh spiking of high amount of Cu.

On December 2020 we first ran bibliographic research on WOS looking for Cu AND (*disponibili* OR availab*) AND soil AND TOPIC function. Secondly, we completed this research with getting into the references of the founded articles. Then we collected the relationships provided to estimate Kd on the basis of total Cu and soil pedogeochemical characteristics. We only selected relationships using pedogeochemical characteristics commonly measured such as soil OM or soil Corga, DOC, CEC, clay percentage and pH.

2.2 Soil data

In this study, we used European data for the different soil parameters (pH, organic C) originated from the LUCAS topsoil data of Join Research Center. It only covers European Union Member States' territory. This data set provides us with pH (https://esdac.jrc.ec.europa.eu/content/copper-distribution-topsoils), organic matter https://esdac.jrc.ec.europa.eu/content/topsoil-soil-organic-carbon-lucas-eu25). It has been regridded at a spatial resolution of 0.5° (approximately 50 km) using cdo commands (Schulzweida, 2019) to fit the resolution of the land surface models used to estimate runoffs and presented in section 2.3.

2.3. Runoff data from land surface models

Runoff is the result of precipitation and soil hydric conductivity. To study runoff's changes across century we then used two land-surface schemes – ORCHIDEE and LPJmL – and two climate models – IPSL-CM5a and GDFL-ESM2m (further named CM5a and ESM2m). We used simulations performed within the Inter-Sectoral Impact Model Intercomparison Project Phase 2b (ISIMIP2b) that distribute land surface models simulations driven with several bias-adjusted climate forcing and land use change scenarios from 1861 to 2099 (Frieler et al., 2017).The climate forcing used by the ISIMIP2b are gridded, daily bias-adjusted climate from different CMIP5 global circulation models (GCMs) (Lange, 2016; Frieler et al., 2017), global annual atmospheric CO_2 concentration, and harmonized annual land use maps (Goldewijk et al., 2017). In the simulation protocols a spin-up is first performed using pre industrial era conditions and then historical and future simulations are run. A detailed protocol is available at https://www.isimip.org/protocol/#isimip2b. The use of bias-adjusted climate data ensures the climate used by the land surface models are in line with observations obtained during the last 40 years of the historical period. Moreover, climate forcing used by the land surface models ensure the continuity of climate forcing between the past and the future. We chose to compare historical data at the beginning of the 21st century (2001-2005) computed by the different models and used with mid (2051-2055) and end (2091-2095) of the century simulation outputs. We therefore compared three periods evenly distributed over the 21st century. For future simulations, we used two century-scaled scenarios, named Representative Concentration Pathway (RCP) and defined by the IPCC (van Vuuren et al., 2011) according to Shared Socioeconomic Pathways followed by countries: (i) RCP 2.6 representing an active reduction of greenhouse gas emissions in order to meet the Paris agreement and (ii) RCP 6.0 which is more or less *business as usual*. RCP 2.6 is thus estimated to produce a radiation forcing of 2.6W.m^{-2} and RCP 6.0 a radiation forcing of 6 W.m^{-2}.

For each climate change scenario (RCP 2.6 or 6.0) applied to each land-surface (LPJmL or ORCHIDEE) and GCMs (CM5a or ESM2m) we computed the five years mean at the beginning (2001-2005), the middle (2051-2055) and the end (2091-2095) of the century to get rid of the inter-annual variability. The cross scheme of 2 land surface models and 2 GCMs allows us to determine if predictions of runoff are rather driven by soil hydrologic properties representation or by rainfall projection. In the first case we would observe highest differences in runoff prediction between LPmL-(CM5a or ESM2m) and ORCHIDEE-(CM5a or ESM2m) projection than between LPJmL-CM5a and ORCHIDEE-CM5a or between LMJmL-ESM2m and ORCHIDEE-ESM2m. In the second case we would observe highest differences in runoff prediction between LPmL-CM5a and ORCHIDEE-CM5a or between LPJmL-ESM2m and ORCHIDEE-ESM2m projection than between LPJmL-CM5a and LMJmL-ESM2m or between ORCHIDEE-CM5a and ORCHIDEE-ESM2m.

2.4. Statistical test to determine AP and LP area

Areas with AP or LP were identified by the comparison of the K_f and runoff value of each grid points to their respective spatial median. Median runoffs were calculated over the whole Europe for each five years mean time period considered. Area with LP correspond to low K_f and high runoff, area of AP to the opposite (cf. Equation (II.1.B.1)). A classical approach proposed by Reimann et al., (2005) is to consider as "high" or "low" outliers to exclude those which are highest than the median +2 median average deviation (MAD) and as low values those which are smallest than median -2 median average

deviation. In our case, we don't aim at excluding outliers' points but rather at identifying points with particularly high or low values. Thus, we use a lower threshold with 1 MAD threshold.

Hence, for each couple of land-use scheme (ORCHIDEE or LPJmL) and climate forcing (CM5a or ESM2m) and each time period (t=2001-2005; 2051-2055 or 2019-2095) of climate change scenario (RCP 2.6 or RCP 6.0), we defined LP and AP as follow:

- Area of high potentiality of leaching under 1 MAD threshold (named LP) for the 5 years mean time period *t* correspond to area where grid points *i* has

$$\begin{cases} K_f(i) < Median\left(European\ K_f\right) - 1\ MAD\left(European\ K_f\right) \\ Runoff(t,i) > Median\ (European\ runoff\ (t) + 1\ MAD\ (European\ Runoff(t)) \end{cases}$$

- Area of low potentiality of leaching under 1 MAD threshold (named AP) for the 5 years mean time period *t* correspond to area where grid points *i* has

$$\begin{cases} K_f(i) > Median\left(European\ K_f\right) + 1\ MAD\left(European\ K_f\right) \\ Runoff(t,i) < Median\ (European\ runoff\ (t) - 1\ MAD\ (European\ Runoff(t)) \end{cases}$$

Some of the advantages brought by this method are that it gets us rid of the absolute character of the values only to get the highest (and lowest) values, and that it is not affected by land use or the set of coefficients chosen to compute K_f.

We used Python 3.8 (van Rossum and Drake, 2009) with NumPy (NumPy developers., 2017), Cartopy (Office, 2015) netCDF4 (http://doi.org/10.5065/D6H70CW6) and Matplotlib (D. Hunter, 2021) to compute outliers and produce our figures.

3. RESULTS

3.1. K_f estimation at the European scale

Empirical equations to estimate K_f are presented in table II.1.B.1. We collected 19 equations with K_f as coefficient of partition between total and Cu in solution. Among all the empirical equations, pH was found the more determining factor in K_f estimation (12/19 relationships).

K_f is positively correlated to pH with partial slope for pH around 0.1 so that the more alkaline the soil is, the lowest the ratio Cu in solution /total Cu is. K_f is globally positively correlated to OM with partial slope for OM around 0.6, even if Mondaca et al., (2015) found negative partial slope for soil OM or dissolved organic C in a study on chilies soils (Table II.1.B.1, eq. II.1.B.12d) . However, the equation also includes a positive partial slope of CEC. CEC can be roughly assimilated to the sum of clay and soil OM, so that the over whole place of OM is compensated in that particular situation.

Table II.1.B.1.: Transfer functions reviewed from literature to estimate distribution constant of Cu. R.V is for response variable and Int. for intercept. In most cases studies fitted K_f defined $K_f = [Cu]_{solution}/[Cu]_{soil}^{n}$ in $L.kg^{-1}$, Cu tot is in $mg.kg^{-1}$, DOC in $mg.L^{-1}$, OM and OC are in $g.kg^{-1}$, clay in percentage, CEC in $cmol.kg^{-1}$

Author	Eq	R.V	Int.	Log (Cu tot)	pH	Log (OM)	Log (DOC)	Log (clay)	other	n-opt	R2	number of data	Range CuTot	Range OM	Range OC	Range pH
(Vulkan et al., 2000)	II.1.B.4	Log (K_f)	1.74		0.34		-0.58				0.42	21	19-8645		9.8-69.8	5.5-8
(Sauvé et al., 2000)	II.1.B.5a	Log (K_f)	1.49 (±0.13)		0.27 (±0.02)						0.29	447	6.8-82850			
(Sauvé et al., 2000)	II.1.B.5b	Log (K_f)	1.75 (±0.12)		0.21 (±0.02)	0.51 (±0.06) (%)					0.42	353	6.8-82850			
(Römkens et al., 2004)	II.1.B.6a	Log (K_f)	-2.61		0.12	0.60 (%)	-0.27	0.23		0.59	0.65	1466	0.2-305.7	2-734		1.8-7.9
(Römkens et al., 2004)	II.1.B.6b	Log (K_f)	-3.55		0.16	0.48		0.18		0.47	0.62	1466	0.2-305.7	2-734		1.8-7.9
(Römkens et al., 2004)	II.1.B.6c	Log (K_f)	-3.07		0.12	0.45	-0.27	0.12	0.35 log (Fe+AloX) mmol.kg^{-1}	0.6	0.66	1466	0.2-305.7	2-734		1.8-7.9
(Römkens et al., 2004)	II.1.B.6d	Log (K_f)	-3.25		0.67	0.87		0.23		0.59	0.89	1466	0.2-305.7	2-734		1.8-7.9
(Degryse et al., 2009)	II.1.B.7a	Log (K_f)	0.6		0.37						0.34	129				

(Degryse et al., 2009)	II.1.B.7b	Log (K_f)	0.45		0.34				0.65 log (CEC %)		0.44	128				
(Unamuno et al., 2009)	II.1.B.8a	Log (K_f)	1.95		0.16						0.15	29	18-10389			
(Unamuno et al., 2009)	II.1.B.8b	Log (K_f)	2.383	0.46							0.61	29	18-10389			
(Unamuno et al., 2009)	II.1.B.8c	Log (K_f)	1.99	0.42	0.06						0.63	29	18-10389			
(Groenenberg et al., 2010)	II.1.B.9a	Log (K_f)	2.26		0.89	0.9 (%)				0.85	0.87	216	0.1-326	2-97.8		3.3-8.3
(Ivezić et al., 2012)	II.1.B.10a	Log (K_f)	3.98			0.48 (%)	-0.59				0.5	74	5.7-141		0.9-10.2	4.3-8.1
(Mondaca et al., 2015)	II.1.B.11a	Log (K_f)	1.05	0.7		-1.06 (%)					0.46	86	56-4441	12.0-62		6.2-7.8
(Mondaca et al., 2015)	II.1.B.11b	Log (K_f)	2.88	0.41			-1.03				0.77	86	56-4441	12.0-62		6.2-7.8
(Li et al., 2017)	II.1.B.12a	Log (K_f)	3.12	0.47			-0.66				0.28	34				

(Li et al., 2017)	II.1.B.12b	Log (K_f)	2.179	-0.452 * log (Cu solution) $\mu mol.L^{-1}$							0.42	34				
(Li et al., 2017)	II.1.B.12c	Log (K_f)	2.59	0.617			-1.55				0.88	20				

The estimation of K_f between total and Cu in solution defined by Sauvé et al., (2000a) in eq.II.1.B. 5a,bTable II.B.1.1) is unambiguously the most commonly used. He provided two equations based on a meta-analysis of roughly 400 data points from long term contaminated samples, one of them taking OM values into account, the other not because of missing information in the collected data. Also, the equation (II.1.B.5b was selected for application at the Europe and K_f was calculated following:

K_f values varies between 4600 and 21500 L kg^{-1} with median values at 9829 L kg^{-1}. Values below 8000 L kg^{-1} and above 12000 L kg^{-1} are respectively low and high outliers for K_f. The application of eq. II.1.B.5b at the European scale show an heterogeneous distribution (Fig. II.1.B.1). Apart from countries not in administrative European union (Switzerland, Norway…), a lack of data can be observed in some mountainous areas where the OM contents are not provided by the JRC. Low partition of Cu in soil solution phases can be found around the Mediterranean Sea, Great Britain, Baltic states and Scandinavia where values of K_f are high (>12000 L kg^{-1}). On the contrary, high partition of Cu into soil solution may be found near Portugal and Poland where values of K_f are low (<8000 L kg^{-1}).

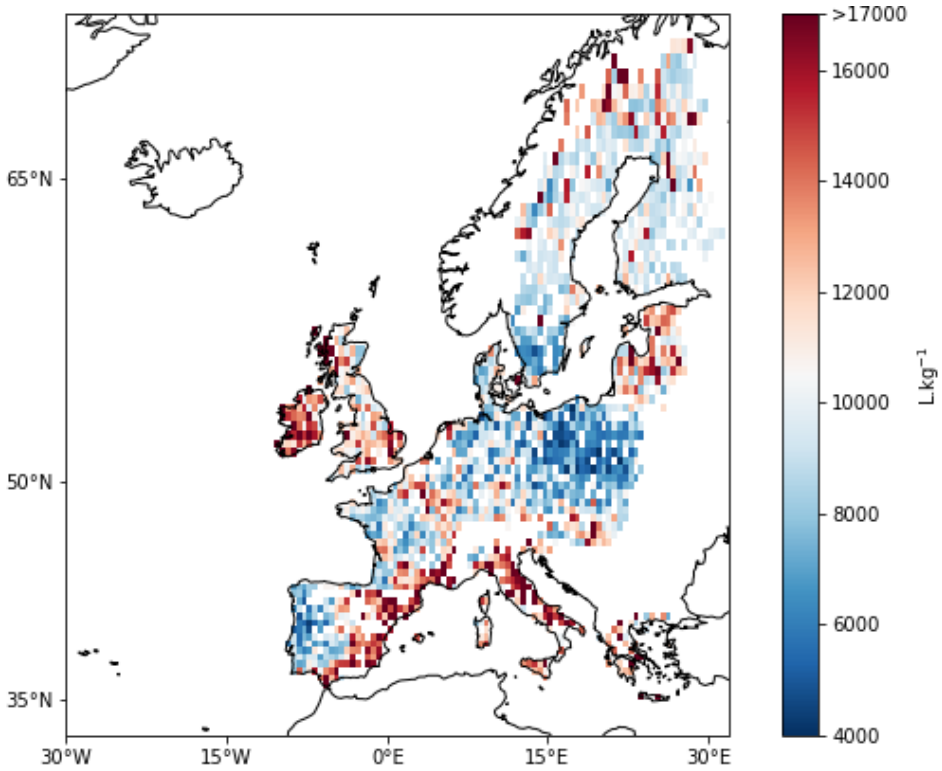

Fig. II.1.B.1: Map of K_f in Europe at 0.5° following eq. II.1.B.5b

3.2. Potential leaching and accumulation in Europe at the beginning of the century (2001-2005)

Over the 2 LSMsx 2 climate forcing, runoffs in 2001-2005 varies between 1.9. 10^{-7} (±1.9 10^{-7} mean, standard deviation of the 4 models) and 4.10^{-5} kgH_2O $m^{-2}.s^{-1}$ (±2.2 10^{-6}) with median value at 8.6 10^{-6} kgH_2O $m^{-2}.s^{-1}$. ORCHIDEE_CM5a combination has the smallest runoff estimation with runoff varying from 3 10^{-8} to 5.10^{-5} kgH_2O $m^{-2}.s^{-1}$ and mean at 9.6 10^{-6} kgH_2O $m^{-2}.s^{-1}$ while LPJmL_ESM2m has the largest runoff estimation

with runoff varying from 4.5 10^{-7} kgH_2O $m^{-2}.s^{-1}$to 4.5 10^{-5} kgH_2O $m^{-2}.s^{-1}$ and mean at 1.03. $10^{-5}.s^{-1}$. Values below 2.9 10^{-6}, 3.8 10^{-6}, 5.5 10^{-6} , 5.7 10^{-6} kgH_2O $m^{-2}.s^{-1}$ and above 1.3 10^{-5}, 1.4 10^{-5}, 1.2 10^{-5} and 1.2 10^{-5} kgH_2O $m^{-2}.s^{-1}$ are respectively low and high outliers for the current runoffs for ORCHIDEE_CM5a, ORCHIDEE_ESM2m, LPJmL_CM5A and LPJmL_ESM2m. Runoffs values are especially high beyond 40th degree latitude with the exception of a few limited areas. As runoffs are especially high compared to the rest of Europe near areas without data, it reduces the robustness of our analysis done by crossing K_d and runoffs data.

Fig. II.1.B.2 represents the LP and AP area for the 2001-2005 time period for the different combination of LSMs and climate forcing. The amount of grid cells concerned by LP and AP varied between LSMs-climate forcing combination (see fig II.1.B.3 with historical scenario) but spatial pattern are well conserved. LP are located mostly in Northern Portugal with scattered points around France, Germany, Poland and Scandinavia. AP are mostly found in South East of Spain and South-Adriatic coast of Italy. Similarities are however larger for a same land surface scheme than for a same climate forcing. For instance, with the LPJmL land surface scheme AP area in South Spain is larger, and LP in France and East Europe are more scattered than with the ORCHIDEE land surface scheme.

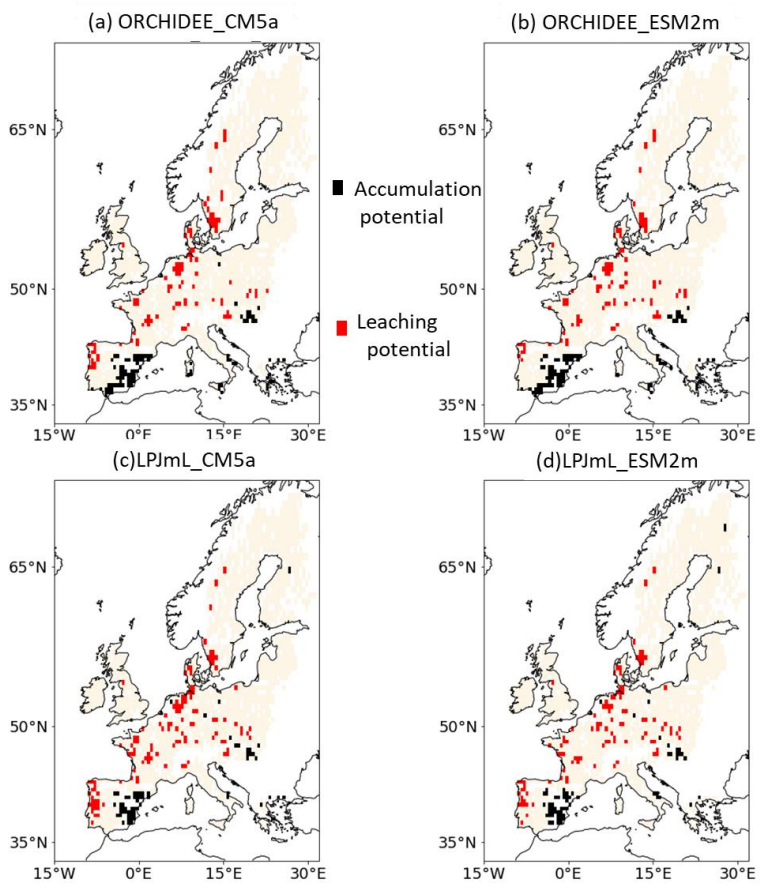

Fig. II.1.B.2: Area of leaching (LP) and accumulation (AP) potential for the historical (2001-2005) period for the different combination of land surface scheme (ORCHIDEE in (a), (b) ; LPJmL in (c), (d)) and climate forcing (CM5a in (a), (c) and ESM2m in (b), (d)).

Over the 4 combinations of LSMs and climate forcing, 5.9 ±1.34 % (median, median deviation) of the grid cells are concerned by LP (fig. II.1.B.3.A) and 4.9 ±1.4 % by AP (fig. II.1.B.3.B) for the historical period (2011-2005). ORCHIDEE_ESM2m combination has the smallest percentage of the grid cells concerned by LP with 4.7% of the grid cells. LPJmL_CM5A has the largest percentage of the grid cells concerned by LP with 7.5% of the grid cells. ORCHIDEE_ESM2M and ORCHIDEE_CM5a have the largest percentage of the grid cells concerned by AP with 5.9% and LPJmL_CM5a the smallest percentage of the grid cells concerned by AP with 3.9% of the grid cells (fig. II.1.B.3.B).

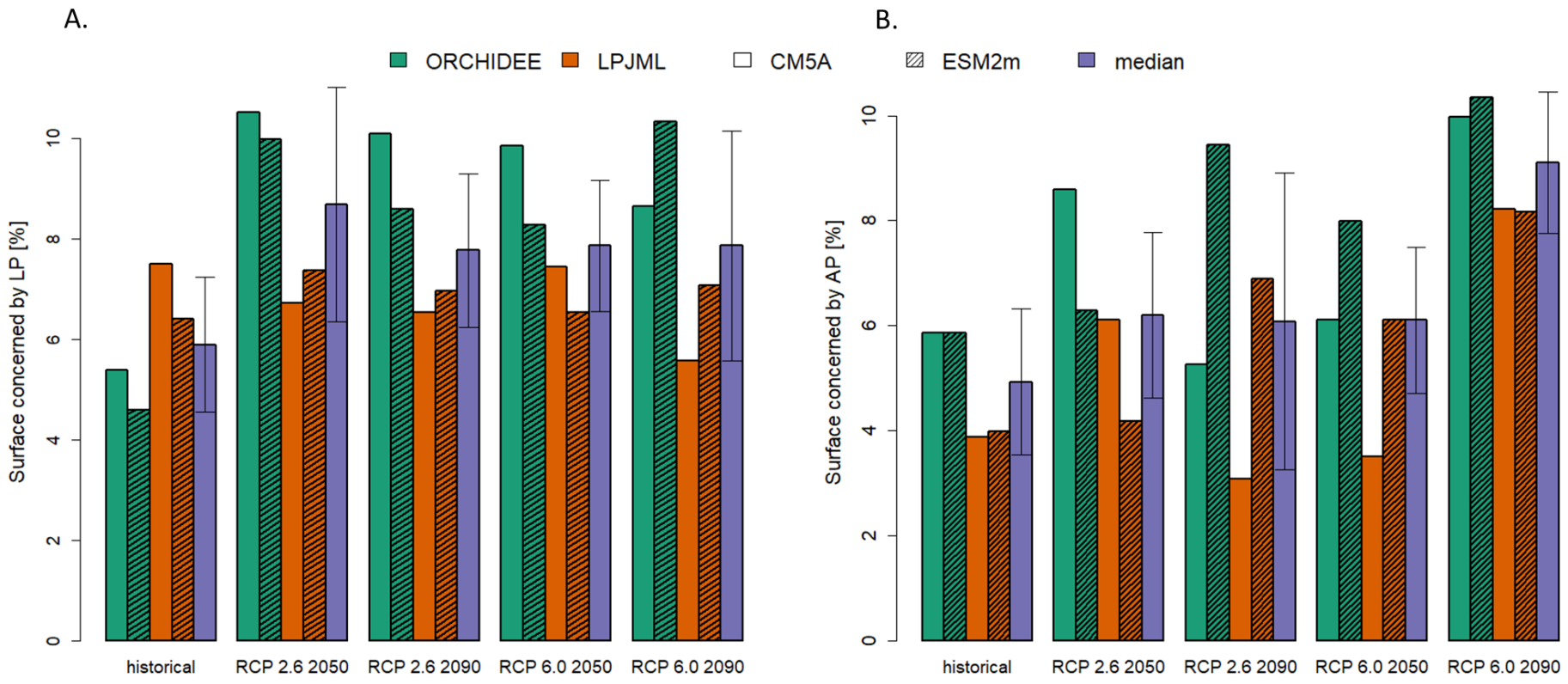

Fig. II.1.B.3: Percentage of the grid cells concerned by LP (A.) and AP (B.) for the different scenario (historical=2001-2005, RCP 2.6 horizon 2050 and 2090 and RCP 6.0 horizon 2090). The 4 combinations of the 2 LSMs (ORCHIDEE in gree and LPJmL in orange) and the 2 climates forcing (CM5a fill bars and ESM2m dashed bar) as well than median (purple) of the 4 models and median deviation (bar) are plotted.

3.3. LP and AP evolutions over the century according to the different RCP

For the two scenarii, runoffs are expected to increase over the century with mean runoff of the 2 LSMs x 2 climates forcing. For 2050-2055 runoffs are of 1.01. 10^{-5} $kgH_2O\ m^{-2}.s^{-1}$ ±4.8 10^{-7} with RCP 2.6 and of 1.01 . 10^{-5}± 6. 10^{-7} with RCP 6.0 (mean, standard deviation of the 2LSMsx 2 climate models over the 5 years). For 2091-2095, runoffs are of 1.04 .$10^{-5}$$kgH_2O\ m^{-2}.s^{-1}$±4.4 10^{-7} (with RCP 2.6 and 1.04 .10^{-5} ± 5.2 10^{-7} with RCP 6.0 (mean, standard deviation of the 2LSMsx 2 climate models over the 5 years).

Fig. II.1.B.4 and II.1.B.5 represent the maps of LP and AP for the 2 LSMs and the 2 climate models with RCP 2.6 respectively for the 2050 and 2090 horizons.

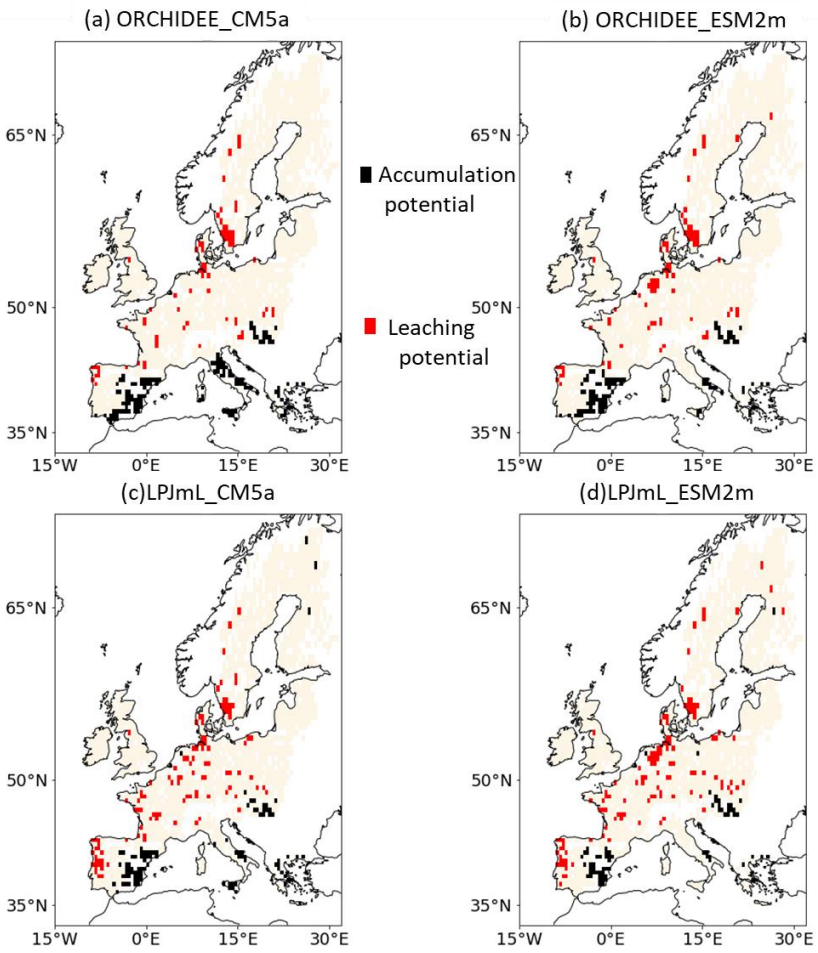

Fig. II.1.B.4: Area of leaching (LP) and accumulation (AP) potential for the RCP2.6 (2051-2055) period for the different combination of land surface scheme (ORCHIDEE in (a), (b) ; LPJmL in (c), (d)) and climate forcing (CM5a in (a), (c) and ESM2m in (b), (d)).

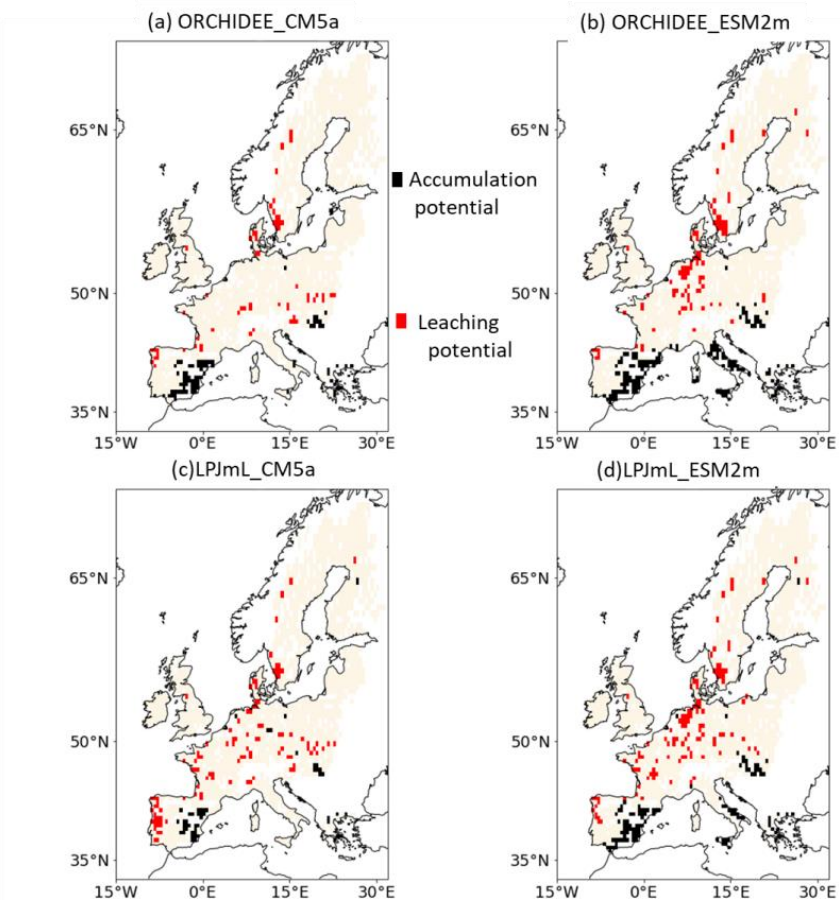

Fig. II.1.B.5: Area of leaching (LP) and accumulation (AP) potential for the RCP 2.6 2091-2095 period for the different combination of land surface scheme (ORCHIDEE in (a), (b) ; LPJmL in (c), (d)) and climate forcing (CM5a in (a), (c) and ESM2m in (b), (d)).

Fig II.1.B.6 and II.1.B.7 represents the map of LP and AP for the 2 LSMs and the 2 climate models with RCP 6.0 respectively for the 2050 and 2090 horizons

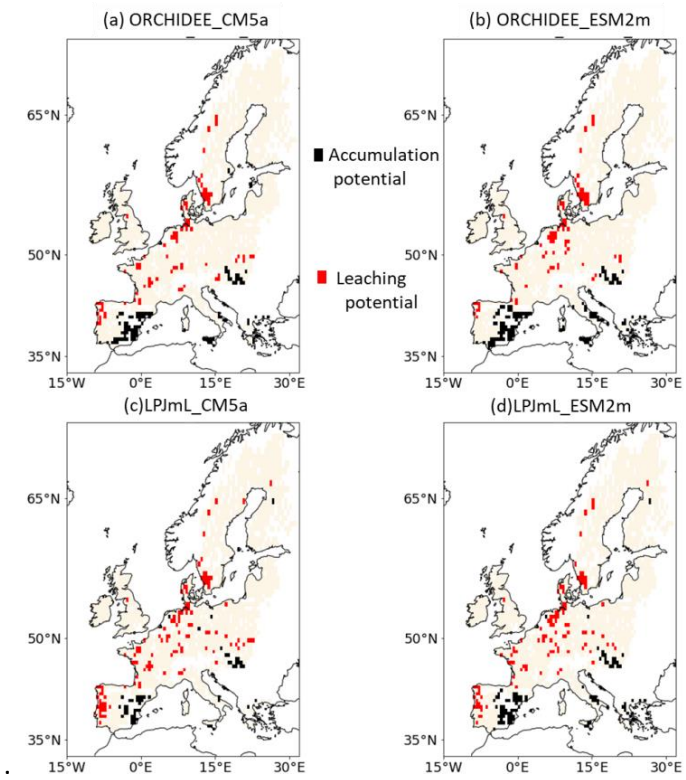

Fig. II.1.B.6: Area of leaching (LP) and accumulation (AP) potential for the RCP 6.0 2091-2095 period for the different combination of land surface scheme (ORCHIDEE in (a), (b) ; LPJmL in (c), (d)) and climate forcing (CM5a in (a), (c) and ESM2m in (b), (d)).

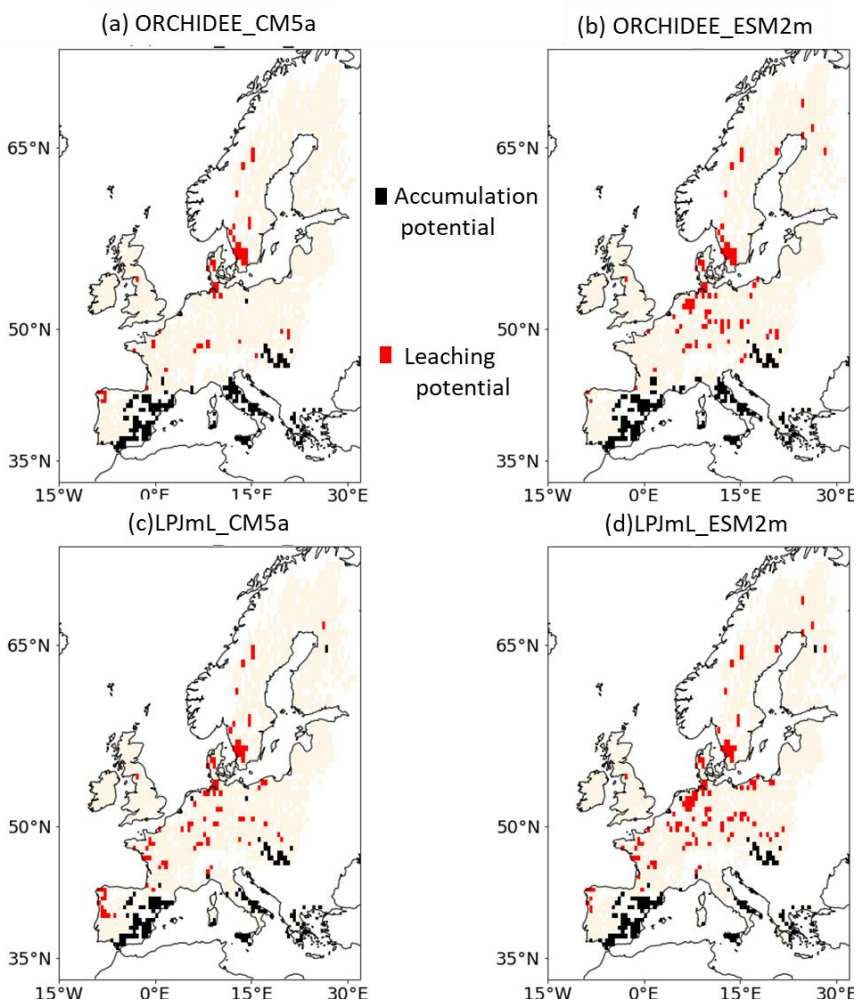

Fig. II.1.B.7: Area of leaching (LP) and accumulation (AP) potential for the RCP 6.0 2091-2095 period for the different combination of land surface scheme (ORCHIDEE in (a), (b) ; LPJmL in (c), (d)) and climate forcing (CM5a in (a), (c) and ESM2m in (b), (d)).

In all cases LP mostly concern Portugal, Scandinavia, Germany and Poland, with more grid cells in East Europe than actually. Models and climate change scenario combination mostly affects the number of scattered points in East Europe and the south extend of Portugal risk. In all cases, AP were found in Sicilia, East Europe and South Spain, but the density and extend of the AP in these regions varied between models and climate change scenario.

At the 2050 horizons, new area concerns by LP concerns scattered points in Sweden and in North Germany with LPJmL_ESm2m. New AP area are found in East Europe and in Greece. Italy is also subject to new AP area (2 LSMs and CM5a climate forcing and ORCHIDEE and ESM2m in the case of RCP2.6 and the 2 LSMs with ESM2m climate forcing in the case of RCPC 6.0). At the 2090 horizon the LP concerns scattered points in central Europe with ESM2m climate forcing and scattered points in East Europe with CM5a. New AP area found in Italy with the ESm2m climate forcing but not with the Cm5a.

The evolution of percentage of Europe concerned by LP for the different scenario and the different LSMs_climate forcing combination over the century are represented in fig. II.1.B.3.A. The median percentage of grid cells concerned by LP increases for all the scenario compared to the current values. With RCP 2.6 median percentage of grid cells concerned by LP decreases from 2050 (8.7 % ± 2.3, median, median deviation) to 2090 (7.7 % ± 1.5, median, median deviation). With RCP 6.0 median percentage of grid cells concerned by LP is stable between 2050 and 2090 at 7.9 % but median deviation increases from 1.2 to 2.3 (fig. II.1.B.3.A).

These trends are followed by all the combination of LSMs and climate forcing for the RCP 2.6 scenario. For the RCP 6.0 the models with CM5a forcing tends to have less grid points concerned by LP (respectively 7.4 to 5.6 % for LPJML_CM5a and 9.9 to 8.7% for ORCHIDEE_CM5a land surface scheme between 2050 and 2090). By contrasts, the models with ESM2m forcing tends to have more grid points concerned by LP (respectively 6.5 to 7% for LPJML and 8.3 to 10.3% for ORCHIDEE land surface scheme in 2050 and in 2090), see fig II.1.B.3.A

The evolution of percentage of Europe concerned by AP for the different scenario and the different LSMs x climate forcing combination over the century are represented in fig. II.1.B.3.B. The median percentage of grid cells concerned by AP increases for all the scenario compared to the current values. With RCP 2.6 median percentage of grid cells concerned by AP in roughly constant from 2050 (6.2 % ± 1.6, median, median deviation) to 2090 (6.1 % ± 2.8, median, median deviation). With RCP 6.0, median percentage of grid cells concerned by AP increases from 6.1 % ± 1.4 in2050 to 9.1% ± 1.34 in 2090. The individual trends of the LSMs and climate forcing are however more variable. Indeed, with RCP2.6 and CM5a climate forcing, the percentage of Europe concerned by AP decreases from 2050 to 2090 and in 2090 the percentage of grid cells concerned by AP is smaller than with historical data (respectively 5.2% and 3.1% in 2090 against 5.8% and 3.9% with historical data for ORCHIDEE and LPJmL land surface model). With ESM2m climate forcing percentage of Europe concern by AP increase from the historical data to 2090. With RCP 6.0 all combination of LSMs and climate forcing increases from the historical data to 2090 except for the LPJmL-CM5a prevision in 2050.

4.DISCUSSION

4.1. Leaching potential versus Cu export

This study aims at identifying potential accumulation and leaching areas for Cu. We focused on partitioning coefficient that take into account soils properties to estimate the proportion of total Cu that get in soil solution. However, our study doesn't take into account the total Cu concentration spatial variability. Indeed, mean total Cu concentration over Europe is 15.76 mg kg^{-1} but spatial variability is high. Yet, highly concentrated zones localized in agricultural area such as vineyards, orchards and olive groves can reach concentration up to more than 100 mg kg^{-1} (Ballabio et al., 2018) mostly in South East of France or Italy. We choose to work on K_f specifically and not on total Cu because Cu in solution is not directly correlated with total Cu and spatial distribution on Cu in solution is largely different from spatial distribution of total Cu (see chapter II.1.A. For our problematic here it was therefore not informative to consider total Cu. For instance, in Eastern Europe low K_f and high runoff resulting in LP but low amount of total Cu limits the amount of total Cu export. By contrast, in Italy, we found high AP for every model for at least one time horizon and one RCP. In these vineyard

regions annual input is relatively high so that Cu will tend to accumulate, resulting in high total Cu concentration that could enter the food web (García-Esparza et al., 2006). Cu would hence partition into soil solution but not be exported through runoff due to their limited amount. In parallel, the North of France and Central-East Europe are not at LP with current scenario but we identified scattered points in all scenario for the rest of the century. Despite rainfall and soil humidity modifications, climate change also induced higher temperature and shorter winter so that, we except a shift in cultures toward North (Hannah et al., 2013). Hence, these regions with few total Cu today may encounter an increase in Cu input through fungicide that could be further exported through freshwater.

4.2. Temporal evolution of data and limits of our analysis

The study conducted here focused on 5-year means, and didn't take into account the seasonal variability of runoffs nor of Cu inputs. Moreover, the K_f we calculated is not dynamic since we had no data to calculate temporal variability of K_f. We also don't investigate i) whether precipitations and runoff will evolved in term of intensity and frequency even if alternance of drying and rewetting events may affect Cu partitioning between phases (Han et al., 2001; Christensen and Christensen, 2003) and ii) whether the time period of year with higher precipitation coincide or not with period of use of Cu for instance in agriculture and vineyards where it's particularly used (Ribolzi et al., 2002; Banas et al., 2010). Indeed, K_f is defined under equilibrium between solid and solution phases assumption, so that, the amount of Cu in solution estimated by this method may be smallest than what occurs just after Cu application and before equilibrium (McBride et al., 1997). Also, if intense rainfall occurs quickly after fungicides application a larger amount than expected may be exported through runoff. Besides, mean precipitation and runoff amount, type of rainfall (duration and intensities) as well than their temporality may thus affect Cu export through runoff. Hence, regional soil Cu budget should be clarified with temporal models taking into account both regular Cu input and output through vegetation or daily runoff.

Furthermore, another punctual driver of movement is soil erosion which sweeps along topsoils charged with Cu and contaminate surface water (El Azzi et al., 2013). Highly erosive storm events being quite frequent in the Mediterranean Basin and predict to increase during the next decades in the Europe is hence another risk factor for freshwater contamination. In this case, most of the exported Cu is solid bound (98% of the exported Cu, (Imfeld et al., 2020)) and can easily be retained into discharge pounds. Hence, the study of leaching potential we conducted should be coupled with erosion risk study (Ballabio et al., 2017) and with retention pond localization to better identified area with exogeneous risk of contamination.

5. CONCLUSION

Our review of Cu K_f equation shows that pH and soil organic matter content are important determinant in Cu partitioning and that OM partial effect is twice larger than pH effect. Based on European map of pedological data we computed the map of K_f at the 0.5° scale we then estimated LP and AP for current and future soil runoff under 2 RCP with 2 climate models and 2 land surface schemes. Historical data show that in median 5.9 ±1.34 % and 4.9 ±1.4 % of the grid cells concerned respectively by LP and AP. In median, LP and AP were found to increase during the century compared to the current estimation for the 2 RCP. With RCP 2.6, 7.8 ±1.5% of the grid cells are concerned by LP in 2090 and 6.1 ±2.8 % by AP. With RCP 6.0, 8.9 ±2.3 % of the grid cells are concerned by LP in

2090 and 9.1 ±1.3 % by AP. Between 2050 and2090, the amount grid cells concerned by LP and AP depends on the RCP scenario followed. With RCP 2.6 area concerned by LP decreases between 2050 and 2090 and area concerned by AP increase with ESM2m climate forcing but decreases with CM5a climate forcing. With RCP 6.0 area concerned by LP decreases from 2050 to 2090 using the CM5a climate forcing and increases with ESM2m climate forcing. Area concerned by AP increases from 2050 to 2090 for the 2 LSMs and the 2 climates forcing. However, even if the number of grid points identified with LP may varied between models and scenario their localization are roughly conserved.

Bibliography:

Babcsányi, I., Chabaux, F., Granet, M., Meite, F., Payraudeau, S., Duplay, J., et al. (2016). Copper in soil fractions and runoff in a vineyard catchment: Insights from copper stable isotopes. *Sci. Total Environ.* 557–558, 154–162. doi:10.1016/j.scitotenv.2016.03.037.

Ballabio, C., Borrelli, P., Spinoni, J., Meusburger, K., Michaelides, S., Beguería, S., et al. (2017). Mapping monthly rainfall erosivity in Europe. *Sci. Total Environ.* 579, 1298–1315. doi:10.1016/j.scitotenv.2016.11.123.

Ballabio, C., Panagos, P., Lugato, E., Huang, J. H., Orgiazzi, A., Jones, A., et al. (2018). Copper distribution in European topsoils: An assessment based on LUCAS soil survey. *Sci. Total Environ.* 636, 282–298. doi:10.1016/j.scitotenv.2018.04.268.

Banas, D., Marin, B., Skraber, S., Chopin, E. I. B., and Zanella, A. (2010). Copper mobilization affected by weather conditions in a stormwater detention system receiving runoff waters from vineyard soils (Champagne, France). *Environ. Pollut.* 158, 476–482. doi:10.1016/j.envpol.2009.08.034.

Broos, K., Warne, M. S. J., Heemsbergen, D. A., Stevens, D., Barnes, M. B., Correll, R. L., et al. (2007). Soil factors controlling the toxicity of copper and zinc to microbial processes in Australian soils. *Environ. Toxicol. Chem.* 26, 583–590. doi:10.1897/06-302R.1.

Christensen, J. H., and Christensen, O. B. (2003). Severe summertime flooding in Europe. *Nature* 421, 805–806. doi:10.1038/421805a.

Chu, H., Wei, J., Qiu, J., Li, Q., and Wang, G. (2019). Identification of the impact of climate change and human activities on rainfall-runoff relationship variation in the Three-River Headwaters region. *Ecol. Indic.* 106. doi:10.1016/j.ecolind.2019.105516.

D. Hunter, J. (2021). Matplotlib: Python plotting. *Matplotlib*, 1. Available at: https://matplotlib.org/%0Ahttps://matplotlib.org/%0Ahttps://matplotlib.org/%0Ahttps://matplotlib.org/3.1.1/index.html%0Ahttps://matplotlib.org/.

Degryse, F., Smolders, E., and Parker, D. R. (2009). Partitioning of metals (Cd, Co, Cu, Ni, Pb, Zn) in soils: concepts, methodologies, prediction and applications - a review. *Eur. J. Soil Sci.* 60, 590–612. doi:10.1111/j.1365-2389.2009.01142.x.

El Azzi, D., Viers, J., Guiresse, M., Probst, A., Aubert, D., Caparros, J., et al. (2013). Origin and fate of copper in a small Mediterranean vineyard catchment: New insights from combined chemical extraction and δ65Cu isotopic composition. *Sci. Total Environ.* 463–464, 91–101. doi:10.1016/j.scitotenv.2013.05.058.

Elzinga, E. J., Van Grinsven, J. J. M., and Swartjes, F. A. (1999). General purpose Freundlich isotherms for cadmium, copper and zinc in soils. *Eur. J. Soil Sci.* 50, 139–149. doi:10.1046/j.1365-2389.1999.00220.x.

Flemming, C. A., and Trevors, J. T. (1989). Copper toxicity and chemistry in the environment: a review. *Water. Air. Soil Pollut.* 44, 143–158. doi:10.1007/BF00228784.

Frieler, K., Lange, S., Piontek, F., Reyer, C. P. O., Schewe, J., Warszawski, L., et al. (2017). Assessing the impacts of 1.5°C global warming - Simulation protocol of the Inter-Sectoral Impact Model Intercomparison Project (ISIMIP2b). *Geosci. Model Dev.* 10, 4321–4345. doi:10.5194/gmd-10-4321-2017.

García-Esparza, M. A., Capri, E., Pirzadeh, P., and Trevisan, M. (2006). Copper content of grape and wine from Italian farms. *Food Addit. Contam.* 23, 274–280. doi:10.1080/02652030500429117.

Giller, K. E., Witter, E., and Mcgrath, S. P. (1998). Toxicity of heavy metals to microorganisms and microbial processes in agricultural soils: A review. *Soil Biol. Biochem.* 30, 1389–1414. doi:10.1016/S0038-0717(97)00270-8.

Goldewijk, K. K., Beusen, A., Doelman, J., and Stehfest, E. (2017). Anthropogenic land use estimates for the Holocene - HYDE 3.2. *Earth Syst. Sci. Data* 9, 927–953. doi:10.5194/essd-9-927-2017.

Groenenberg, J. E., Römkens, P. F. A. M., Comans, R. N. J., Luster, J., Pampura, T., Shotbolt, L., et al. (2010). Transfer functions for solid-solution partitioning of cadmium, copper, nickel, lead and zinc in soils: Derivation of relationships for free metal ion activities and validation with independent data. *Eur. J. Soil Sci.* 61, 58–73. doi:10.1111/j.1365-2389.2009.01201.x.

Han, F. X., Banin, A., and Triplett, G. B. (2001). Redistribution of heavy metals in arid-zone soils under a wetting-drying cycle soil moisture regime. *Soil Sci.* 166, 18–28. doi:10.1097/00010694-200101000-00005.

Hannah, L., Roehrdanz, P. R., Ikegami, M., Shepard, A. V., Shaw, M. R., Tabor, G., et al. (2013). Climate change, wine, and conservation. *Proc. Natl. Acad. Sci. U. S. A.* 110, 6907–6912. doi:10.1073/pnas.1210127110.

Imfeld, G., Meite, F., Wiegert, C., Guyot, B., Masbou, J., and Payraudeau, S. (2020). Do rainfall characteristics affect the export of copper, zinc and synthetic pesticides in surface runoff from headwater catchments? *Sci. Total Environ.* 741, 140437. doi:10.1016/j.scitotenv.2020.140437.

Ivezić, V., Almås, Å. R., and Singh, B. R. (2012). Predicting the solubility of Cd, Cu, Pb and Zn in uncontaminated Croatian soils under different land uses by applying established regression models. *Geoderma* 170, 89–95. doi:10.1016/j.geoderma.2011.11.024.

Jacobson, A. R., Dousset, S., Guichard, N., Baveye, P., and Andreux, F. (2005). Diuron mobility through vineyard soils contaminated with copper. *Environ. Pollut.* 138, 250–259. doi:10.1016/j.envpol.2005.04.004.

Komárek, M., Čadková, E., Chrastný, V., Bordas, F., and Bollinger, J. C. (2010). Contamination of vineyard soils with fungicides: A review of environmental and toxicological aspects. *Environ. Int.* doi:10.1016/j.envint.2009.10.005.

Lange, S. (2016). EartH2Observe, WFDEI and ERA-Interim data Merged and Bias-corrected for ISIMIP (EWEMBI). *GFZ Data Serv.*

Li, B., Ma, Y., and Yang, J. (2017). Is the computed speciation of copper in a wide range of Chinese soils reliable? *Chem. Speciat. Bioavailab.* 29, 205–215. doi:10.1080/09542299.2017.1404437.

McBride, M., Sauvé, S., and Hendershot, W. (1997). Solubility control of Cu, Zn, Cd and Pb in contaminated soils. *Eur. J. Soil Sci.* 48, 337–346. doi:10.1111/j.1365-2389.1997.tb00554.x.

Mimikou, M. A., Baltas, E., Varanou, E., and Pantazis, K. (2000). Regional impacts of climate change on water resources quantity and quality indicators. *J. Hydrol.* 234, 95–109. doi:10.1016/S0022-1694(00)00244-4.

Mondaca, P., Neaman, A., Sauvé, S., Salgado, E., and Bravo, M. (2015). Solubility, partitioning, and activity of copper-contaminated soils in a semiarid region. *J. Plant Nutr. Soil Sci.* 178, 452–459. doi:10.1002/jpln.201400349.

Noll, M. R. (2003). *Trace Elements in Terrestrial Environments*. doi:10.2134/jeq2002.3740.

NumPy developers. (2017). NumPy — NumPy. *NumPy Website*, All.

Office, M. (2015). cartopy: a cartographic python library with a matplotlib interface. Available at: http://scitools.org.uk/cartopy.

Reimann, C., Filzmoser, P., and Garrett, R. G. (2005). Background and threshold: Critical comparison of methods of determination. *Sci. Total Environ.* 346, 1–16. doi:10.1016/j.scitotenv.2004.11.023.

Ribolzi, O., Valles, V., Gomez, L., and Voltz, M. (2002). Speciation and origin of particulate copper in runoff water from a Mediterranean vineyard catchment. *Environ. Pollut.* 117, 261–271. doi:10.1016/S0269-7491(01)00274-3.

Römkens, P. F. A. M., Groenenberg, J. E., Bonten, L. T. C., de Vries, W., and Bril, J. (2004). Derivation of partition relationships to calculate Cd, Cu, Ni, Pb, Zn solubility and activity in soil solutions. *Alterra* 305, 75. Available at: http://edepot.wur.nl/16988.

Rooney, C. P., Zhao, F. J., and McGrath, S. P. (2006). Soil factors controlling the expression of copper toxicity to plants in a wide range of European soils. *Environ. Toxicol. Chem.* 25, 726–732. doi:10.1897/04-602R.1.

Salminen, R., and Gregorauskiene, V. (2000). Considerations regarding the definition of a geochemical baseline of elements in the surficial materials in areas differing in basic geology. *Appl. Geochemistry*. doi:10.1016/S0883-2927(99)00077-3.

Sauvé, S., Hendershot, W., and Allen, H. E. (2000). Solid-solution partitioning of metals in contaminated soils: Dependence on pH, total metal burden, and organic matter. *Environ. Sci. Technol.* 34, 1125–1131. doi:10.1021/es9907764.

Unamuno, V. I. R., Meers, E., Du Laing, G., and Tack, F. M. G. (2009). Effect of physicochemical soil characteristics on copper and lead solubility in polluted and unpolluted soils. *Soil Sci.* 174, 601–610. doi:10.1097/SS.0b013e3181bf2f52.

van Rossum, G., and Drake, F. L. (2009). *Python 3 Reference Manual.*

van Vuuren, D. P., Edmonds, J., Kainuma, M., Riahi, K., Thomson, A., Hibbard, K., et al. (2011). The representative concentration pathways: An overview. *Clim. Change* 109, 5–31. doi:10.1007/s10584-011-0148-z.

Vidal, M., Santos, M. J., Abrão, T., Rodríguez, J., and Rigol, A. (2009). Modeling competitive metal sorption in a mineral soil. *Geoderma* 149, 189–198. doi:10.1016/j.geoderma.2008.11.040.

Vulkan, R., Zhao, F. J., Barbosa-Jefferson, V., Preston, S., Paton, G. I., Tipping, E., et al. (2000). Copper speciation and impacts on bacterial biosensors in the pore water of copper-contaminated soils. *Environ. Sci. Technol.* 34, 5115–5121. doi:10.1021/es0000910.

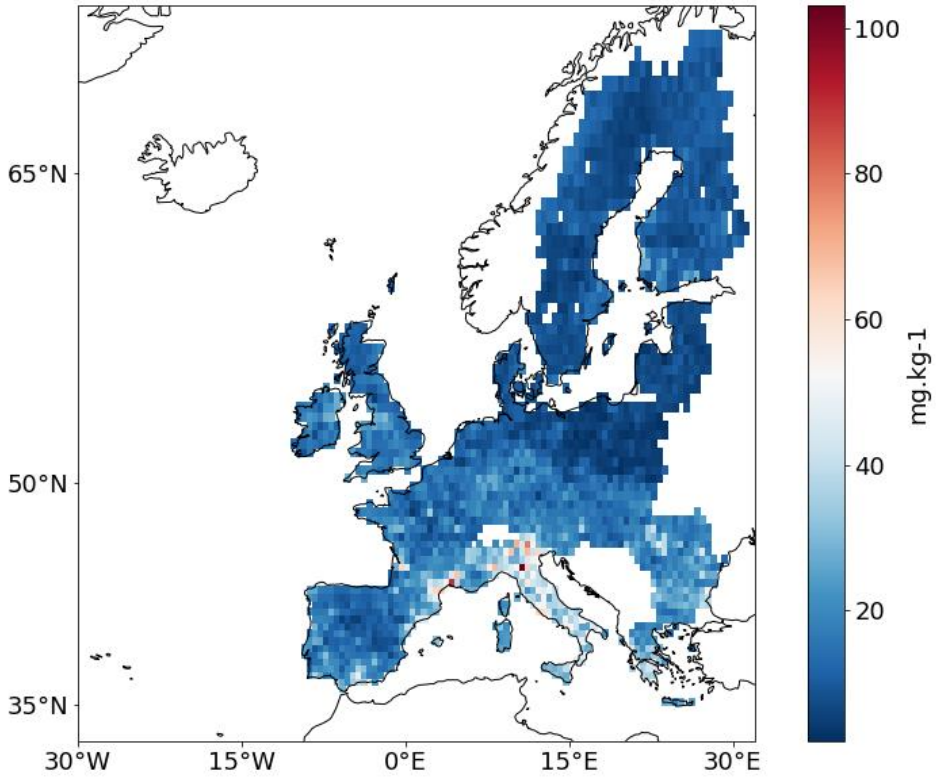

Suppl. Fig II.1.B.1: Map of total Cu (mg.kg soil $^{-1}$) at the European scale regridded at 0.5° from https://esdac.jrc.ec.europa.eu/content/copper-distribution-topsoils

Conclusion intermédiaire (2) :

En II.1.A nous avons pu souligner l'importance des co-facteurs pédologiques dans la définition des zones à risque vis-à-vis de la contamination, tandis que le chapitre II.1.B a permis de mettre en évidence les évolutions des risques avec le changement des précipitations. En II.1.B, la concentration effective en Cu n'a pas été inclue, mais notre étude prospective a permis de souligner les zones les plus à risque d'exporter du Cu actuellement ou dans le futur, et qui sont donc le plus à même de mériter le plus d'attention quant aux quantités de Cu apportées. En parallèle, les zones en aval sont susceptibles de connaître des apports en Cu via les eaux de ruissellement qui auraient pu ne pas être prisent en compte lors d'études locales. En revanche, nous n'avons pas pu considérer les différences de sensibilité des écosystèmes sous l'impact des doubles stress de contamination et de changement de précipitation ni intégrer les variations saisonnières de précipitation et d'humidité du sol.

Ainsi à la suite, le chapitre II.2. porte sur une étude locale de laboratoire précisant les effets de double stress d'humidité et de contamination sur les fonctions de nitrification du sol. L'étude sera menée en suivant 2 indicateurs : le Cu total et le Cu en solution, ce qui permettra donc non seulement d'estimer les effets de double stress sur les fonctions des sols mais également d'estimer les effets des changements pluviométriques sur la partition du Cu.

Chapitre II.2 : Estimation de l'effet d'une contamination au Cu après un stress d'humidité sur l'inhibition d'activités nitrifiantes du sol *

Le chapitre II porte sur l'impact d'un double stress (humidité du sol très faible, élevée ou variable avec des cycles d'humification-dessiccation suivi d'apport de Cu) sur les activités nitrifiantes des sols. Ce chapitre, basé sur des incubations de laboratoire, se découpe en deux sous chapitre : II.2.A. se concentre sur les effets du double stress exprimé en termes d'apport en Cu total sur l'inhibition des activités nitrifiantes, II.2.B cherchera à clarifier les effets d'un historique des précipitations sur la disponibilité du Cu et la pertinence d'un proxy tel que le Cu en solution dans les études éco-toxicologiques en contexte de changement climatique. Dans ce sous chapitre II.2.B, nous chercherons à déterminer si les effets du double stress observés en II.2.A sont dus à des modifications dans la disponibilité du Cu et/ou à une réponse de la communauté nitrifiante.

Le chapitre II.2 se rapporte aux interactions entre climat et contamination (impact des précipitations sur la disponibilité des contaminants), climat et sol (impact des précipitations sur la sensibilité des activités nitrifiantes au stress de Cu) et contamination et sol (impact de la contamination sur les activités nitrifiantes) telles que schématisées ci-dessous :

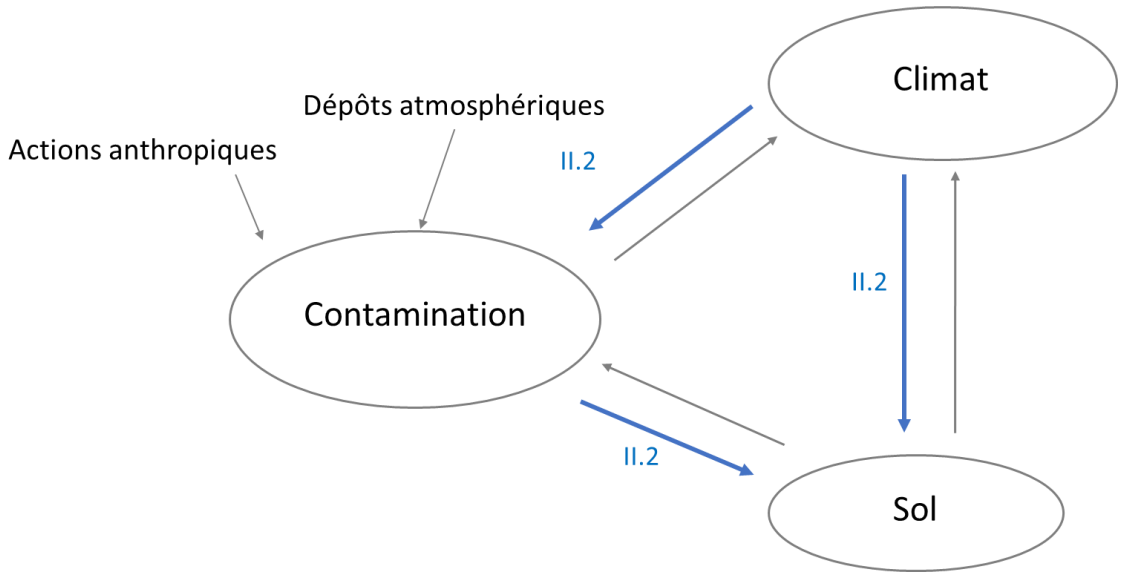

* Les expériences exploitées dans ce chapitre ont été réalisées dans le cadre du stage de M2 de Charlotte Blasi en 2015-2016 : Blasi C. 2017. Impact of climate change on threshold in terrestrial ecotoxicology. Internship report M2 Master Sciences, Technologies, santé, mention STEE et Chimie, spécialité EXCE (Ecotoxicologie et Chimie de l'Environnement), Université Bordeaux, 38pp + Annexes. Encadrement I. Lamy et B. Guenet

II.2.A. : Réponse de l'activité nitrifiante du sol à une contamination au Cu après un stress d'humidité du sol

Résumé en français

Certaines étapes du cycle de l'azote dans le sol, réalisées par un petit nombre de microorganismes du sol, sont sensibles aux pressions environnementales telles que l'humidité ou la contamination du sol. Au cours des prochaines décennies, on s'attend à ce que les régimes de température et de précipitations changent. Ces changements affecteront probablement le fonctionnement microbien ainsi que la disponibilité des contaminants mais restent encore peu documentés. Cette étude vise à évaluer l'importance de l'humidité du sol sur l'impact des contaminations sublétals en cuivre (Cu) sur une fonction du sol. Dans ce but, les activités nitrifiantes potentielles (PNA) ont été jugées être un bioindicateur approprié. Un sol limoneux a été incubé à 30, 60 ou 90% de sa capacité de rétention d'eau (WHC) ou en alternance de périodes de dessication-humectation. Ensuite, les échantillons de sol ont été exposés à un gradient de concentrations de Cu au cours d'un bio-essai. Les courbes dose-réponse de PNA en fonction du Cu ajouté ont été modélisées et nous avons comparé les différentes concentrations effectives de Cu (ECx) produisant x % d'inhibition de PNA pour mettre en évidence les différences dans les valeurs seuils. Les traitements d'humidité de préincubation ont affecté de manière significative les réponses de PNA au stress secondaire de Cu avec, par exemple, des réponses hormétiques dans tous les cas sauf dans le cas d'alternance d'assèchement et de réhumectation. De plus, des différences significatives ont été trouvées dans les ECx estimées pour les traitements d'humidité. De faibles inhibitions de la PNA ont été estimées pour des doses élevées de Cu dans les sols à faible teneur en eau (30% WHC) ou avec plusieurs cycles dessiccation-humectation. Au contraire, l'inhibition des sols soumis à des teneurs en eau élevées ou à une seule période de sécheresse s'est faite pour des teneurs en Cu plus élevées. Ces résultats sont discutés en termes d'impact des multi-stress sur le fonctionnement du sol et de valeurs seuils d'inhibition de la PNA.

II.2.A. Responses of soil nitrification activities to copper after a moisture stress –

Laura Sereni[1]*, Bertrand Guenet[2], Olivier Crouzet[1,3], Charlotte Blasi[1,4], Isabelle Lamy[1]
[1] University Paris-Saclay, INRAE, AgroParisTech, UMR ECOSYS, Ecotoxicology Team, 78026, Versailles, France
[2] Laboratoire de Géologie de l'ENS, PSL Research University, CNRS, UMR 8538, Paris, France
[3] Present address: Office national de la chasse et de la faune sauvage, Site d'Auffargis-Saint-Benoist 78612 Le-Perray-en-Yvelines, France
[4] Present address: Centre Sève, Département de Chimie, Université de Sherbrooke, Sherbrooke, QC, Canada
*Correspondence: Laura Sereni laura.sereni@inrae.fr

Submitted in: Environmental Science and Pollution Research on October 13th 2021

Abstract:

Some steps of the soil nitrogen cycle, performed by a small number of soil microorganisms, are sensitive to environmental pressures like soil moisture or contamination. Temperature and rainfall patterns are expected to change during the next decades, which likely affect microbial functioning as well as contaminant availability in a way that is still poorly documented. This study aimed at assessing the importance of the soil moisture on the impact of sublethal copper (Cu) contaminations on a soil function. In this aim, the potential nitrifying activities (PNA) was selected as a suitable bioindicator. A loamy soil was incubated in either 30, 60, or 90% of its water holding capacity (WHC) or in alternance of drought and rewetting periods. Thereafter, soil samples were exposed to a gradient of Cu concentrations through a bioassay. The dose-response curves of PNA in function of added Cu were modelled and we compared the different effective Cu concentrations (ECx) producing x % of PNA inhibition to highlight differences in threshold values. The preincubation moisture treatments significantly affected the PNA responses to the secondary Cu stress with, for instance, hormetic responses in all cases except for the dry-rewetting treatment. Moreover, significant differences were found in estimated ECx values between moisture treatments. Small PNA inhibitions were estimated for high Cu doses in the soils with a low water content (30% WHC) and with several dry-rewetting cycles contrarily to the pattern observed for high water contents (90% WHC) or submitted to a single period of drought. These results are discussed in terms of multi-stress impact on soil functioning and threshold values of PNA inhibition.

Keywords: successive stress, climate change, dry-rewetting, microbial indicator, toxicological thresholds, dose-response

1. INTRODUCTION

With the current scenarios of climate change, rainfall patterns are expected to change during the next decades (Lee et al., 2014) with more intense and longer drought periods followed by intense rainfalls. These modifications in the rainfall patterns may impact the soil water contents during critic periods. Excess of water or drought may affect soil moisture which is one of the main drivers of the soil microbial activity (Moyano et al., 2013). In parallel, human activities have dispersed significant quantities of contaminants into the environment, such as trace elements which are persistent and potentially toxic for the life soil biota (Giller et al., 2009). Nowadays, the contamination of soils by trace elements coming from atmospheric source or through agricultural practices has become a major concern at a global scale (Song et al., 2012). Trace element contaminations affect several environmental processes such as those performed by soil microorganisms (Giller et al., 2009) and soil microbiological indicators (abundance, diversity or activity) are hugely used to assess soil contamination. Microbial activities related to specific narrow niche processes are among the most sensitive endpoints to assess soil contaminant impacts (Broos et al., 2005). Therefore, bioassays measuring activities performed by microorganisms are useful to assess the severity of stress encountered by the soil ecosystem and possible outcomes on soil functions.

Microbial communities would encounter multi-stress of both global climate changes, soil contaminations and their combined effects, these last ones being less documented. Soils nitrifying communities have been shown to be highly sensitive to heavy metal stress as a Cu contamination (Ruyters et al., 2010; Smolders et al., 2001) as well as to soil moisture variations (Van Groenigen et al., 2015). However, effects of a first more or less mild stress on the response of microbial functions to a secondary stress are not well known, with reported increase or decrease of resistance depending on the stress (Philippot et al., 2008; Rusk et al., 2004). In this context, it is difficult to predict the combined effect of climate change and contamination pressures on soil functions performed by soil organisms.

This work investigated the outcomes of an ecological stress ascribed to soil moisture on a chemical stress induced by copper (Cu). We focused on the effect of new-born exogenous Cu contaminations spiked to a soil which was first submitted to various moisture stresses: constant, small, or high soil moistures but also intermittent intense moisture stresses with drought and rewetting cycles. Cu was used as a model of contaminant because it is widely found in the soils in particular in Europe (Panagos et al., 2018) mainly due to its use as fungicide in agriculture. Cu concentration thresholds for soil management could vary largely depending on the agricultural policies. We also focused on PNA as an end-point. The nitrogen (N) cycle is an important contributor of emissions of greenhouse gases (GHG), particularly from agricultural sector. For instance, N_2O is a powerful GHG with approximatively 256 fold the warning potential of CO_2 on a 100-year time horizon (Myhre et al., 2013). Moreover, N cycle is performed by a limited number of microorganisms, making it more sensitive to environmental pressures than C cycle (Broos et al., 2005). Also, N cycle is highly sensitive to soil moisture as nitrifying and denitrifying communities concur in soils depending of its oxygenation and thus of its moisture (Van Groenigen et al., 2015).

In this context, the aim of our study was to assess the effect of the soil moisture history - used here as one of the factors of climate change - on the impact of added Cu on potential nitrification - used here as a proxy of the soil nitrification process. Thus, a dose-response approach was carried out. First, absolute PNA (aPNA) responses after moisture and Cu stresses were quantitatively analysed. Then relative PNA (rPNA) responses compared to the no-added Cu sample were used to both 1) compare the pattern of the dose-response curves and 2) determine effective Cu concentrations inducing 5, 10, 20, and 50% (EC 5, 10, 20, 50) of decrease in rPNA. We hypothesized that 1) the pre-incubation periods

under various moisture treatments affect the microbial community function related to the N cycle; 2) consequently the dose-response curves rPNA = f(added Cu) show different patterns with the various moisture pre-treatments; and 3) effective Cu concentrations are useful indicators to highlight differences in threshold values when a stress on stress occurs.

2. MATERIALS AND METHODS

2.1 Soil sampling

The soil, described in Obriot et al., (2016) as a luvisol with 11g/kg of organic carbon and pH 6.9, was sampled in January 2017 in the control plot of the experimental Qualiagro site (48°87'N, 1° 97'E 17). This agricultural plot is not contaminated with Cu (no registered inputs since more than 20 years).Its Cu content is around 12 mgCu.kg^{-1} consistent with the regional pedogeochemical background. Several fresh soil samples were pooled and immediately sieved at 5mm and stored at 4°C few days before building-up the microcosms to drive soil moisture regimes. Aliquots of this sieved soil were used to measure the fresh soil moisture at the time of sampling which was 15% and the field capacity as maximum water holding capacity (WHC) which was set up at 32% (w/w).

2.2. Experimental setup

To evaluate the impact of soil moisture on the sensitivity of nitrification to Cu toxicity, a two steps experimental approach was carried out: a first pre-incubation period of five weeks was running under different moisture stresses before application of a secondary metal contamination stress during a 72h bioassay allowing evaluation of the absolute and relative potential nitrifying activities).

2.2.1. Microcosms to drive soil moisture regime

Five microcosms of about 500 g of soil were incubated in five plastic boxes maintained half-open during 35 days and submitted to different treatments. Starting from the known initial moisture, three microcosms were set up at 30%, 60% and 90% of the soil WHC. This WHC was then kept constant by weighting and were made in order to roughly span respectively limiting, optimal, and close to water saturation treatments for the microbial activity. Later on, these three treatments will be called "30%, 60% and 90%", respectively. The two others microcosms were incubated with variable WHC in order to simulate two kinds of drought and dry-rewetting cycles. One was left for about 3 weeks dry period without water inputs (gentle air drying) until 10% of the WHC before progressively rewetting at 60% WHC, while the other was treated with alternative cycles of one-week dry period (10% of the WHC by air-drying) followed by one week near-saturation period (90% WHC). Drying was performed by natural evaporation and moisture control by weighting. These two samples will be called thereafter "Drought" (DO) and "Dry-rewetting" (DR). The concentrations of N-NO_2, N-NO_3, N-NH_4 and dissolved organic carbon (DOC) at the end of the pre-incubation period for the controls without added Cu and for each of the 5 moisture treatments are presented in table II.2.A.1.

Table II.2.A.1: Mean and standard error (Std error) of concentration of N species and dissolved organic carbon (DOC) for the 3 replicants of each pre incubation moisture condition at the end of the preincubation showing negligible values of N-NO_2.

	N-NO_3 (µg / g de sol)	N-NO_2 (µg / g de sol)	N-NH_4 (µg / g de sol)	

Moisture condition	mean	Std error	mean	Std error	mean	Std error	DOC [mg.L-1]
30	14.64	0.53	0.14	0.02	4.26	0.23	5.45
60	18.77	0.05	0.16	0.03	6.84	0.10	4.61
90	23.92	0.32	0.21	0.00	9.91	2.39	4.01
DO	27.43	2.06	0.29	0.08	6.23	1.07	4.41
DR	29.34	0.86	0.22	0.08	4.03	0.82	3.73

2.2.2. Bioassay to assess further Cu impact

After the pre-incubation period, the soil bioassays were immediately performed by measuring nitrate (NO_3^-) production rates over a short-term aerobic incubation in soil slurries (ratio soil:solution 1:6) with ammonium in excess and in the presence of gradients of Cu concentrations. The soil potential nitrification was then calculated on the basis of NO_3^- measurement over the time period. The PNA bioassays were adapted from the methods proposed by (Tom-Petersen et al., 2004). Briefly, 5 g of fresh soil (approximately 4.7g of soil equivalent dry weight), were mixed in a Falcon® tubes with 29mL of a 10 mM HEPES buffer solution (hydroxyethyl piperazineethanesulfonic acid, Sigma-Aldrich, France) to maintain a constant pH under Cu spiking and nitrification activity, and containing the substrate $(NH_4)_2SO_4$ (3 mM) (Sigma-Aldrich, France). Then, 1mL of Cu solutions at different concentrations were added to reach final added Cu concentrations of 50, 100, 250, 500, 750, 1000 and 2000 mgCu. kg^{-1} soil. Controls with only Milli-Q® water (Millipore) were also performed. Three independent samples (n = 3) from each pre-incubation treatment were ran in three concomitant bioassays for each Cu concentrations. Following an initial horizontal shaking step (250 rpm, 10 min), the soil slurries were left incubated on a rotary shaker (150rpm), under aerobic treatments, at 25°C during 72h. After 10 min, 24 h and 72 h of incubation, 2 mL aliquots of the soil-solution mixture were transferred in Eppendorf® vials and centrifuged for 5 min at 13000 *g* at 4°C. The supernatants were collected and stored in microplates at – 20 °C until analyses of NO_3^- and NO_2^- by colorimetric determinations, following the reduction of NO_3^- in NO_2^- by vanadium(III) and then the detection of NO_2^- by the acidic Griess reaction (Miranda et al., 2001). Three different aliquots from each bioassay tube were analysed. Finally, the absolute value of PNA, aPNA in µg N-NO_3 g^{-1} soil h^{-1}, was calculated on the basis of N-NO_3^- + N-NO_2^- concentrations measured at the different time steps. The points Cu=0 allowed us to verify that NO_2^- contents were negligible (table II.2.A.1), so that aPNA followed eq. II.2.A.1, by checking the linear production rate between 2 h, 24 h and 72h:

$$(\text{II. 2. A. 1.})\ aPNA = \frac{[NO_3^-]_{Tfinal} - [NO_3^-]_{Tinitial}}{Tfinal - Tinitial} \times Vs \div W$$

With

Vs: Volume of solution

W: Weight of fresh soil

T: Time of incubation

For each moisture treatment, the relative PNA values, rPNA values in %, were calculated by dividing aPNA for each added Cu level by the aPNA without added Cu.

2.3. Statistical analysis for the different moisture treatment on Cu comparison

Data of aPNA values between the different moisture treatments were compared for each Cu level with the use of Kruskal Wallis test followed by a post-hoc Dunnett test. Adjustment of p-value for multiple comparison was made by Holm procedure to limit false negatives.

Dose responses curves for rPNA were analysed with the DRC package, following recommendations of (Ritz 2010; Ritz et al., 2015). For the dose responses curves fitted by the same functions, the parameters were compared using the compParm function of the DRC package (see 2.4).

ECx comparisons were made through the estimated confidence intervals (IC), so that for each ECx the moisture treatment with overlapping IC was not significant different.

All analysis were conducted using R v4.1 (R Core Team 2021).

2.4. Dose-response curves analysis

To fit the dose-response curves, we have proceeded by different steps according to our aims of both estimate and compare the variations in rPNA due to Cu contamination stress under the different moisture stresses. Expected results are to provide EC5, EC10, EC20 and EC50 values as % response (at 95% confidence interval) expressed as rPNA for each moisture treatment.

For the first aim, i.e. estimating the variations in rPNA, the selection of the best dose-response model able to fit the experimental data was achieved by testing the following widely used models in ecotoxicology studies (Ritz et al., 2015): the log-normal (LN) dose-response model, or the log-logistic (LL) and their Weibull derivative (W1 or W2), or the hormetic models as the Cedergreen models (CD, tested with alpha =1 and alpha=0.25), the Gompertz (G) model, or the Braincousens models (BC.4 or BC.5 depending of the number of parameters to be fitted). Lower asymptotes were fixed to 0 and upper to 1 except for the hormetic models.

For the second aim, we considered that the comparison of the dose response curves and their parameters as a whole between all the moisture treatments better required using a common model for all the curves, contrarily to ECx determinations that required more precise fits to extract ECx values. We thus compared the five best models per moisture treatment according to AIC and logLik criteria and confirmed the choices by visual confidence interval accordance (limited confidence interval). From these five pre-treatments x 5 models we looked for a common model. If no common type of model was found powerful enough to extract ECx values, we selected more types of models for these extractions.

3. RESULTS

3.1. Absolute PNA evolution under successive stresses

Fig 1 shows the mean, 1st and 3rd quartile of aPNA values obtained for all pre-incubation treatments (DR, DO and, 30, 60 and 90% WHC treatments) in function of the Cu concentration gradient.

The comparison between the control bioassay without Cu (Fig. 1, Cu 0) and the values in the presence of added Cu shows that the moisture pre-incubation treatments significantly affect the aPNA. Significant differences were found between aPNA for soils incubated under DR stress and soils incubated under 60% WHC, with aPNA values roughly smaller by one third in the soils submitted to dry and rewetting cycles (DR treatment).

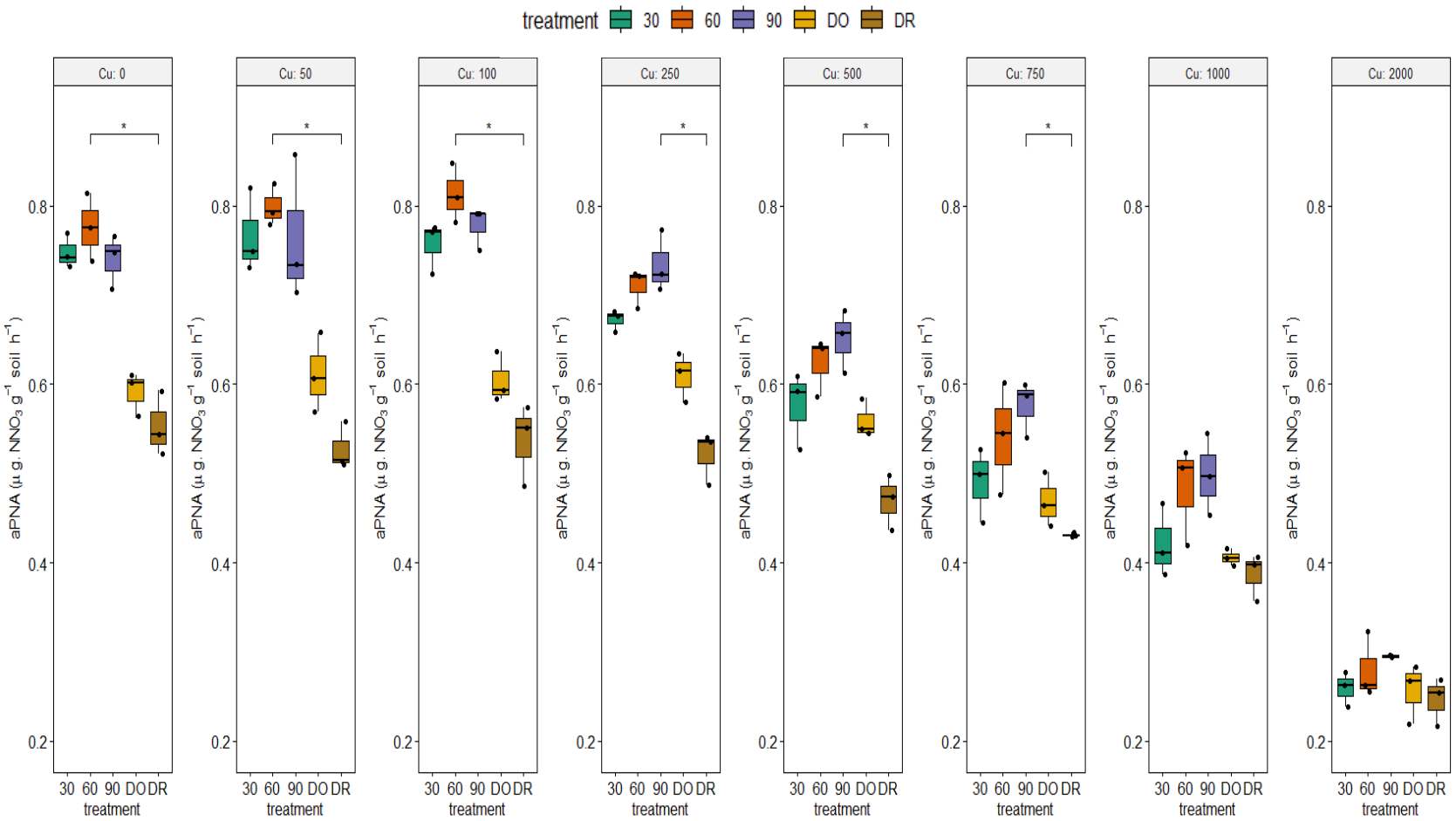

Fig. II.2.A.1: Mean, 1st and 3rd percentile of aPNA measured at the end of the bioassay for each incubation treatment and added Cu concentration. Preincubation treatment are represented per color with 30%WHC in green, 60% in orange, 90% in purple, DR in yellow and DO in brown. For each Cu level, post hoc Dunett test with Holm procedure was applied. Significant differences in PNA between moistures treatments are indicated by brackets branches and notated with stars (* : p.v <0.05)

The aPNA values decreased with increasing soil Cu concentrations and the moisture pre-treatment differently affected the aPNA inhibition by Cu stress. At the highest Cu doses (>1000 mgCu.kg^{-1}), no more differences in aPNA values could be observed whatever the moisture treatments. Therefore, above a threshold of 1000 mgCu.kg^{-1}, the effects on the nitrification processes were the same whatever the initial moisture pre-incubation.

3.2. Relative PNA evolution under successive stresses analysis with dose responses curves

3.2.1 Selection of dose responses models for ECx estimation.

Suppl. Table II.2.A.1 gives the values of the criteria obtained for the five best fit of each of the dose-response curves: rPNA inhibition = f (total added soil Cu). Model selection based on the lowest value of AIC and higher value of LogLikelihood criteria showed that Cedergreen (alpha=1) and Braincousens or Weibull models are the best ones describing the inhibition of rPNA in function of total added Cu for incubation performed under constant moisture treatments (Supp Table II.2.A.1a). Cedergreen and Braincousens models integrate hormesis parameters, so that modelling included our observations of an increase in rPNA at small Cu inputs in several moisture treatments (Fig. II.2.A.2A).

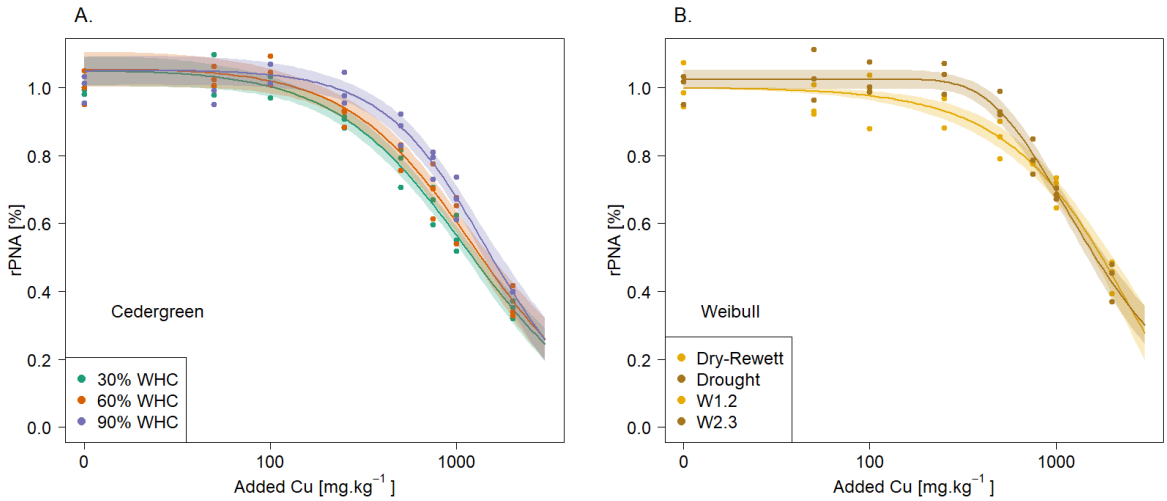

Fig. II.2.A.2: Fit of the selected function on the AIC criteria to model rPNA responses to added Cu with 95% confidence interval. A. In the case of the incubation performed at constant moisture (30% in green, 60% in orange and 90% WHC in purple) with fit of Cedergreen functions. B. In the case of the incubation performed under DR (dry rewet, yellow) and DO (dry only, brown) moisture treatment with fit of Weibull functions. Weibull model of the first type was used in the case of the dry-rewet incubation and Weibull model of the second type was used in the case of the dry only treatment.

If we consider the AIC criterion, inhibition of rPNA in DO incubated soils were better described by Braincousens or Weibull II and DR by Weibull I models (Suppl. table II.2.A.1b). But for DO the Weibull fit indicators (AIC, Lack of Fit…) were close to those of Braincousens, and we chose using Weibull for homogeneity with the DR modelling to further extract ECx values. This means that rPNA inhibition of soils incubated under DO treatment was poorly affected by the Cu gradient for low Cu concentrations. On the contrary, soils incubated under DR treatment are largely affected by variations of moderate Cu concentrations but poorly by the highest (Fig. II.2.A.1, II.2.A.2).

In order to compare the parameters of the dose-responses models selected taking into account their biological meaning, only one type of dose response model had to be selected. For that, we looked at using a single model whatever the pre-treatments. We also tested specifically the Cedergreen modelling function in the case of DO and DR conditions for two reasons: i) Braincousens and Cedergreen models are both hormetic models and ii) the Cedergreen fits were found acceptable compared to Braincousens for all the constant moisture treatments.

3.2.2 Effect of pre incubation on dose-response curves.

The Cedergreen parameter models finally obtained are given in table 2, and are significantly different from 0 ($p < 0.05$) for all pre-incubation treatments except the hormesis effect in DR. This means that stimulation of the rPNA at low Cu concentration is not possible in the case of DR treatment (table II.2.A.2, Fig II.2.A.2B). No differences in the size of the hormetic effect (f parameter, table II.2.A.2) were found between all the four other treatments. For these four other treatments, we were able to estimate the maximum estimated response (e.g. the maximum increase in the potential nitrifying activities) and associated Cu concentration. In all cases (30, 60, 90 %WHC and DO), the increase in rPNA

at small doses of added Cu is limited to 5% (maximal response expected from 1.047 to 1.052 % of aPNA). The associated Cu concentration modelled by the Cedergreen fit was roughly twice higher for the 90% WHC and the DO treatment than for the 30 and 60% WHC treatments (22 and 26 mgCu.kg^{-1} against 11and 14 respectively).
In parallel, the "b" parameter which represents the steepness of the curve after hormesis is found significantly higher in the DO case than in the four other treatments, whereas it was found significantly smallest in the 30% WHC case. This means that for DO treatments the decrease in rPNA is higher for smaller Cu concentration and that for 30 % WHC the decrease in rPNA is smallest with the increase in Cu concentration.

No straightforward interpretation of the "e" parameter could be draw as it only represents the low limit for the EC50 values and not a precise estimate. However, from the fitted results we may expet highest EC50 values with highest moisture incubation treatments and even more with DR and DO treatments (table II.2.A.2).

Table II.2.A.2. Estimated coefficients and standard error for the Cedergreen model used to fit all the dose-response curves of rPNA against total added Cu concentration in the form
$rPNA = \frac{1+f*\exp\left({}^{-1}/_{Cu\ tot}\right)}{1+\exp\left(b*\log(Cu\ tot)-\log(e)\right)}$.
p-value are reported for test against 0. Last column refers to comparison of the 5 pre treatment for each coefficient. Coefficient sharing the same letter in the last column are not statistically different.

coefficient	Estimate	Standard Error	p-value	Moisture Condition	Statistical comparisons
b	1.22	0.13	1E-15	30	a
	1.28	0.13	1E-15	60	ab
	1.56	0.15	8E-18	90	b
	1.67	0.15	5E-19	DO	bc
	1.59	0.19	1E-13	DR	b
e	1120.2	75.6	9E-28	30	a
	1243.8	78.0	3E-30	60	a
	1450.4	77.3	1E-35	90	cd
	1558.4	81.6	3E-36	DO	de
	1805.5	114.4	9E-30	DR	e
f	0.056	0.029	0.06	30	a
	0.060	0.027	0.02	60	a
	0.053	0.021	0.01	90	a
	0.051	0.020	0.008	DO	a
	-0.030	0.020	0.1	DR	NS

3.3. Estimation of the effective Cu concentrations inducing PNA inhibitions

ECx extraction was made on the basis of Cedergreen models for the constant moisture treatment and on Weibull models for the treatment with various moisture (Weibull II for DO, Weibull I for DR).

Table 3 gives the values of EC5, EC10, EC50 for each soil moisture status. For a given percentage of rPNA inhibition, we found significant differences in the estimated amounts of Cu inhibiting rPNA between the different moisture pre-treatments (Table II.2.A.3). For instance, a 5% rPNA inhibition was predicted for a low soil Cu contents of 185 (±66) $mgCu.kg^{-1}$ for the 30% WHC pre-treatment but a higher soil Cu content of 405 (±88) $mgCu.kg\ soil^{-1}$ was predicted for soils pre-incubated under DO treatment. In parallel, a 20% rPNA inhibition was predicted for a low soil Cu content of 440 (±88) $mgCu.kg^{-1}$ for the 30% WHC pre-treatment but for a higher soil Cu content of 721 (±95) $mgCu.kg\ soil^{-1}$ for soils pre-incubated under DO treatment. These results suggest that drought is highly affecting for a subsequent Cu contamination compared to drought followed by a progressive rehumectation. This pattern is found again for all the x levels except for the 50% level. Taken into account the lower and upper values of EC5, we estimated that rather small Cu total concentrations added to soil around 185 $mgCu.kg^{-1}$ are able to induce a decrease in potential nitrifying activities when the soils is at 30% and 60% WHC but not for soils at 90% WHC or when soil is subjected to DO pre-treatment. In the same manner, we estimated that a value of around 400 $mgCu.kg^{-1}$ reduced rPNA by only 5% in the sample subjected to DO pre-treatment while about roughly 20% of rPNA inhibition was observed in the soil sample at 30% WHC.

Except for x = 50, the ECx values calculated for DO were always found higher than for DR. However, the differences were only significant in the case of EC5. On the other hand, and for a given pre-incubation, we observed no significant differences between the estimated EC5 and 10 (Table II.2.A.3). For x = 50, the EC50 values were found significantly higher after DR pre-treatment (1763 ± 230 $mgCu.kg^{-1}$) than at 30% WHC (1220 ± 179 $mgCu.kg^{-1}$ for the 30% WHC, table II.2.A.3), and tend to be higher for DR than for DO but with no significant differences.

Table II.2.A.3: Effective Cu concentration ECx inducing x% of rPNA inhibition with x = 5, 10, 20, or 50%. ECx estimates are in $mgCukg^{-1}$ soil and derivate from the functions cedergreen (method= CD) or weibull (method= W) taken into account the total added Cu concentrations. Lower and upper estimated values (95% CI) are given in $mgCukg^{-1}$ soil; moistures of 30, 60 and 90 refer to conditions of pre-treatments with 30, 60 and 90 % WHC, DR to dry rewet and DO to dry only. Last column refers to comparison of the 5 pre treatment for each x level. Coefficient sharing the same letter in the last column are not statistically different.

X level	Moisture	Estimate	Lower	Upper	Method	Comparison
5	30	184.9	119.2	250.7	CD	a
	60	231.3	156.6	306.1	CD	a
	90	348.8	253.0	444.7	CD	ab
	DO	404.8	316.8	492.7	W2	b
	DR	189.4	111.6	267.1	W1	a
10	30	265.8	193.8	337.8	CD	a
	60	323.4	241.3	405.4	CD	ab
	90	465.4	366.2	564.7	CD	b
	DO	516.9	425.2	608.6	W2	b
	DR	350.9	249.7	452.1	W1	ab
20	30	439.8	352.0	527.6	CD	a
	60	517.8	421.4	614.2	CD	ab
	90	693.1	586.8	799.3	CD	b
	DO	721.1	626.3	815.9	W2	b
	DR	667.6	552.8	782.4	W1	b
50	30	1221.9	1042.8	1401.0	CD	a
	60	1358.9	1155.7	1562.0	CD	ab
	90	1548.7	1329.0	1768.5	CD	ab
	DO	1577.7	1374.3	1781.1	W2	b
	DR	1763.4	1533.1	1993.7	W1	b

4. DISCUSSION

4.1. Use of PNA as indicator of successive moisture and chemical stress events

PNA is a frequently used indicator of soil contamination and of loss of soil functions (Broos et al., 2007; Hund-Rinke & Simon, 2008) despite its high variability in non-polluted soils (Sauvé et al., 1999). Here we submitted the soil samples first to a moisture stress before applying a secondary metallic stress, and we focused on the potential soil nitrification activities response to these two conjugated stresses. Thus, aPNA measured in our bioassay is a reflection of the activity of the whole nitrifying community selected through microcosm moisture treatments and its ability to resist to a subsequent Cu stress. Dry-rewetting cycles for soils have been reported to enhance C and N mineralization due to nutrient flush with rewetting (Birch, 1958) but with various effects on NO_3^- concentrations depending on the soil use or on the number of dry-rewetting cycles (Fierer & Schimel, 2002). Our hypothesis was that the various moisture stresses do not select the same communities inducing different nitrate production abilities. This is consistent with our results showing that rPNA values were affected by the pre-incubation moisture with roughly 30% inhibition in the soils incubated under DO or DR treatments compared to the soils incubated at a constant moisture.

PNA measurements can also be used as a sensitive tool to define ecotoxicological guidelines (Broos et al., 2005). In the literature, it is often noticed that EC50 values are difficult to obtain mostly due to the fact that dose-response curves are rarely fully complete until the end-point being zero. The determination of EC50 values by extrapolation could thus be less interesting and more ambiguous than the determination of threshold with smallest ECx with x<50. In our experiments, we only measured 2 cases where rPNA was inhibited higher than 50% whatever the pre-incubation treatment, and we never reached a plateau in rPNA inhibition. Despite the fact that satisfying at least one of these two conditions is a guarantee to provide accurate estimates (Sebaugh, 2011), our results showed limited incertitude around the estimated ECx values. For the high EC values we obtained an incertitude of 14% in added Cu in mean compared to the 31% of total added Cu in mean concentration for the small EC (EC5).

The beginning of the dose-responses fits for the small concentrations of added Cu provided hormesis effects with different ranges (table II.2.A.2 and estimated max PNA). This variability in the range of the small dose effects is not captured by ECx values with small x, but rather lead to large incertitude's in EC5 determinations. Such incertitude decreased for EC10 and EC20. Also, if ECx data are useful threshold providing values easily transferable in terms of contamination management, their determination after modelling may be not sufficient to identify smallest dose effects. Finally, the use of PNA as indicator of successive moisture and chemical stress events was powerful in our conditions to highlight an effect of moisture on the response of a soil to a Cu stress, and to allow comparison of ECx for different moisture pre-treatment in particular for x = 20.

4.2. Effects of a double stress as preliminary moisture stress followed by a Cu stress

In the present laboratory study the Cu stress was applied secondary of the dry-rewet or constant moisture events. In the field, it can also happen that dry rewet events occur in Cu contaminated soils, which is another scenario as the one we studied.

In this framework, our results show that moisture soil history changes the soil PNA response to a supplementary stress. Soil samples submitted to a single long dry cycle (DO) or staying at 90% WHC seemed to be more tolerant to a subsequent Cu stress than for those submitted to dry-rewetting cycles periods (DR) or 30% WHC (Fig. II.2.A.1, table II.2.A.3). The 60% WHC microcosms were found in-between these two cases. This can be clearly seen through the higher EC5 to EC20 values for DO soils. The rather surprising result concerning DO could be due to our experimental design where the last week the sample was gently moistened back from 10 to 60%WHC. For DR, we hypothesized that this incubation strongly selected communities. Indeed, it has been shown that less diverse microbial communities may be more sensitive to subsequent stress (Hallin et al., 2012). The hypothesis of a highest primary stress in the soils incubated under DR treatment is somehow supported by the absence of hormesis, whereas in the four others treatments low Cu concentrations induced slight increases in PNA, suggesting that microbial communities could have enough resources to do so.

For the soils incubated at 30% WHC, no effect of pre-incubation period was noticed on PNA without added Cu but we noticed a high sensitivity to Cu contamination that could be due either to a low pool of microorganisms resistant to Cu or to a high level of Cu bioavailability.

On the contrary, the soils incubated at 90% WHC showed high resistance to Cu that could either be due to a lower Cu availability in the soil solution or to a higher pool of soil bacterial communities resistant to Cu. To disentangle between these hypotheses, it could be interesting to design the experiments by including proxy of Cu availability as well as characterization of the communities (structure or diversity) after the first stress to assess potential differences in the modifications of microbial communities between the pre-incubations.

Finally, we observed that the aPNA values were found different between the constant and various moisture pre-treatments only for the lowest part of the dose-response curves, thus for low added Cu concentrations, and became similar at highest added Cu concentrations (Fig. II.2.A.1). Such a result suggests that the pre-incubation patterns have modified the sensitivity (Cu concentration initializing a loss of function) but not the resistance (disappearance of the function) of aPNA. However, we cannot conclude if the aPNA measured under 2000 mgCu.kg^{-1} are minimal values (Fig. II.2.A.1) due to microbial highly resistant groups or if higher levels of Cu would have reduced aPNA.

5. CONCLUSION:

Our study showed that pre-incubated soils at low moisture (30% WHC) were more sensitive to a secondary Cu stress than those pre-incubated at a higher moisture (60 and 90% WHC), with EC5 values defined respectively around 185 (±66), 231 (±75) and 349 (± 96) mgCu.kg^{-1}. Soils submitted to gentle drought (DO) then gentle rewetting were surprisingly less sensitive to Cu with a EC5 value at 404 (± 88) mgCu.kg^{-1} whereas soils submitted to drastic changes in moistures (DR) lost nitrification activities as soon as low amounts of Cu (EC5 = 189 (±78) mgCu.kg^{-1}) indicating their sensitivity to the second stress. These Cu amounts in agricultural parcels are not seldom with Cu inputs through fertilizers or pesticides resulting from several years of cumulative inputs (Panagos et al., 2018). Nevertheless, our results showed that climate and particularly rainfall patterns have to been considered because micro-organisms and the soils functions they provide may be differentially affected by Cu stress depending on the soil moisture history. Our results showed that differences in PNA values between the moisture

histories we studied decrease when the Cu contamination increases. We also show that ecotoxicological studies based on ECx determination should be complete by dose-responses curves fitting analysis that highlight more precise patterns. Indeed, this permit us to emphasize small increases in PNA for low added Cu concentration close to 20 mgCu.kg^{-1} for four to five preincubation treatments that were not exemplified through ECx determinations. Considering the key roles of the soil N emissions in the GHG emissions, our results could be useful to provide a combined estimation of nitrification and denitrification fluxes and activities of the microbial communities involved in these functions in the context of climate change and soil contamination.

Conflict of interests:
The authors declare there is no conflict of interests

Acknowledgments:
Parts of this study were financially supported by the ANR CESA-13-0016-01 through the CEMABS project and the Labex BASC through the Connexion project. LS thanks ENS for funding her PhD. The author thanks Amélie Trouvé for her help in soil data analysis, Sébastien Breuil for soil processing and Christelle Marrauld for her help in the bioassay design.

References

Birch HF. 1958. The effect of soil drying on humus decomposition and nitrogen availability. Plant Soil. doi:10.1007/BF01343734.

Broos K, Mertens J, Smolders E. 2005. Toxicity of heavy metals in soil assessed with various soil microbial and plant growth assays: A comparative study. Environ Toxicol Chem. 24(3):634–640. doi:10.1897/04-036R.1.

Broos K, Warne MSJ, Heemsbergen DA, Stevens D, Barnes MB, Correll RL, McLaughlin MJ. 2007. Soil factors controlling the toxicity of copper and zinc to microbial processes in Australian soils. Environ Toxicol Chem. doi:10.1897/06-302R.1.

Fierer N, Schimel JP. 2002. Effects of drying-rewetting frequency on soil carbon and nitrogen transformations. Soil Biol Biochem. doi:10.1016/S0038-0717(02)00007-X.

Giller KE, Witter E, McGrath SP. 2009. Heavy metals and soil microbes. Soil Biol Biochem. doi:10.1016/j.soilbio.2009.04.026.

Van Groenigen JW, Huygens D, Boeckx P, Kuyper TW, Lubbers IM, Rütting T, Groffman PM. 2015. The soil n cycle: New insights and key challenges. Soil. 1(1):235–256. doi:10.5194/soil-1-235-2015.

Hallin S, Welsh A, Stenström J, Hallet S, Enwall K, Bru D, Philippot L. 2012. Soil Functional Operating Range Linked to Microbial Biodiversity and Community Composition Using Denitrifiers as Model Guild. PLoS One. 7(12). doi:10.1371/journal.pone.0051962.

Hund-Rinke K, Simon M. 2008. Bioavailability assessment of contaminants in soils via respiration and nitrification tests. Environ Pollut. 153(2):468–475. doi:10.1016/j.envpol.2007.08.003.

Lee JW, Hong SY, Chang EC, Suh MS, Kang HS. 2014. Assessment of future climate change over East Asia due to the RCP scenarios downscaled by GRIMs-RMP. Clim Dyn. 42(3–4):733–747. doi:10.1007/s00382-013-1841-6.

Miranda KM, Espey MG, Wink DA. 2001. A rapid, simple spectrophotometric method for simultaneous detection of nitrate and nitrite. Nitric Oxide - Biol Chem. 5(1):62–71. doi:10.1006/niox.2000.0319.

Moyano FE, Manzoni S, Chenu C. 2013. Responses of soil heterotrophic respiration to moisture availability: An exploration of processes and models. Soil Biol Biochem. 59:72–85. doi:10.1016/j.soilbio.2013.01.002.

Myhre G, Shindell D, Bréon F-M, Collins W, Fuglestvedt J, Huang J, Koch D, Lamarque J-F, Lee D, Mendoza B, et al., 2013. Anthropogenic and natural radiative forcing. In: Press C university, editor. Climate Change 2013 the Physical Science Basis: Working Group I Contribution to the Fifth Assessment Report of the Intergovernmental Panel on Climate Change. Vol. 9781107057. Stocker. p. 659–740.

Obriot F, Stauffer M, Goubard Y, Cheviron N, Peres G, Eden M, Revallier A, Vieublé-Gonod L, Houot S. 2016. Multi-criteria indices to evaluate the effects of repeated organic amendment applications on soil and crop quality. Agric Ecosyst Environ. 232:165–178. doi:10.1016/j.agee.2016.08.004. http://dx.doi.org/10.1016/j.agee.2016.08.004.

Panagos P, Ballabio C, Lugato E, Jones A, Borrelli P, Scarpa S, Orgiazzi A, Montanarella L. 2018. Potential sources of anthropogenic copper inputs to European agricultural soils. Sustain. doi:10.3390/su10072380.

Philippot L, Cregut M, Chèneby D, Bressan M, Dequiet S, Martin-Laurent F, Ranjard L, Lemanceau P. 2008. Effect of primary mild stresses on resilience and resistance of the nitrate reducer community to a subsequent severe stress. FEMS Microbiol Lett. doi:10.1111/j.1574-6968.2008.01210.x.

R Core Team. 2021. R core team (2021). R A Lang Environ Stat Comput R Found Stat Comput Vienna, Austria URL http//www R-project org.:ISBN 3-900051-07-0, URL http://www.R-project.org/

Ritz C. 2010. Toward a unified approach to dose-response modeling in ecotoxicology. Environ Toxicol Chem. 29(1):220–229. doi:10.1002/etc.7.

Ritz C, Baty F, Streibig JC, Gerhard D. 2015. Dose-response analysis using R. PLoS One. 10(12):1–13. doi:10.1371/journal.pone.0146021.

Rusk JA, Hamon RE, Stevens DP, McLaughlin MJ. 2004. Adaptation of soil biological nitrification to heavy metals. Environ Sci Technol. doi:10.1021/es035278g.

Ruyters S, Mertens J, Springael D, Smolders E. 2010. Stimulated activity of the soil nitrifying community accelerates community adaptation to Zn stress. Soil Biol Biochem. 42(5):766–772. doi:10.1016/j.soilbio.2010.01.012. http://dx.doi.org/10.1016/j.soilbio.2010.01.012.

Sauvé S, Dumestre A, McBride M, Gillett JW, Berthelin J, Hendershot W. 1999. Nitrification potential in field-collected soils contaminated with Pb or Cu. Appl Soil Ecol. 12(1):29–39. doi:10.1016/S0929-1393(98)00166-8.

Sebaugh JL. 2011. Guidelines for accurate EC50/IC50 estimation. Pharm Stat. 10(2):128–134. doi:10.1002/pst.426.

Smolders E, Brans K, Coppens F, Merckx R. 2001. Potential nitrification rate as a tool for screening toxicity in metal-contaminated soils. Environ Toxicol Chem. 20(11):2469–2474. doi:10.1002/etc.5620201111.

Song L, Gu D, Huang M, Chen L, Huang Q, Tong M, He Y. 2012. Spatial distribution and contamination assessments of heavy metals in sediments of Wenruitang River, Wenzhou, China. In: Iranpour, R and Zhao, J and Wang, A and Yang, FL and Li, X, editor. Advances In Environmental Science And Engineering, Pts 1-6. Vol. 518–523. Laublsrutistr 24, Ch-8717 Stafa-Zurich, Switzerland: Trans Tech Publications Ltd. (Advanced Materials Research). p. 2196–2203.

Tom-Petersen A, Hansen HCB, Nybroe O. 2004. Time and Moisture Effects on Total and Bioavailable Copper in Soil Water Extracts. J Environ Qual., doi:10.2134/jeq2004.5050.

Suppl table II.2.A.1. Indicators of fit (logLik=log Likehood, AIC= Awaike Criteria information, Lack of fit and Res Var= residual variance) for the 5 first models following AIC criteria to fit PNA inhibition under total Cu gradient for each of the moisture condition a) for the 3 pre-incubations at constant moisture of 30, 60 and 90% WHC, b) for the bioassays with various moisture during the pre-incubation period with DR = Dry Rewet and DO = Dry Only. Cedergreen is for cedergreen model with 4 parameters to fit, BC is for braincousen with 4 or 5 (BC4 or BC5) to fit, LL is for log logistic with 2 (LL2.2), 3 (L3) , 4 (LL2.4) or 5 parameters (LL.5) to fit, LN.3 is for log normal model with 3 parameters to fit.

a.

logLik	AIC	Lack of fit	Res var	Moisture condition	model
45.17	-80.34	0.98	1.63E-03	30	Cedergreen, alpha 1
45.17	-80.34	0.98	1.63E-03	30	Cedergreen alpha 0.25
43.89	-79.77	0.81	1.73E-03	30	BC.4
43.89	-79.77	0.81	1.73E-03	30	BC.5
43.01	-78.02	0.62	1.86E-03	30	LL.5
39.12	-70.24	0.61	2.57E-03	60	LN.3
39.97	-69.94	0.68	2.51E-03	60	Cedergreen alpha 1
39.95	-69.91	0.68	2.52E-03	60	Cedergreen alpha 0.25
39.39	-68.79	0.54	2.64E-03	60	W2.4
38.31	-68.63	0.45	2.75E-03	60	BC.4
39.13	-70.26	0.93	2.57E-03	90	BC.4
39.13	-70.26	0.93	2.57E-03	90	BC.5
38.96	-69.92	0.90	2.60E-03	90	LN.3
39.78	-69.57	0.98	2.55E-03	90	Cedergreen alpha 1
39.75	-69.49	0.98	2.56E-03	90	Cedergreen alpha 0.25

b.

logLik	AIC	Lack of fit	Res var	Moisture condition	model
42.20	-76.40	0.95	1.99E-03	DO	BC.4
42.20	-76.40	0.95	1.99E-03	DO	BC.5
41.78	-75.56	0.88	2.06E-03	DO	W2.3
42.23	-74.47	0.90	2.08E-03	DO	W2.4
40.03	-74.05	0.62	2.27E-03	DO	W2.2
39.56	-73.11	0.96	2.36E-03	DR	W1.2
39.15	-72.30	0.91	2.45E-03	DR	LL.4
39.83	-71.66	0.96	2.42E-03	DR	W1.3
39.75	-71.50	0.95	2.44E-03	DR	L.3
39.61	-71.21	0.92	2.47E-03	DR	LN.3

II.2.B : Estimation de l'effet de l'historique des précipitations sur la mise en solution du Cu et son impact sur les activités nitrifiantes.

L'expérience présentée en II.2.A a été complétée par des mesures de Cu en solution à la fin du bio-essai et les résultats sont présentés ici. Comme décrit précédemment, cinq microcosmes ont été pré-incubés 5 semaines sous des conditions d'humidité variables (30, 60, 90 % de la capacité de rétention en eau, CRE, DR et DO avec des cycles d'assèchement-dessèchement plus ou moins long). A la fin de ces cinq semaines, des bio-essais mesurant l'activité nitrifiante potentielle (PNA) après ajout de gradient de Cu ont été conduit et les teneurs de Cu en solution utilisé comme proxy de la disponibilité environnementale ont été mesurées à la fin de ce bio-essai. Cela permet ainsi :

i) D'établir des relations entre Cu total et Cu en solution après différents historiques de précipitation.
ii) Déterminer des courbes doses réponses entre Cu en solution et activité nitrifiante potentielle pour chaque condition de pré-incubation.
iii) D'estimer des valeurs de concentration en Cu en solution inhibant l'activité nitrifiante de X (5, 10, 20, 50) %

Un protocole complet du design expérimental et des méthodes d'analyse des résultats est donné au chapitre II.2.A.-2 (material and methods). A celui-ci s'ajoute un dosage du Cu en solution à la fin des 3 jours de bioessai. Pour cela, le mélange sol : solution contenant le cuivre a été centrifugé et le surnageant utilisé pour la mesure du Cu. La concentration de Cu dans cette solution de sol a été déterminée par spectroscopie d'absorption atomique à flamme (FAAS, Varian SpectrAA 220, limite de quantification 0.03 $mgCu.L^{-1}$ équivalent à 0.26 $mgCu.kg^{-1}$ en sol sec).

1. Effet de la pré-incubation sur la teneur en Cu en solution du bioessai

Les teneurs de Cu en solution mesurées suivent des relations log-normales avec les valeurs de Cu total ajoutées dans les microcosmes (Fig. II.2.B.1). Dans le cas des sols incubés à 90 % de la CRE les teneurs de Cu en solution mesurées pour 750 $mgCu.kg^{-1}$ et pour 1000 $mgCu.kg^{-1}$ sont anormalement faibles (inférieures à celles mesurées pour 500 et pour 2000 $mgCu.kg^{-1}$). Nous n'avons cependant pas pu recommencer l'expérimentation par faute de matériel disponible. Ces deux valeurs ont donc été gardées telles qu'elles malgré une suspicion d'erreur de manipulation
Néanmoins, nos résultats permettent de montrer un effet significatif ($p.v<0.01$ pour l'anova sur les modèles log-normaux) des conditions d'incubation sur les teneurs de Cu en solution avec des valeurs de Cu en solution dans les sols incubés à DR et DO inférieures à celles mesurées dans les sols incubés à humidité constante.

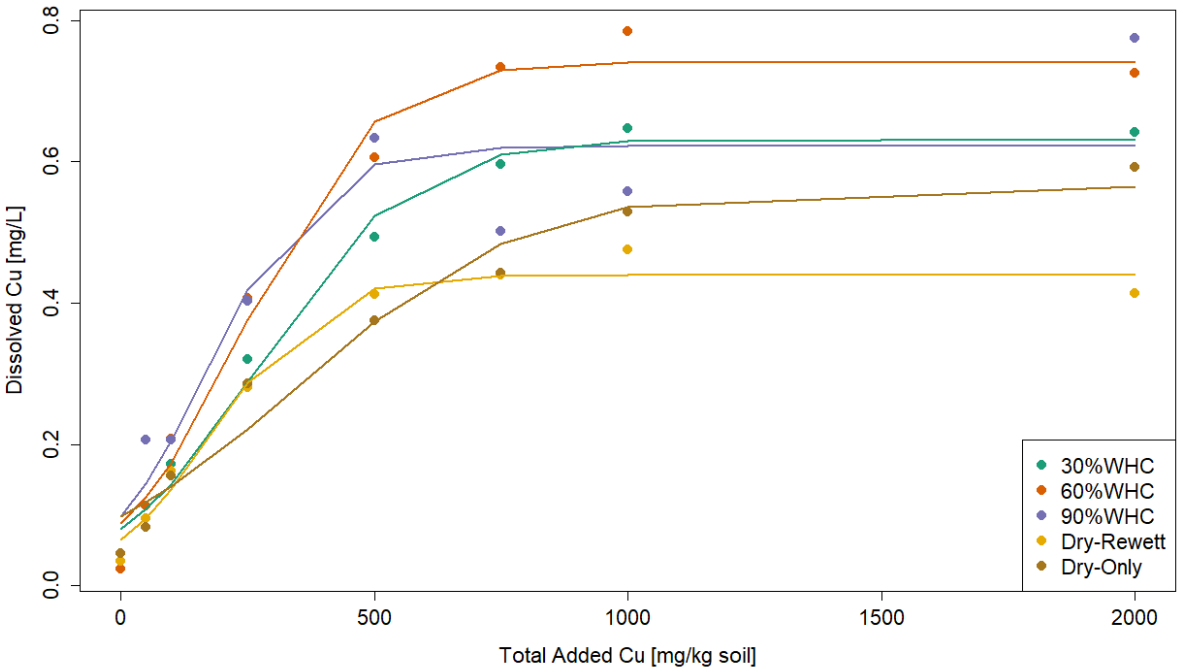

Fig. : II.2.B.1: Cu en solution (mgCu.L^{-1}) mesuré pour les concentrations de Cu ajouté (mgCu.kg^{-1}, representation log) pour chaque condition de preincubation, vert pour 30% CRE, orange pour 60 % CRE, violet pour 90% CRE, jaune pour Dry Rewett et marron pour Dry Only.

2. Détermination de courbes dose-réponses : inhibition de la PNA en fonction du Cu en solution

Sur la base des critères d'AIC et log Lik, l'inhibition de la PNA en fonction du Cu en solution est le mieux représenté par des modèles de type Weibull pour les 5 conditions de pré-incubation. Les microcosmes exposés à 30 et 90% de l'humidité ainsi que ceux sous DR suivent un modèle de type Weibull I (Eq. II.2.B.1), les microcosmes exposés à 60 et DO un modèle de type Weibull II (Eq.II.2.B.2).

(Eq. II.2.B.1) $$\%\ PNA\ inhibtion = \exp\left(-\exp\left(b(log(Cu\ en\ solution) - \log(e))\right)\right)$$

(II.2.B.2) $$\%\ PNA\ inhibtion = 1 - \exp\left(-\exp\left(b(log(Cu\ in\ solution) - \log(e))\right)\right)$$

Ces 2 modèles dérivent des log-logistiques par aplatissement des asymptotes. Ainsi, le modèle Weibull I correspond à une forte sensibilité à des variations dans les faibles concentrations en Cu tandis que le modèle Weibull II correspond à une forte sensibilité à des variations dans les fortes concentrations en Cu (fig. : II.2.B.2).

La table II.2.B.1 donne les estimations des paramètres b et e dans les différentes conditions (II.2.B.1.a pour les conditions 30, 90 %CRE et DR modélisées par des courbes de type Weibull I et II.2.B.1.b pour les conditions 60% CRE et DO modélisées par des courbes Weibull II). Le paramètre « b » représente la pente relative de la courbe autour du point d'inflexion et le paramètre « e » la valeur de ce point d'inflexion.

La pente autour du point d'inflexion n'est pas significativement différente entre les conditions 30, ou 90 % CRE et DR. L'intensité de variation de cette pente est également équivalente dans le cas de DO avec

$$|b|_{DO} \sim |b|_{30,\,90,\,DR}.$$

Elle est en revanche plus faible dans le cas de 60 % CRE ce qui signifie que la sensibilité de la PNA aux fortes concentrations de Cu est moins importante dans ce dernier cas que dans les 4 autres. Le point d'inflexion estimé se situe entre 0.52 et 0.82 $mgCu.L^{-1}$ selon les conditions de pré-incubation. La valeur est significativement plus faible dans le cas de DO (plus forte sensibilité atteinte pour des concentrations en Cu plus faible) et plus forte dans le cas de 90 % CRE. Néanmoins, i) les valeurs de Cu en solution similaires pour de fortes valeurs de Cu ajouté dans le cas de 90 % CRE et les fortes incertitudes dans la modélisation de la courbe DR réduisent la précision de ces estimations.

Table II.2.B.1. Paramètres estimés des modèles, écart type et p.value de test contre 0, (a) pour les modèles Weibull I de la forme :

$$\%\ PNA\ inhibtion = \exp\left(-\exp\left(b(log(Cu\ en\ solution) - \log(e))\right)\right)$$

et (b) pour les modèles de type Weibull II de la forme :

$$\%\ PNA\ inhibtion = 1 - \exp\left(-\exp\left(b(log(Cu\ in\ solution) - \log(e))\right)\right)$$

Les conditions partageant une même lettre dans la dernière colonne ne sont pas significativement différentes l'une de l'autre

(a)

Paramètre	Estimation	Ecart type	p-value	Condition de pré incubation	
b	3.77	1.16	1.86E-03	30	a
	3.90	0.79	5.97E-06	90	a
	2.17	0.81	9.02E-03	DR	a
e	0.70	0.04	5.05E-30	30	b
	0.82	0.04	1.76E-30	90	a
	0.71	0.14	4.18E-06	DR	ab

(b)

Paramètre	Estimation	Ecart type	p-value	Condition de pré incubation	
b	-1.92	0.49	0.0003	60	c
	-3.34	0.64	4.92E-06	DO	d
e	0.69	0.026	2.50E-29	60	b
	0.52	0.014	1.32E-35	DO	d

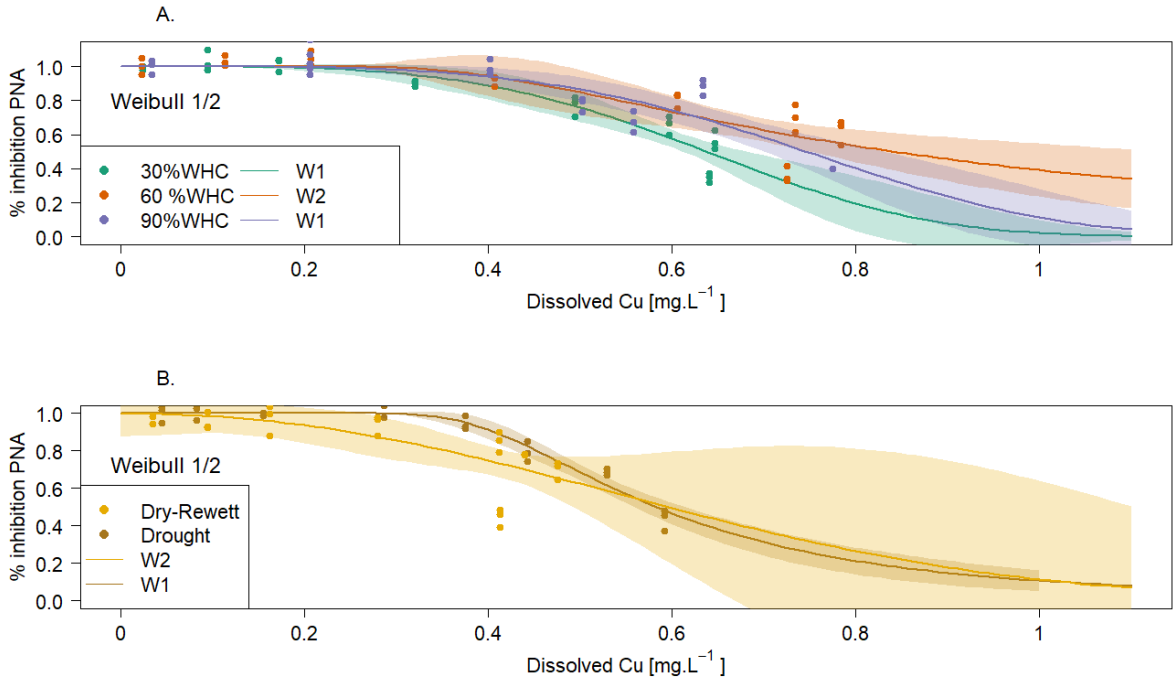

Fig. II.2.B.2. Ajustements des modèles Weibull du premier type (W1) pour 30% CRE, 90% CRE et DO, et des modèles Weibull du second type (W2) pour les conditions 60 % CRE et DR. Les ajustements et les intervalles de confiances à 95% sont représentés

3. Estimation des concentrations ECx en Cu en solution induisant une diminution de X% de la PNA

Sur la base des modèles Weibull décrits précédemment nous avons pu extraire les doses de Cu correspondant à des inhibitions de la PNA de 5, 10, 20 et 50 %. Les résultats sont présentés dans la table II.2.B.2. Pour les EC5 (0.36 ± 0.032 mg Cu L^{-1}, moyenne et écart type sur les 5 conditions de pré-incubation), 10 (0.422 ± 0.029 mg Cu L^{-1}, moyenne et écart type sur les 5 conditions de pré-incubation) et 20 (0.050 ±0.038 mg Cu L^{-1}, moyenne et écart type sur les 5 conditions de pré-incubation), nos résultats montrent une tendance non significative à avoir de plus fortes valeurs d'EC pour les microcosmes pré-incubés de 30 à 90 % CRE à humidité constante. Les microcosmes pré-incubés à DR et DO ont des valeurs d'ECx de l'ordre de grandeur de ceux pré-incubés à 30% CRE.

Les EC50 déterminés pour 30 % CRE (0.64 ±0.03 mg $Cu.L^{-1}$) sont significativement plus faibles que ceux pour 60 (0.84 ±0.15) et 90% CRE (0.75 ±0.06 mg $Cu.L^{-1}$). Les EC50 estimés pour les microcosmes pré-incubés à DO et DR sont de l'ordre de ceux du microcosme à 30 % CRE mais les incertitudes plus importantes ne les rendent pas significativement différent de ceux à 60 et 90 % CRE.

Table II.2.B.2: Concentrations effectives de Cu en solution (mg Cu .L^{-1}) ECx (x = 5, 10, 20, ou 50% d'inhibition de la PNA) estimées à partir des modèles Weibull de réponse au Cu en solution, avec leurs estimations basses et hautes (intervalle de confiance à 95%) exprimées en concentrations de Cu en solution avec les valeurs basses et hautes d'estimations (95% CI) derivées de fonctions Weibull ; les conditions d'humidité de 30, 60 et 90 se réfèrent à 30, 60 et 90 % CRE, DR à dessiccation-ré-humectation et DO à dessiccation seulement.

X niveau	Condition pré incubation	Estimation	Limite basse	Limite haute
5	30 % CRE	0.32	0.21	0.43
	60 % CRE	0.39	0.22	0.56
	90 % CRE	0.38	0.28	0.49
	DR	0.32	0.18	0.46
	DO	0.39	0.22	0.56
10	30 % CRE	0.39	0.29	0.48
	60 % CRE	0.45	0.3	0.6
	90 % CRE	0.46	0.37	0.55
	DR	0.39	0.26	0.51
	DO	0.42	0.27	0.58
20	30 % CRE	0.47	0.4	0.54
	60 % CRE	0.54	0.43	0.66
	90 % CRE	0.56	0.49	0.62
	DR	0.47	0.38	0.56
	DO	0.48	0.37	0.59
50	30 % CRE	0.64	0.61	0.67
	60 % CRE	0.84	0.69	0.99
	90 % CRE	0.75	0.68	0.81
	DR	0.64	0.6	0.67
	DO	0.64	0.59	0.69

Cette étude visait à prendre en compte le Cu en solution en complément de la précédente étude qui ne considérait que le Cu total ajouté. La prise en compte du Cu en solution avait pour but d'approcher l'exposition des microorganismes via la solution du sol plutôt qu'en considérant que la teneur totale en cuivre était impactante. Nous avons pu montrer i) que la disponibilité du Cu était affectée par les conditions d'humidité lors de la préincubation et ii) que les PNA des microcosmes pré-incubés à 30, 90 %CRE et DR étaient sensibles à des variations de teneurs pour des concentrations faibles de Cu en solution, alors que les microcosmes pré incubés à 60 % CRE et DO étaient sensibles à des variations de teneurs dans la gamme des fortes concentrations en Cu solution. Cependant, les incertitudes dans l'estimation des courbes dose-réponses restent grandes, et nous n'avons pas pu observer de différences significatives entre les conditions de préincubations pour les ECx < EC20 , les

estimations des EC50 étant quant à elles soumises à réserve car il n'y a qu'un point au-delà de 50% d'inhibition pour ajuster les courbes.

Les plus faibles valeurs de Cu en solution mesurées pour les microcosmes pré-incubés avec des variations d'humidité (DR et DO) peuvent être dues à des modification dans la structure du sol (Denef et al., 2001a). En effet, les cycles de dessiccation-ré-humectation peuvent affecter le nombre et la taille des agrégats et augmenter les surfaces de sorption spécifiques ou diminuer la force ionique du sol (Walworth, 1992). Des études ont pu montrer que cela pouvait provoquer une augmentation de la quantité de Cu en phase solide, ce qui concorderait avec les plus faibles quantités de Cu en solution que nous avons pu mesurer (Huang et al., 2014; Wang et al., 2015). Enfin, nous avons également pu mesurer de plus faibles quantités de carbone organique dissous (II.2.A table1) dans les microcosmes DR et DO, ce qui peut également expliquer les plus faibles quantités de Cu en solution, le carbone organique dissouts favorisant le Cu en solution en s'y liant (Oorts et al., 2006).

Les évolutions des PNA au regard des concentrations en Cu en solution suggèrent une meilleure résistance aux fortes concentrations des microcosmes pré-incubés à 60 % CRE (paramètre « b » des modèles Weibull plus faible, tableau II.2.B.1) que dans les autres cas. On estime également que la diminution forte de la PNA pour les microcosmes incubés à 90% CRE commence à des concentrations en Cu supérieures à celles des autres microcosmes (paramètre « e » des modèles Weibull supérieur).

Ce résultat rejoint ceux que nous avons pu voir en II.2.A où les microcosmes pré-incubés à 90% CRE et dans une moindre mesure 60 % présentaient des ECx supérieures aux autres conditions quand elles sont exprimées en fonction de la teneur totale en cuivre. Les valeurs de Cu en solution mesurées supérieures dans le cas des microcosmes incubés à DO par rapport à DR ne permettent en revanche pas d'expliquer que les ECx estimés en Cu total (II.2.A) pour DO soient supérieurs à ceux estimés pour DR.

Cette étude confirme donc la nécessité de prendre en compte les facteurs climatiques en plus des facteurs pédologiques lors de l'étude de contamination, qu'il s'agisse d'étude portant sur la disponibilité ou sur les effets toxicologiques sur les fonctions biologiques. En particulier, nous avons pu montrer qu'il était important de prendre en compte l'historique des conditions climatiques, là où les conditions climatiques contemporaines sont le plus souvent considérées (Noyes et al., 2009; Augustsson et al., 2011).

Conclusion intermédiaire (3) :

Le chapitre II.1 a pu mettre en évidence, à partir des grandes variations dans les concentrations des sols en Cu total, des teneurs estimées en Cu libre ou Cu en solution également hétérogènes à l'échelle de l'Europe ainsi que des variations dans les quantités de pluies et leurs évolutions. La mesure du Cu en solution en II.2.B n'a pas permis de mettre en évidence une meilleure corrélation entre

réponse de l'activité nitrifiante et Cu en solution qu'entre réponse de l'activité nitrifiante et Cu total. En revanche, nos résultats suggèrent que les alternances de sécheresse et ré humectation peuvent affecter la partition du Cu. Ceci est étayé par les plus faibles concentrations en Cu en solution mesurées pour ces sols que pour ceux ayant été maintenus à une humidité constante. Les régions identifiées en II.1.B comme ayant à la fois une forte probabilité de relarguer du Cu en solution (K_f faible) et d'augmentation de débit due à une augmentation des quantités de précipitations pourraient donc être moins à risque d'exporter du Cu *via* la solution du sol qu'estimé en II.1.B si cette augmentation résulte d'événements ponctuels plus que d'une augmentation générale de pluviométrie annuelle. Pour autant, i) les concentrations en Cu étudiées en laboratoire en II.2. restent plus élevées que celles issues des campagnes de mesure *in situ* reportées en II.1. et ii) les redondances de communautés et fonctions impliquées dans les émissions de gaz à effet de serre (C ou N) des sols n'autorisent pas de façon rigoureuse d'estimer l'amplitude des variations d'émissions imputable à la contamination des sols sur de larges échelles.

La partie III qui fait suite cherchera ainsi à quantifier l'effet de la contamination des sols en Cu sur les émissions de C et N. Trois angles seront abordés : premièrement, on cherchera à établir un diagnostic de la capacité des modèles actuels de surface continentale à prendre en compte cet effet. Deuxièmement, nous chercherons à estimer une fonction générique de réponse des émissions de CO_2 à une contamination au Cu. Enfin, nous proposerons un modèle prenant en compte les effets des modifications de changement de précipitations et de contamination au Cu sur les émissions d'azote des sols.

Partie III : Importance de la prise en compte explicite de la contamination des sols dans les modèles mécanistiques de surface continentale

Les modèles de surface continentale sont largement utilisés à des fins prospectives afin d'estimer les effets de scénarii d'émissions de GES sur les cycles biogéochimiques ou sur le climat, tandis que la contamination des sols est dépendante localement de l'usage qui est fait des sols mais aussi des politiques de régulations d'apport mises en place. Dans cette partie III notre objectif était double : i) identifier si les effets d'une contamination *in situ* en Cu, constatée en partie II comme pouvant concerner de grandes surfaces mais non prise en compte dans ces modèles, est d'ampleur suffisante pour affecter significativement les prévisions de respiration hétérotrophe de ces modèles et ii) si pertinent, proposer des fonctions prenant en compte la contamination du Cu pour être incorporées dans ces modèles.

Cette partie est ainsi divisée en trois chapitres., Le chapitre III.1 cherchera à établir si les erreurs d'estimations de Rh des modèles de surface continentale s'expliquent par la non prise en compte de la contamination des sols au Cu dans ces modèles. Le chapitre III.2 visera à établir une fonction réponse générale entre contamination au Cu des sols et Rh. Le chapitre III.3 aura pour but de compléter le modèle de biogéochimie continentale DNDC par des fonctions prenant en compte l'effet du Cu sur le cycle de l'azote pour différentes conditions d'humidité du sol. Ce modèle (DNDC-Cu) sera ensuite utilisé pour prédire les émissions d'espèces azotées en fonction de la concentration en Cu et pour différentes conditions d'humidité du sol.

Le premier chapitre de cette partie III concerne les interactions entre la contamination et les sols (effet d'une contamination en Cu sur les fonctions du sol), entre le climat et le sol (effet des précipitations sur les émissions azotées) et entre les sols et le climat (modification des émissions de C et N dans les sols contaminés) schématisées ci-dessous

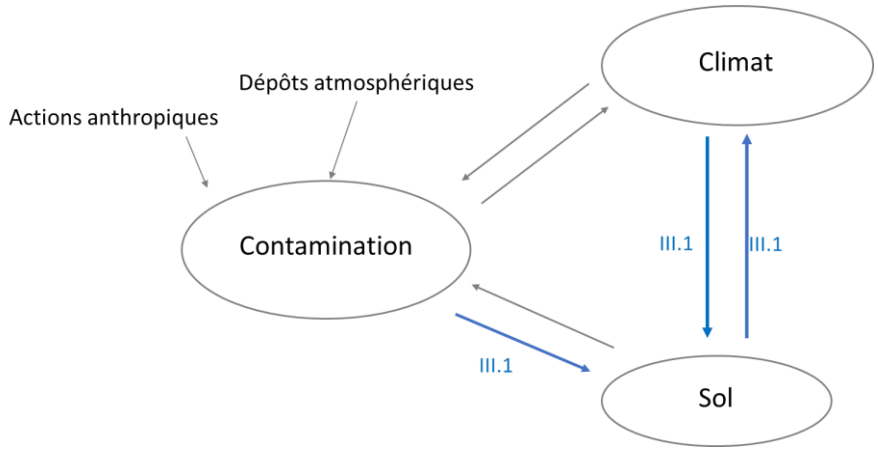

III.1. La contamination des sols, un facteur manquant dans la dynamique du carbone des sols des modèles de surface continentale. Cas d'étude du Cu

La contamination des sols est-elle un paramètre à prendre en compte pour l'estimation de la respiration hétérotrophe par les modèles de surface continentale ? Cas d'étude du Cu

En cours de soumission pour Global Change Biology

Résumé en français :

Les modèles de surface continentale sont des composantes importantes des modèles de système Terre utilisés pour estimer l'effet des émissions de gaz à effet de serre (GES) anthropiques sur le climat de la Terre. Cependant, en plus des changements d'utilisation des terres et des émissions directes de GES pris en compte dans ces modèles, les activités anthropiques sont également associées à l'émission et aux apports de contaminants. Or, malgré l'effet de la contamination sur les processus du sol (comme les émissions de GES), celle-ci n'est pas encore considérée comme un paramètre important à prendre en compte dans les modèles de surface continentale.

Ici, nous avons cherché à évaluer l'importance de la contamination du sol dans les émissions de CO_2 du sol sous la forme de la respiration hétérotrophe (Rh). Par conséquent, nous avons analysé, à l'échelle de l'Europe, si la contamination du sol peut expliquer les résidus de Rh modélisés à partir de 4 modèles de surface continentale par rapport aux produits de Rh dérivés d'observations. Nous avons utilisé un modèle mixte généralisé des moindres carrés (GLS) pour évaluer les principaux facteurs des résidus du modèle. Parmi les contaminants, nous nous sommes concentrés sur le Cu qui est largement utilisé dans l'industrie ou dans l'agriculture, provoquant une contamination diffuse sur de grandes surfaces. De plus, il a été montré que la Rh du sol et la disponibilité du Cu pour la faune du sol dépendaient fortement des paramètres pédologiques et climatiques du sol. Notre analyse a donc été complétée par l'inclusion des paramètres pédo-environnementaux et par l'analyse du Rh par rapport au Cu libre - un proxy du Cu biodisponible.

Nos résultats montrent que le Cu est un paramètre non négligeable pouvant expliquer les inexactitudes dans la modélisation des Rh, que ce soit en considérant le Cu total ou le Cu libre. L'effet partiel du Cu s'est avéré aussi fort que d'autres facteurs pédologiques tels que l'argile ou le pH et dans certains cas que la température pour expliquer les résidus des modèles. Lorsque le Cu (total ou libre) a été jugé significatif, la différence entre Rh modélisé et observé s'est avérée augmenter avec l'augmentation de la concentration de Cu dans le sol pour des concentrations en Cu modérées à élevées et diminuer pour les plus élevées. Le seuil de Cu auquel les tendances des différences entre le Rh modélisé et observé s'inverse s'est cependant avéré différent selon les modèles et les produits d'observation considérés.

Conclusion intermédiaire (4) :

Le chapitre III.1 est basé sur des estimations statistiques de la respiration des sols (Rh) et des concentrations en Cu. Cela a permis de mettre en évidence que la contamination au Cu en Europe, non prise en compte dans les modèles de surface continentale pouvait expliquer une partie significative de l'erreur de modélisation des flux de Rh de ces modèles. La prise en compte du Cu sous sa forme de Cu libre au chapitre III.1 n'a pas permis d'améliorer les capacités prédictives des modèles par rapport à la considération conjointe d'un effet du pH et d'un effet de la concentration en Cu. Les chapitres III.2 et III.3, basés sur des mesures de laboratoire où les concentrations en Cu et les valeurs de Rh ont été systématiquement mesurées visent à affiner la modélisation prédictive d'un effet du Cu sur Rh et sur les émissions d'espèces azotées des sols par la détermination d'équations.

Le chapitre III.2 concerne les interactions schématisées ci-dessous

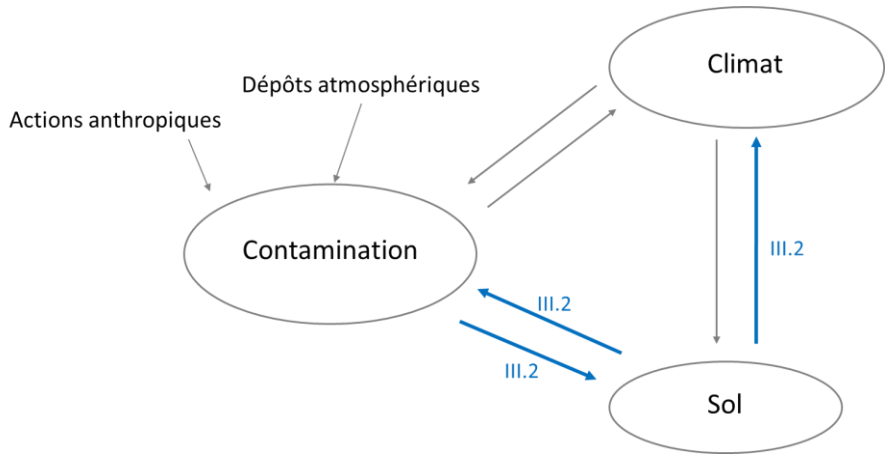

III.2 La contamination en cuivre des sols affecte-t-elle leurs émissions de CO_2 ? Etude bibliographique

Accepté dans Frontiers

Résumé en français :

Les sols contaminés sont très répandus et l'on sait que la contamination a un impact sur plusieurs processus biotiques du sol. Cependant, on ne sait toujours pas dans quelle mesure la contamination du sol affecte l'efflux de carbone du sol (CO_2) dû à la respiration de la microfaune du sol. Du fait des grands stocks de carbone organique (Corga) stockés dans les sols, même des changements limités dans les flux sortants peuvent modifier substantiellement la concentration de CO_2 atmosphérique et avoir des rétroactions importantes sur le climat. Dans cette étude, nous avons cherché à évaluer et à quantifier l'impact d'une contamination du sol sur sa respiration. Pour cela, nous avons effectué une

revue quantitative de la littérature en nous concentrant sur i) les mesures de respiration hétérotrophe du sol, excluant ainsi la respiration autotrophe des plantes, ii) la contamination du sol par le cuivre, et iii) l'influence des paramètres pédo-climatiques tels que le pH, la teneur en argile ou le type de climat. Sur la base de 389 données ainsi récupérées, nous avons montré une diminution des émissions de CO_2 du sol avec une augmentation de la contamination en cuivre du sol. Les données spécifiques provenant d'expériences de contamination ex-situ ont pu être facilement différenciées de celles provenant de la contamination in-situ en raison de la diminution plus marquée de la minéralisation de Corga dans ces sols. Grâce aux données des contaminations ex-situ nous avons pu déterminer un seuil dans les teneurs en Cu du sol affectant les émissions de CO_2 : les émissions de CO_2 augmentent pour des apports inférieurs à 265 $mgCu.kg^{-1}$ de sol et diminuent au-dessus de cette concentration. Les données sur les contaminations in situ de long terme dues aux activités anthropogéniques (industrialisation, agriculture, ...) ont également montré un impact sur la minéralisation du carbone du sol, en particulier pour les contaminations industrielles (fonderie, boues d'épuration, ...) où les émissions de CO_2 diminuent lorsque la contamination en Cu augmente. Le pH du sol a été identifié comme étant un facteur significatif dans l'effet du Cu sur les émissions de CO_2. En effet, la minéralisation du carbone du sol s'est avérée plus sensible à la contamination par le Cu dans les sols acides que dans les sols neutres ou alcalins. Inversement, la teneur en argile et le type de climat n'expliquent pas de manière significative les effets du Cu sur la minéralisation du carbone dans le sol. Enfin, les données recueillies ont été utilisées pour proposer une équation empirique quantifiant l'effet d'une contamination au Cu sur la respiration du sol. La diminution des émissions de CO_2 du sol ne peut cependant pas se traduire comme un effet « puit de carbone » car elle s'accompagne d'une diminution de la biomasse microbienne du sol.

Conclusion intermédiaire (5) :

L'étude conduite au chapitre III.2 nous a permis d'établir une relation générique entre contamination des sols au Cu et respiration hétérotrophe à travers une grande variété de type de sols et de climats. Nous avons pu confirmer un effet de la concentration en Cu totale sur la respiration hétérotrophe, mais aussi la nécessité d'inclure le pH comme co-facteur. La gamme de concentration en Cu plus étendue que celle rencontrée *in-situ* et utilisée en III.1 a permis de montrer que les concentrations très élevées en Cu s'accompagnaient d'une diminution de la respiration hétérotrophe et de la biomasse microbienne.

La revue quantitative nous a permis de mettre en évidence un effet du climat du lieu de prélèvement dans les respirations hétérotrophes. Cet effet n'a cependant pu être inclus que sous un aspect qualitatif prenant en compte de grands types de régime hydriques. D'autre part, nous n'avons pu prendre en compte cet effet qu'en terme de modulation de l'ordonnée à l'origine, c'est-à-dire pour de faible niveau de (« sans ») Cu. Pour autant, les variations des communautés bactériennes avec le climat peuvent également induire des réponses différentes (c'est-à-dire différentes pentes dans notre III.2) au Cu.

En parallèle, outre les émissions de CO_2, les espèces azotées sont d'importants gaz à effet de serre, en termes de quantité comme de pouvoir de réchauffement. Les émissions d'N étant moins bien renseignées que celles de carbone, la définition de fonction réponse entre émissions d'espèces azotées et contamination au Cu ne peut se faire par revue quantitative. L'étude II.2. a permis de mettre en évidence l'effet du double stress environnemental (chimique et de contamination) sur les fonctions de nitrification mais pas d'estimer les retombées sur les émissions. L'objectif du III.3. a donc été de proposer un modèle prenant en compte les effets conjoints du Cu et de différents régimes hydriques sur les émissions d'espèces azotées des sols.

Le chapitre III.3 concerne les interactions schématisées ci-dessous :

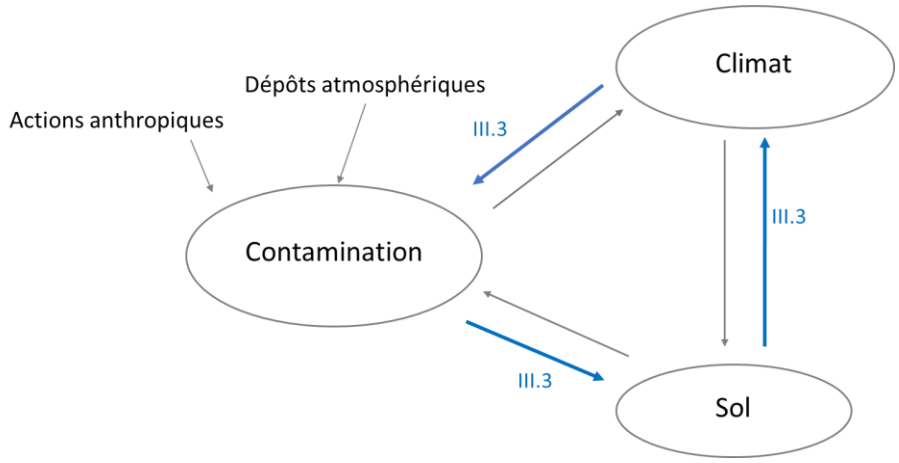

III.3. Dans quelle mesure les stress d'humidité et de contamination des sols peuvent affecter leurs émissions de gaz à effet de serre ? Calibration d'un modèle de nitrification-dénitrification*.

Soumis à Biogeosciences

Résumé en francais:

Les modèles biogéochimiques continentaux sont couramment utilisés pour investiguer l'effet de l'usage des terres, de l'apport de matière organique exogène ou du changement climatique sur les émissions de gaz à effet de serre des sols. Cependant, ils ne peuvent pas encore être utilisés pour étudier l'effet de la contamination du sol, alors même que l'on sait qu'elle affecte plusieurs processus des sols et concerne une grande partie de la surface terrestre. Nous avons implémenté un modèle couramment utilisé pour estimer les émissions d'azote (N) des sols, le modèle DeNitrification DeCompostion (DNDC), avec une fonction prenant en compte la contamination du sol par le cuivre (Cu) dans la modulation de la production de nitrate. Ensuite, nous avons utilisé ce modèle pour prédire les émissions de $N\text{-}N_2O$, $N\text{-}NO_2$ NOx et $N\text{-}NH_4$ en présence de Cu et dans le contexte de changements des précipitations. Pour cela, des incubations de sols ont été réalisées à différentes humidités de sol afin de mimer les régimes pluviométriques attendus au cours des prochaines décennies et notamment la sécheresse et l'excès d'eau. L'effet de ce double stress sur la production de nitrate du sol a ensuite été étudié avec un bio-essai. Ensuite, les données de production de nitrate obtenues pour chaque traitement d'humidité ont été utilisées pour paramétrer le modèle DNDC et estimer les émissions de N du sol en considérant les différents effets du Cu. Quelle que soit l'humidité de la préincubation, les résultats expérimentaux ont montré une diminution de la production de $N\text{-}NO_3$ lors de l'ajout de Cu mais avec une nette différence selon l'humidité du sol. La version de DNDC-Cu que nous avons proposée a été capable de reproduire les effets observés du Cu sur la concentration en nitrate du sol avec r2>0.99 et RMSE<10% pour tous les traitements dans la gamme de calibration du DNDC-Cu (>40% de la capacité de rétention d'eau) mais a montré de mauvaises performances pour les sols secs. Nous avons modélisé un effet du Cu induisant une augmentation de la concentration et des émissions de $N\text{-}NH_4$ dans le sol en raison d'une activité de nitrification réduite, et donc une diminution des concentrations et des émissions de $N\text{-}NO_3$, $N\text{-}N_2O$ et N-NOx. L'effet de l'ajout de Cu était plus important sur les émissions de $N\text{-}N_2$ et $N\text{-}N_2O$ que sur les autres espèces d'azote et plus important pour les sols incubés sous humidité constante que variable.

* Les expériences exploitées dans ce chapitre ont été réalisées dans le cadre du stage de M2 de Charlotte Blasi en 2015-2016 : Blasi C. 2017. Impact of climate change on threshold in terrestrial ecotoxicology. Internship report M2 Master Sciences, Technologies, santé, mention STEE et Chimie, spécialité EXCE (Ecotoxicologie et Chimie de l'Environnement), Université Bordeaux, 38pp + Annexes. Encadrement I. Lamy et B. Guenet

Conclusion intermédiaire (6) :

Au cours du chapitre III nous avons pu mettre en évidence que la contamination au Cu, à des niveaux environnementaux de contamination diffuse comme à des concentrations très supérieures de laboratoire, affectait la respiration hétérotrophe du sol. Le chapitre III.1 a permis de mettre en évidence que les surfaces et concentrations concernées par une contamination en Cu affectaient significativement les capacités prédictives de respiration hétérotrophe des modèles de surface continentale. Les études à grande échelle conduites sur les effets de la concentration en Cu des sols et leur respiration hétérotrophe (III.1 et III.2) n'ont pas mis en évidence de palier dans les effets du Cu, mais plutôt une réponse bi-type où les émissions de CO_2 augmentent à de faibles concentrations en Cu et diminuent à de plus fortes concentrations. Le chapitre III.2 a permis de déterminer une équation générique pour prédire les effets d'une contamination au Cu sur les émissions de CO_2 du sol émanant de Rh. Les expériences conduites dans le chapitre III.3 ont permis de prendre en compte les effets d'une contamination au Cu sur les émissions d'azote ainsi que les effets du double stress de contamination et de modification des précipitations dans le modèle DNDC-Cu. Nos résultats montrent que les émissions azotées diminuent quand la concentration en Cu augmente et que cette diminution est plus faible pour des sols soumis à des changements d'humidité du sol (assèchement dessèchement) que pour des sols soumis à des humidités constantes.

Chapitre III.1.: Contamination as a missing driver of soil carbon dynamic in land surface models. A study case with copper-

Is soil contamination a missing driver of soil heterotrophic respiration in land surface models? A study case with copper –

Laura Sereni, Isabelle Lamy, Philippe Peylin, Bertrand Guenet

Expected journal for submission: Global Change Biology

Abstract:
Land Surface Models (LSMs) are important components of Earth System Models used to estimate the effect of anthropogenic greenhouse gases (GHG) emission on Earth climate. However, in complement to land use change and to direct GHG emissions, anthropogenic activities also paired with contaminant emission and deposition. Despite recognized effect of contamination on soil processes like GHG emissions, soil contamination is however still not considered as an important parameter to take into account into LSMs.

Here we aimed at assessing the importance of soil contamination for soil CO_2 emissions under the form of heterotrophic respiration (Rh). Therefore, we analyzed how European soil contamination mays explain residues of modelled Rh from 4 LSMs against Rh products derived from observations. We used a generalized least squared mixed models to evaluate the main drivers of the model residues. Among contaminant, we focused on Cu that is widely used in industry or in agriculture leading to large diffuse contamination. Furthermore, it has been shown that soil Rh and Cu availability to soil fauna were strongly dependent of soil pedological and climatic parameters. Hence, our analysis was complete by the inclusion of pedo-environmental parameter and by the analysis of Rh against free Cu -a proxy of bioavailable Cu.

Our results show that Cu is a non negligeable parameter to explain Rh modeled inaccuracy considering either total or free Cu forms. Cu partial effect was found as strong as other pedological factors such as clay or pH effect and in some cases as temperature to explain models' residues. When Cu (total or free) was found significant, the difference between model and observed Rh was found to decrease with increase in soil Cu concentration for moderate to high Cu concentration and to decrease for the highest. Threshold of Cu for trends inversions of differences between model and observed Rh were however found different depending on the models and observations products considered.

Keywords: Heterotrophic respiration, contaminant availability, gls, stepAIC, regional model

1.INTRODUCTION

Land surface models (LSMs) are used within Earth Systems Models since the 70's to predict climate from physical atmospheric and oceanographic models (Fisher and Koven, 2020). Since years they've been recognized as useful and improved by several components such as continental biogeochemical cycle to take into account the large fluxes of carbon (C) (and more recently nitrous N) between soils and atmosphere (Cox et al., 2000; Friedlingstein et al., 2006; Zaehle and Friend, 2010; Vuichard et al., 2018). However, despite improvement during the last decades there is still uncertainties in modeling some of the major processes. For instance, soil C stocks represents 1500 PgC and C fluxes between soils and atmosphere are on the order of 75 PgC $year^{-1}$ (Schlesinger and Andrews, 2000). Anav et al., (2013) estimates that only 6 over the 15 Earth system models tested correctly reproduce the land carbon sink while looking at the Northern Hemisphere, all models underestimated C sink from 200 to 50 %.

Up to now model of soil C fluxes are mostly governed by soil temperature, moisture, clay, the amount of soil organic carbon and the C input to the soil through primary production (Fisher and Koven, 2020; Blyth et al., 2021). Yet, growing anthropisation not only affects greenhouse gases (GHG) emissions but also drastically modifies the soils contamination. For instance, industrial activities, urban traffic or agriculture can increase the soil concentration of contaminants as heavy metals or pesticides that can in turns affect soil functions (Cao et al., 1984; Bååth, 1989; Steinnes et al., 1997; Yang et al., 2006). Also, the soil contamination is expected to vary during the next decades, largely depending on international or more local policies (Ballabio et al., 2018; Panagos et al., 2018). Thus, if the soil contamination affects soil GHG emission, it is of particular importance to take it into account into LSMs to 1) adjust the scenario of climate change under the current contamination and 2) to take into account the variation due to contamination into GHG emission and climate change when prospecting land use change scenario or defining contamination guidelines. Among land-atmosphere fluxes, soil heterotrophic respiration (Rh) while soil contamination has been found to affect soil's microbes at the origin of Rh (Giller et al., 1998, 2009; Sereni et al., 2021).

Among pollutants, Cu is widely used in industry or in agriculture through fertilizers and pesticides with natural concentration varying from 5 to 50 mg Cu kg^{-1} soil due to parental material (Thornton and Webb, 1980) and concentration up to 150 mg Cu kg^{-1} in vineyards or event 3000 mg Cu kg^{-1} close to industries (Smorkalov and Vorobeichik, 2011; Ballabio et al., 2018). Soil Cu concentrations have been found to affect soil CO_2 emissions over a wide range of contamination cases (laboratory spikes, industrial or agricultural fields, forests…), but its effect on soil CO_2 emission at field scale still remains uncertain (Sereni et al., 2021).

The effect of soil Cu on GHG emission is expected to occur through its effects on soil microbes' respiration. However, it is widely accepted that all total metal content is not biologically available. For instance, free ion activity models argues that only the small amount of Cu in the form of free ion in the soil solution is effectively bio-available and impacting for soil fauna (Parker et al., 2001; Lanno et al., 2004; Thakali et al., 2006; Lofts et al., 2013). Indeed, Cu availability is highly dependent on soils properties such as soil pH, soil organic C, so that available Cu increase at low pH and low organic matter content (McBride et al., 1997). Moreover, it has been found that Cu input to soils were closely related

to soils factors like pH, clay, $CaCO_3$ or organic matter content (Ballabio et al., 2018). Thus, in our case it is possible that total Cu is not a good proxy to estimate the effect of soil contamination on GHG emission and that free Cu should be preferred.

Thus, we will investigate both the effect of total Cu and the effect of free Cu (considered as bio available) on soil CO_2 emissions. However, available databases which could be further easily reused in large scale soil models recorded total Cu because it is easier to measure than free Cu (Tóth et al., 2016; Ballabio et al., 2018). Thus, to derive bioavailable Cu, we used among the numerous empirical existing equations the Tipping et al.'s, (2003) estimation which is the most cited and used a transfer function based on more than 90 observations. Therefore, we will use its equation and the data on soil properties provided by the JRC to estimate free Cu at EU-scale.

The aim of our study was to examine whether the errors of continental biogeochemical models in reproducing observation based products of heterotrophic respiration are partially explained by the Cu content. Continental land surface (LSM) biogeochemical models differ in the mechanism they reproduce and the inclusion of environmental variables. Also, the spatial variations of soil Rh are different between models. Models intercomparison is then often used to estimate patterns of models' residue and improvement required and to distinguish individual misrepresentation from missing first order drivers that need to be better represented (Huntzinger et al., 2017). Thus, we will use models output from the TRENDY database to investigate whether the soil Cu concentration may drive models' residue. Because large scale observation of Rh fluxes are seldom and rarely direct, we will used two different products of observation with hypothesis that bias of importance were different between both products.

2. MATERIALS AND METHODS:

2.1.: Sources of soil data

Data of soil total Cu, soil organic C (Corga), soil pH, soil clay percentage, soil cationic exchange capacity (CEC) and soil $CaCO_3$ content were downloaded from the JRC data files. References can respectively be found in Ballabio et al., (2018) for total Cu, de Brogniez et al., (2015) for Corga, in Ballabio et al., (2016) for clay and in Ballabio et al., (2019) for $CaCO_3$ and CEC values. NPP observations values used are the products provided by Smith et al., (2016). This product relies on the Moderate Resolution Imaging Spectroradiometer NPP algorithm, driven by long-term Global Inventory Modeling and Mapping Studies (GIMMS) fraction of photosynthetically active radiation and leaf area index data, to calculate a 30-year global data set of satellite-derived NPP (1982–2011).

We hypothesis that soil Cu concentration was roughly constant over the last decades, thus that data provided by the JRC in 2015 may be used for comparison over the 1982-2010 time period. Concentration of free Cu was calculated as proxi of bio available Cu (Parker et al., 2001). Free ion Cu^{2+} concentration was expressed as $pCu=-\log(Cu^{2+})$ with the equation III.1.1:

Eq. III.1.1: $pCu = 1.17\ pH - 1.09\ \log_{10}Cu + 0.52\ \log_{10}(2.Corga) - 5.35$

(Tipping et al., 2003) . Co-variables used to calculate Cu in solution and free Cu were from the JRC databases.

Data were collected at the 0.5km scale and regridded using the climate data operator cdo at 0.5° to fit with the TRENDY models resolution.

2.2.: Observations of heterotrophic respiration data

Two products of observation for heterotrophic respiration were used for comparison: one was provided by Hashimoto as yearly means over the 1901-2010 period and at the 0.5° scale (Hashimoto et al., 2015). Most of the observation were made after 1990. Hashimoto's product is based on semi-empirical approach that defines heterotrophic respirations response to temperature and precipitation based on few hundreds' measurement, then estimates heterotrophic respiration at the global scale on the basis on climatic measurement. These observations will be further named Rh Hashimoto. The other is provided by Warner as mean of the 1961 – 2010 period at the 1km scale (Warner et al., 2019). The other observations product arose from machine learning trained on few hundreds 'observations. Warner et al. (2019) data base procures soil respiration fluxes and two derivations of heterotrophic fluxes from it. As both derivations are linear products of the same co-factors we only use the estimation of heterotrophic respiration from Subke derivation (further named Rh Warner_S). These observations were regridded at the 0.5° to be coherent with the Trendy simulation resolution.

2.3.: Model respiration data

The TRENDY-v9 project (Sitch et al., 2015) provides the land component of the Global Carbon Project 2020 Budget with an ensemble of land carbon simulations provided by and accessible for a consortium of DGVM groups. Models are forced over the 1700-2019 period with changing CO_2, climate and land use according to the S3 protocol detailed in https://sites.exeter.ac.uk/trendy (last access 17. September 2021). Briefly, models are forced over 1901-2019 by the monthly or 6 hours Climate Research Units (CRU) historical forcing provided by Ian Harris at UEA 1901-2019 and available at ttps://crudata.uea.ac.uk/cru/data/hrg/cru_ts_4.04/ (Mitchell et al., 2004). Atmospheric CO_2 data for the 1700-2019 time period are derived from ice core CO_2 data merged with NOAA resolution from 1958 onwards. Land Use change data are based on updated data from HYDE for the years 1960-2020 and the latest FAO wood harvest data. Trendy-v9 data base provide results for 20 models with variables data in separate netcdf files. Files from a same model were combined into a single netcdf file at the 0.5° and aggregated in yearly data for the 1900-2019 and then an average over the period 1980-2011 was calculated. Models with coarser resolution were removed from the comparison.

Because Rh is strongly correlated with NPP, soil moisture, air temperature and soil Corga content we aimed at including these variables from the models before comparison with observations. Also, from the whole TRENDY database we removed models missing one of these variables. Finally, we ended up with: ISAM, LPX, ORCHIDEE, ORCHIDEE v3,

2.4.: Statistical analysis

We investigated the differences between Rh estimated by each model and each Rh from observation-based products. To identify the drivers of the model residues we used two different set of predictors.

Set A was: clay, CEC, pH, total Cu, temperature, soil moisture, the differences of NPP following eq. III.1.2, CaCO3 and the differences of Corga following eq. III.1.3. Set B was clay, CEC, free Cu (considered as a proxy for bioavailable Cu and defined based on eq. III.1.1), temperature, soil moisture, the differences of NPP (ΔNPP = NPP from model i – NPP observed) and CaCO3.

$\Delta NPP_i = NPP_i - NPP\ observed$ (eq. III.1.2)

$\Delta Corga_i = Corga_i - Corga\ observed$ (eq. III.1.3)

With *i* being a trendy model, NPP observed and Corga observed being dataset described in section 2.1

As we were looking for second order processes, because we hypothesized threshold in Cu effect and because neither raw neither log transformed variables (except for (Cu)) were normally distributed classical model such as linear mixed effect model were not relevant. Also, it was hypothesized that our covariables were spatially correlated. Thus, we proceed with a twofold methodology. 1. We compare several linear generalized least square models with no or different spatial structures (gaussian, exponential, spherical, linear or rational (gls package)). Based on AIC values we selected exponential spatial correlation that had the smallest AIC values for the following analysis 2. We used polynomial generalized least square estimations (gls, package) with all terms represented at their 3rd degree with exponential spatial correlation 3. We selected variables to keep in the final model thanks to the stepAIC function that aimed at keeping the more parsimonious model based on the AIC criteria. All statistical analysis were made using R v3.5 (R Core Team, 2018). Finally, because the Cu maps provided by the JRC are done at EU-scale, all the analysis were done over the EU territory.

3. RESULTS

3.1. Observed heterotrophic respiration fluxes.

Maps of mean heterotrophic respiration fluxes period for the Europe are presented in fig. III.1.1 respectively for the Hashimoto (a) and the Warner_S (b) observations-derived products.

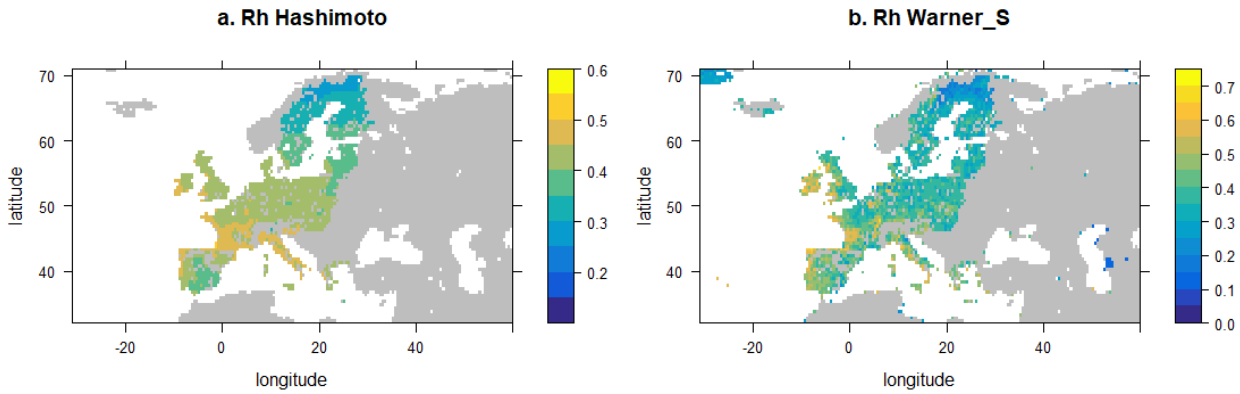

Fig. III.1.1. Heterotrophic respiration (Rh) fluxes from the observations products in kgC m^{-2} $year^{-1}$. a. Rh Hashimoto, b. Rh Warner_S filtered over the EU territory.

Hashimoto Rh's fluxes were about 0.40 ± 0.05 kgC m^{-2} y^{-1} (mean, sd) with minimal at 0.27 and max at 0.51 whereas Warner_S Rh's fluxes were about 0.38 kgC m^{-2} y^{-1} (mean, sd) and varied from 0.16 to 0.66 kgC m^{-2} y^{-1} (table III.1.1) The Rh Warner_S also show more coarser variation in Rh than the observation of Hashimoto. In both case the Rh fluxes increase from the south-west to the north east of Europe. However, Rh Warner_S have more scattered pattern with more isolated variations. For instance, with Rh Warner_S, Croatia and North West Italy have highest fluxes than South Alpes while with Hashimoto's database the whole region has similar fluxes.

Table III.1.1: Descriptive statistics of Rh with minimal, 1st quartile, median, mean, 3rd quartile and maximal values for the 2 products of observation Rh Hashimoto and Rh Warner_S and the 4 models ORCHIDEE, ORCHIDEE v3, ISAM and LPX expressed in kgC m^{-2} $year^{-1}$

	min	1st quartile	median	mean	3rd quartile	max
Rh Hashimoto	0.27	0.38	0.41	0.40	0.44	0.51
Rh Warner_S	0.16	0.33	0.38	0.39	0.43	0.67
Rh ISAM	0.00	0.34	0.54	0.47	0.61	0.79
Rh LPX	0.00	0.31	0.38	0.38	0.45	0.70
Rh ORCHIDEE	0.04	0.31	0.38	0.39	0.48	0.69
Rh ORCHIDEE v3	0.05	0.32	0.40	0.40	0.46	1.10

3.2. Modeled heterotrophic respiration fluxes at the European scale

Mean Rh fluxes of the 4 models are 0.28 kgC m^{-2} y^{-1} with max at 1.1 and min at 0. Most of the highest respiration fluxes are modelized by ISAM (ISAM median Rh 0.35 kgC m^{-2} y^{-1} and 3rd quartile 0.54 kgC.m^{-2}.y^{-1}) but maximum value is obtained with ORCHIDEE v3 (1.1 kgC m^{-2} y^{-1}), see table III.1.1. Fig. III.1.2 shows the modeled Rh fluxes at the EU scale. Most of the models reproduce the North-East gradient of increase in Rh fluxes but their spatial patterns differ. For instance, ISAM shows the highest contrast and ORCHIDEE v3 the lightest with particularly highest respiration in North Germany but not in Scotland. Highest respiration fluxes in North Spain and Italy are modeled in the case of ISAM and ORCHIDEE while LPX and ORCHIDEE v3 modeled little increase in Rh fluxes in these regions.

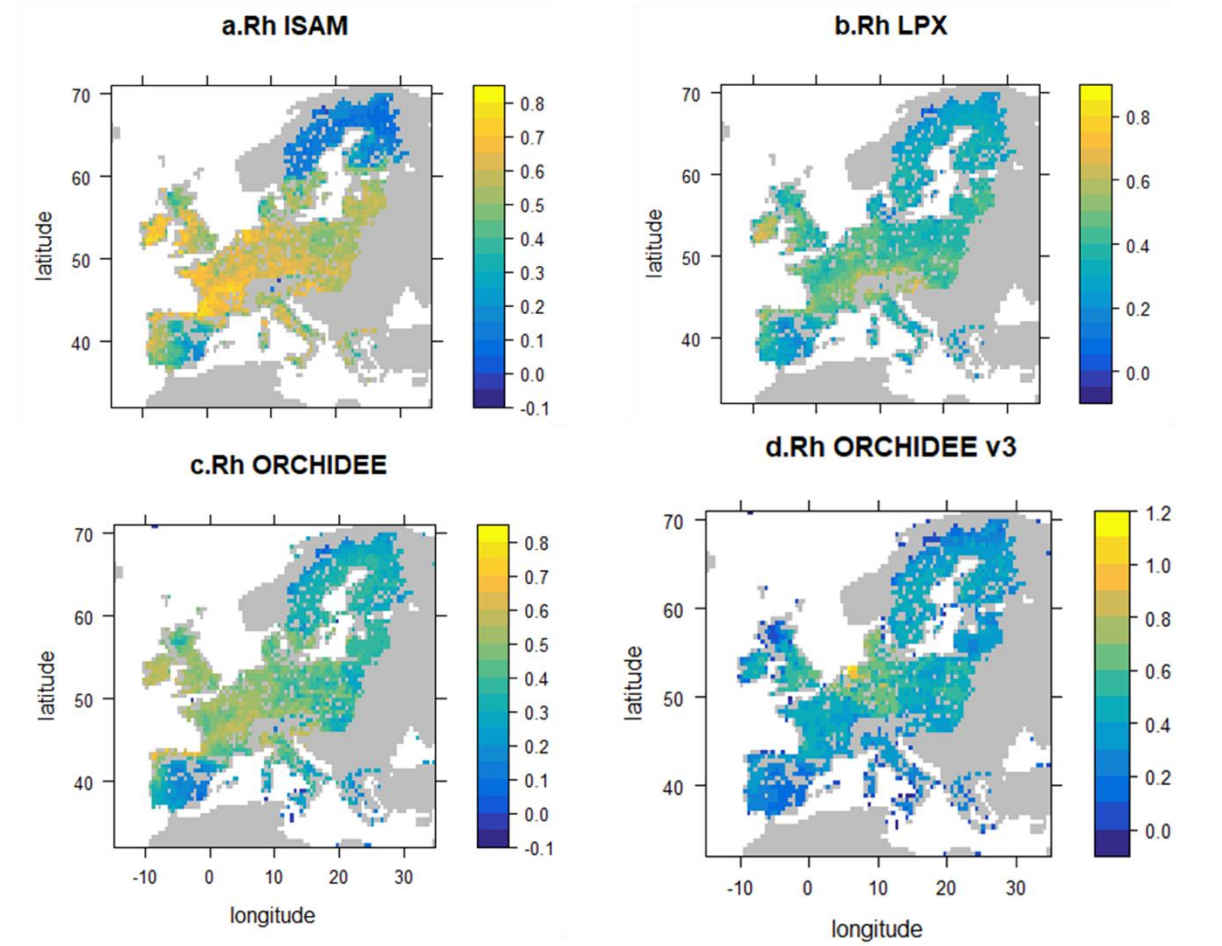

Fig. III.1.2. Heterotrophic respiration (Rh) fluxes from the different LSM models in kgC m^{-2} $year^{-1}$. a. ISAM model, b. LPX model, c. ORCHIDEE model, d. ORCHIDEE v3 model filtered over the EU territory.

3.3. Residues of modeled Rh

On the studied area, we observed a global underestimation of Rh fluxes (median values for differences between model and observed Rh <0) for all models except ISAM when compared with the Hashimoto's Rh products. Nevertheless, when compared with Rh Warner_S products, we observed a global overestimation of Rh fluxes (median values for differences between model and observed Rh >0), see table III.1.2. For all models, the global underestimation of Rh fluxes in comparison to Hashimoto's Rh is balanced by overestimation at some grid points (3rd quartile and/or maximum values of differences between model and observed Rh>0). Fig III.1.3 shows the differences between modeled Rh and Hashimoto's Rh. ISAM model mostly overestimated Rh in West Europe and underestimated it in Scandinavia and South Europe. LPX is less contrasted but there is an underestimation in Spain and overestimation in North Alps. ORCHIDEE show similar pattern than ISAM despite smallest overestimation. ORCHIDEE v3 mostly underestimated Rh in Central west and south Europe but overestimated Rh in North central Europe. Fig. III.1.4 shows the differences between modeled Rh and Warner_S Rh's. Three models (LPX, ISAM, ORCHIDEE) show a global overestimation of Rh in central

and East Europe and an underestimation in Scandinavia and South Europe. In these cases, the contrasts are more pronounced. ORCHIDEE v3 mostly overestimate Rh in North Europe.

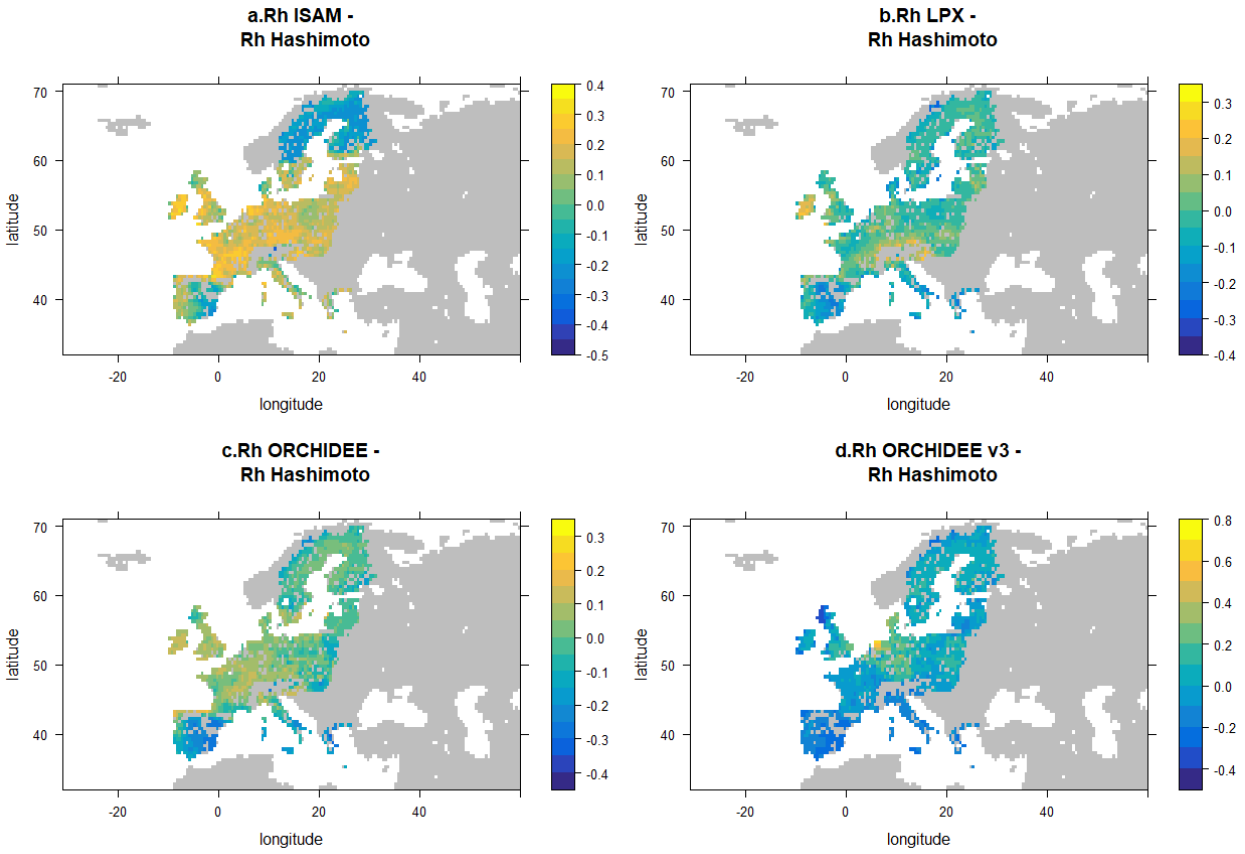

Fig III.1.3. Differences between modeled Rh and observed Rh from Hashimoto observation product for the different LSMs expressed in $kgC.m^{-2}.year^{-1}$. a. Between ISAM and Hashimoto, b. between, LPX and Hashimoto, c. between ORCHIDEE and Hashimoto, d. between ORCHIDEE v3 and Hashimoto

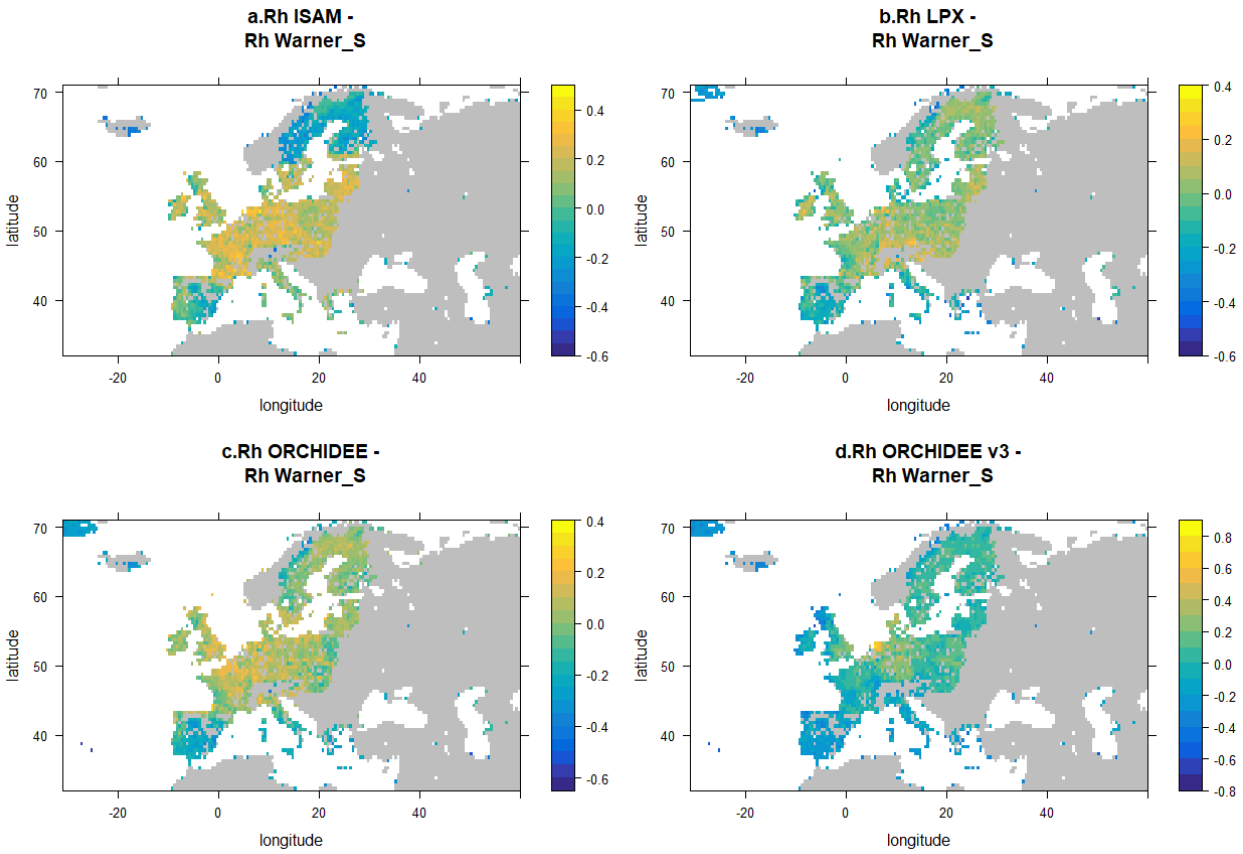

Fig. III.1.4: Differences between modeled Rh and observed Rh from Warner_S observation product for the different LSMs expressed in $kgC.m^{-2}.year^{-1}$. a. Between ISAM and Warner_S, b. between, LPX and Warner_S, c. between ORCHIDEE and Warner_S, d. between ORCHIDEE v3 and Warner_S

Table III.1.2.: Descriptive statistics Rh with minimal, 1st quartile, median, mean, 3rd quartile and maximal values for the 2 differences between the two products of observation Rh and the 4 models ORCHIDEE, ORCHIDEE v3, ISAM and LPX expressed in kgC $m^{-2}.year^{-1}$ a. differences with Rh Hashimoto and b. differences with Rh Warner_S

a.

Model Rh -Rh Hashimoto	Min	1st quartile	median	mean	3rd quartile	Max
Rh ISAM	-0.38	-0.06	0.13	0.07	0.18	0.32
Rh LPX	-0.29	-0.05	-0.02	-0.02	0.02	0.24
Rh ORCHIDEE	-0.34	-0.05	0	-0.01	0.05	0.2
Rh ORCHDEE v3	-0.34	-0.05	0	-0.01	0.05	0.2

b.

Model -Rh Warner_S	Min	1st quartile	mediane	mean	3rd quartile	max
ISAM	-0.43	-0.05	0.14	0.09	0.21	0.40
LPX	-0.49	-0.06	0.01	-0.01	0.06	0.25
ORCHIDEE	-0.43	-0.05	0.02	0.00	0.08	0.26
ORCHIDEE v3	-0.43	-0.05	0.02	0.00	0.08	0.26

3.4. Statistical models to explain modeled Rh residue

a. Effect of pedo-climatic predictors to explain modeled Rh residue

The Rh residues for the different models (difference between model and observed Rh) were analyzed against several driving factors (see 2.4.). The differences between modeled and observed Rh were better explain by the gls in the case of ORCHIDEE where the residual standard error is the smallest. AIC are also the smallest with few terms conserved by the stepAIC procedures. By contrast, the largest residual standard error and AIC are found for the comparison of Rh ORCHIDEE v3. (see table III.1.3).

Table III.1.3.: Predictors selected by the step AIC procedure to explain differences between modeled and observed Rh with A set of predictors in initial gls model. Crosses indicate that a predictor (column) has been selected as significant to explain difference between model Rh (row) and observed Rh.

Residual standard error and AIC of the final model are indicated. Corresponding partial plots are presented in suppl. Fig III.1.1, III.1.3, III.1.5, III.1.7 for Rh Hashimoto and Suppl. Fig. III.1.2, III.1.4, III.1.6, III.1.8 for Rh Warner_S a.: with Rh Hashimoto for comparison b.: with Rh Warner_S for comparison ; c. is the number of times where each predictor is conserved over a. and b.

a.

Rh Model - Rh Hashimoto	Soil moisture	temperature	Cu	Δ Corga	Δ NPP	pH	clay	CEC	CaCO3	residual standard error	AIC
ISAM	X	X	X	X	X	X	X	X		0.11	-5006
LPX	X	X	X	X	X	X	X			0.064	-6180
ORCHIDEE	X	X			X	X			X	0.060	-12833
ORCHIDEE v3	X	X	X	X	X		X			0.156	-4869

b.

Rh Model - Rh Warner_S	Soil moisture	temperature	Cu	Δ Corga	Δ NPP	pH	clay	CEC	CaCO3	residual standard error	AIC
ISAM	X	X		X	X		X	X		0.086	-4410
LPX		X	X	X	X		X		X	0.11	-3955
ORCHIDEE			X			X	X			0.088	-5039
ORCHIDEE v3	X	X		X	X	X	X			0.22	-3852

c.

Predictor	Soil moisture	temperature	Cu	Δ Corga	Δ NPP	pH	clay	CEC	CaCO3
N° times conserved over the 8 regressions	6	7	5	6	7	5	7	2	2

Table III.1.4.: Predictors selected by the step AIC procedure to explain differences between modeled and observed Rh with B set of predictors in initial gls model. Crosses indicate that a predictor (column) has been selected as significant to explain difference between model Rh (row) and observed Rh. Residual standard error and AIC of the final model are indicated. Corresponding partial plots are presented in suppl. Fig III.1.9, III.1.11, III.1.13, III.1.15 for Rh Hashimoto and Suppl. Fig. III.1.10, III.1.12, III.1.14, III.1.16 for Rh Warner_S a.:with Rh Hashimoto for comparison b.: with Rh Warner_S for comparison. c. is the number of times where each predictor is conserved over a. and b.

a.

Rh Mod - Rh Hashimoto	soil moisture	temperature	pCu	Δ NPP	clay	CEC	CaCO3	residual standard error	AIC
ISAM	X	X	X	X		X		0.11	-3943
LPX	X	X	X	X	X	X		0.065	-6121
ORCHIDEE	X	X	X	X			X	0.060	-12826
ORCHIDEE v3	X	X		X				0.156	-4836

b.

Rh Mod - Rh Warner_S	soil moisture	temperature	pCu	Δ NPP	clay	CEC	CaCO3	residual standard error	AIC
ISAM	X	X		X	X	X		0.11	-3943
LPX		X	X	X	X			0.087	-4392
ORCHIDEE			X		X		X	0.089	-5042
ORCHIDEE v3	X	X	X	X	X			0.22	-3829

c.

Predictor	Soil moisture	temperature	pCu	Δ NPP	clay	CEC	CaCO3
N° times conserved over the 8 regressions	6	7	6	7	5	3	2

Soil moisture and air surface temperature were conserved by stepAIC selection in all cases when Rh Hashimoto was used for comparison (table III.1.3a, III.1.4a). When using Rh Warner_S, soil moisture was only conserved by the stepAIC in the case of ISAM and ORCHIDEE v3 and air surface temperature in ISAM, LPX and ORCHIDEE v3 (table III.1.3b, III.1.4b). Similarly, the difference between modeled NPP and NPP from the GIMMS product was selected as an explaining variable of the all the models residues when using Rh Hashimoto. When compared with Rh Warner_S, the difference between modeled NPP and NPP from the GIMMS product was also selected as an explaining variable of the all the models residues except for ORCHIDEE. Soils CEC and $CaCO_3$ were less conserved by the stepAIC selection: CEC was found significant to explain the models residues in 5 over the 16 studied cases (table III.1.3c and 4c). CEC was conserved to explain the models residues between Rh ISAM and Rh Hashimoto and Rh Warner_S but not for the other models except for the comparison of Rh LPX and Rh Hashimoto taking pCu into account. $CaCO_3$ was only conserved for the analysis of Rh ORCHIDEE's residues except for the comparison of Rh modeled to Rh Hashimoto with set A of predictor into account. In the case of comparison of Rh Hashimoto with set A of predictor, $CaCO_3$ was conserved in the Rh LPX residues analysis but not for the Rh ORCHIDEE residues analysis. Clay was conserved in all the cases when Rh Warner_S was used for comparison. When using Rh Hashimoto for comparison, clay was found significant in all except ORCHIDEE case when using total Cu as a predictor but only in the LPX case when using pCu as a predictor. The difference between modeled and measured soil Corga is only involved when using total Cu as a predictor because soil Corga is used for pCu calculation. In these cases, Δ Corga was found significant in all cases except ORCHIDEE.

b. Effect of total Cu or bio-available Cu as predictor of modeled Rh residue

Total Cu was conserved by the stepAIC selection in 5 over the 8 studied cases while pCu was conserved in 6 over the 8 studied cases by the stepAIC selection (table III.1.3c and III.1.4c respectively). The terms conserved by the stepAIC selection and Rh are respectively displayed in table III.1.3a, III.1.4a for the comparison with Rh Hashimoto and III.1.3b, III.1.4b for the comparison with Rh Warner_S considering set A (table III.1.3) or set B (table III.1.4) as predictor. With comparison to the Rh Hashimoto data base, Cu was conserved for the ISAM and LPX models considering both total and free Cu content. The total Cu content was also found to explain the difference between Rh ORCHIDEE v3 and Rh Hashimoto while

pCu was found to explain the difference between Rh ORCHIDEE and Rh Hashimoto. With use of Rh Warner_S for comparison, total Cu was conserved by the stepAIC selection for Rh LPX and Rh ORCHIDEE and pCu for Rh LPX, Rh ORCHIDEE and Rh ORCHIDEE v3. Hence, total and free Cu were conserved in all cases for LPX models, in ¾ cases for ORCHIDEE and in half of the cases for ISAM and ORCHIDEE v3 (table III.1.4c). Thus, in models selected by the stepAIC, Cu and pCu are considered as significant variables as many times as clay or soil moisture and 2-3 times more than CEC or CaCO3.

Fig. III.1.5 and III.1.6 show the partial effects of total Cu, fig. III.1.7 and III.1.8 those of pCu as a predictor of differences between models and observed Rh (when Cu or pCu were not conserved by the regression the plots are not shown). When conserved, Cu partial effect was found of the same order (10^{-1}) of magnitude to explain Rh residue than the other predictor except the temperature that has 10 times larger effect. Partial plot showing the regressions of the selected term in gls models are provided in suppl. fig. III.1.1 to III.1.8 (full gls before terms selection using set A of predictors) for the differences between the 4 models and the two observations products and III.1.9 to III.1.16 (full gls before terms' selection using set B of predictors) for the differences between the 4 models and the two observations products.

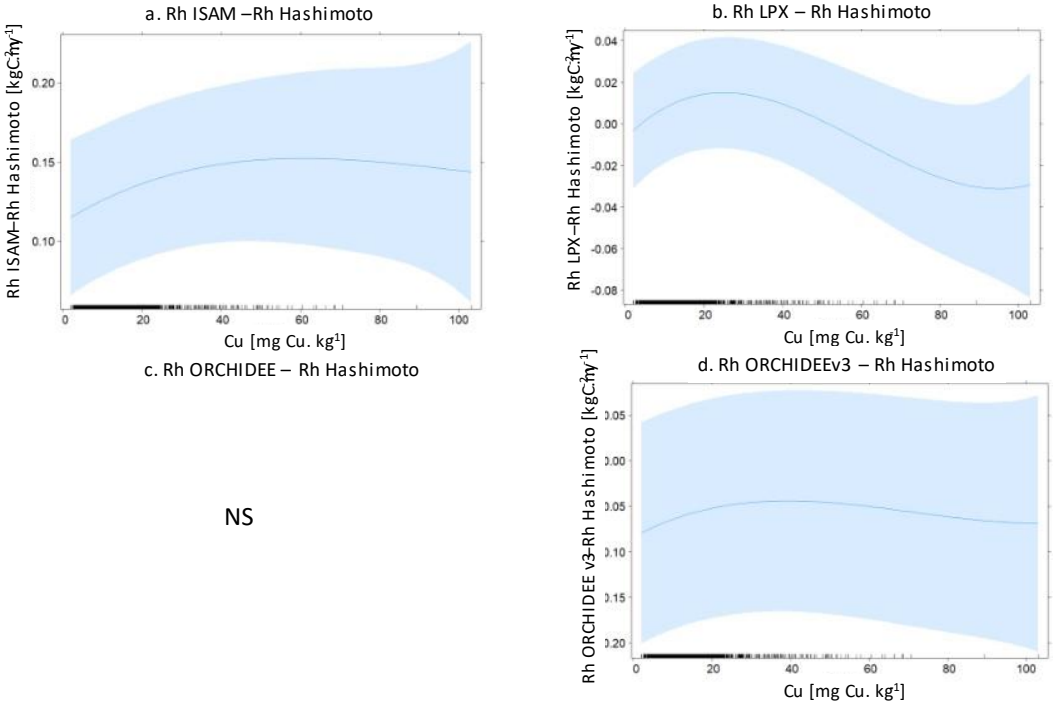

Fig. III.1.5.: Partial Cu effects plots for the differences between the four models and Rh Hashimoto. A. for ISAM, b. for LPX, c. for ORCHIDEE, d. for ORCHIDEE v3

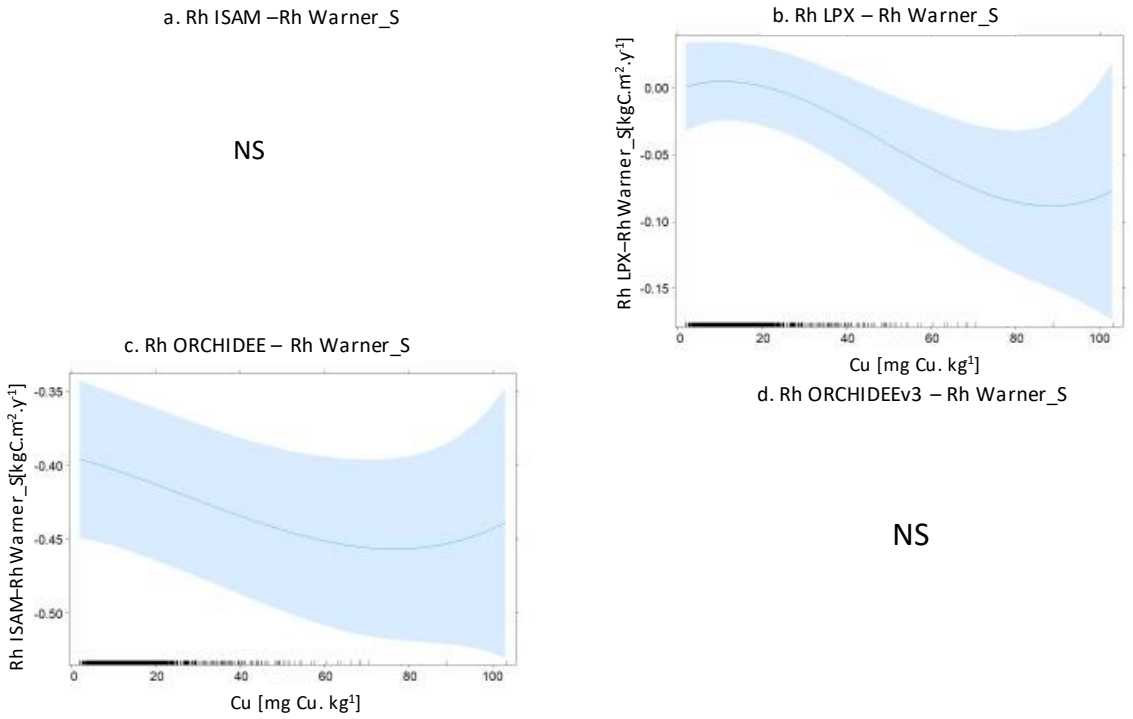

Fig III.1.6. Partial Cu effects plots for the differences between the four models and Rh Warner_S. A. for ISAM, b. for LPX, c. for ORCHIDEE, d. for ORCHIDEE v3

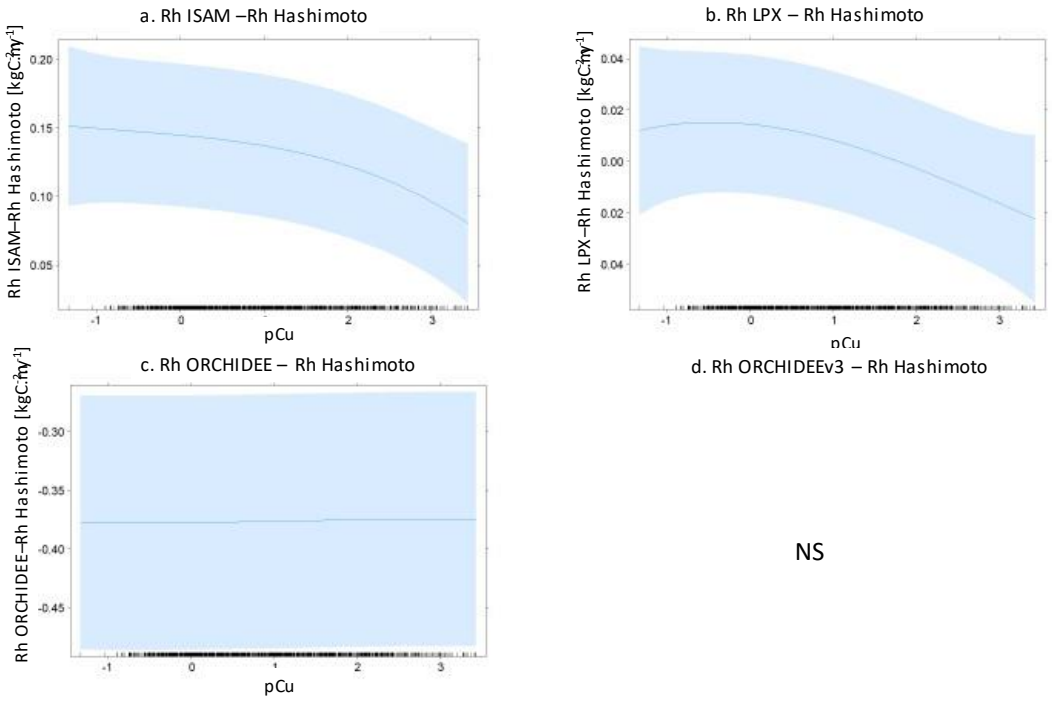

Fig III.1.7. Partial pCu effects plots for the differences between the four models and Rh Hashimoto. A. for ISAM, b. for LPX, c. for ORCHIDEE, d. for ORCHIDEE v3

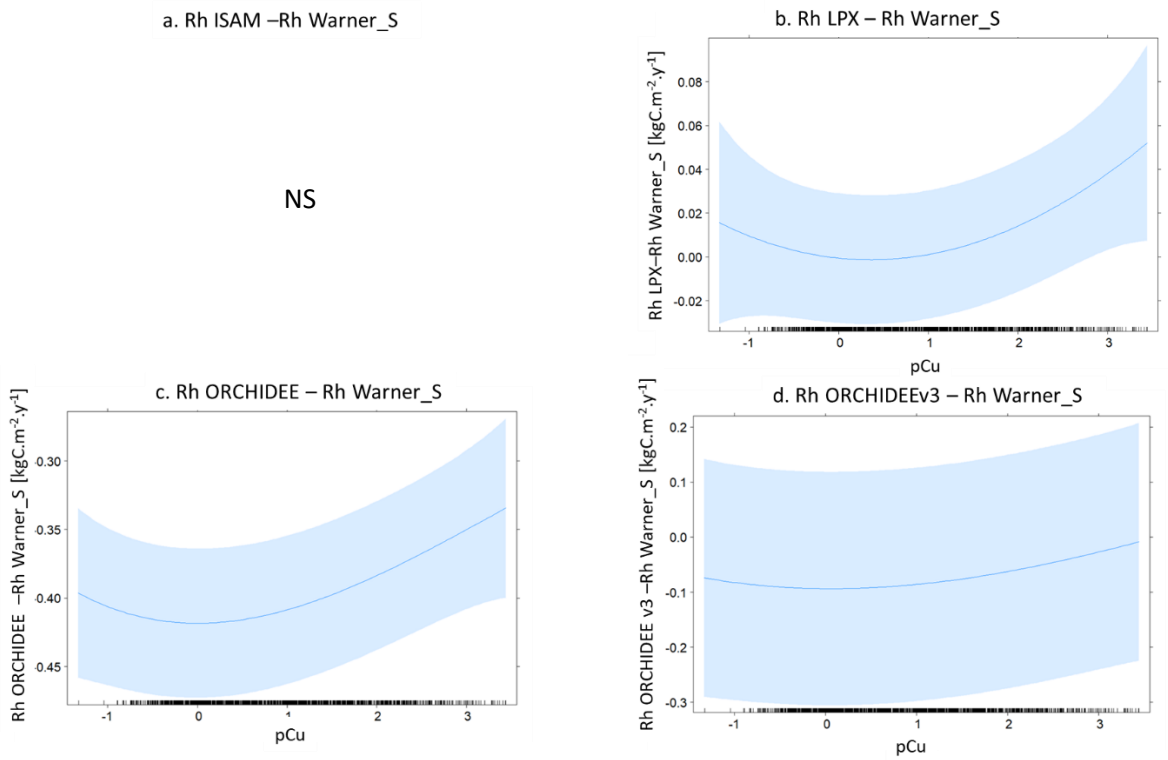

Fig III.1.8. Partial pCu effects plots for the differences between the four models and Rh Warner_S. A. for ISAM, b. for LPX, c. for ORCHIDEE, d. for ORCHIDEE v3

Considering the four models and the two bases of observation there is a global increase in differences between model and observed Rh with moderate increase in soil total Cu, then a decrease. However, the shifts in trends differ depending on the models and the observations products. Considering Rh ISAM- Rh Hashimoto or Rh ORCHIDEE v3- Rh Hashimoto the maximum differences are for Cu concentrations around 40 mgCu kg^{-1} while for Rh LPX- Rh Hashimoto or Rh LPX- Rh Warner_S the maximum differences are for Cu concentrations below 20 mg Cu kg^{-1}. Furthermore, in these two last cases and in the Rh ORCHIDEE- Rh Warner_S case the differences show a second increase for the higher Cu concentration >80 mg Cu kg^{-1} (fig. III.1.5b, III.1.6b, III.1.c).

With use of set B of predictors, the results differ depending on the source of observation. With use of Rh Hashimoto's, there is an increase in difference between model and observed Rh for very small pCu (high free Cu) and a decrease in difference between model and observed Rh for high pCu (low free Cu), see fig. III.1.7. By contrast, the differences between models Rh and Rh Warner_S increase for low pCu (high free Cu), decrease for moderate pCu and increase for high pCu (low free Cu), see fig. III.1.8.

4. DISCUSSION

4.1.: Integrating soil contamination into LSMs

In the present study we found that soil Cu concentration was a significant factor to explain differences between modeled Rh and Rh from observation products. Hence, taking soil Cu concentration into

account in LSMs may improve their predictive capacities. Taking a new parameter into account may be achieved either 1. by the definition of empirical functions that correct the models on the basis of their difference to observations products either 2. By the definition of mechanistic functions that adjust the modeled component affect by the soil contamination.

The first approach required large data base of chosen endpoints (Rh, NPP, GPP etc…) and of soil contamination to calibrate the model. The present study illustrates the limitation of this approach, with different results depending on the observation products and the models considered. Moreover, the calibration of statistical functions on the basis of observational databases limits the possibility to use the resulting functions for prospective studies. Indeed, the strength of such calibration is to reproduce as well as possible the current status of endpoints in response to the current soil contamination. However, the extrapolation over the range of calibration is difficult. Some ecotoxicological studies used a space for time scheme of study to estimate the future of area that are currently not contaminated but are about to be. This approach may be reliable for close area but it has been shown that climatic conditions may affects ecosystem response to soils contamination (Tobor-Kapłon et al., 2006; Moe et al., 2013; Li et al., 2017). Thus, the extrapolation of response functions to soils contamination may be not applicable over large area.

The second approach is more suitable for prospective studies as laboratory studies may easily use large concentration of contaminant to investigate endpoints response. However, this requires to process a large number of experimental studies taking into account the multiplicity of co-factors (soils pH, texture, climate…). Moreover, the processes studied into micro or mesocosms for the purpose of calibrations functions may be not illustrative of the ecosystem's response and the large-scale processes modeled. For instance, it has been shown that soil contamination may affect both the microbial efficiency and the microbial amount. These two effects have different consequences on long term key processes of LSMs (for instance soil CO_2 emissions and Corga concentration) but the explicit representation of microbial biomass being not implemented in LSMs yet, the integration of responses function to soil contamination should be adapted model per model. More generally the explicit representations of fine scale processes into LSMs is still under investigation (Fisher and Koven, 2020).

4.2.: Regional analysis of soil contamination

This study was conducted at the 0.5° scale which is one of the finest scale for LSMs but a coarse resolution for geochemical and contaminant variations (Anav et al., 2013; Tóth et al., 2016). Indeed, the mapping of soil Cu at 0.5° we used here limits the hot spots of Cu concentration, with for instance 1/1570 grid points with Cu >100 mg Cu.kg $^{-1}$ and 13/1570 grid points with Cu >50 mg Cu.kg^{-1}. Also, the results presented here concerned more diffuse contamination, e.g. limited to few decades to hundred mg Cu. kg $^{-1}$ but for area of at least 0.5°. By contrast, Cu concentration >100 mgCu .kg^{-1} was found in 1.1% of the samples in the Ballabio et al.'s, (2018) soil survey study and vineyards' Cu mean was found close to 50 mg Cu.kg^{-1}. Previous study on laboratory incubation found a general decrease in soil Rh with increase in soil Cu contamination despite an increase in soil Rh at limited Cu concentration for freshly contaminated soils (Sereni et al., 2021). Due to the small number of grid points at high concentration we used here, it is difficult to determine the robustness of the decreased tendency observed. Moreover, we limited our study to the European scale while ecosystems response to

external disturbance may largely varied across biomes (Clements and Rohr, 2009; Bowler et al., 2020; Beaumelle et al., 2021). With growing interest of soil Rh, databases at large scale and coarse resolutions are regularly published based on different aggregations procedures, hence the analysis we conducted here may be reinforced with comparison to coarser and broader databases (Bond-Lamberty et al., 2020; Jian et al., 2021).

Moreover, we focused on the soil Cu contamination as a model for soil contamination because it is widely used in agricultural sectors and well-studied. However, soil contamination rarely occurs with single contaminant. Indeed, atmospheric deposition from industries or transports are often a mixture of heavy metals while agricultural fungicides and pesticides are also made of organic component. For instance, Tóth et al., (2016) found that in Europe, Cu concentrations were highly correlated to Co, Cr, Mn, Ni and Sb concentrations. Multi-contaminations effects on soils functions are hard to estimate. In some cases, an adaptation to a contaminant limits the effects of the other while in other cases stress conjugations increase effect's on fauna or functions (Wakelin et al., 2014; Rillig et al., 2019; Zandalinas et al., 2021). Finally, contaminants have different sources and environmental mobility also, scale of contamination diffusion may vary. Hence, if our study emphasized the Cu contamination importance for 0.5° Rh dominant contaminant may differs with spatial resolution.

4.3.: Uncertainties in Rh estimations

In this study we observed differences between the Rh for Warner_S observation's derived product and the observation derived product from Hashimoto et al., (2015). These two products are based on different statistical mapping at the worldwide scale based on few thousand points so that the predictors conserved to explain Rh for the 2 observation products differs. The strong dependency of Rh Hashimoto on climate factors might be explained by its construction as a semi empirical function of temperature and precipitation (Hashimoto et al., 2015). By contrast, Rh Warner_S constructed with a random forest algorithm is also explained by several pedological factors even if the conserved factors for data base construction were restrained to temperature, precipitation (annual mean and mean from November to January) and enhanced vegetation index. Over Europe, Ballabio et al., (2018) found that Cu soil concentration was correlated with spring temperature and rainfall. More precisely, Cu concentration was found higher in the humid and hot area were fungicides application to fight against down mildew are frequent and much particularly in vineyards. Then, with the inclusion of enhanced vegetation index in Rh Warner_S random forests algorithm predictors as $CaCO_3$, clay, pH or Cu. Hence, due to their statistical derivations, the observations products differ in their strength of Rh variability reproduction. Therefore, the models residues analysis required to use several observations products for comparison to limits false positive as well than false negative due to observation products derivations methods.

5. CONCLUSION

The comparison of Rh to soil Cu concentration databases show that soil Cu concentration was a relevant predictor for Rh defined at 0.5° scale. Indeed, no significant effect of Cu was found by comparison to Rh Hashimoto whereas significant effect of Cu was found by comparison to Rh Warner_S, that we previously identified with coarser variations. Our results also show that total Cu as well than free Cu were relevant predictors of Rh, without gaining in accuracy with use of free Cu. In the two cases, soil Rh was found to increase with increase in soil Cu concentration.

The analysis of the 4 LSMs show that Cu may in most of the cases explain their residue. Indeed, in 11 of the 16 studied cases, Cu (express as a total content or as a bioavailable) was found significative. In 10 of these cases the Cu effect was found of the same order of magnitude than the other soils factors. General trends were an increase in difference between model and observed soil Rh at small Cu concentrations then a decrease. However, the Cu concentration of inversion from an increase to a decrease largely varied among the models and the observations considered. None of these models considered Cu. Also, the various responses we observed should come from the different calibration of response functions to co-varying parameters like pH or climate.

References:

Anav, A., Friedlingstein, P., Kidston, M., Bopp, L., Ciais, P., Cox, P., et al. (2013). Evaluating the land and ocean components of the global carbon cycle in the CMIP5 earth system models. *J. Clim.* 26, 6801–6843. doi:10.1175/JCLI-D-12-00417.1.

Bååth, E. (1989). Effects of heavy metals in soil on microbial processes and populations (a review). *Water. Air. Soil Pollut.* 47, 335–379. doi:10.1007/BF00279331.

Ballabio, C., Lugato, E., Fernández-Ugalde, O., Orgiazzi, A., Jones, A., Borrelli, P., et al. (2019). Mapping LUCAS topsoil chemical properties at European scale using Gaussian process regression. *Geoderma*. doi:10.1016/j.geoderma.2019.113912.

Ballabio, C., Panagos, P., Lugato, E., Huang, J. H., Orgiazzi, A., Jones, A., et al. (2018). Copper distribution in European topsoils: An assessment based on LUCAS soil survey. *Sci. Total Environ.* 636, 282–298. doi:10.1016/j.scitotenv.2018.04.268.

Ballabio, C., Panagos, P., and Monatanarella, L. (2016). Mapping topsoil physical properties at European scale using the LUCAS database. *Geoderma*. doi:10.1016/j.geoderma.2015.07.006.

Beaumelle, L., Thouvenot, L., Hines, J., Jochum, M., Eisenhauer, N., and Phillips, H. R. P. (2021). Soil fauna diversity and chemical stressors: a review of knowledge gaps and roadmap for future research. *Ecography (Cop.).* 44, 845–859. doi:10.1111/ecog.05627.

Blyth, E. M., Arora, V. K., Clark, D. B., Dadson, S. J., De Kauwe, M. G., Lawrence, D. M., et al. (2021). Advances in Land Surface Modelling. *Curr. Clim. Chang. Reports* 7, 45–71. doi:10.1007/s40641-021-00171-5.

Bond-Lamberty, B., Christianson, D. S., Malhotra, A., Pennington, S. C., Sihi, D., AghaKouchak, A., et al. (2020). COSORE: A community database for continuous soil respiration and other soil-atmosphere greenhouse gas flux data. *Glob. Chang. Biol.* 26, 7268–7283. doi:10.1111/gcb.15353.

Bowler, D. E., Bjorkman, A. D., Dornelas, M., Myers-Smith, I. H., Navarro, L. M., Niamir, A., et al. (2020). Mapping human pressures on biodiversity across the planet uncovers anthropogenic threat complexes. *People Nat.* 2, 380–394. doi:10.1002/pan3.10071.

Cao, H., Chang, A. C., and Page, A. L. (1984). Heavy Metal Contents of Sludge-Treated Soils as Determined by Three Extraction Procedures been recommended as availability indices of metals in soil (Lagerwerff , 1971 ; John et al ., 1972 ; Symeonides Reisenauer , 1982). Under experimental conditions ,. 2–4.

Clements, W. H., and Rohr, J. R. (2009). Community responses to contaminants: using basic ecological principles to predict ecotoxicological effects. *Environ. Toxicol. Chem.* 28, 1789–1800. doi:10.1897/09-140.1.

Cox, P. M., Betts, R. A., Jones, C. D., Spall, S. A., and Totterdell, I. J. (2000). Acceleration of global warming due to carbon-cycle feedbacks in a coupled climate model. *Nature* 408, 184–187. doi:10.1038/35041539.

de Brogniez, D., Ballabio, C., Stevens, A., Jones, R. J. A., Montanarella, L., and van Wesemael, B. (2015). A map of the topsoil organic carbon content of Europe generated by a generalized additive model. *Eur. J. Soil Sci.* doi:10.1111/ejss.12193.

Fisher, R. A., and Koven, C. D. (2020). Perspectives on the Future of Land Surface Models and the Challenges of Representing Complex Terrestrial Systems. *J. Adv. Model. Earth Syst.* 12. doi:10.1029/2018MS001453.

Friedlingstein, P., Cox, P., Betts, R., Bopp, L., von Bloh, W., Brovkin, V., et al. (2006). Climate-carbon cycle feedback analysis: Results from the C4MIP model intercomparison. *J. Clim.* 19, 3337–3353. doi:10.1175/JCLI3800.1.

Giller, K. E., Witter, E., and Mcgrath, S. P. (1998). Toxicity of heavy metals to microorganisms and microbial processes in agricultural soils: A review. *Soil Biol. Biochem.* 30, 1389–1414. doi:10.1016/S0038-0717(97)00270-8.

Giller, K. E., Witter, E., and McGrath, S. P. (2009). Heavy metals and soil microbes. *Soil Biol. Biochem.* doi:10.1016/j.soilbio.2009.04.026.

Hashimoto, S., Carvalhais, N., Ito, A., Migliavacca, M., Nishina, K., and Reichstein, M. (2015). Global spatiotemporal distribution of soil respiration modeled using a global database. *Biogeosciences* 12, 4121–4132. doi:10.5194/bg-12-4121-2015.

Huntzinger, D. N., Michalak, A. M., Schwalm, C., Ciais, P., King, A. W., Fang, Y., et al. (2017). Uncertainty in the response of terrestrial carbon sink to environmental drivers undermines carbon-climate feedback predictions. *Sci. Rep.* 7. doi:10.1038/s41598-017-03818-2.

Jian, J., Vargas, R., Anderson-Teixeira, K., Stell, E., Herrmann, V., Horn, M., et al. (2021). A restructured and updated global soil respiration database (SRDB-V5). *Earth Syst. Sci. Data* 13, 255–267. doi:10.5194/essd-13-255-2021.

Lanno, R., Wells, J., Conder, J., Bradham, K., and Basta, N. (2004). The bioavailability of chemicals in soil for earthworms. in *Ecotoxicology and Environmental Safety* doi:10.1016/j.ecoenv.2003.08.014.

Li, J., Liu, Y. R., Cui, L. J., Hu, H. W., Wang, J. T., and He, J. Z. (2017). Copper Pollution Increases the Resistance of Soil Archaeal Community to Changes in Water Regime. *Microb. Ecol.* doi:10.1007/s00248-017-0992-0.

Lofts, S., Criel, P., Janssen, C. R., Lock, K., McGrath, S. P., Oorts, K., et al. (2013). Modelling the effects of copper on soil organisms and processes using the free ion approach: Towards a multi-species toxicity model. *Environ. Pollut.* 178, 244–253. doi:10.1016/j.envpol.2013.03.015.

McBride, M., Sauvé, S., and Hendershot, W. (1997). Solubility control of Cu, Zn, Cd and Pb in

contaminated soils. *Eur. J. Soil Sci.* 48, 337–346. doi:10.1111/j.1365-2389.1997.tb00554.x.

Mitchell, T. D., Carter, T. R., Jones, P. D., Hulme, M., and New, M. (2004). A comprehensive set of high-resolution grids of monthly climate for Europe and the globe : the observed record (1901-2000) and 16 scenarios (2001-2100). *Geography* 55, 30. Available at: http://www.ipcc-data.org/docs/tyndall_working_papers_wp55.pdf.

Moe, S. J., De Schamphelaere, K., Clements, W. H., Sorensen, M. T., Van den Brink, P. J., and Liess, M. (2013). Combined and interactive effects of global climate change and toxicants on populations and communities. *Environ. Toxicol. Chem.* 32, 49–61. doi:10.1002/etc.2045.

Panagos, P., Ballabio, C., Lugato, E., Jones, A., Borrelli, P., Scarpa, S., et al. (2018). Potential sources of anthropogenic copper inputs to European agricultural soils. *Sustain.* doi:10.3390/su10072380.

Parker, D. R., Pedler, J. F., Ahnstrom, Z. A. S., and Resketo, M. (2001). Reevaluating the free-ion activity model of trace metal toxicity toward higher plants: Experimental evidence with copper and zinc. *Environ. Toxicol. Chem.* doi:10.1002/etc.5620200426.

R Core Team (2018). R software: Version 3.5.1. *R Found. Stat. Comput.* doi:10.1007/978-3-540-74686-7.

Rillig, M. C., Ryo, M., Lehmann, A., Aguilar-Trigueros, C. A., Buchert, S., Wulf, A., et al. (2019). The role of multiple global change factors in driving soil functions and microbial biodiversity. *Science (80-.).* 366, 886–890. doi:10.1126/science.aay2832.

Schlesinger, W. H., and Andrews, J. A. (2000). Soil respiration and the global carbon cycle. *Biogeochemistry* 48, 7–20. doi:10.1023/A:1006247623877.

Sereni, L., Guenet, B., and Lamy, I. (2021). Does Copper Contamination Affect Soil CO2 Emissions? A Literature Review. *Front. Environ. Sci.* 9, 29. doi:10.3389/fenvs.2021.585677.

Sitch, S., Friedlingstein, P., Gruber, N., Jones, S. D., Murray-Tortarolo, G., Ahlström, A., et al. (2015). Recent trends and drivers of regional sources and sinks of carbon dioxide. *Biogeosciences* 12, 653–679. doi:10.5194/bg-12-653-2015.

Smith, W. K., Reed, S. C., Cleveland, C. C., Ballantyne, A. P., Anderegg, W. R. L., Wieder, W. R., et al. (2016). Large divergence of satellite and Earth system model estimates of global terrestrial CO2 fertilization. *Nat. Clim. Chang.* 6, 306–310. doi:10.1038/nclimate2879.

Smorkalov, I. A., and Vorobeichik, E. L. (2011). Soil respiration of forest ecosystems in gradients of environmental pollution by emissions from copper smelters. *Russ. J. Ecol.* 42, 464–470. doi:10.1134/S1067413611060166.

Steinnes, E., Allen, R. O., Petersen, H. M., Ramb??k, J. P., and Varskog, P. (1997). Evidence of large scale heavy-metal contamination of natural surface soils in Norway from long-range atmospheric transport. *Sci. Total Environ.* 205, 255–266. doi:10.1016/S0048-9697(97)00209-X.

Thakali, S., Allen, H. E., Di Toro, D. M., Ponizovsky, A. A., Rodney, C. P., Zhao, F. J., et al. (2006). A Terrestrial Biotic Ligand Model. 1. Development and application to Cu and Ni toxicities to barley root elongation in soils. *Environ. Sci. Technol.* 40, 7085–7093. doi:10.1021/es061171s.

Thornton, I., and Webb, J. S. (1980). “Trace Elements in Soils and Plants,” in *Food Chains and Human Nutrition* doi:10.1007/978-94-011-7336-0_12.

Tipping, E., Rieuwerts, J., Pan, G., Ashmore, M. R., Lofts, S., Hill, M. T. R., et al. (2003). The solid-solution partitioning of heavy metals (Cu, Zn, Cd, Pb) in upland soils of England and Wales. *Environ. Pollut.* 125, 213–225. doi:10.1016/S0269-7491(03)00058-7.

Tobor-Kapłon, M. A., Bloem, J., and De Ruiter, P. C. (2006). Functional stability of microbial communities from long-term stressed soils to additional disturbance. *Environ. Toxicol. Chem.* doi:10.1897/05-398R1.1.

Tóth, G., Hermann, T., Szatmári, G., and Pásztor, L. (2016). Maps of heavy metals in the soils of the European Union and proposed priority areas for detailed assessment. *Sci. Total Environ.* 565, 1054–1062. doi:10.1016/j.scitotenv.2016.05.115.

Vuichard, N., Messina, P., Luyssaert, S., Guenet, B., Zaehle, S., Ghattas, J., et al. (2018). Accounting for Carbon and Nitrogen interactions in the Global Terrestrial Ecosystem Model ORCHIDEE (trunk version, rev 4999): multi-scale evaluation of gross primary production. *Geosci. Model Dev. Discuss.* doi:10.5194/gmd-2018-261.

Wakelin, S., Gerard, E., Black, A., Hamonts, K., Condron, L., Yuan, T., et al. (2014). Mechanisms of pollution induced community tolerance in a soil microbial community exposed to Cu. *Environ. Pollut.* 190, 1–9. doi:10.1016/j.envpol.2014.03.008.

Warner, D. L., Bond-Lamberty, B., Jian, J., Stell, E., and Vargas, R. (2019). Spatial Predictions and Associated Uncertainty of Annual Soil Respiration at the Global Scale. *Global Biogeochem. Cycles* 33, 1733–1745. doi:10.1029/2019GB006264.

Yang, Y., Campbell, C. D., Clark, L., Cameron, C. M., and Paterson, E. (2006). Microbial indicators of heavy metal contamination in urban and rural soils. *Chemosphere* 63, 1942–1952. doi:10.1016/j.chemosphere.2005.10.009.

Zaehle, S., and Friend, A. (2010). Carbon and nitrogen cycle dynamics in the O-CN land surface model: 1. Model description, site-scale evaluation, and sensitivity to parameter estimates. *Global Biogeochem. Cycles* 24. doi:10.1029/2009GB003521.

Zandalinas, S. I., Fritschi, F. B., and Mittler, R. (2021). Global Warming, Climate Change, and Environmental Pollution: Recipe for a Multifactorial Stress Combination Disaster. *Trends Plant Sci.* xx, 1–12. doi:10.1016/j.tplants.2021.02.011.

Supplementary materials :

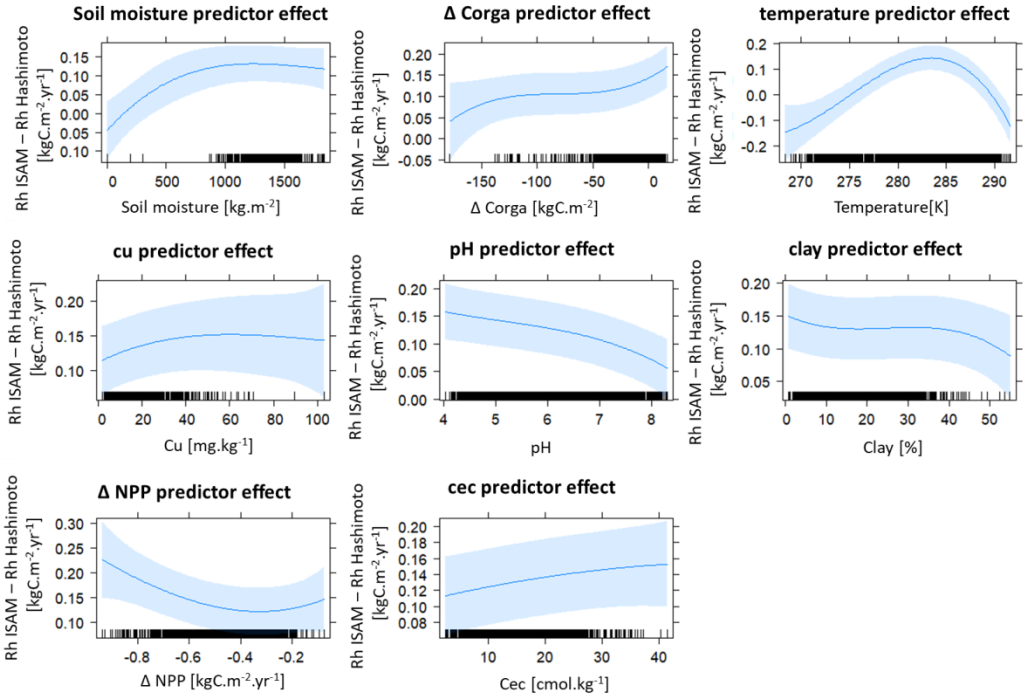

Supplementary fig III.1.1.: partial effects plot for the different predictors selected by the stepAIC procedure using set I of predictors to explain the difference Rh ISAM - Rh Hashimoto

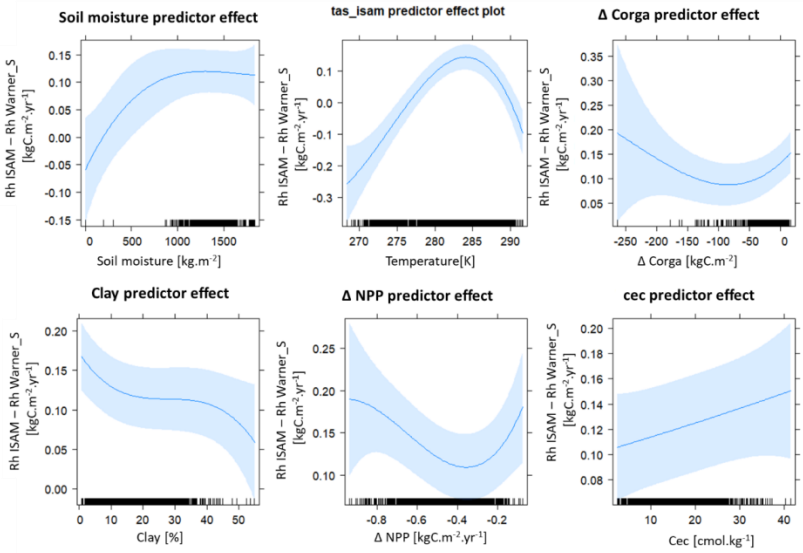

Supplementary fig III.1.2.: partial effects plot for the different predictors selected by the stepAIC procedure using set I of predictors to explain the difference Rh ISAM - Rh Warner_S

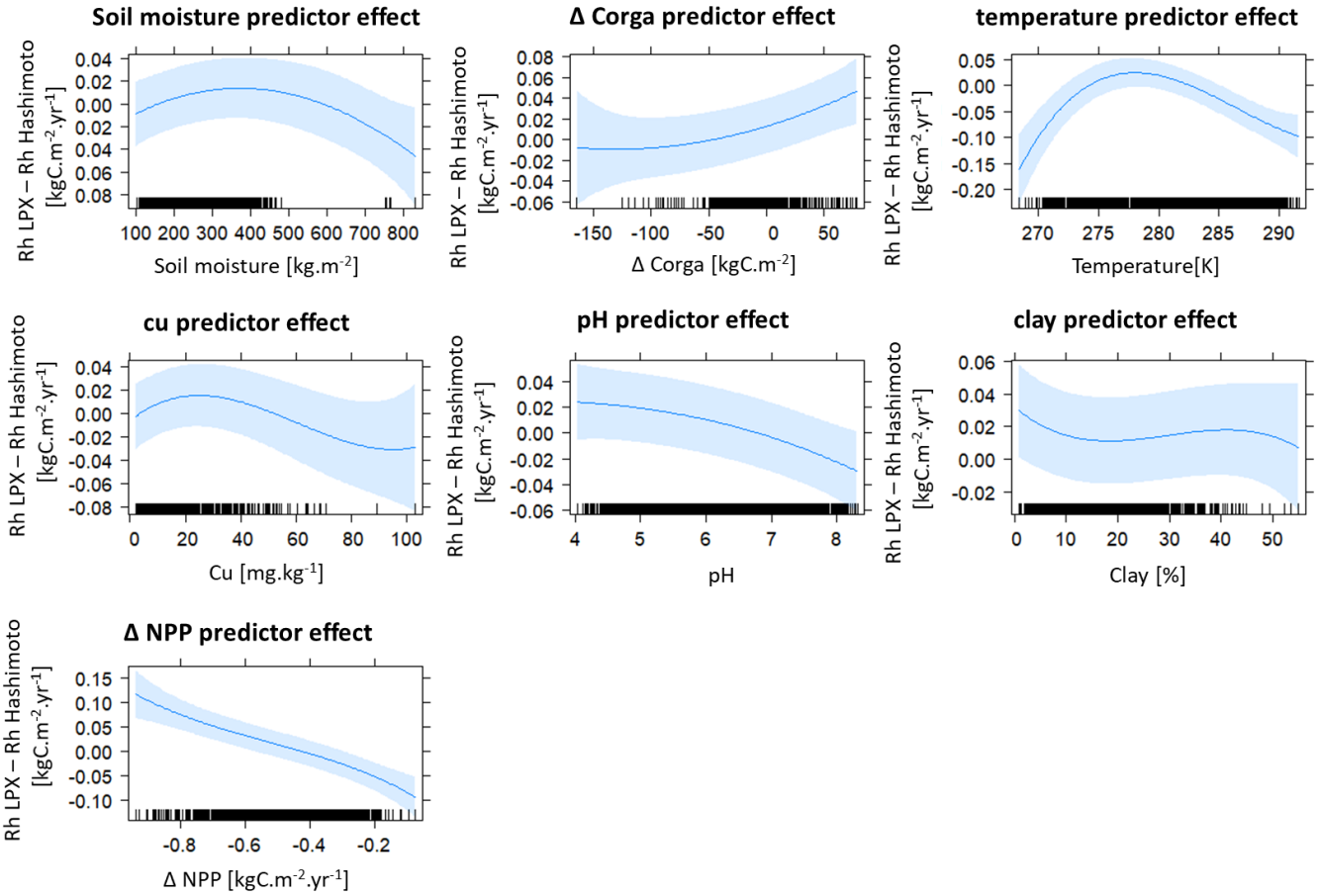

Supplementary fig III.1.3.: partial effects plot for the different predictors selected by the stepAIC procedure using set I of predictors to explain the difference Rh LPX - Rh Hashimoto

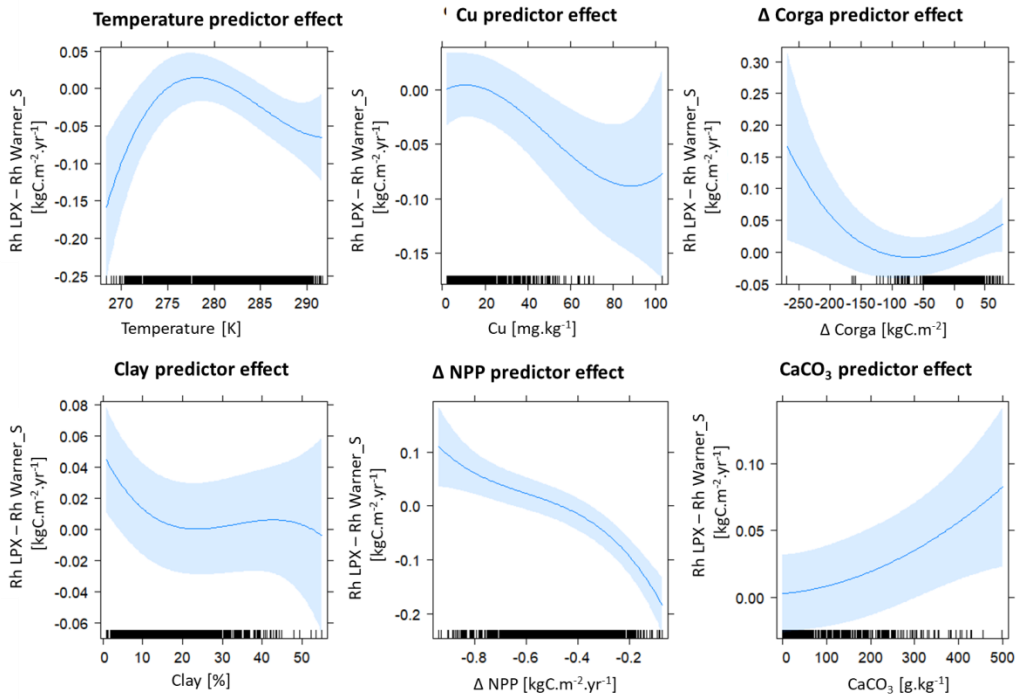

Supplementary fig III.1.4: partial effects plot for the different predictors selected by the stepAIC procedure using set I of predictors to explain the difference Rh ISAM - Rh Warner_S

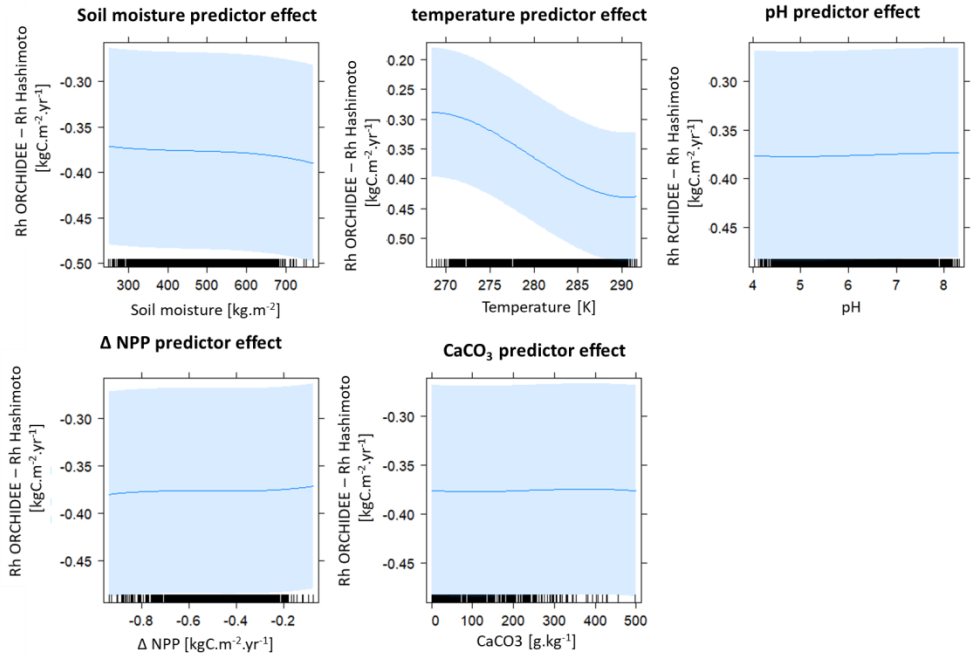

Supplementary fig III.1.5.: partial effects plot for the different predictors selected by the stepAIC procedure using set I of predictors to explain the difference Rh ORCHIDEE - Rh Hashimoto

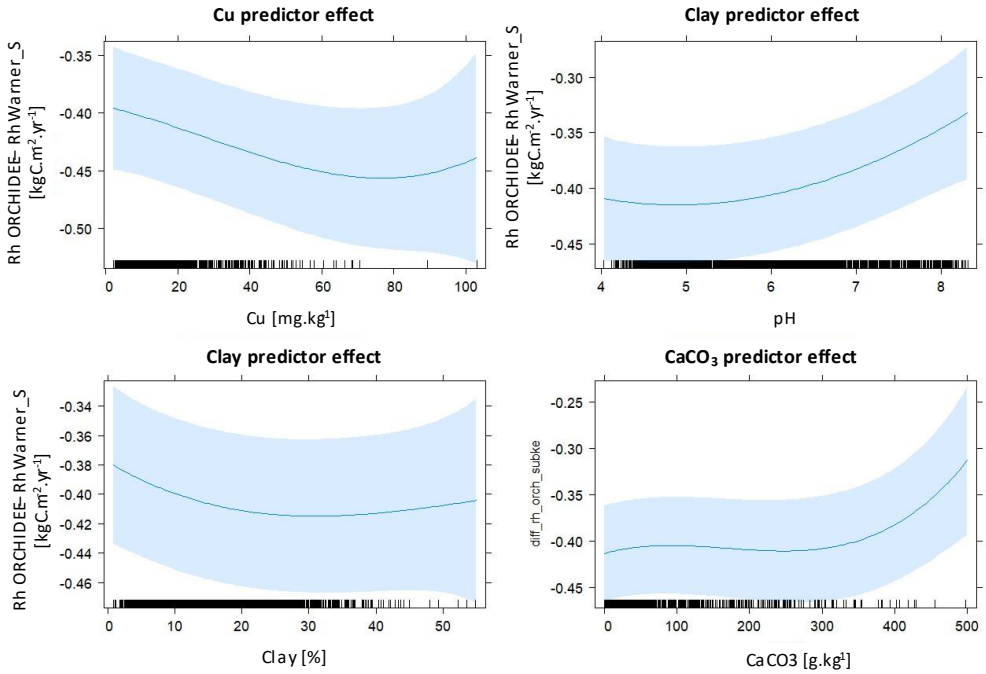

Supplementary fig III.1.6.: partial effects plot for the different predictors selected by the stepAIC procedure using set I of predictors to explain the difference Rh ORCHIDEE- Rh Warner_S

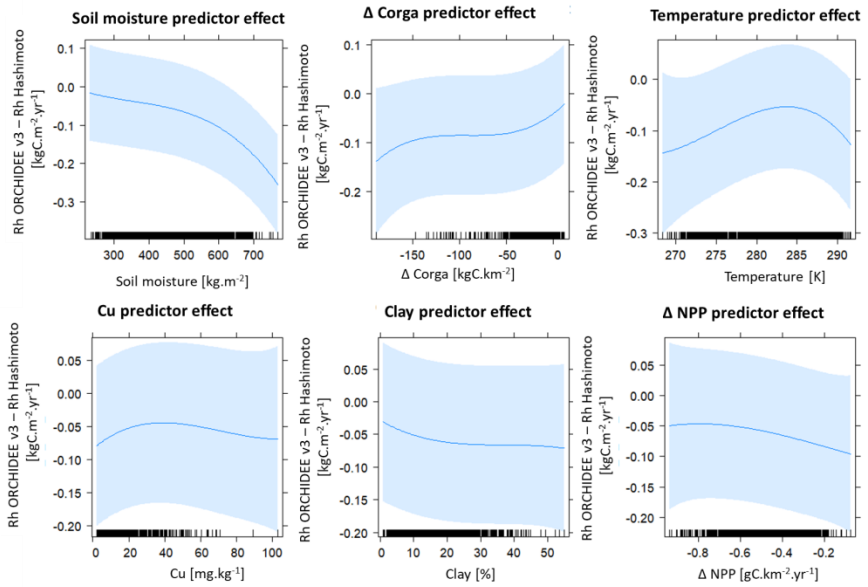

Supplementary fig III.1.7.: partial effects plot for the different predictors selected by the stepAIC procedure using set I of predictors to explain the difference Rh ORCHIDEE v3- Rh Hashimoto

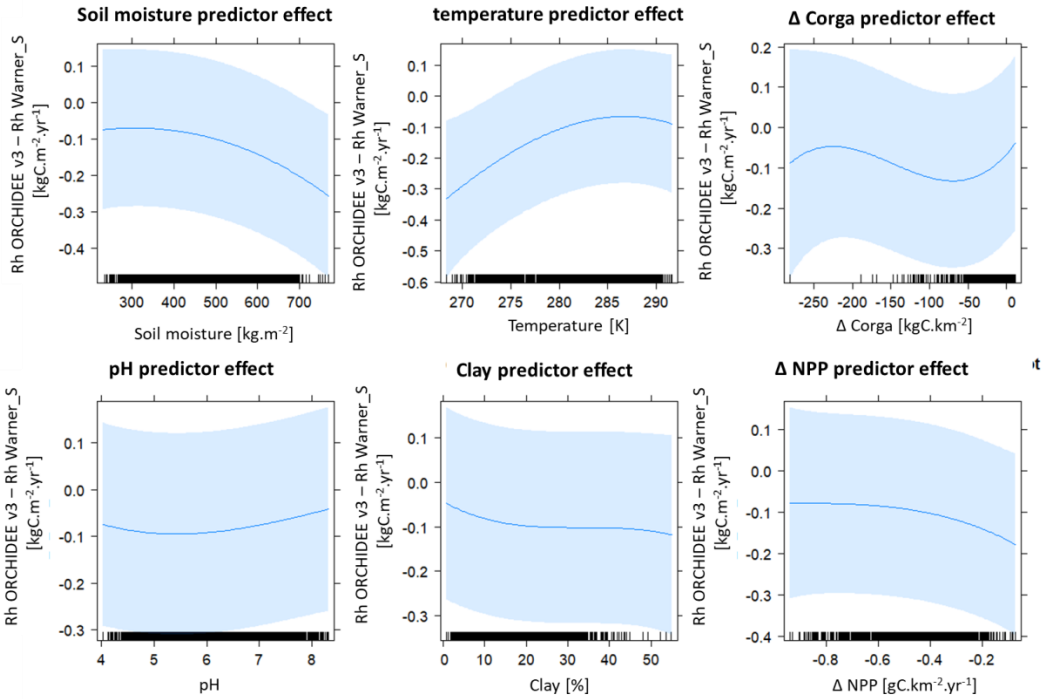

Supplementary fig III.1.8.: partial effects plot for the different predictors selected by the stepAIC procedure using set I of predictors to explain the difference Rh ORCHIDEE v3- Rh Warner_S

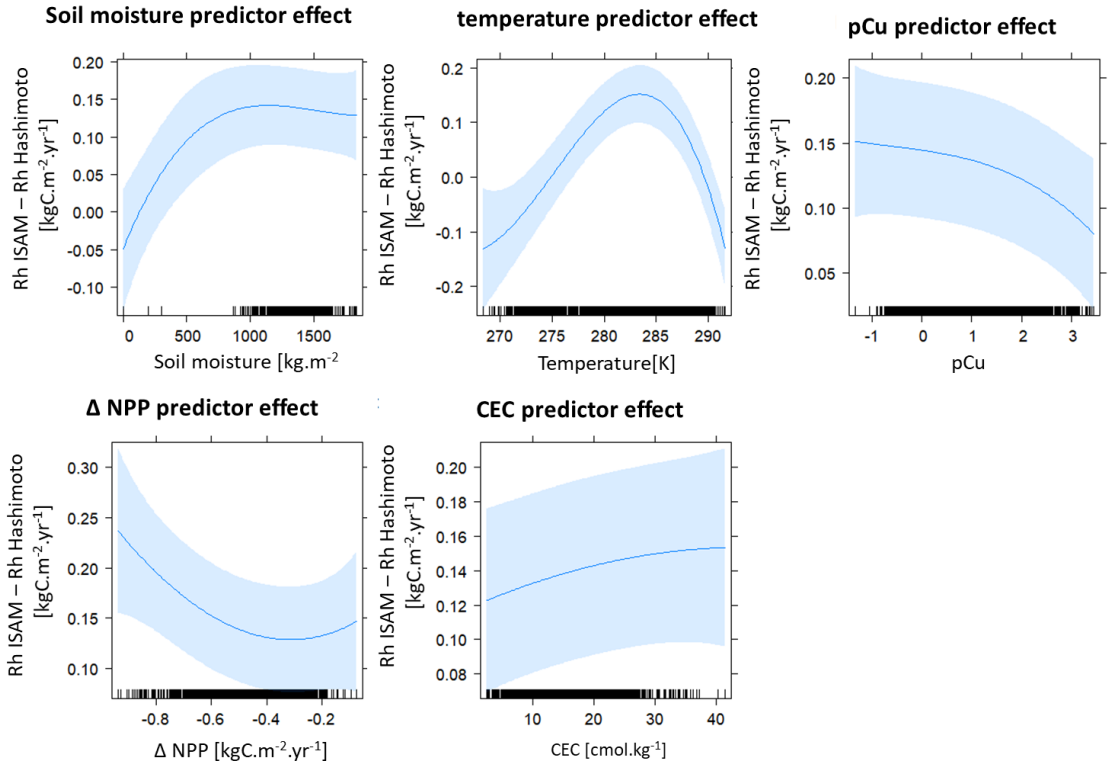

Supplementary fig III.1.9.: partial effects plot for the different predictors selected by the stepAIC procedure using set II of predictors to explain the difference Rh ISAM - Rh Hashimoto

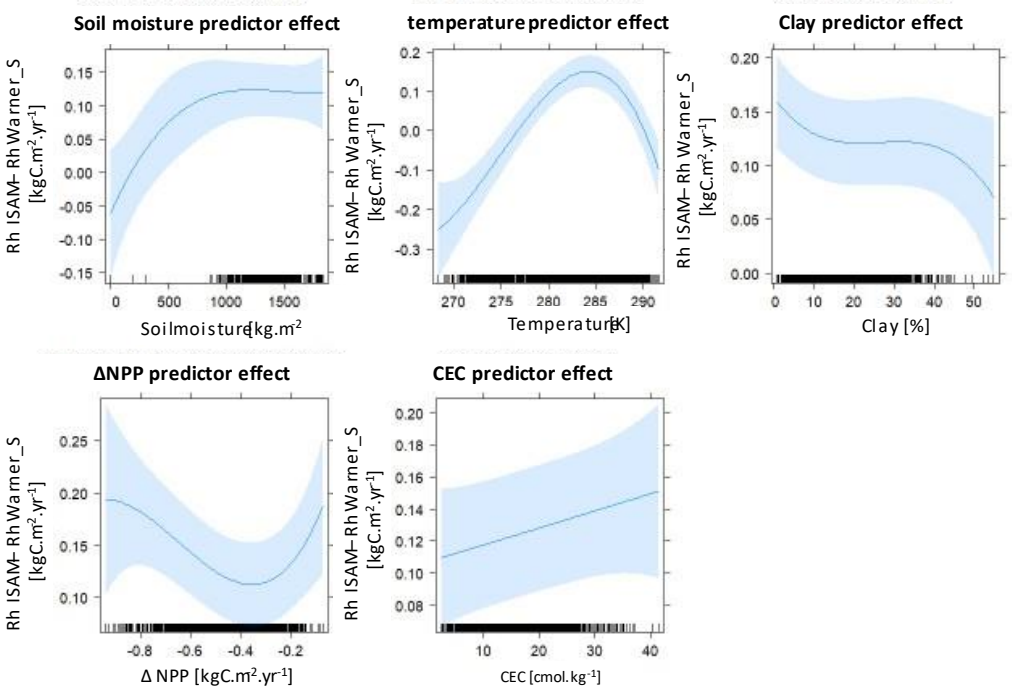

Supplementary fig III.1.10.: partial effects plot for the different predictors selected by the stepAIC procedure using set II of predictors to explain the difference Rh ISAM - Rh Warner_S

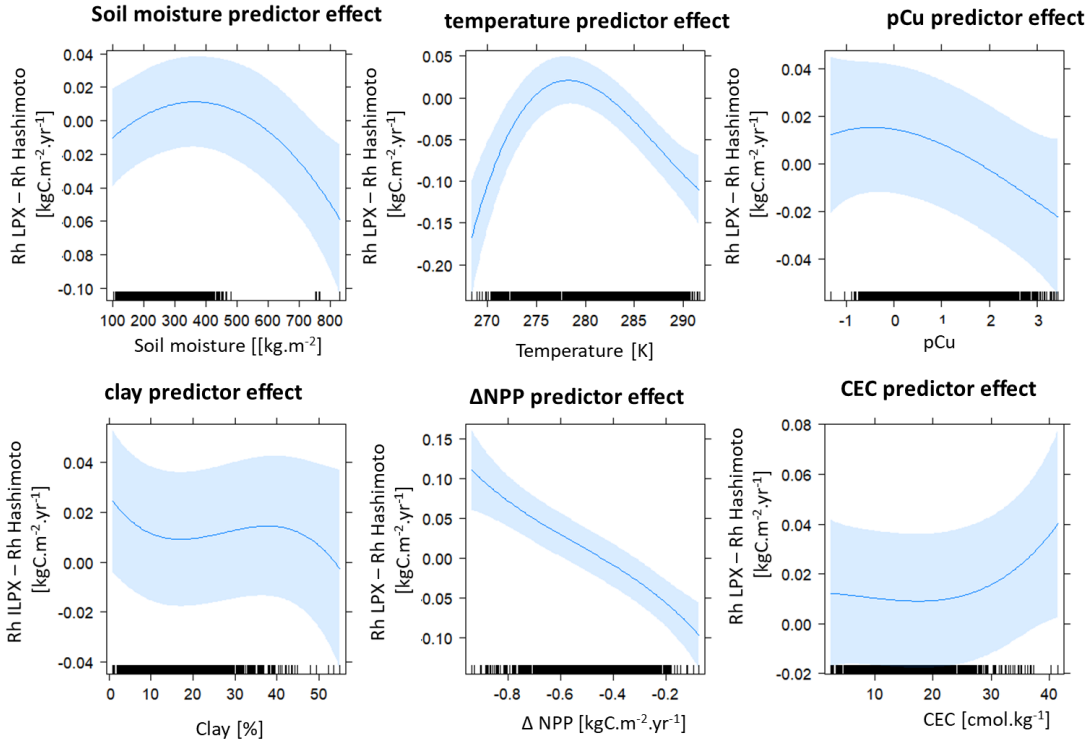

Supplementary fig III.1.11.: partial effects plot for the different predictors selected by the stepAIC procedure using set II of predictors to explain the difference Rh LPX - Rh Hashimoto

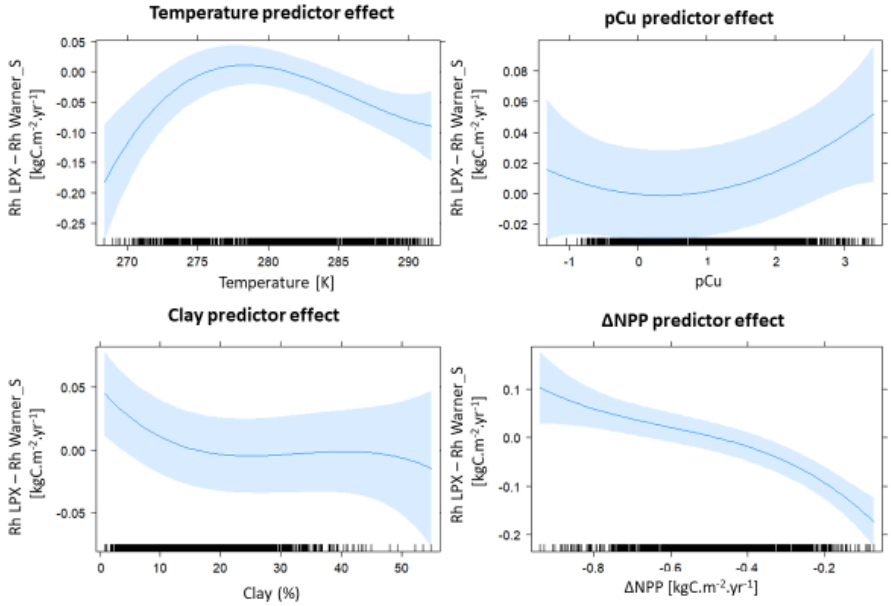

Supplementary fig III.1.12.: partial effects plot for the different predictors selected by the stepAIC procedure using set I of predictors to explain the difference Rh LPX - Rh Warner_S

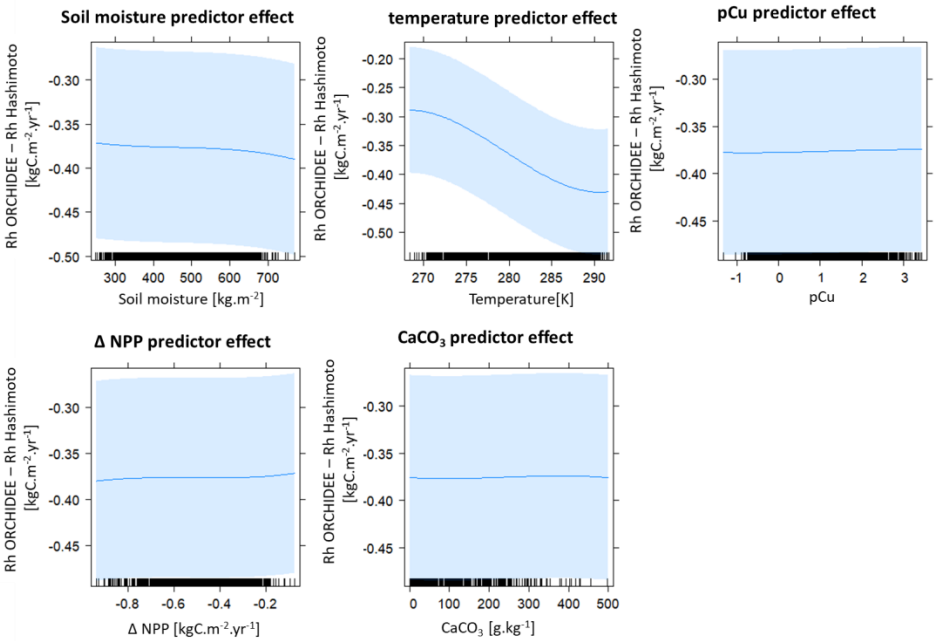

Supplementary fig III.1.13.: partial effects plot for the different predictors selected by the stepAIC procedure using set II of predictors to explain the difference Rh ORCHIDEE - Rh Hashimoto

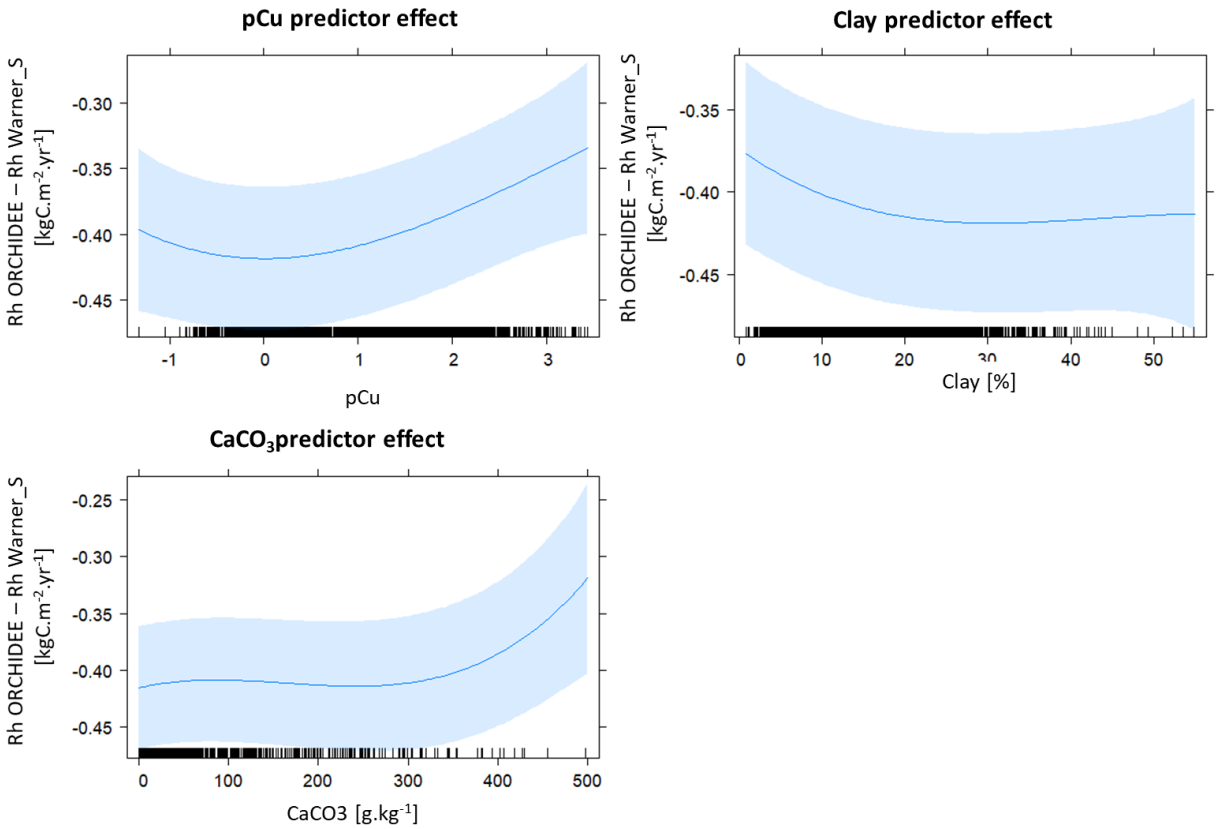

Supplementary fig III.1.14.: partial effects plot for the different predictors selected by the stepAIC procedure using set II of predictors to explain the difference Rh ORCHIDEE – Rh Warner_S

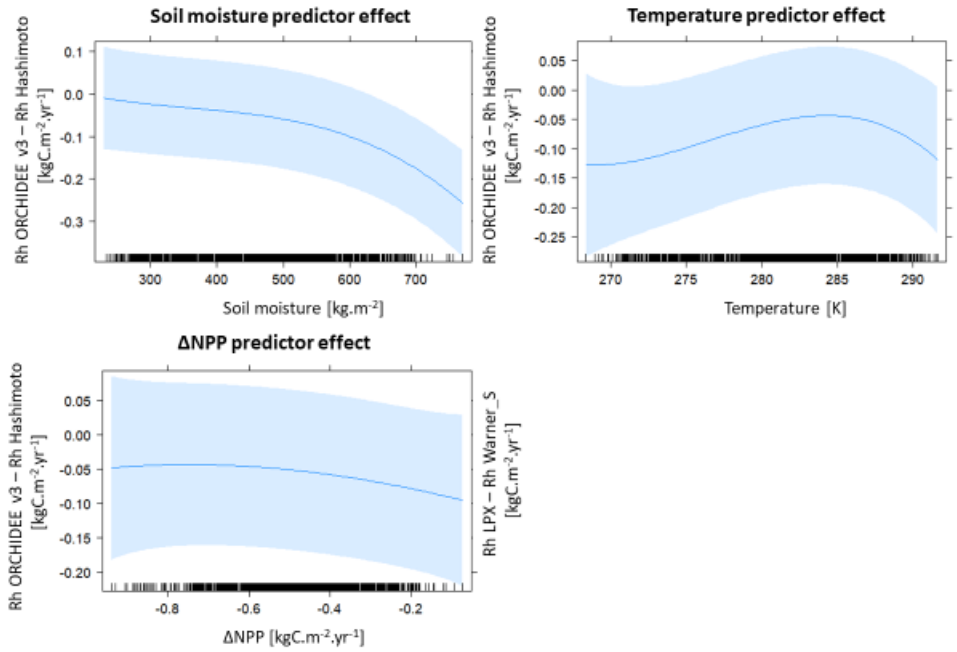

Supplementary fig III.1.15.: partial effects plot for the different predictors selected by the stepAIC procedure using set II of predictors to explain the difference Rh ORCHIDEE V3 - Rh Hashimoto

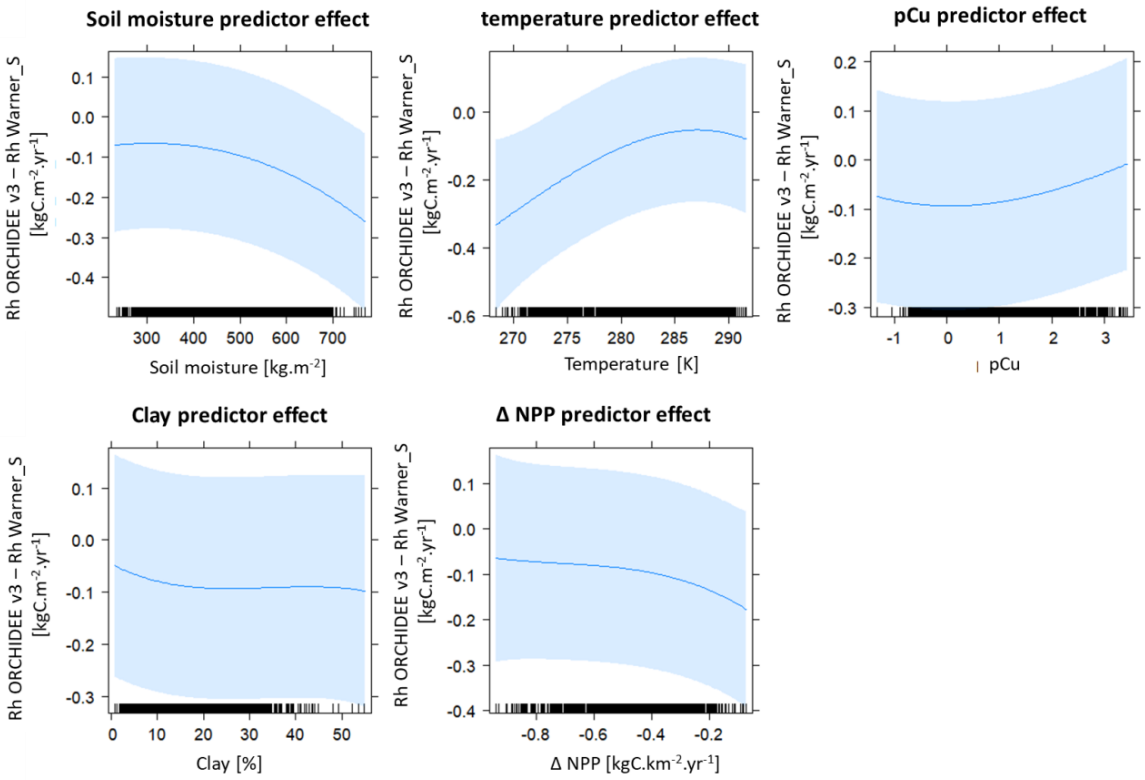

Supplementary fig III.1.16.: partial effects plot for the different predictors selected by the stepAIC procedure using set II of predictors to explain the difference Rh ORCHIDEE v3- Rh Warner_S

Chapitre III.2. : Does Copper Contamination Affect Soil CO_2 Emissions? A Literature Review

Laura Sereni[1*], Bertrand Guenet[2], Isabelle Lamy[1]

[1] Université Paris-Saclay, INRAE, AgroParisTech, UMR ECOSYS, Ecotoxicology Team, 78026, Versailles, France
[2] Laboratoire des Sciences du Climat et de l'Environnement, LSCE/IPSL, CEA-CNRS-UVSQ, Université Paris-Saclay, 91191 Gif-sur-Yvette, France

*** Correspondence:** Laura Sereni laura.sereni@inrae.fr

Published in frontiers, April 13th 2021

Highlights:

* A literature review assessed soil Cu contamination and basal respiration links

* Soil Cu was found to decrease basal respiration specifically in acidic soils

* Taking into account microbial biomass specific respiration increases with soil Cu

* Soil respiration decreased after a 265 $mgCu.kg^{-1}$ threshold as assessed in laboratory

ABSTRACT:

Contaminated soils are widespread and contamination is known to impact several biotic soil processes. But it is still not clear to what extent soil contamination affects soil carbon efflux (CO_2) occurring through soil microfauna respiration. Regarding the large stocks of organic carbon (Corga) stored in soils, even limited changes in the outputs fluxes may modify atmospheric CO_2 concentration with important feedbacks on climate. In this study, we aimed at assessing and quantifying how soil respiration is affected by contamination. For that, we performed a quantitative review of literature focusing on i) soil heterotrophic respiration measurements thus excluding autotrophic respiration from plants, ii) soil copper contamination, and iii) the influence of pedo-climatic parameters such as pH, clay content or the type of climate.

Using a dataset of 389 data, we showed a decrease in soil CO_2 emission with an increase in soil copper contamination. Specific data from *ex-situ* spiking experiments could be easily differentiated from the ones originated from *in-situ* contamination due to their sharper decrease in soil Corga mineralization. Interestingly, *ex-situ* spikes data provided a threshold in soil Cu contents for CO_2 emissions: CO_2 emission increased for inputs below 265 $mgCu.kg^{-1}$ soil and decreased above this concentration. Data from long-term *in-situ* contaminations due to anthropogenic activities (industrialization, agriculture, …) also displayed an impact on soil carbon mineralization, much particularly for industrial contaminations (smelter, sewage sludge, …) with decreased in CO_2 emissions when Cu contamination increased. Soil pH was identified as a significant driver of the effect of Cu on CO_2 emissions, as soil C mineralization was found to be more sensitive to Cu contamination in acidic soils than in neutral or alkaline soils. Conversely the clay content and the type of climate did not significantly explain the

responses in soil C mineralization. Finally, the collected data were used to propose an empirical equation quantifying how soil respiration can be affected by a Cu contamination. The decrease in soil CO_2 emission can however not be translate in term of C sink as it comes together with a decrease in soil microbial biomass.

Key words: ecotoxicology, climate change, statistical analysis, basal respiration, greenhouse gases, respiration quotient

1. INTRODUCTION

Soils play a key role in different ecosystem services such as water storage, food production or carbon sequestration. The last one is of particular interest due to the strong interactions with all the other ecosystems services and its direct impact on the climate system (FAO and ITPS, 2015; Adhikari and Hartemink, 2016). In the context of an increase in atmospheric greenhouse gas concentrations, soil carbon management is hence of major importance with a roughly three times larger carbon (C) pool in soils than in atmosphere (2400 GtC vs 800 GtC (Batjes, 2014; Friedlingstein et al., 2019)). However, the soil C residence times vary from years to millennia depending on land use, climate or soil mineral composition (Sorensen, 1981; Liang and Balser, 2011; Schmidt et al., 2011).

Carbon fluxes from soils to atmosphere are estimated from 75 (Schlesinger, 2000) to 91 $Pg.C.year^{-1}$ (Hashimoto et al., 2015) and represent the second largest carbon fluxes after photosynthesis between terrestrial ecosystems and the atmosphere (Xu and Shang, 2016). Soil microbial respiration would account for around 56 % of these C fluxes (Hashimoto et al., 2015) with a magnitude depending on environmental factors such as soil mineralogy (Müller & Höper, 2004; Wang, et al., 2003) or pH (Rousk et al., 2009). The soil microbial respiration results from soil organic matter (OM) decomposition and is driven by the amount of microbial biomass and by how much is respired by microbes. Microbial activities are driven by environmental factors (temperature, soil moisture, etc.) but are also affected by contamination (Baath, 1989). The ratio of respiration ($C\text{-}CO_2$) per unit of microbial carbon biomass (Cmic) is called specific respiration or metabolic quotient (qCO_2) depending of the authors. Jones (2001) identified the metabolic quotient as an interesting indicator of stress related to organic contaminations with higher metabolic quotients in soils contaminated by pesticides. Metabolic quotient is thus commonly used as a suitable indicator to investigate the impact of environmental conditions on soil microbial communities (Anderson and Domsch, 1993). Soil contaminant effect on soil microbial community structure is complex and can varies with time (Deary et al., 2018). However, soil contaminants are expected to alter soil ecosystem services by i) a general decrease in microbial communities sizes ii) a replacement by competitor or a lack in trophic-chain (Wakelin et al., 2010) due to differential mortality in communities, iii) an increase in respiratory activities per unit of microbial biomass in reaction to stress (Odum, 1995), and/or iv) an impact on the soil OM degradation due to a decrease in soil OM availability following associations between OM and contaminants (Dumestre et al., 1999a; Sauvé et al., 2000).

It has been estimated during the 90's that more than 22 Gha of soils over the globe were contaminated by organic and/or metallic substances from numerous origins (FAO, 2008). These contaminations were due either to atmospheric deposition near roadside (Kumar et al., 2016; Venuti et al., 2016), or near industries, or to water treatment plant or landfill (Baderna et al., 2011).

Agricultural practices have also provided different soil contaminants through the spreading of pesticides, or mineral or organic fertilizers which have been widely used in developed countries since the 50's. In the attempt to estimate the effect of soil pollution on the soil functions, microbial respiration measurements have been mainly used in ecotoxicological studies. Bååth, (1989) claimed that microbial respiration is "the oldest and most studied variable in connection with metal pollution", because it is a key process in the soil C storage function. But the use of this indicator and the ways of interpreting it were shown to be contrasted, depending on the pollutant and on local conditions. Consequently no clear pattern arose across studies on the effects of contaminants on soil respiration, even with respiration values normalized by microbial community size or soil OM content as suggested by Brookes, (1995).

Among metal pollutants, copper (Cu) is of major environmental and toxicological concern (Komárek et al., 2010) and many data can be found in the literature (Panagos et al., 2018). Soil Cu contamination has various origins including both industrial or agricultural activities. Mine tailing or atmospheric deposition can increase soil Cu concentration regarding to geochemical background as well as the agricultural practices with the use of Cu-based fungicide or the application of enriched Cu animal manure or sewage sludge. As a cation, Cu is easily complexed by the negatively charged soil OM more than other metallic cations, inducing high Cu concentrations in the upper layers of soils where OM concentration are higher (FAO, 2008). Cu contamination was shown to affect soil respiration, but some studies provided contrasting results. For instance, without supplement in carbohydrates (the source of energy for microorganisms) Soler-Rovira et al. (2013) had not detected any effect of Cu contamination on soil respiration while other studies showed either a decrease or an increase in respiration with an increase in Cu soil concentration (Keiblinger et al., 2017; Li et al., 2005; Merrington et al., 2002). The type of soil appears as a key factor modulating the effect of Cu on soil respiration due to biotic or abiotic Cu bounds with soil constituents (Komárek et al., 2010). Dominant mechanisms, however, are still not clearly assessed, even when using the various technics mimicking the bio-available pool of Cu such as soil extractions with $CaCl_2$, ethylenediaminetetraacetic (EDTA), or diethylenetriaminepentaacetic acid (DTPA) solutions (Wang, et al., 2018). Other parameters like soil OM content or soil pH have been proposed to explain some of the contrasting results observed in the literature (Fernandez-Calvino & Baath, 2016; Moreno et al., 2009). Finally, if soil Cu contamination unambiguously can have an impact on soil respiration, it is not clear if a generic relationship can be defined or if observed results are site-specific. Such a generic and empiric relationship, however, could be useful to take into account soil contamination in various modelling prospective scenario involving carbon cycle like those of climate change.

In this context, the aim of this study was twofold: i) to establish a generic relationship describing soil Cu contamination effect on soil CO_2 emissions using available literature data and ii) to identify the main drivers of CO_2 emissions, following a gradient of soil Cu contamination. We carried out a quantitative review of peer review published available data and created a database by collecting soil respiration data in the presence of Cu contamination together with available pedo-climatic conditions of the samples used for the measured data. We took into account both papers dealing either with data involving in situ Cu contamination or those dealing with ex situ Cu spikes under laboratory conditions. To be environmentally relevant, we chose to focus the present study on basal respiration,

defined as the steady state of respiration in soil which originates from the mineralization of soil OM by microorganisms and the associated CO_2 fluxes (Pell, et al., 2006). Thus, we do not to take into account data where carbohydrates were added. Selected papers were those which only provided data both from soil basal respiratory activities and soil total Cu concentrations. In order to highlight the drivers of the changes in soil C mineralization, collected data included total soil Cu concentration, and when they were available the microbial biomass carbon, pedological factors as soil pH, clay and OM content values. We also included the origin of the soil contamination, and the climatic zone of the soil samples as, different climatic conditions can impact microbial communities evolution (Fierer, 2017). Data were discussed by exploring the main factors best explaining the Cu contamination effect on soil C mineralization.

2. MATERIALS AND METHODS

2.1 Bibliographic research

To find data linking soil C emissions and soil Cu concentrations, we ran a Wos Core Collection research using the following equation of research:

TS = (("soil C" OR "soil organic C*" OR "soil organic matter") NEAR/10 (minerali* OR decomposition)) OR TS = ((soil near/4 ("CO2 emission" OR "CO2 release" OR "basal respiration" OR respiration)) OR "soil respiration") AND TS = (Cu OR cupric OR copper)

Where “TS” refers to the titles, abstracts or subjects of research papers. NEAR was used to restrict the research to the “C mineralization” nominal group related to soil processes. Four and ten spacing between words were defined by successive research looking for a maximum of results with a minimum of noise and usable number of papers. The research was lastly actualized in December 2019

This provided 238 papers published between 1983 and 2019. To focus only on soil heterotrophic basal respiration, we excluded from this selection through careful reading the papers where litter or lake sediment respiration were measured, or when studies focused on substrate induced respiration. In order to focus mainly on Cu effect, we also excluded papers from multi-contaminated soil if the contribution of Cu contamination was identified by the authors as minor compared to other contaminants. Finally, we excluded soil remediation studies using mineral (lime, beringite, Ca) or biochar amendment because these soil inputs introduced a bias in the soil carbon emissions and their side effects were poorly documented.

The final selection consisted in 92 papers from both in-situ or ex-situ (laboratory) Cu contamination. Papers with unclear protocols regarding to the incubation lengths, or with supply in carbohydrates or in the presence of plant (particularly in the case of field measurements) were also discarded. Furthermore we extracted data giving outcomes only with long term measurements (> 7 days) to avoid the parts corresponding to the Birch effect, i.e. the known major increase in mineralization rate due to soil re-humidification (Birch, 1958). None of the papers dealing with in situ field measurements satisfied our standards (e.g. absence of plants, knowledge of total Cu content, …), so they were not kept in our final selection. This ended to 46 papers describing incubations experiments using either

uncontaminated soils which were further copper contaminated, or already contaminated soils. These papers allowed us to have access to 389 data including their associated control in order to build the database. Fourteen from those 46 papers where published between 1990 and 2000, 24 between 2000 and 2010 and 17 between 2010 and December 2019. Graphical values were exported with the Engauge digitizer (v12.0) software (Engauge digitizer v12.0).

2.2. Database construction

We gathered 389 experimental laboratory measurements. At a minimum, all contained total Cu in soil (mg kg soil^{-1}) and the corresponding basal heterotrophic respiration (C-CO_2 kg soil^{-1} d^{-1}). When available soil Corga, soil pH, clay percentage and microbial C biomass (Cmic gC.kg soil^{-1}) were also reported. When soil carbon data were originally expressed in OM we converted them in Corga using Corga = OM/2 (Pribyl, 2010). When total carbon was measured without mention of carbonates, we assumed that total C = Corga. Data were expressed in dry soil weight. When original data were expressed on fresh soil weight basis, we converted fresh soil weight data in dry soil weight data using water holding capacity (WHC) and soil moisture information's when given. In the absence of mention on the humidity state of the samples used in the experiments, we hypothesized that data were expressed on a dry weight basis. For 7 papers (corresponding to 33 data) where the soil Cu concentrations in the control samples were not explicitly given, we used as a surrogate the corresponding copper concentration given by the map of Ballabio et al. (2018) for the position.

The database was supplemented when possible with two types of calculated data:

1) In order to take into account soil Corga concentration, daily mineralization was divided by the soil Corga and was further named soil C mineralization (expressed as fluxes per day). When soil C respiration was reported with cumulative measurements (e.g. amount of C released during incubation time) we calculated a daily respiration from the data after the equilibration period (i.e; after rewetting) using the two last points from curve of cumulative C release to provide an amount of C release per day at the end of the incubation period.

2) The Response Ratio (R.R, eq. III.2.1) for each incubation experiment involving laboratory copper contamination, defined as the ratio of C mineralization in contaminated conditions on C mineralization for the control:

Eq.III.2.1 : $$R.R = \frac{Mineralisation\ in\ contaminated\ condition}{Mineralisation\ without\ supplementary\ contamination}$$

Finally, the database was also supplemented with two other extractable data: 1) the climatic origin of the soil samples and 2) the origin of the Cu contamination. This latter being linked to the form under which it is present (organic or mineral, in solution or included in a solid phase for example). For each data we gathered the climatic origin of the soil samples using the Koeppen classification system (Rudolf Geiger, 1954) with ten subdivisions corresponding to the main geographic repartition of climate in the world. Thereafter two letters were used in accordance with the Koeppen classification system: the first letters refer to the main type of climate (A = Tropical, B = Dry, C = Temperate, D = continental), and the second letters will refer to the rainfall pattern (f = humid all year long, m = monsoon, s = dry summer, w = dry winter).

To fill in the database with the origin of the Cu contamination and in order to take into account the magnitude of the Cu contamination together with the exposition time in the effect on soil C mineralization, we collected explicit information regarding the site where the soils were sampled. We have thus divided the contamination information into four main categories: 1) the "non contaminated" sites (thereafter named Nc) used as "non-polluted" controls in the laboratory experiments, or often sampled in situ under grassland or forest, 2) the agricultural sites (thereafter named Agr) with moderate but chronic contamination, 3) the industrial sites (thereafter named Ind) with high mostly multi-contaminated soils during the last 100 years from industrial effluents or atmospheric dust deposition; and 4) a category we called "Other sites" (thereafter named Oth) in which the Cu contamination was from various or from undefined origin (city park, roadside…). In addition to this information on contamination, a suffix was added to distinguish the various ex-situ experiments: i) the addition of a non-contaminated OM like straw or grass to a soil sample (thereafter called + OM), ii) the addition of an already Cu contaminated OM like pig slurry or sewage sludge to a soil sample (thereafter called + OMc), iii) the addition of Cu spikes under mineral forms to soils (thereafter called + S), or iv) the addition of both OM and Cu spikes to soils (thereafter called OM+S).

All these subdivisions introduced in the database were made to provide clusters in order to interpret the whole set of data and assess the genericity of the soil C mineralization answers to soil Cu contamination.

2.3. Statistical analysis

Statistics were used here to overcome two main difficulties in dealing with our bibliographic data : 1) the missing data across papers and in particular pedological data, and 2) the fact that because some studies performed several treatments, data extracted from a same paper were less independent from each other than data from different papers. Thus, two successive and complementary statistical approaches were conducted, one descriptive and the other predictive.

To explain daily soil Corga mineralization we first analyzed the data with the maximum number of parameters including the pedo-climatic ones (thus with the smallest number of data) using the descriptive statistics PCA (R packages FactoMineR and factoextra) and Random Forest (R package randomforest) to determine which parameters have to be firstly considered. This prevents us to deal with parameters which restrict the number of data to be analyzed simultaneously (due to a lack of this information in some papers). This also prevents us to deal with co-correlation. Random Forest results were exploited through the partial modelled plots and the % of Mean Standard Error (MSE) Increase. This percentage represents the increase in MSE predictions of a randomly chosen variable being permuted among all the variables.

The following step consisted in using the stepwise regression on linear mixed effects models (*lme*, stepAIC, MASS package, with bidirectional selection) as predictive statistics. This method takes a given number of variables as fixed effect and selects the better ones as predictors to explain a response variable by minimizing the model AIC. It was used on the sub-dataset defined thanks to the use of Random Forest and PCA. A final model was then gradually built by adding or deleting variables which were or were not linearly related to the response variable. The model was selected thanks to the AIC criterion. The final selected model had to provide the maximum likelihood for the minimum number

of response variables. It could happen that one variable is selected in the final model even if its p-value does not appear as particularly relevant: this is because the final model would have been particularly degraded without this variable.

The three following variables: i) soil C mineralization, ii) respiration per microbial C biomass also named metabolic quotient thereafter called qCO_2 and iii) response ratio (R.R.) were tested as response variables whereas soil Cu content, pH, % of clay or microbial C biomass (Cmic) were fixed quantitative effect. Interactions between response variable were also tested, but were limited to Cu and pH interaction due to the lack of data for the other response variables. The rainfall pattern (corresponding to the 2nd letter of the Koeppen classification), the ex-situ additions of contamination (under the form of added organic or mineral Cu contents) and the nature of the in-situ contamination (agricultural, industrial or "other" as well as non-contaminated) were tested as fixed qualitative variables. Data originating from a same paper -thus a same set of experiment- were less independent from each other than data from different articles. To tackle this problem, we used those articles from which the data came from as a random effect in linear mixed model. In our case the complementary use of descriptive and predictive statistics was used to confirm the robustness of the results. All analyses were performed using R v3.5.1 and log transformed data to satisfy normal distributions hypothesis tested using Kurtosis and skewness tests.

3. RESULTS

3.1 Collected data and structure of the database

The complete database can be found in the attached data.

The main characteristics of the database are given Table III.2.1 with the descriptors used in this study. Compared to the number of data we gathered for soil total Cu and pH (389), Corga (385), or mineralization of Corga (382), the data much missing were the microbial biomass Cmic (128 data). The number of data we could account for the response ratio was also limited (173 data) because R.R was calculated only with the set of papers dealing with added Cu contamination during laboratory experiments (spikes or contaminated organic matter). The percentage of clay was also a data not frequently specified (206 data). Furthermore, papers reported either Cmic or clay values but both were very seldom reported (43 data, 9 papers) which prevents us from analyzing collectively these two predictors. The range of values covered by the data was large (Table 1) which allows working with wide gradients. In particular, the Cu gradient covers a large range of soil Cu contents from non-contaminated to highly contaminated soils, with a total soil Cu concentration of 586 ± 65.6 mg.kg^{-1} (mean and standard error) due to the various sources of Cu. The number of data in each categories of type of climate is given in Supplementary Table III.2.1. Data covered a wide range of ecosystems but not equally distributed (Supplementary Figure III.2.1): main data come from European countries and temperate climate, either with or without dry seasons, while the least well represented is the dry climate.

Table III.2.1. Number of collected data after the final selection of the 46 papers and their corresponding ranges of values given as minimal (Min), medium (Med), maximal (Max), 1st and 3rd

quadrant (Qua) and mean (Mean) values. Corga is the soil organic carbon content, R.R is the Response Ratio calculated according to eq. (III.2.1), Cmic is the microbial C biomass.

	Min	1st Qua	Med	Mean	3rd Qua	Max	Number of data
Cu soil (mg.kg^{-1})	1.0	32.4	122	586.3	500	8052	389
Corga. (g.kg sol^{-1})	0. 6	17.2	30.1	66.12	58.6	480	385
pH	2.5	5.3	5.9	6.1	7.2	9.2	389
Clay (%)	2	12	18.3	18.4	23.0	60	206
Incubation length (day)	7	28	31	87	84	630	356
Mineralization eq.(mgC.kgsoil^{-1}.day^{-1})	0.01	1.26	5.2	16.0	22.5	149.11	386
R.R	0.09	0.64	0.95	1.39	1.24	13.92	194
Mineralization/Corga (mgC.gCorga-^{1} day^{-1}	0.0001	0.05	0.13	0.82	0.54	27	382
Cu/Corga. (mg.g^{-1})	0.003	0.79	3.71	31.3	16.6	2234	385
Cmic (gC.kg soil^{-1})	0.01	0.17	0.31	0.67	0.88	6.2	128

In the dataset, spiked samplesto introduce Cu contamination represent almost half of the data (Supplementary Table III.2.2) and the highest values of added Cu concentrations pull up the average. When excluding laboratory contaminated experiments, most of the reported soil Cu concentrations ranged around 140 ± 19 mg.kg^{-1} as mean and standard error respectively calculated for all the sites classified A, Nc, O or I in Supplementary Table III.2.2. This value largely overwhelmed the mean Cu concentration measured in Europe (16.85 mg.kg^{-1}) as reported by the European Soil Data Centre (ESDAC in Ballabio et al., 2018). But comparing with the measured concentration in vineyard soils (mean at 49.26 mg.kg^{-1}) and considering that more than 14% of vineyard samples have values higher than 100 mg.kg^{-1}), the mean 140 mg.kg^{-1} describing our database is in the upper Cu range of European soils. The database also reported few high spots of soil Cu contents in the so-called 'industrial contamination' group of data but the mean Cu concentration was around 190 mgCu.kg^{-1} (with a median at 95 mg.kg^{-1}).

The discrepancy in the number of data per category had ambivalent impacts on our dataset. In one hand it confers some large sub-groups (for instance the "spiked" or the soils under agriculture) to carry out the analysis, but on the other hand the analysis of cross subgroups were not possible. For instance,

industrial soils further contaminated by contaminated OM just provided 4 data. It was also not possible to cross rainfall pattern with the origin of the contamination (see Supplementary Table III.2.1, III.2.2).

3.2. Selection of the predictive variables

A first selection of the predictive variables (also called thereafter predictors) was made by Random Forest on all the variables (numerical variables: Cu, clay, pH, microbial C biomass, and soil C mineralization but also categorical variables: main climate, rainfall pattern, soil use type and type of contamination).

A small number of papers (9) presented both values for clay percentage and Cmic, thus the analyzed data associated was 43. Random Forest explained 78.9% of the soil C mineralization variance. Random Forest emphasizes an effect of seasonal rainfall pattern (Fig III.2.1A) which account for 19.7% of increase in MSE per standard deviation. pH, microbial biomass carbon and clay represent a second pool of variable of interest as these variables account respectively for 13.7,12.7 and 12.2 % of increase in MSE per standard deviation (Fig III.2.1A). Finally, Random Forest attributes a moderate part of the variation of the soil C mineralization to soil Cu contamination (4.3 % of increase in MSE per standard deviation, Fig III.2.1A).

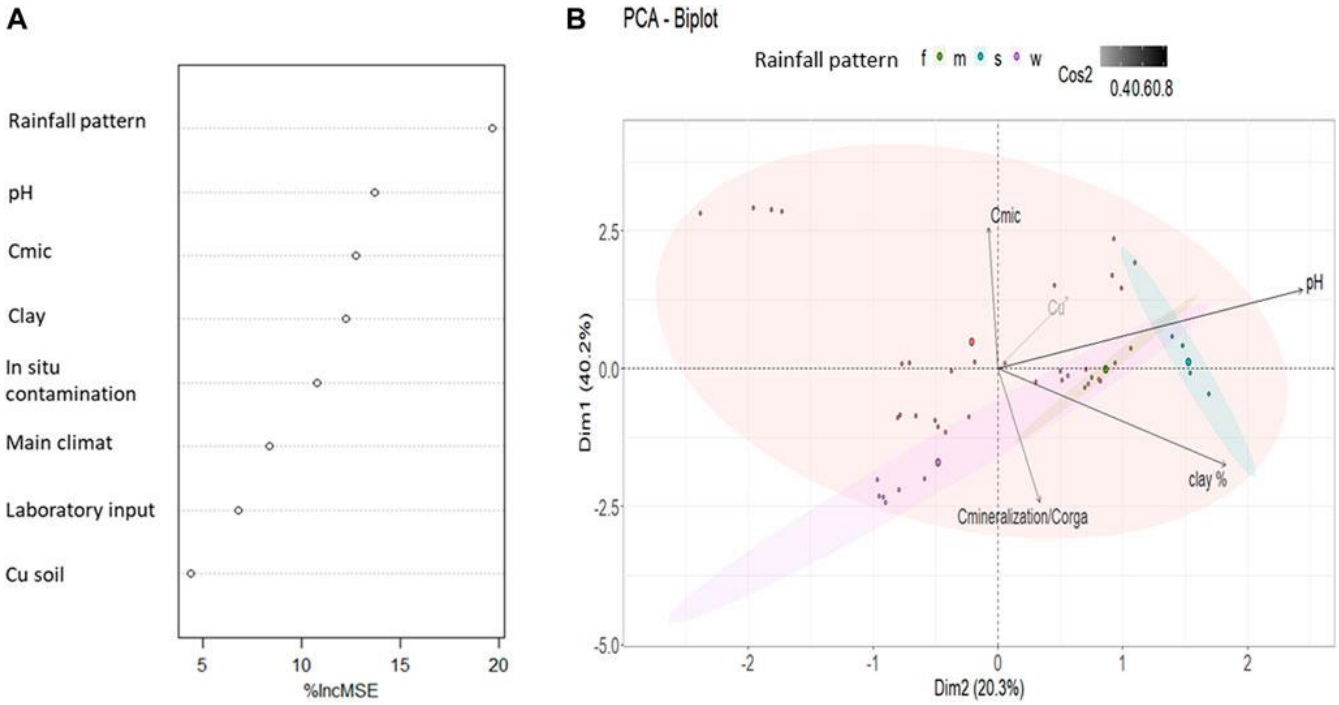

Fig III.2.1.: Analytical statistic description of the 43 data with all recorded variables set by two statistical approaches (A) Random Forest analysis with the % of increase in mean standard deviation (%IncMSE) due to each variable for soil C mineralization per soil organic carbon (B) PCA with the 2 first dimensions contributing to 60.5 % of variance in the data set. Quality of representation through PCA construction of quantitative variables (axes component) are represented through the colour of the arrow (cos2). Rainfall pattern is illustrated with the colour of the data point, ellipse are the 95% confidence interval of groups representation in the PCA space estimation. Cmic is expressed in g per kg of soil, clay in percentage of soil, soil Cu in mg of Cu per kg of soil and C mineralization in mg of C-CO2 per g of soil Corga.

Sensus stricto PCA analyses cannot use categorical variables to define axis. Thus, the PCA was run on the same numerical variables than Random Forest (Cmic, pH, clay, Cu, mineralization per Corga). The component space (build on the numerical variables) was represented and then the data were added with respect to their categorical variables (climate, type or in or type of ex situ contamination). Their category was illustrated in color (Fig III.2.1B) but they were not use to build the axes. The PCA explained 60.5 % on the two first axes ~~(Dim 1-2)~~ of the data set variance (Fig III.2.1B), all variables being well reproduced (cos^2>0.2) through these 2 dimensions. The 5 variables account significantly in the data set description with a highest contribution in the PCA construction of pH and Cmic (respectively 27 and 23%) and a smallest contribution for soil Cu (7%). Based on the PCA representation we could expect a positive correlation between Cu and Cmic and a negative one between Cu and soil C mineralization.

Compared to the Random Forest analysis, the exclusion of categorical variables in the PCA only slightly decreased the explanation of variances. The representation of data's rainfall pattern is shown in Fig III.2.1B. The PCA analysis doesn't show significant differences between the different rainfall patterns, which also have a small number of soils sampled and large variation, particularly for the "w" soils. The other categorical variables (main climate, rainfall pattern, types of in situ and type of ex situ contamination) where not displayed by the PCA (Fig III.2.1B for the rainfall pattern, other data not shown). Random Forest partial model plot (not shown) also showed that the rainfall pattern had weak interaction with the pH or with the nature of in situ contamination and no interaction with the other covariables. From our database, the rainfall pattern is thus suggested to impact the microbial biomass amount but the relationships with the effect of soil Cu and C mineralization were less clear and will have to be clarified using *lme*.

3.3. Global soil copper contamination effect on soil C mineralization and influence of specific descriptors

In order to assess the specific impacts of the several descriptors, the first results with Random Forest and PCA have guided the further analyses on Cu effect on soil C mineralization using linear mixed effect models. Successive analyses were made on five types of dataset: (1) on the maximum dataset thus including only the co-variables always recorded (soil C mineralization and Cu contents) to clarify the effect of soil Cu on soil C mineralization; (2) on a dataset including in addition pH, rainfall pattern and clay percentage, as these co-variables were shown to be of main importance by our previous analysis (but not Cmic); (3) on a dataset replacing rainfall pattern by Cmic then using the analyses of metabolic quotient qCO_2 as response variable; (4) on a dataset restricted to response ratio measurements thus

corresponding only to copper contamination supplied in laboratory; (5) on a dataset restricted to natural, in situ contamination in order to point out the influence of the origin of the contamination.

3.3.1 Modulation of soil organic C mineralization by soil Cu content

We checked the influence of soil Cu per se with a *lme* analysis using the 382 data concerning soil C mineralization (as the response variable), Cu contents (as the fixed effect) and the papers as random effects as described in material and methods. Fig III.2.2 shows the results confirming a non-negligible effect of soil Cu content on soil C mineralization as soil C mineralization decreases when soil copper content increases. The relationship was defined as:

Eq. III.2.2: $\log\left(\frac{mineralisation}{soil\ C\ orga}\right) = -1.04 - 0.09 \log\left(Cu\right)$, R^2=0 .92 , p-value < 0.001

3.3.2 Influence of clay, rainfall pattern, and pH

Once clay, pH and rainfall pattern were included in the linear model selection, the selected model after stepwise regression (R^2 = 0.92, 206 data) excluded clay but included pH and Cu as explaining variables as well than their interactions. However, p-values weren't below acceptance rate (Cu p-value = 0.08; pH p-value = 0.70 and pH-Cu interactions p-value = 0.1, Supplementary Table III.2.3). Rainfall pattern did not significantly affect soil C mineralization.

Investigations were then pursued without clay values and focusing on pH taking into account that pH is expected to be a determining factor based on PCA and Random Forest analysis (Fig III.2.1). pH was a parameter always recorded in our database, thus, a largest number of soil C mineralization data could be analyzed (382). The selected model shows that an increase in soil Cu significantly decreases the soil C mineralization (p-value <0.005) and that the soil pH increase was related to an increase in soil C mineralization (p-value<$2e^{-16}$). The interaction between pH and Cu weren't selected in the final model. The analysis also showed an effect of the rainfall pattern: the soil C mineralization was significantly higher in the case of the "w" soils than in the case of the "f" ones. The adjusted effects of soil C mineralization with rainfall pattern are presented in Table III.2.2, and the global equation of soil C mineralization is:

Table III.2.2. (A) Slope and intercept (± standard error (s.e.)) between log (mineralization/organic C) and variables selected through stepwise analyses with the linear mixed model for different dataset (all data, data with pH≤5.3, data with 7>pH>5.3 and data with pH≥7) as well as the metrics associated to each model. (B) Shift of the intercept for log (mineralization/organic C) between the different groups of qualitative variable (rainfall pattern) (s=dry summer, w=dry winter) and the reference one (f=humid all year long). P-values of each estimate are symbolised by NS for p-value>0.1, by ° for p-value<0.1, by * for p-value<0.05; by ** for p-value<0.01 and by *** for p-value<0.001.

(A)

Log (Mineralization / Organic C)	**Intercept** (±s.e.)	**pH** (±s.e.)	**log (Cu tot)** (±s.e.)	**AIC**	**BIC**	**logLIK**	**R2**
(all data, n=382)	**-2.68**** (± 0.51)	**+0.19***** (± 0.04)	**-0.07**** (± 0.02)	922	954	-453	0.92
(pH≤5.3, n=102)	**-2.61** ** (± 0.77)	**0.24** (± 0.1)	**-0.06**^{NS} (± 0.04)	229	247	-107	0.96
(7>pH>5.3, n=159)	**-1.85**** (± 0.47)	**Not selected by the stepwise regression**	**-0.11**** (± 0.04)	406	425	-197	0.90
(pH≥7, n=121)	**-1.13** ** (± 0.45)	**Not selected by the stepwise regression**	**Not selected by the stepwise regression**	323	331	-158	0.89

(B)

Log (Mineralization / Organic C)	Rainfall pattern	Intercept (±s.e.)
(all data, n=382)	**s**	**0 .57^{NS}**(± 0.69)
	m	**3.41^{NS}** (± 2.2)
	w	**1.4*** ** (± 0.36)
(pH≤5.3, n=102)	**s**	**0 .61^{NS}** (± 1.22)
	m	**Not selected by the stepwise regression**
	w	**1.69***** (± 0.38)
(7>pH>5.3, n=159)	**s**	**0 .24^{NS}** (± 1.22)
	m	**Not selected by the stepwise regression**
	w	**1.3*** (± 0.51)
(pH≥7, n=121)	**s**	**Not selected by the stepwise regression**
	m	**Not selected by the stepwise regression**
	w	**Not selected by the stepwise regression**

Eq. III.2.3: $\log(\frac{C\ mineralization}{soil\ C\ orga}) = -2.3 + 0.2\ pH - 0.08 \log(Cu)$ all p-value < 0.005, general $R^2 = 0.92$

The small size effective of the different rainfall pattern doesn't allow to assess if the Cu effect (understood as Cu slope) was significantly different between rainfall patterns.

3.3.3 Specific influence of pH

Taking into account specifically the pH values allows us to work with a larger number of data analyzed. A first analysis showed that the interaction between soil pH and soil Cu concentration weren't selected by the step wise (see section 3.3.2). To disentangle the effect of soil Cu across pH from a potential threshold effect on the soil C mineralization, we completed this first result with a splitting of the database in 3 subgroups defined on the basis of a decisional tree (not shown): i) 102 data with data pH≤5.3, ii) 159 data with 7>pH>5.3, iii) 121 data with pH≥7.

For the acidic soils (pH≤5.3) the *lme* analysis showed a significant effect of pH but not of Cu on soil C mineralization. Cu was however maintained in the final model through the selection procedure even if the p-value wasn't significant (p-v = 0.15) as explained in the material and method section (Table III.2.2, Fig III.2.2). For the soils with pH in the range]5.3; 7[soil C mineralization is expected to decrease with increase in soil Cu but no effect of pH was found (Table III.2.2, Fig III.2.2). For the soils with alkaline pH values soil C mineralization was not correlated neither to pH nor Cu (Table III.2.2). In the two first cases the soils samples under "w" (dry winter) rainfall pattern were found to have soil C mineralization highest than the soils samples under the other rainfall patterns whereas the rainfall pattern was not supposed to modulate the soil C mineralization in the last case.

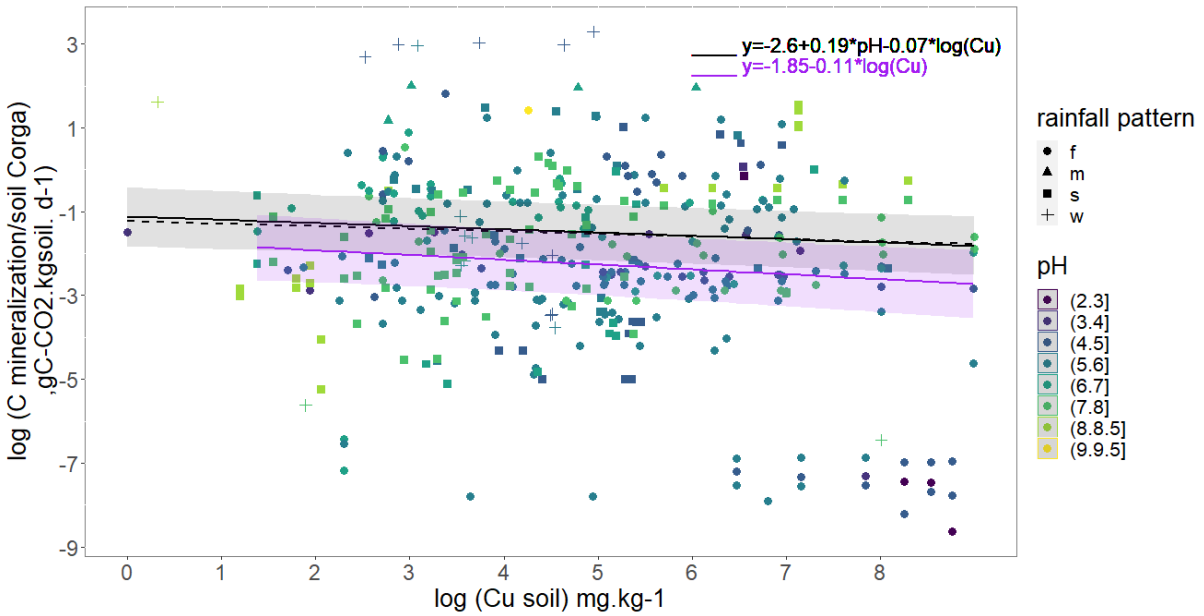

Fig III.2.2.: Daily Soil C mineralization per g organic C per day as a function of soil Cu concentration. Soil pH is coloured scale and rainfall pattern represented with point shape. The full black line models copper effect on daily mineralization for all data considering median pH (5.9), R^2=0.90. The black dash line models copper effect on daily mineralization for data with pH<5.3. The purple line models copper effect on daily mineralization for data with pH €[5.3,7]. The shaded area are 95% confidence interval for all data in black and data with pH €05.3,7] in purple. Rainfall patterns are the following : f=humid all year long, m= monsoon, s=dry summer, w=dry winter.

Finally, no clear interactions between Cu and pH were found, but we found different Cu effects on soil C mineralization depending on the ranges of pH values. The selection of Cu through stepwise for pH < 7 tends to show that soil Cu mostly affects soil C mineralization in acidic soil pH conditions, but the limited associated p-v for pH lower than 5.3 doesn't allow us to draw general conclusion.

3.3.4 Cu contamination and microbial parameters effects on soil organic carbon mineralization: use of the metabolic quotient qCO_2

Based on the descriptive statistics, microbial C biomass was also an important variable to explain C mineralization variability. However, only few C-CO_2 emission data were found associated with both clay and Cmic values while both variables were pointed out by descriptive analyses. We thus considered microbial carbon biomass rather than clay percentage in the explanatory variables (128 values), and did not find any significant Cu effect on soil C mineralization variability, which was found to only depend on Cmic and pH (general R^2 = 0.90, Supplementary Table III.2.4).

Based on the dependency of soil C mineralization on Cmic and because it has been shown that relative variables were most informative than absolute (Brookes, 1995) we modified our *lme* equation in order to use the metabolic quotient e.g daily mineralization per microbial carbon biomass (Fig III.2.3) to use it as response variable in the *lme.* The final selected model shows that qCO_2 increases with pH and Cu without evident interaction between the two variables. Neither rainfall pattern nor soil Corga were selected and the relationship obtained was:

Eq III.2.4: $\log(qCO_2) = 1.5 + 0.2 \times pH \times \log(Cu)$,general $R^2 = 0.94$.

From equation III.2.2 we showed that soil C mineralization decreases with an increase in soil Cu concentration, and we also showed that soil CO_2 emission increases with soil C microbial biomass (*lme* result, Supplementary Table III.2. 4). The effect of soil Cu on metabolic quotient was hence refined with the use of Cmic as response variable and Corga, soil Cu, pH and rainfall pattern as fixed explanatory variable. The model selection shows that microbial C biomass increases with soil Corga, but decreases when soil Cu content increases (p-value. respectively 0.02 and 0.008, general $R^2 = 0.84$ see Supplementary Table III.2.5). Rainfall pattern wasn't selected by this step AIC selection.

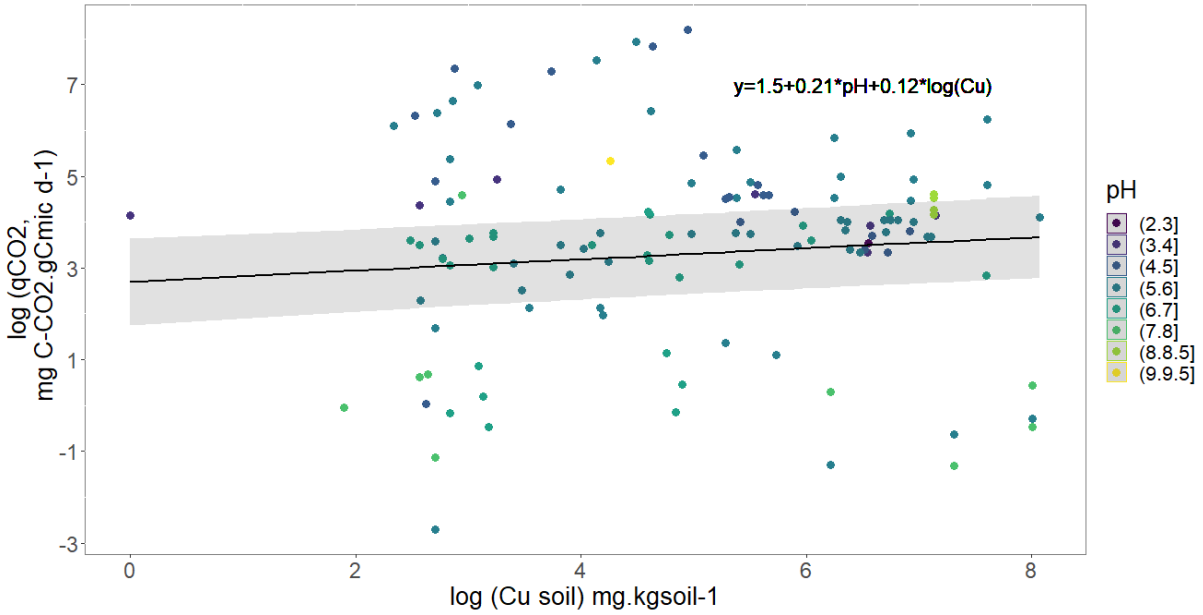

Fig III.2.3.: Variation of the metabolic quotient (qCO_2) in mg C-CO_2 respired per g of C of soil microbes as a function of soil copper concentration and pH represented through the colour of points. The black full line models soil Cu effect on qCO_2 with median pH value (5.7), R2=0.94

3.3.5 Influence of Cu contamination supplied ex-situ using the analysis of response ratio

Several data from our dataset concerned experiments introducing Cu contamination into soil microcosms in the form of Cu in solution (spikes), sometimes with OM (grass residues…) or in the form of Cu contaminated OM (Supplementary Table III.2.2). These experiments represent an artificial, non-repetitive and short-term contamination. Consequently, the microbial community has no time to develop evolutional response and must adapt thanks to phenological plasticity in contrary to more chronic, long-term diffuse contaminations where microbes can evolve to adapt. It was thus interesting to analyze these data *per se*, and in particular the R.R calculated as the variation of a given soil sample to a sudden increase in Cu content compared to a control (eq. III.2.1). To include a maximum number of data in the response ratio analyses we didn't take soil clay percentage into account. Soil pH and soil Corga were however kept in the analysis because they were well reported thus didn't limit the number of data (176) to be analyzed.

Results show that R.R decreases when soil copper content increases (Table III.2. 3A) but increases when pH increases following equation III.2.5:

Eq. III.2.5: $\log(R.R) = -0.1\ (\pm 0.4) + 0.12\ (\pm 0.04)pH - 0.10\ (\pm 0.04)\log\ (Cu)$, general $R^2 = 0.74$

Interestingly, Fig III.2.4 shows that response ratio is higher than 1 (log(R.R)>0) for low soil Cu concentrations, meaning that the soil C mineralization is highest in contaminated soils than in the control ones. For all the OM+S and OMc contaminated samples, mean R.R was higher than 1. In these cases it is important to note that R.R, for the OM+S data, were calculated with the OM contamination as a control, thus largest soil C mineralization fluxes could not be attributed to organic matter supply. Figure 4 also shows that R.R lower than 1 (log (R.R) <0) is expected for a soil Cu concentration exceeding a threshold value. From our dataset the soil Cu threshold was found controlled by the pH following the eq. III.2.6:

Eq. III.2.6: $Cu_{threshold} = e^{\frac{-0.076}{0.109}+\frac{0.115}{0.109}pH}$

As an example, a threshold value of 265 mg Cu.kg soil^{-1} can be calculated taking into account the mean reported pH 5.95 value in artificially contaminated samples. In those conditions, such a threshold value means that i) for Cu inputs below 265 mg Cu.kg soil^{-1} the soil C mineralization fluxes will increase, ii) the soil C mineralization in contaminated soil is lower than in the control for soil Cu higher than 265 mg.kg soil^{-1}, and iii) the highest the Cu inputs the lowest the R.R.

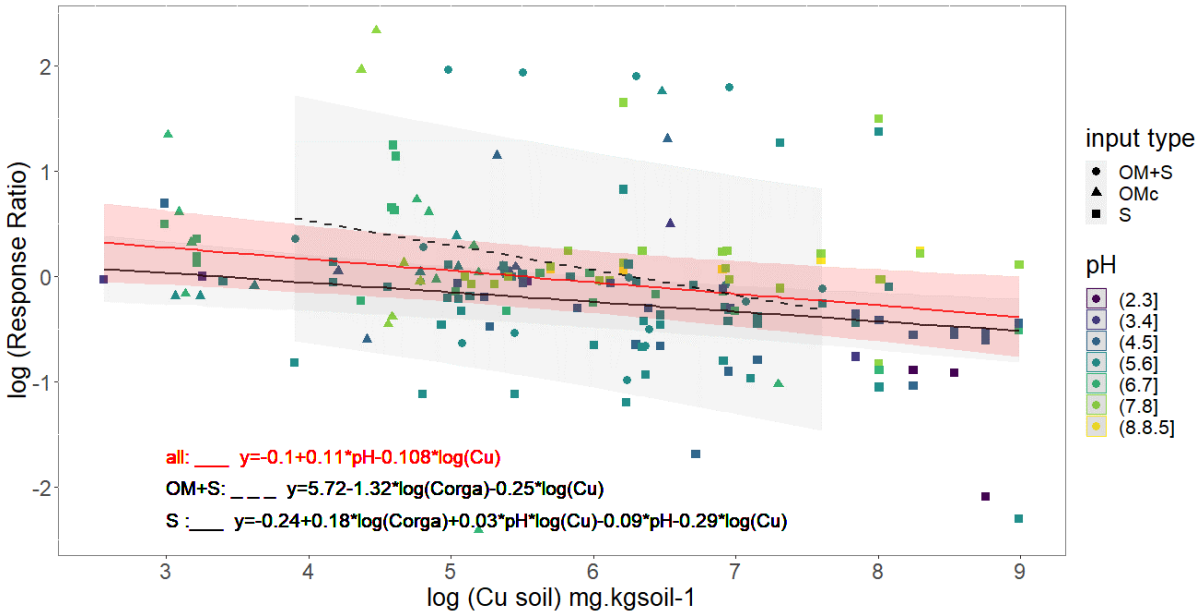

Fig III.2.4.: Variation in soil C mineralization due to artificial contamination. pH and nature of artificial contamination are represented through colour and shape. Black red line models soil Cu effect on log(Response Ratio) for all supplementary contamination with median pH value (5.9), black full line for Spike contamination with median pH and Corga (5.7 and 29.4 g.kgsoil^{-1}) value and black dashed line for organic matter +spike data with median Corga value (27 g.kg soil^{-1}). Mean Response Ratio are calculated according to eq. III.2.1 and soil respiration in contaminated condition is equal to control respiration for log (Response Ratio) = 0 which is the grey dashed line.

The type of added contamination (spikes only or in the presence of organic matter) could affect the soil response due to different Cu speciation as inputs. It would have been useful to include the interaction between the type of inputs and Cu in the R.R analysis through *lme*. However, due to the effective size we could only include the type of inputs but not their interactions with Cu. Nevertheless, results given in Table III.2.3 show that the type of inputs affected the range of R.R values. Indeed, different intercepts were defined but the influence of the type of contamination on the Cu effect on C mineralization was less clear.

Table III.2.3. (A) Slope and intercept (±standards errors, s.e.) between log (R.R) and variables selected through stepwise analysis with the linear mixed model for different dataset (all contamination, spikes and contamination due to organic matter additions). (B) Shift of the intercept for log (R.R) between the different groups of qualitative variable (different type of laboratory contamination, S = Spike, OMc= contaminated organic matter) and the reference one (Spike + Organic matter contamination) only calculated for the full dataset. p-values symbols are explained in the legend of Table III.2.2.

(A)

Log (R.R)	**Intercept** (±s.e.)	**pH** (±s.e.)	**.log (Cu tot)** (±s.e.)	**log (Cu tot)*pH** (±s.e.)	**Log(Corga)**	**AIC**	**BIC**	**logLIK**	**R2**
(all contamination, n=173)	**1.8°** (± 0.9)	**0.12^{NS}** (± 0.15)	**-0.30*** (± 0.12)	**0.03°** (± 0.02)	**Not selected by the stepwise regression**	278	303	-131	0.81
(S, n=123)	**0.24^{NS}** (± 0.79)	**-0.1^{NS}** (± 0.12)	**-0.29**** (± 0.10)	**0.04*** (± 0.02)	**0.04*** (± 0.02)	133	153	-59.8	0.73
(OM+S, n=18)	**5.32**** (± 0.87)	**Not selected by the stepwise regression**	**-0.23*** (± 0.09)	**Not selected by the stepwise regression**	**-1.32***** (± 0.16)	30	35	-11	0.97
(OMc, n=32)	**5.9^{NS}** (± 4.30)	**-1.00^{NS}** (± 0.70)	**-1.08^{NS}** (± 0.14)	**0.21^{NS}** (± 0.84)	**Not selected by the stepwise regression**	65	75	-26.9	0.94

(B)

	Type of contamination	**Intercept** (±s.e.)
Log (R.R) (all contamination, n=382)	**S**	**-0.74***** (± 0.15)
	OMc	**0.2^{NS}** (± 0.38)

In order to improve the quantification of the effect of different kinds of added contamination (pure spike contamination, spike with non-contaminated OM and OM associated contamination) we

analyzed separately the different subgroups. Results show that copper contamination effect was different depending of the contamination cases (Table III.2.3A, III.2.3B) so that:

- For pure spikes contaminations (123 data) and spikes with non-contaminated OM (16 data) we observed a decrease in R.R when Cu concentration increased (p-value = 0.005, general R^2 = 0.89 and p-value = 0.01, general R^2 = 0.80 respectively). Nevertheless, co-factors were found different between these two cases. In the cases of spikes, R.R is expected to increase with an increase in pH and in Corga. In the cases of spikes with non-contaminated OM, R.R is expected to decrease with an increase in Corga (see Table III.2.3A, III.2.3B and Fig III.2.4)

- For contamination associated with OM (32 data), the effect of soil Cu on R.R was not significant even though Cu was kept in the model selection but with a p-value > 0.1. No effect of pH nor of Corga were found.

Thus, a strong influence on the nature of the Cu contamination supplied ex-situ was assess using R.R and the dataset restricted to laboratory conditions.

3.3.6 Effect of the origin of Cu contamination on soil C mineralization: case of in situ copper contamination

To investigate specifically data of in situ Cu contaminated soils without laboratory added Cu contamination (eg when limiting the data set to the « non added contamination »), the soil clay content data were not included because the number of data from industrial or “other” soils would have been too small. Our analyses were then restricted to Cu and pH effects on soil C mineralization without investigation of other parameters. On their whole the 189 data thus obtained and analyzed by *lme* showed a slight tendency of a soil C mineralization to decrease with an increase in soil Cu (p-value = 0.08) and an increase with an increase in soil pH (p-value = 0.08) (Supplementary Table III.2.6A).

Focusing on the 105 data with pH < 6.2 (taking the mean value of the 105 data as threshold) we found a significant and negative effect of soil Cu (p-value = 0.02) on soil C mineralization (Table III.2.4A) as well as an effect of soil contamination type.

Table III.2.4. (A) Slope and intercept (±standards errors, s.e.) between log (mineralization/organic C) and variables selected through step wise analyse for the linear mixed model for different dataset (all nature of the in situ contamination with pH≤6.2, agricultural soils with pH≤6.2, industrial soils with pH≤6.2, non-contaminated soils with pH≤6.2). (B) Shift of the intercept for log (mineralization/organic C) between the different groups of qualitative variable (different type of in situ contamination with pH≤6.2, industrial soils with pH≤6.2, non-contaminated soils with pH≤6.2) and the reference one (agricultural soils,) only calculated for the full dataset. p-values symbols are explained in the legend of Table III.2.2.

(A)

Log (Min / Org C)	**Intercept** (±s.e.)	**pH** (±s.e.)	**.log (Cu tot)** (±s.e.)	**log (Cu tot)*pH** (±s.e.)	**AIC**	**BIC**	**logLIK**	**R2**
(all nature of the in situ contamination, with pH≤6.2 n=105)	**-0.12^{NS}** (± 1.20)	**-0.16^{NS}** (± 0.20)	**-0.5*** (± 0.21)	**0.07°** (± 0.04)	219	243	-101	0.98
(agricultural soils, with pH≤6.2 n=29)	**-3.5^{NS}** (± 0.9)	**+0.34^{NS}** (± 0.11)	**Not selected by the stepwise regression**	**Not selected by the stepwise regression**	64	79	-28	0.97
(industrial soils, with pH≤6.2 n=26)	**-2.5°** (± 1.7)	**0.48°** (± 0.24)	**-0.27**** (± 0.08)	**Not selected by the stepwise regression**	58	65	-24.6	0.99
(non contaminated soils, with pH≤6.2 n=46)	**-3.7°** (± 2.2)	**0.34^{NS}** (± 0.41)	**1.22^{NS}** (± 0.08)	**-0.23** (± 0.15)	121	132	-54	0.98

(B)

	Type of contamination	**Intercept** (±s.e.)
Log (Min / Org C) (all nature of the in situ contamination, n=109)	**Ind**	**-0.43°** (± 0.26)
	Nc	**-0.41*** (± 0.19)
	Oth	**0.57^{NS}** (± 0.41)

Aggregating all the in situ contamination type the soil Cu contamination effect on soil C mineralization was modelled as eq III.2.7:

Eq. III.2.7: $\log\left(\frac{Cmineralization}{soil\ C\ orga}\right) = -0.8\ (\pm 1.15) - 0.1\ (\pm 0.2) \times pH - 0.40(\pm 0.21) \times \log Cu + 0.06\ (\pm 0.04) \times pH \times \log(Cu)$

The p-values were 0.6; 0.06; and 0.1 for pH, Cu and their interactions respectively, with a $R^2 = 0.97$.

We did not find any effect of soil Cu on the soil C mineralization when agricultural type of contamination was involved (29 data, Table III.2.4A). The same was found when the non-contaminated samples at the background Cu level were involved (46 data, Table III.2.4A) but we did find an effect of soil Cu on soil C mineralization for the industrially contaminated soil types (26 data, Table III.2.4A). The "other" sources of contamination were not examined separately because of the small number of data (n=4). Hence, even for a diffuse and chronic in situ Cu contamination, the increase in soil Cu concentration can be related to a decrease in soil C mineralization. As previously we noticed a more pronounced effect of soil Cu on soil C mineralization in the acid soils. However, the differences in soil pH or soil Cu concentration could not explain the different relationships for the acid agricultural or industrial sites. In fact, for Agr soils 1st and 3rd quartile of pH are 4.7 and 5.9 against 4.6 and 5.7 for Ind soils whereas mean and max Cu concentration are 148 and 992 $mgCu.kg^{-1}$ for Agr soils and 109 and 898$mgCu.kg^{-1}$ for Ind soils. The multicontamination occurring in the industrial sites could artificially increase the effect of soil Cu on soil C mineralization in these sites, but we also observed a decreasing tendency in the whole naturally contaminated data set, which comfort us in the hypothesis of an observable in situ soil Cu effect.

4.DISCUSSION

4.1. From general to specific relationship of soil copper content effect on soil CO_2 emissions

Our general bibliographic approach allowed us to construct a large database with soil Cu concentrations associated to soil C mineralization for a large panel of ecosystems and contamination cases and with a broad range of soil pedological characteristics. Most of the *in situ* soil Cu content values (1st and 3rd quartile are respectively 16 and 133.4 $mgCu.kg\ soil^{-1}$) used in these studies are in the range of European values from ESDAC Database (Supplementary Table III.2. 2 and (Ballabio et al., 2018)). Moreover, for some cases (industrial fields) the Cu values were higher than data reported by ESDAC (1st and 3rd quartile respectively 44.6 and 216.3 mg $Cu.kg^{-1}$ but max at 1251 $mgCu.kg\ soil^{-1}$). This might be due to the spatial heterogeneity of the Cu distribution at smaller scale (Chopin and Alloway, 2007) not reflected by the European database ESDAC despite their large (22,000) number of samples (Ballabio et al., 2018). Hence our industrial contamination database provides 8 data in the range of the highest spike contamination Cu concentration we also recorded. The high concentrations reached with spikes overwhelmed by several orders of magnitude most of the in-situ reported Cu concentrations. But they can still be considered as environmentally relevant because industrial sites or amended agricultural soils like vineyard soils are known to exhibit such concentrations (Aoyama & Nagumo, 1997b; Usman, et al., 2005; Zimakowska-Gnoińska et al., 2000).

The complementarity uses of PCA and Random Forest allowed us to establish important cluster of analysis while analysis with *lme* limited the statistical bias in the small size factor classes. Using our quantitative analysis approach, we were able to define a generic relationship between soil C mineralization and soil Cu contamination and thus confirm an effective impact of Cu contamination on soil C mineralization. Several authors reported different effects of Cu on microbial characteristics and functions in soils (biomass, C mineralization, …) depending of local soil properties, soil type (Doelman

and Haanstra, 1984; Broos et al., 2007; Li et al., 2016), OM content, clay types (Li et al., 2015), pH (Fernández-Calviño and Bååth, 2016) or specific environmental conditions (freezing exposure (Salminen et al., 2002). Hence, from our global dataset, we confirmed the possibility of obtaining a general log linear relationship between soil C mineralization and soil Cu content, that shows a decrease in soil C mineralization when soil Cu content increase (Eq. III.2.2). Furthermore, we identified specific cases based on general soil properties such as pH but not clay. Even if equations III.22 and III.2.3 relying soil C mineralization to soil Cu contents were different, it is notable that their slopes were rather identical (near -0.08, Eq. III.2.2 and III.2.3). Thus, effect of soil Cu contamination on soil C mineralization was similar whatever the co-factor.

Soil contamination history, which was here roughly assimilated to the in situ contamination and soil use type, has also been identified as a non-negligible co-factor in Cu effect on soil C mineralization. The relationship between soil C mineralization and Cu contamination was also refined for the industrial sites or acidic soils. To better understand the impact of soil contamination on soil CO_2 emissions, we looked at three response variables: qCO_2, R.R and soil C mineralization. The equations thus obtained can be further used in other works depending on the desired expression of soil C mineralization or CO_2 emission of interest and the available data mostly as soil pH and Corga.

4.2 How environmental factors influence the effect of soil Cu contamination on soil C mineralization?

We have shown that the global decrease in soil respiration with the increase in soil Cu contents could be refined considering the soil pH or the origin of contamination (Table III.2.2). Our results showed that this decrease was i) particularly marked for acidic soils and ii) somehow influenced by OM.

The highest sensitivity of soil C mineralization to Cu contamination in the case of acidic soil compared to neutral or alkaline soil conditions is consistent with the fact that cationic Cu species are known to readily associate with OM, hence be less bioavailable for microbial communities. This was shown for moderate Cu concentrations but not for too high concentrations (Fließbach et al., 1994). In acidic soils, H^+ and Cu^{2+} can compete to link with the functional reactive groups of OM so that for a same amount of soil Cu and soil OM, more Cu can be bioavailable in acidic soil (Khan and Scullion, 2000; Sauvé et al., 2000; Li et al., 2015). Furthermore, soil Cu concentration has been found positively correlated with soil pH (Panagos et al., 2018). Thus, the highest sensitivity of soil C mineralization in acidic soils found in laboratory conditions can be counter-balanced by the fact that in situ these soils are generally found to be less contaminated. As a result, the global effect of soil Cu contamination on soil C mineralization could be limited.

Numerous studies emphasize the potentiality of OM bindings to limit Cu bioavailability (Degryse et al., 2009; Amery et al., 2010; Groenenberg et al., 2010; Ren et al., 2015) particularly in the case of organic fertilizer amendments. Our results do not allow us to clearly assess the OM effect on Cu contamination. However, we saw that Corga could not be excluded from R.R analyses in spiked cases (Table III.2.4B). In the case of spikes, the increase in R.R with OM tends to show that the negative Cu effect on soil C mineralization would be mitigated by the soil organic matter. But in the case of contamination with

both spikes and OM inputs (OM+S), the negative influence of C organic could be due to confounding effects between an increase in soil Cu and an increase in soil Corga. Moreover, in this last case R.R is expected to be largely higher than 1 for the lowest Cu input but to decrease more abruptly with Cu concentration than in the case of spike only. Finally, no clear effect on soil C mineralization was found when dealing with the OMc samples for which Cu was provided in tight association with OM. Nonetheless our results are consistent with previous studies reporting that high soil OM contents diminished to a certain extent Cu availability (Smolders et al., 2012; Laurent et al., 2020), hence somewhat diminished the decrease in soil C mineralization due to Cu contamination. Thus, the soil C mineralization of soils with high C contents could be less impacted by Cu contamination than the one in soils with low Corga contents.

4.3 For the soil Cu contamination effect, does the nature of the input matter?

It was interesting to investigate external, anthropogenic factors, as they are known to influence the soil responses. We thus separated the impact of land use through the analysis of the different natures of in situ contamination cases, and the cases of artificial laboratory contaminations. The comparison was not straightforward between short-term artificial contaminations in laboratories and chronic low inputs as in natural in situ environmental samples. Artificial Cu inputs are expected to rapidly and temporary decrease soil pH, whereas naturally in situ contaminated soils progressively equilibrate through various processes called “aging processes” or “natural attenuation” leading to less available contamination and less toxicity (Orts et al., 2006; Smolders et al., 2009). Moreover on the long term, soil microbial community adaptation to successive metal stress has been shown (Niklińska et al., 2006; Philippot et al., 2008). Hence, compared to naturally contaminated samples, a larger effect of soil Cu content on soil respiration is expected for the ex-situ contamination experiments. Our results are consistent with these findings: the effect of soil Cu content on soil C mineralization is clearly assessed in the case of laboratory contamination, but only slightly assessed when considering the entirety of in situ Cu contaminated soil data.

The influence of the nature of the in situ contamination, however, was not clear: Cu effect on soil C mineralization was noticed for all the in situ contaminated acid soils (pH<6.2) with different intercept values (Table III.2.4B) depending on the contamination type. However, focusing on each subgroups of in situ contamination (Agr, Ind, Nc, Oth, Supplementary Table III.2.2 the effect of soil Cu contamination on soil C mineralization was only assessed for the industrial soils. Multi-contaminations occurring in industrial sites (Wilson and Pyatt, 2007) have often been proposed to explain strong decline in soil functions (Ramsey, et al., 2005; Romero-Freire, et al. 2016). Some of the samples with “other” Cu source were also multi-contaminated, as they include for instance contamination from roadside. Unfortunately, the small (7) number of samples does not allow us to investigate the effect of soil Cu contamination on C mineralization in those soils and to affine the potential effect of multi-contamination. Hence, we just observed a downward trend in CO_2 emissions with an increase in Cu contamination for in-situ contaminated sites. The effects were more pronounced in acids industrial sites. However, for low contaminated agricultural or other soils, no effect was detected.

4.4 Implication for the climate of the soil Cu contaminations as seen by the variations in CO_2 emissions

Nowadays, several environmental policies aim at reducing atmospheric CO_2 according to scenarios included in predictive atmospheric CO_2 models. Soil pollution is still not included in models projection used to define policies, even if soil contamination is suspected to alter soil CO_2 emissions. Our study focuses on Cu as a common pollutant known to affect several biological processes like plant productivity, microfauna reproduction or their biomass (Eijsackers et al., 2005; Tobor-Kapłon et al., 2006). Here we focused on one soil function which is the soil C mineralization and we showed that soil C mineralization and thus CO_2 emissions tended to decrease when soil Cu concentrations increased. This is the results of two compensating processes: i) the specific respiration (e.g the amount of respired C per unit of microbial biomass) increases in particular for high contamination levels and low soil pHs and ii) soil microbial biomass decreases when Cu increases. Analyses of response ratio data also showed the same trend: as Cu concentration increases, R.R decreases when contamination stays below an estimated threshold of about 265 $mg.kg^{-1}$, meaning that Cu inputs will increase the respiration of a contaminated soil compared to its uncontaminated level (see section 3.3.5).

Heavy metals such as Cu are known to accumulate in surface soils for a long time (Pietrzak and McPhail, 2004) and can be predicted to increase progressively as they are not biodegradable and poorly mobile in the soil profile. In accordance with our results, and following a Cu accumulation with time, contaminated soils will be supposed to emit less CO_2 than non-contaminated ones. Furthermore, the increase in soil C mineralization noticed for Cu input below 265mgCu. kg^{-1} would likely not be observed in the case of field contamination in scenarios with increasing Cu inputs. Finally, considering minimal and mean Cu contents in the case of in situ contamination from 1 to 140 mg Cu.kg soil $^{-1}$ (Table III.2.1, Supplementary Table III.2.2 and eq. III.2.2), we can predict with the geochemical models of soil CO_2 emission an overestimation from roughly 41%.

Nevertheless, the general observed lower soil C mineralization in contaminated soils gets with an increase in the specific respiration rate (respired CO_2 per unit of microbial biomass) at higher copper level. Thus, even though toxic high Cu contaminations reduce soil microbial biomass we can notice that CO_2 respired per microbial biomass unit increases. Thus, our results rather show that if soil Cu contamination result in a decrease in soil C-CO_2 emissions it is accompanied by a loss of soil function but not by an increase in C storing potential. Hence, a decrease in soil respiration does not necessary mean that more C is stored in the soil for a long time but it could be that less C is converted in biomass and biological products as microbial C biomass decreases. According to Ding et al., (2016) and Liang et al., (2017) the microbial biomass and more specifically the necromass are the primary contributors of stable soil C pool. Hence, taking into account the decrease of microbial biomass in contaminated soils, the over whole stabilization of C in soil is not expected to increase. Some biogeochemicals models include microbial biomass dynamics (Changsheng Li, et al., 1992; Kuijper, et al., 2005; Moore et al., 2004) and their use could be useful to predict longer term effect of soil Cu pollution on C stock. In particular, the generic relationships between soil CO_2 emission and soil Cu concentration obtained here could be used as a first step to complete continental biogeochemical models including soil Cu pollution and to refine soil CO_2 emission scenarii. We propose that such a modified model should be used when

prospecting futures of CO_2 atmospheric concentrations and climate with, for instance, soil land use modifications and the estimated associated Cu pollution.

5. CONCLUSION:

The aim of this study was to quantify a generic effect of soil Cu contamination on soil Corga mineralization and thus on soil CO_2 emissions. By taking into account various soils types and contamination cases our study established that Cu contamination may decrease soil carbon mineralization and a generic relationship was established (eq III.2.2). This simple relationship between soil carbon emissions and soil Cu could, however, be refined to include soil parameters such as pH, Corga content and, when available the origin of the contamination. Our study points out that soil Cu contamination significantly affect soil C mineralization for soil Cu contents above 265 $mg.kg^{-1}$ and also for acidic soils. Artificial acute Cu contaminations lead to highest decreases in soil C mineralization than in situ contamination. However if we raise our acceptation p-value to 0.1 the in situ contamination could be considered as significant. So that, even chronic long term contamination of soils due to anthropogenic activities can be related to a decrease in soil C mineralization. Our statistical analysis of soil microbial C content with Cu contamination showed a decrease of Cmic and an increase in carbon emission per unit of microbial biomass in some contaminated environments. Thus, it must not be concluded that the observed decrease in soil C mineralization in contaminated soils may be associated with a way to store more C in soils. On the contrary, the observed decrease in Cmic is expected to favor loss of soil functions and of resiliency to face supplementary stresses like extreme climatic events (Visser and Parkinson, 1992; Tobor-Kapłon et al., 2006).

Although very comprehensive, our study faces the lack of information on i) soil carbon mineralization kinetics, ii) field measurements and iii) studies with extreme climate samples. Particularly i) and iii) are factors of interest in long-term soil carbon release estimation to model CO_2 cycle, CO_2 atmospheric concentration and climate. The poor number of data concerning field measurements as well as the over-representation temperate and continental climates are damageable for global Earth functioning comprehension. To better anticipate the climate changes, we need studies in extreme climate conditions that get out of our methodological approach but would provide more reliable results. Nonetheless the generic equation we obtained relying soil C mineralization to soil Cu concentration can be considered as a step forward to improve the soil biogeochemical models and further climate projections. Moreover, some important drivers of soil OM mineralization had to be ignored in our study because of missing data such as microbial community composition or activity.

6. Additional Requirements

The full database has been deposited on data.inrae.fr and is available at:
https://data.inrae.fr/dataset.xhtml?persistentId=doi:10.15454/P6XPF6

7.Conflict of Interest

The authors declare that the research was conducted in the absence of any commercial or financial relationships that could be construed as a potential conflict of interest.

8. Authors contributions

LS created the database and performed the analysis. IL and BG designed the study. All authors equally contributed the interpretation and the writing.

9. Fundings

We acknowledge support from the Agence Nationale de la Recherche with the LabEx BASC (ANR-11-LABX-0034) and the CONNEXION project.

10.Acknowledgements

The authors thank Christine Sireyjol for her help in the bibliographic search process, Olivier Crouzet for his advices in results exploitation. They also thank the LabeX BASC for its funding through the CONNEXION project. Laura Sereni also thanks the ENS for her grant.

References

Adhikari, K., and Hartemink, A. E. (2016). Geoderma Linking soils to ecosystem services — A global review. *Geoderma* 262, 101–111. doi:10.1016/j.geoderma.2015.08.009.

Amery, F., Degryse, F., Van Moorleghem, C., Duyck, M., and Smolders, E. (2010). The dissociation kinetics of Cu-dissolved organic matter complexes from soil and soil amendments. *Anal. Chim. Acta*. doi:10.1016/j.aca.2010.04.047.

Anderson, T. H., and Domsch, K. H. (1993). The metabolic quotient for CO2 (qCO2) as a specific activity parameter to assess the effects of environmental conditions, such as ph, on the microbial biomass of forest soils. *Soil Biol. Biochem.* doi:10.1016/0038-0717(93)90140-7.

Aoyama, M., and Nagumo, T. (1997). Effects of heavy metal accumulation in apple orchard soils on microbial biomass and microbial activities. *Soil Sci. Plant Nutr.* 43, 601–612. doi:10.1080/00380768.1997.10414786.

Bååth, E. (1989). Effects of heavy metals in soil on microbial processes and populations (a review). *Water. Air. Soil Pollut.* 47, 335–379. doi:10.1007/BF00279331.

Baderna, D., Maggioni, S., Boriani, E., Gemma, S., Molteni, M., Lombardo, A., et al. (2011). A combined approach to investigate the toxicity of an industrial landfill's leachate: Chemical analyses, risk assessment and in vitro assays. *Environ. Res.* doi:10.1016/j.envres.2011.01.015.

Ballabio, C., Panagos, P., Lugato, E., Huang, J. H., Orgiazzi, A., Jones, A., et al. (2018). Copper distribution in European topsoils: An assessment based on LUCAS soil survey. *Sci. Total Environ.* 636, 282–298. doi:10.1016/j.scitotenv.2018.04.268.

Batjes, N. H. (2014). Total carbon and nitrogen in the soils of the world. *Eur. J. Soil Sci.* doi:10.1111/ejss.12114_2.

Birch, H. F. (1958). The effect of soil drying on humus decomposition and nitrogen availability. *Plant Soil*. doi:10.1007/BF01343734.

Brookes, P. C. (1995). The use of microbial parameters in monitoring soil pollution by heavy metals. *Biol. Fertil. Soils*. doi:10.1007/BF00336094.

Broos, K., Warne, M. S. J., Heemsbergen, D. A., Stevens, D., Barnes, M. B., Correll, R. L., et al. (2007). Soil factors controlling the toxicity of copper and zinc to microbial processes in Australian soils. *Environ. Toxicol. Chem.* 26, 583–590. doi:10.1897/06-302R.1.

Changsheng Li, Frolking, S., and Frolking, T. A. (1992). A model of nitrous oxide evolution from soil driven by rainfall events: 1. Model structure and sensitivity. *J. Geophys. Res.* doi:10.1029/92jd00509.

Chopin, E. I. B., and Alloway, B. J. (2007). Distribution and mobility of trace elements in soils and vegetation around the mining and smelting areas of Tharsis, Ríotinto and Huelva, Iberian Pyrite Belt, SW Spain. *Water. Air. Soil Pollut.* doi:10.1007/s11270-007-9336-x.

Deary, M. E., Ekumankama, C. C., and Cummings, S. P. (2018). Effect of lead, cadmium, and mercury co-contaminants on biodegradation in PAH-polluted soils. *L. Degrad. Dev.* doi:10.1002/ldr.2958.

Degryse, F., Smolders, E., and Parker, D. R. (2009). Partitioning of metals (Cd, Co, Cu, Ni, Pb, Zn) in soils: concepts, methodologies, prediction and applications - a review. *Eur. J. Soil Sci.* 60, 590–612. doi:10.1111/j.1365-2389.2009.01142.x.

Ding, J., Chen, L., Zhang, B., Liu, L., Yang, G., Fang, K., et al. (2016). Linking temperature sensitivity of soil CO2 release to substrate, environmental, and microbial properties across alpine ecosystems. *Global Biogeochem. Cycles*. doi:10.1002/2015GB005333.

Doelman, P., and Haanstra, L. (1984). Short-term and long-term effects of cadmium, chromium, copper, nickel, lead and zinc on soil microbial respiration in relation to abiotic soil factors. *Plant Soil* 79, 317–327. doi:10.1007/BF02184325.

Dumestre, A., Sauvé, S., McBride, M., Baveye, P., and Berthelin, J. (1999). Copper speciation and microbial activity in long-term contaminated soils. *Arch. Environ. Contam. Toxicol.* 36, 124–131. doi:10.1007/s002449900451.

Eijsackers, H., Beneke, P., Maboeta, M., Louw, J. P. E., and Reinecke, A. J. (2005). The implications of copper fungicide usage in vineyards for earthworm activity and resulting sustainable soil quality. *Ecotoxicol. Environ. Saf.* doi:10.1016/j.ecoenv.2005.02.017.

FAO (2008). Soil Pollution a hidden reality. doi:10.2105/ajph.12.5.426-b.

FAO, and ITPS (2015). The World's Soil Resources: Main Report.

Fernandez-Calvino, D., and Baath, E. (2016). Interaction between pH and Cu toxicity on fungal and bacterial performance in soil. *SOIL Biol. Biochem.* 96, 20–29. doi:10.1016/j.soilbio.2016.01.010.

Fernández-Calviño, D., and Bååth, E. (2016). Interaction between pH and Cu toxicity on fungal and bacterial performance in soil. *Soil Biol. Biochem.* 96, 20–29. doi:10.1016/j.soilbio.2016.01.010.

Fierer, N. (2017). Embracing the unknown: Disentangling the complexities of the soil microbiome. *Nat. Rev. Microbiol.* doi:10.1038/nrmicro.2017.87.

Fließbach, A., Martens, R., and Reber, H. H. (1994). Soil microbial biomass and microbial activity in soils treated with heavy metal contaminated sewage sludge. *Soil Biol. Biochem.* doi:10.1016/0038-0717(94)90144-9.

Friedlingstein, P., Jones, M. W., O'Sullivan, M., Andrew, R. M., Hauck, J., Peters, G. P., et al. (2019). Global carbon budget 2019. *Earth Syst. Sci. Data*. doi:10.5194/essd-11-1783-2019.

Groenenberg, J. E., Koopmans, G. F., and Comans, R. N. J. (2010). Uncertainty analysis of the nonideal competitive adsorption - Donnan model: Effects of dissolved organic matter variability on predicted metal speciation in soil solution. *Environ. Sci. Technol.* doi:10.1021/es902615w.

Hashimoto, S., Carvalhais, N., Ito, A., Migliavacca, M., Nishina, K., and Reichstein, M. (2015). Global spatiotemporal distribution of soil respiration modeled using a global database. *Biogeosciences* 12, 4121–4132. doi:10.5194/bg-12-4121-2015.

Jones, W. J., and Ananyeva, N. D. (2001). Correlations between pesticide transformation rate and microbial respiration activity in soil of different ecosystems. *Biol. Fertil. Soils*. doi:10.1007/s003740100365.

Keiblinger, K. M., Schneider, M., Gorfer, M., Paumann, M., Deltedesco, E., Berger, H., et al. (2017). Assessment of Cu applications in two contrasting soils—effects on soil microbial activity and the fungal community structure. *Ecotoxicology* 27, 217–233. doi:10.1007/s10646-017-1888-y.

Khan, M., and Scullion, J. (2000). Effect of soil on microbial responses to metal contamination. *Environ. Pollut.* doi:10.1016/S0269-7491(99)00288-2.

Komárek, M., Čadková, E., Chrastný, V., Bordas, F., and Bollinger, J. C. (2010). Contamination of vineyard soils with fungicides: A review of environmental and toxicological aspects. *Environ. Int.* doi:10.1016/j.envint.2009.10.005.

Kuijper, L. D. J., Berg, M. P., Morriën, E., Kooi, B. W., and Verhoef, H. A. (2005). Global change effects on a mechanistic decomposer food web model. *Glob. Chang. Biol.* doi:10.1111/j.1365-2486.2005.00898.x.

Kumar, V., Kothiyal, N. C., and Saruchi (2016). Analysis of Polycyclic Aromatic Hydrocarbon, Toxic Equivalency Factor and Related Carcinogenic Potencies in Roadside Soil within a Developing City of Northern India. *Polycycl. Aromat. Compd.* doi:10.1080/10406638.2015.1026999.

Laurent, C., Bravin, M. N., Crouzet, O., Pelosi, C., Tillard, E., Lecomte, P., et al. (2020). Increased soil pH and dissolved organic matter after a decade of organic fertilizer application mitigates copper and zinc availability despite contamination. *Sci. Total Environ.* doi:10.1016/j.scitotenv.2019.135927.

Li, J., Ma, Y. B., Hu, H. W., Wang, J. T., Liu, Y. R., and He, J. Z. (2015). Field-based evidence for consistent responses of bacterial communities to copper contamination in two contrasting agricultural soils. *Front. Microbiol.* 6, 1–12. doi:10.3389/fmicb.2015.00031.

Li, J., Wang, J. T., Hu, H. W., Ma, Y. B., Zhang, L. M., and He, J. Z. (2016). Copper pollution decreases the resistance of soil microbial community to subsequent dry-rewetting disturbance. *J. Environ. Sci. (China)*. doi:10.1016/j.jes.2015.10.009.

Li, Y. T., Becquer, T., Quantin, C., Benedetti, M., Lavelle, P., and Jun, D. (2005). Microbial activity indices: Sensitive soil quality indicators for trace metal stress. *Pedosphere* 15, 409–416.

Liang, C., and Balser, T. C. (2011). Microbial production of recalcitrant organic matter in global soils: Implications for productivity and climate policy. *Nat. Rev. Microbiol.* doi:10.1038/nrmicro2386-c1.

Liang, C., Schimel, J. P., and Jastrow, J. D. (2017). The importance of anabolism in microbial control over soil carbon storage. *Nat. Microbiol.* 2, 1–6. doi:10.1038/nmicrobiol.2017.105.

Mark Mitchell, Muftakhidinov, Winchen, B. T., Badshah400, B. van S., Wilms, A., Kylesower, et al. Engauge digitizer. doi:10.5281/zenodo.3558440.

Merrington, G., Rogers, S. L., and Van Zwieten, L. (2002). The potential impact of long-term copper fungicide usage on soil microbial biomass and microbial activity in an avocado orchard. *Aust. J. Soil Res.* 40, 749–759. doi:10.1071/SR01084.

Moore, J. C., Berlow, E. L., Coleman, D. C., De Suiter, P. C., Dong, Q., Hastings, A., et al. (2004). Detritus, trophic dynamics and biodiversity. *Ecol. Lett.* doi:10.1111/j.1461-0248.2004.00606.x.

Moreno, J. L., Bastida, F., Ros, M., Hernandez, T., and Garcia, C. (2009). Soil organic carbon buffers heavy metal contamination on semiarid soils: Effects of different metal threshold levels on soil microbial activity. *Eur. J. Soil Biol.* 45, 220–228. doi:10.1016/j.ejsobi.2009.02.004.

Müller, T., and Höper, H. (2004). Soil organic matter turnover as a function of the soil clay content: Consequences for model applications. *Soil Biol. Biochem.* doi:10.1016/j.soilbio.2003.12.015.

Niklińska, M., Chodak, M., and Laskowski, R. (2006). Pollution-induced community tolerance of microorganisms from forest soil organic layers polluted with Zn or Cu. *Appl. Soil Ecol.* 32, 265–272. doi:10.1016/j.apsoil.2005.08.002.

Odum, E. P. (1995). Expected Trends in stressed ecosystem. *Bioscience* 35, 419–422.

Oorts, K., Bronckaers, H., and Smolders, E. (2006). Discrepancy of the microbial response to elevated copper between freshly spiked and long term contaminated soils. 25, 845–853.

Panagos, P., Ballabio, C., Lugato, E., Jones, A., Borrelli, P., Scarpa, S., et al. (2018). Potential sources of anthropogenic copper inputs to European agricultural soils. *Sustain.* doi:10.3390/su10072380.

Pell, M., Stenström, J., and Granhall, U. (2006). *Microbiological methods for assessing soil quality*. , eds. B. J., D. W. Hopkins, and A. Benedetti CAB international Wallingford Oxfordshire, UK.

doi:10.1079/9780851990989.0000.

Philippot, L., Cregut, M., Chèneby, D., Bressan, M., Dequiet, S., Martin-Laurent, F., et al. (2008). Effect of primary mild stresses on resilience and resistance of the nitrate reducer community to a subsequent severe stress. *FEMS Microbiol. Lett.* doi:10.1111/j.1574-6968.2008.01210.x.

Pietrzak, U., and McPhail, D. C. (2004). Copper accumulation, distribution and fractionation in vineyard soils of Victoria, Australia. *Geoderma*. doi:10.1016/j.geoderma.2004.01.005.

Pribyl, D. W. (2010). A critical review of the conventional SOC to SOM conversion factor. *Geoderma* 156, 75–83. doi:10.1016/j.geoderma.2010.02.003.

Ramsey, P. W., Rillig, M. C., Feris, K. P., Moore, J. N., and Gannon, J. E. (2005). Mine waste contamination limits soil respiration rates: A case study using quantile regression. *Soil Biol. Biochem.* 37, 1177–1183. doi:10.1016/j.soilbio.2004.11.016.

Ren, Z. L., Tella, M., Bravin, M. N., Comans, R. N. J., Dai, J., Garnier, J. M., et al. (2015). Effect of dissolved organic matter composition on metal speciation in soil solutions. *Chem. Geol.* doi:10.1016/j.chemgeo.2015.01.020.

Romero-Freire, A., Garcia Fernandez, I., Simon Torres, M., Martinez Garzon, F. J., and Martin Peinado, F. J. (2016). Long-term toxicity assessment of soils in a recovered area affected by a mining spill. *Environ. Pollut.* 208, 553–561. doi:10.1016/j.envpol.2015.10.029.

Rousk, J., Brookes, P. C., Bååth, E., Rousk, J., Brookes, P. C., and Bååth, E. (2009). Contrasting Soil pH Effects on Fungal and Bacterial Growth Suggest Functional Redundancy in Carbon Mineralization Contrasting Soil pH Effects on Fungal and Bacterial Growth Suggest Functional Redundancy in Carbon Mineralization □ †. 75. doi:10.1128/AEM.02775-08.

Rudolf Geiger, W. P. (1954). Eine neue Wandkarte der Klimagebiete der Erde nach W. Köppens Klassifikation (A New Wall Map of the Climatic Regions of the World According to W. Köppen's Classification). *Erdkunde*.

Salminen, J., Liiri, M., and Haimi, J. (2002). Responses of microbial activity and decomposer organisms to contamination in microcosms containing coniferous forest soil. *Ecotoxicol. Environ. Saf.* 53, 93–103. doi:10.1006/eesa.2001.2215.

Sauvé, S., Hendershot, W., and Herbert E., A. (2000). Solid-Solution Partitioning of Metals in Contaminated Soils: Dependence on pH, Total Metal Burden, and Organic Matter. *Am. Chem. Soc.*, 1125–1131. doi:10.1021/es9907764.

Schmidt, M. W. I., Torn, M. S., Abiven, S., Dittmar, T., Guggenberger, G., Janssens, I. A., et al. (2011). Persistence of soil organic matter as an ecosystem property. *Nature*. doi:10.1038/nature10386.

Smolders, E., Oorts, K., Lombi, E., Schoeters, I., Ma, Y., Zrna, S., et al. (2012). The Availability of Copper in Soils Historically Amended with Sewage Sludge, Manure, and Compost. *J. Environ. Qual.* doi:10.2134/jeq2011.0317.

Smolders, E., Oorts, K., Van Sprang, P., Schoeters, I., Janssen, C. R., McGrath, S. P., et al. (2009). Toxicity of trace metals in soil as affected by soil type and aging after contamination: Using calibrated bioavailability models to set ecological soil standards. *Environ. Toxicol. Chem.* doi:10.1897/08-592.1.

Soler-Rovira, P., Fernández-Calviño, D., Arias-Estévez, M., Plaza, C., and Polo, A. (2013). Respiration parameters determined by the ISO-17155 method as potential indicators of copper pollution in vineyard soils after long-term fungicide treatment. *Sci. Total Environ.* 447, 25–31. doi:10.1016/j.scitotenv.2012.12.077.

Sorensen, L. H. (1981). Carbon-nitrogen relationships during the humification of cellulose in soils containing different amounts of clay. *Soil Biol. Biochem.* doi:10.1016/0038-0717(81)90068-7.

Tobor-Kapłon, M. A., Bloem, J., and De Ruiter, P. C. (2006). Functional stability of microbial communities from long-term stressed soils to additional disturbance. *Environ. Toxicol. Chem.* doi:10.1897/05-398R1.1.

Usman, a., Kuzyakov, Y., and Stahr, K. (2005). Effect of clay minerals on immobilization of heavy metals and microbial activity in a sewage wludge-contaminated soil. *J. Soils Sediments* 5, 245–252. doi:10.1065/jss2005.05.141.

Venuti, A., Alfonsi, L., and Cavallo, A. (2016). Anthropogenic pollutants on top soils along a section of the Salaria state road , central Italy. *Ann. Geophys.* 59, 11. doi:10.4401/ag-7021.

Visser, S., and Parkinson, D. (1992). Soil biological criteria as indicators of soil quality: Soil microorganisms. *Am. J. Altern. Agric.* doi:10.1017/S0889189300004434.

Wakelin, S. A., Chu, G., Broos, K., Clarke, K. R., Liang, Y., and McLaughlin, M. J. (2010). Structural and functional response of soil microbiota to addition of plant substrate are moderated by soil Cu levels. *Biol. Fertil. Soils* 46, 333–342. doi:10.1007/s00374-009-0436-1.

Wang, Q. Y., Sun, J. Y., Xu, X. J., and Yu, H. W. (2018). Integration of chemical and toxicological tools to assess the bioavailability of copper derived from different copper-based fungicides in soil. *Ecotoxicol. Environ. Saf.* doi:10.1016/j.ecoenv.2018.06.041.

Wang, W. ., Dalal, R. ., Moody, P. ., and Smith, C. . (2003). Relationships of soil respiration to microbial biomass, substrate availability and clay content. *Soil Biol. Biochem.* 35, 273–284. doi:10.1016/S0038-0717(02)00274-2.

Wilson, B., and Pyatt, F. B. (2007). Heavy metal dispersion, persistance, and bioccumulation around an ancient copper mine situated in Anglesey, UK. *Ecotoxicol. Environ. Saf.* doi:10.1016/j.ecoenv.2006.02.015.

Xu, M., and Shang, H. (2016). Contribution of soil respiration to the global carbon equation. *J. Plant Physiol.* doi:10.1016/j.jplph.2016.08.007.

Zimakowska-Gnoińska, D., Bech, J., and Tobias, F. J. (2000). Assessment of the heavy metal pollution effects on the soil respiration in the Baix Llobregat (Catalonia, NE Spain). *Environ. Monit. Assess.* 61, 301–313. doi:10.1023/A:1006105329210.

Supplementary Table III.2.1. Number of collected data for the categories of climate based on the Koeppen classification system. The first letter refers to the main type of climate (A = Tropical, B = Dry, C = Temperate, D = continental), the second letter refers to the rainfall pattern (f = humid all year long, m = monsoon, s = dry summer, w = dry winter).

Climate in the sampling sites	**Af** Equatorial	**Am** Moonsonic	**Aw** Savannah with dry summer	**Bs** steppe	**Bw** Desert	**Cf** Temperate without dry season	**Cs** Temperate with dry summer	**Cw** Temperate with dry winter	**Df** Continental whithout dry season
Number of data	5	4	12	20	1	152	106	8	81

Supplementary Table III.2.2. Number of collected data from the different ex-situ soil contamination related to the various in situ samples. For each set of data mean ± standard error of the total soil Cu concentrations are given in parenthesis. None = no added Cu contamination

In situ Contamination / **Ex situ supplementary contamination**	**Agricultural**	**Non Contaminated**	**Other**	**Industrial**
None	51 (259 ± 345)	99 (45.5 ± 6.31)	9 (285 ± 215)	36 (194 ± 43.9)
Spike	41 (1206±324)	80 (1615±220)	2 (447± 382)	
Organic Matter + Spike (OM+S)	6 (276±89.2)	10 (753±182)		
Contaminated Organic Matter (OMc)	12 (155 ±17.7)	24 (64.2±7.69)	4 (105±5.35)	5 (727±209)
Organic Matter (OM)	2 (46.1±36.2)	3 (39.6±11.6)		3 (1251±0)
Contaminated organic matter + Spike (S+OMc)		2 (270±150)		

Supplementary Table III.2.3. (A) Characteristics of the relationship between log (mineralization/ Corga) and the variables selected through the stepwise analyses with the linear mixed model given as intercept and slopes (±standard errors, s.e) . P-values of each estimate are symbolised with NS for p-value>0.1, with "°" for p-value<0.1, with "*" for p-value<0.05 ; with "**" for p-value<0.01 and with "***" for p-value<0.001.

(B) Shift of the intercept for log (mineralization/organic C) between the different groups of qualitative variable (rainfall patterns s, m, w) and the reference one (f) only calculated for the full dataset.

(A)

	Intercept (±s.e.)	**pH** (±s.e.)	**.log (Cu tot)** (±s.e.)	**log (Cu)*pH** (±s.e.)	**Log(clay)**	**AIC**	**BIC**	**logLIK**	**R2**
Log (Mineralization / Corga) (n=206)	**-0.6^{NS}** (± 1.20)	**-0.07 °** (± 0.17)	**-0.27°** (± 0.16)	**+0.03^{NS}** (± 0.02)	**Not selected by the step wise regression**	483	503	-135	0.92

(B)

Log (Mineralization / Corga) (n=206)	**s**	**Not selected by the stepwise regression**
	m	**Not selected by the stepwise regression**
	w	**Not selected by the stepwise regression**

Supplementary Table III.2.4 (A) Slope and intercept (± standards errors, s.e.) between log (mineralization/ Corga) and variables selected through step wise analyse for the linear mixed model. (B) Shift of the intercept for log (mineralization/ Corga) between the different groups of qualitative variable (rainfall patterns s, m, w) and the reference one (f) only calculated for the full dataset. P-values symbols are explained in the legend of supplementary Table III.2.3

(A)

	Intercept (±s.e.)	**pH** (±s.e.)	**.log (Cu tot)** (±s.e.)	**log (Cu)*pH** (±s.e.)	**Log (Cmic)** (±s.e.)	**AIC**	**BIC**	**logLIK**	**R2**
Log (Mineralization / Corga) (n=128)	**-1.87*** (± 0.73)	**+0.26**** (± 0.09)	**Not selected by the step wise regression**	**Not selected by the step wise regression**	**+0.44***** (± 0.01)	324	338	-157	0.91

(B)

Log (Mineralization / Corga) (n=128)	**s**	**Not selected by the stepwise regression**
	m	**Not selected by the stepwise regression**
	w	**Not selected by the stepwise regression**

Supplementary Table III.2.5 (A) Slope and intercept (±standards errors, s.e.) between log (microbial biomass) and variables selected through stepwise analyse for the linear mixed model. (B) Shift of the intercept for log (microbial biomass) between the different groups of qualitative variable (rainfall patterns s, m, w) and the reference one (f) only calculated for the full dataset. P-values symbols are explained in the legend of supplementary Table III.2.3.

(A)

	Intercept (±s.e.)	**pH** (±s.e.)	**.log (Cu tot)** (±s.e.)	**Log (Corga)** (±s.e.)	**AIC**	**BIC**	**logLIK**	**R2**
Log (microbial biomass) (n=128)	**-1.31*** (± 0.73)	**Not selected by the step wise regression**	**-0.11**** (± 0.03)	**+0.27*** (± 0.1)	273	287	-131	0.82

(B)

Log (microbial biomass C) (n=128)	**s**	**Not selected by the stepwise regression**
	m	**Not selected by the stepwise regression**
	w	**Not selected by the stepwise regression**

Supplementary Table III.2.6 (A) Slope and intercept (±standards errors , s.e.) between log (mineralization/Corga) and variables selected through step wise analyse for the linear mixed model. B) Shift of the intercept for log (mineralization/Corga) between the different groups of qualitative variables (in situ contamination, agricultural soils, industrial soils, non-contaminated soils) and the reference one (agricultural soil) only calculated for the full dataset. P-values symbols are explained in the legend of supplementary Table III.2.3

(A)

	Intercept (±s.e.)	**pH** (±s.e.)	**.log (Cu tot)** (±s.e.)	**Log (Corga)** (±s.e.)	**AIC**	**BIC**	**logLIK**	**R2**
Log (Mineralization /Corga) for all in situ contamination cases (n=189)	**-1.99**** (± 0.63)	**-0.15°** (± 0.08)	**-0.08°** (± 0.05)	**+0.27*** (± 0.1)	507	524	-248	0.93

(B)

Log (Mineralization / Corga) (n=189)	**Ind**	**Not selected by the stepwise regression**
	Nc	**Not selected by the stepwise regression**
	Oth	**Not selected by the stepwise regression**

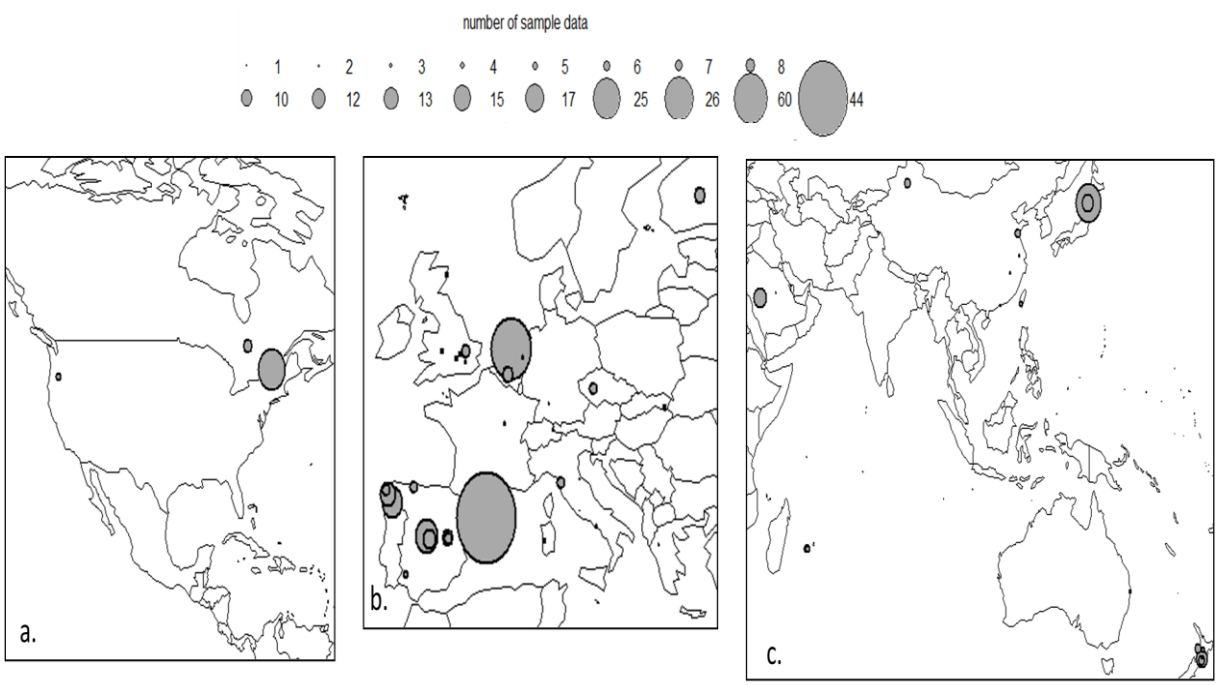

Supplementary Figure III.2.1: Repartition at an international scale of the sample site origins of the 389 data extracted from the 46 selected papers. The size of the point represent the number of data samples. a. for the North American continent, b for the European continent and c for the Asian continent.

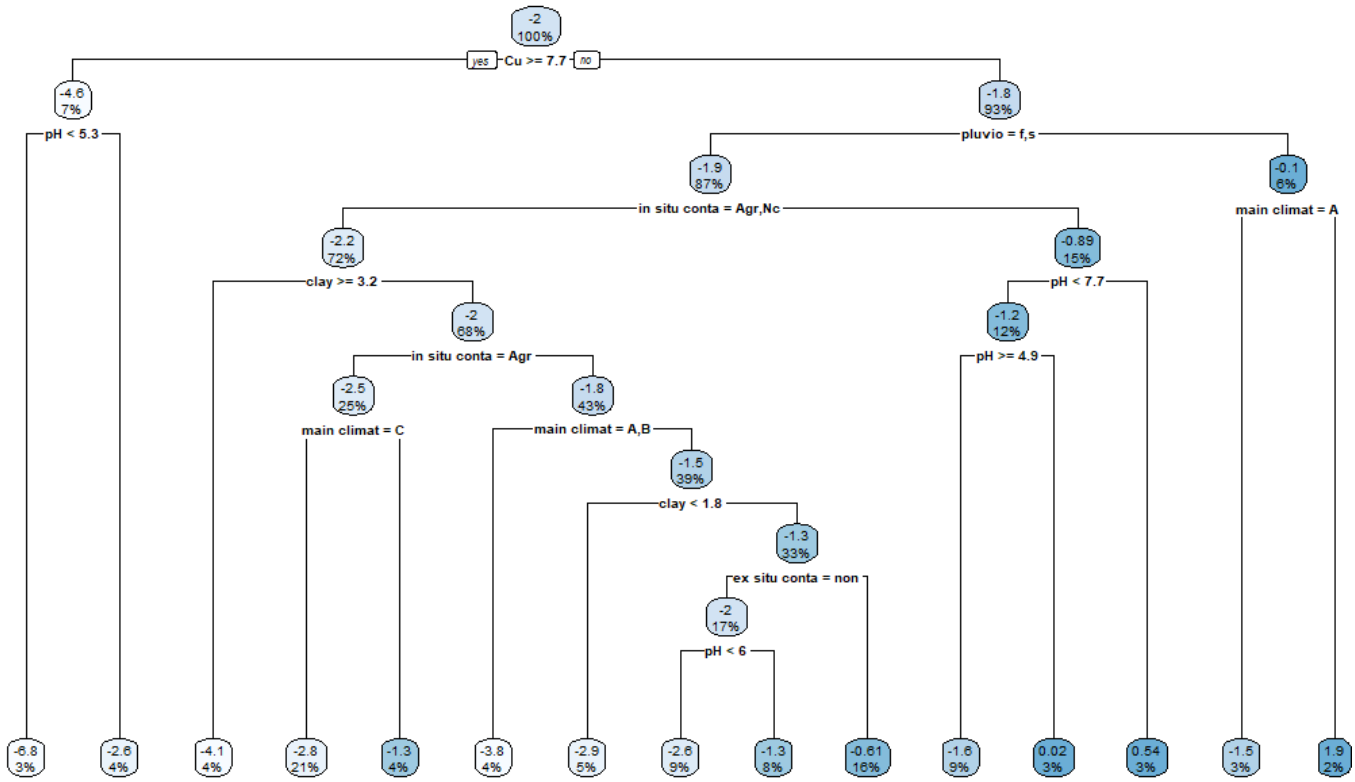

Supplementary fig IIII.2.2.: Decision tree build for the determination of main factors and thresholds values which account for the variation of Mineralization/Corga. Decision tree was build on 382 couple of data with Mineralization/Corga values. From this decision tree we can see the importance of pluviometric regime and pH in the determination of Mineralization/Corga. A major effect of highest contamination (exp(7.7)=2208mgCu.kg soil^{-1}) with decrease of Mineralization is also emphasized.

Chapitre III.3.: To what extend a soil contamination can affect greenhouse gas emissions? An attempt to calibrate a nitrification/denitrification model-

Laura Sereni[1*], Bertrand Guenet[2], Charlotte Blasi[1,3], Olivier Crouzet[1,4], Jean-Christophe Lata[5,6] Isabelle Lamy[1]

[1]Université Paris-Saclay, INRAE, AgroParisTech, UMR ECOSYS, Ecotoxicology Team, 78026, Versailles, France
[2]Laboratoire de Géologie de l'ENS, PSL Research University, CNRS, UMR 8538, IPSL, Paris, France
[3]Present address: Centre Sève, Département de Chimie, Université de Sherbrooke, Sherbrooke, QC, Canada
[4]Present address: Office national de la chasse et de la faune sauvage, Site d'Auffargis-Saint-Benoist 78612 Le-Perray-en-Yvelines, France
[5]Sorbonne Université, Université de Paris, UPEC, CNRS, INRAE, IRD, UMR 7618, Institute of Ecology and Environmental Sciences – Paris, iEES Paris, 7 quai St Bernard 75252, Paris, France
[6]Department of Geoecology and Geochemistry, Institute of Natural Resources, Tomsk Polytechnic University, 30, Lenin Street, Tomsk, 634050, Russia
*_Correspondence to_ Laura Sereni (laura.sereni@inrae.fr)
Submitted in: Biogeosciences, October 15th 2021

Abstract

Continental biogeochemical models are commonly used to prospect the effect of land use, exogenous organic matter input or climate change on soil greenhouse gas emission. However, they can still not be used to investigate the effect of soil contamination while it is known to affect several soil processes and to concern a large fraction of land surface. We implemented a commonly used model estimating soil nitrogen (N) emission, the DeNitrification DeCompostion (DNDC) model, with a function taking into account soil copper (Cu) contamination in nitrate production modulation. Then, we aimed at using this model to predict N-N_2O, N-NO_2 NOx and N-NH_4 emissions in the presence of contamination and in the context of changes in precipitations. For that, incubations of soils were performed at different soil moistures in order to mimic expected rainfall patterns during the next decades and in particular drought and excess of water. The effect of this double stress on soil nitrate production was studied using a bio-assay. Then, data of nitrate production obtained under each moisture treatment were used to parameterize the DNDC model and estimate soil N emission considering the various effect of Cu. Whatever the moisture preincubation, experimental results showed a N-NO_3 decreasing production when Cu was added but with different sharpness depending on soil moisture. The DNDC-Cu version we proposed was able to reproduce these observed Cu effects on soil nitrate concentration with r2>0.99 and RMSE<10% for all treatments in the DNDC-Cu calibration range (>40% of the water holding capacity) but showed poor performances for the dry treatments. We modelled a Cu-effect inducing an increase in N-NH_4 soil concentration and emissions due to a reduced nitrification activity, and therefore a decrease in N-NO_3, N-N_2O and N-NOx concentrations and emissions. The effect of added Cu was larger on N-N_2 and N-N_2O emissions than on the other N species and larger for the soils incubated under constant than variable moisture.

Keywords: copper, DNDC modelling, rainfall pattern, ecotoxicology, soil function

1. INTRODUCTION

The increase in atmospheric greenhouse gases [GHG] like CO_2, CH_4, or N_2O is expected to induce a global climate change with e.g. higher mean temperature or changes in precipitation patterns with projections of increased precipitations or droughts depending on regions (Knutti and Sedláček 2012). These modifications in rainfall patterns may impact soil moisture which is one of the main drivers of soil microbial activity (Moyano et al. 2013). Microbial communities ensure key activities supporting numerous ecosystem functions, such as those involved in nitrogen (N) cycle influencing N_2O emissions (Jones et al. 2014) and are at the origin of more than 80% of N_2O fluxes (IPCC 2019). In particular, nitrification/denitrification processes are largely controlled by the local (an-)oxic treatments and therefore by soil moisture, denitrification being the main source of soil N_2O emission for moist soils whereas dry soil N_2O emissions are mainly due to nitrification (Bateman and Baggs 2005). This strong dependency to local soil O_2 availability (Khalil et al. 2004), by playing on the realization of nitrification/denitrification reactions and N species diffusion (Conrad 1996; Schurgers et al. 2006), makes N soil fluxes dynamics particularly difficult to predict at larger scales. Despite this, some continental biogeochemical have shown improved predictions when N cycle is explicitly represented (Kesik et al. 2005; Butterbach-Bahl et al. 2009; Vuichard et al. 2018).

In addition to climate change, human activities introduce significant quantities of contaminants into the environment, such as trace elements (TE) which are persistent and can be toxic for soil biota (Bech et al. 1997; Giller et al. 2009). Indeed, the contamination of soils by TE has become a major concern at global scale (De Vleeschouwer et al. 2007; Khan et al. 2008) coming from atmospheric sources (Steinnes et al. 1997) or through the use of pesticides (Nicholson et al. 2003). In particular, TE contaminations are known to largely affect soil microorganisms (Giller et al. 2009) and their activities, such as nitrification/denitrification processes (Broos et al. 2007; Mertens et al. 2010). Therefore, the combined effect of climate change and of soil contamination may largely impact the emissions of NO_x and N_2O from soils (Holtan-Hartwig et al., 2002; Vásquez-Murrieta et al. 2006). However, the effect of the interactions between climate change and soil contamination on the GHG emissions is still poorly documented (Rillig et al. 2019; Zandalinas et al. 2021).

Despite recent progress, the Earth system models (ESMs) used to predict future climate change still don't take into account soil contamination effect on GHG emissions (Anav et al. 2013) whereas a large fraction of the soils are impacted by contaminants (Lado et al. 2008). Furthermore, soil biogeochemical models are often used to estimate loss or accumulation of N species (ammoniac NH_4 volatilization, nitrate NO_3 leaching - Giltrap et al. 2010) or they respective concentrations under scenarii of organic fertilizer amendments, but do not take into account the contamination which often occurs simultaneously (Wuana and Okieimen 2011). Thus, there is a growing need to provide continentals models combining ecotoxicological/contamination and climate change concerns. Among biogeochemical models DeNitrification DeCompostion (DNDC, Changsheng Li et al. 1992) is a relatively simple model handling both biogeochemistry of denitrification and microbial growth (Li et al. 2000), and on which Land Surface Model-soil N component -a part of ESMs- like ORCHIDEE are built (Vuichard et al. 2018).

For this purpose, this study combines in an innovative way experimental and modelling approaches in order to evaluate the impact of soil moisture on the sensitivity of nitrification to copper (Cu) toxicity and consequently on N-GHG emissions. Cu was chosen as a model of soil contamination due to its relevance in agricultural soils and available data in the literature. Soil incubations were run during two months by applying chosen soil moisture from drought to water saturation. Then, a bioassay estimating NO_3 production was performed under a gradient of Cu added by spiking. The experimental data were then used to calibrate a new model, DNDC-Cu, able to predict NO_x and N_2O emissions with the implementation of new functions to consider the effect of Cu concentration ([Cu]) on nitrification/denitrification processes. Our hypothesis is that the building of such a model will permit to gain in understanding on the effect of a soil [Cu] on NO_x and N_2O and NH_4 cycling in a climate change context. Hence, data are also used here to discuss on knowledge gaps in such modelling approaches, and to question the use of soil contamination data in climate change scenarios.

2. MATERIALS AND METHODS

2.1 Soil sampling

The soil was sampled in January 2017 at the surface layer (0–20 cm) of a control plot at the Qualiagro experimental site (48°87'N, 1° 97'E - https://www6.inrae.fr/valor-pro_eng/Experimental-devices/QualiAgro/QualiAgro-web-site). The soil sample was immediately wet sieved at 5mm and shortly stored at 4°C until microcosm build-up. Aliquots of this sieved soil were used to measure the initial water content in addition to the maximum water holding capacity (WHC) for the further microcosm experiments. This site is located at Feucherolles near Paris, France, and had been designed to evaluate urban compost fertility together with the monitoring of contaminant inputs (Cambier et al. 2019). Soil is a luvisol with 15% clay, 78% silt and 7% sand, a pH of 6.9, organic carbon (Corg) and total N contents at 10.5 ± 0.2 and 1.00 ± 0.03 g kg^{-1} soil, respectively, and with a CEC of 7.9 ± 0.8 $cmol^{+}$ kg^{-1} soil. This soil is not contaminated with Cu, and basal [Cu] measured by ICP-AES after HF-$HClO_4$ extraction was of 12 mg $Cu.kg^{-1}$ soil.

2.2 Experimental setup

In order to evaluate the impact of soil moisture on the sensitivity of nitrification to Cu toxicity, we carried out a two-step experiment. The first step consisted in 5 different WHC incubation during 45 days, and the second to a 3-day bioassay with spiked Cu gradient (Fig 1.).

Five microcosms were built up with about 5g of sampled soil. Three of them were set up with a constant moisture corresponding to 30%, 60% and 90% of their WHC in order to span respectively limiting, optimal, and saturating conditions for the microbial activities. These three samples will be called thereafter "30%, 60% and 90%", respectively. Their water contents were verified by weighting every two days and water added if necessary. The two other microcosms were incubated in order to simulate two kinds of drought and dry-rewetting cycles. One, thereafter called "Drought" (or DO), started with one week at 60% WHC and then the soil was left for 3 weeks without added water to

mimic a dry period until 10% of the WHC before rewetting at the initial 60% WHC. The other, thereafter called "Dry-rewetting" (or DR) encountered alternatives cycles of one-week dry period (10% of the WHC) followed by one-week near-saturation period (90% WHC). The moisture states of microcosms were performed by air-drying and controlled by weighting.

At the end of the incubation period, we performed a nitrification bioassay in triplicate using incubated soils and following an adaptation of the method proposed by Petersen et al. (2012). Soils were first spiked with a gradient of increasing Cu^{2+} in the presence of an excess of NH_4^+ and the resulting potential nitrification activity (PNA) measured. The microcosms incubated at constant moisture were kept at their moisture level (30, 60 or 90% of WHC) whereas those incubated at variable moisture were set at 60% WHC. The NO_3^-production rates were measured in soil slurries over a short-term aerobic incubation, for each Cu added concentration. Briefly, 1mL of Cu solution at different concentrations were added in soil slurries (soil solution 1:12) to reach final added [Cu] of 50, 100, 250, 500, 750,1000 and 2000 mg Cu.kg $soil^{-1}$ (final soil [Cu] of 62, 112, 262, 512, 762, 1012 and 2012 mg Cu.kg $soil^{-1}$). The pH was adjusted to 7. Then, microcosms were incubated on a rotary shaker (150rpm) under aerobic conditions at 25°C until 72h. After 0, 24 and 72h of incubation, 2 ml aliquots of 3g were transferred in Eppendorf vials and centrifuged. The supernatants were collected and stored in microplates at – 20 °C until analyses of NO_3^- and NO_2^- by colorimetric determinations, following the reduction of NO_3^- in NO_2^- by vanadium(III) and then the detection of NO_2^- by the acidic Griess reaction (Miranda et al. 2001). Finally, PNA (µg N-NO_3 g^{-1} soil h^{-1}) was calculated on the basis of N-NO_3^- + N-NO_2^- concentrations measured at different time steps. In our bioassay, [NO_2^-] were negligible and PNA was thus calculated following eq. III.3.1, by checking the linear production rate of NO_3^- between 2 h, 24 h and 72h:

(III.3.1) $$PNA = \frac{[NO_3^-]_{Tfinal} - [NO_3^-]_{Tinitial}}{Tfinal - Tinitial} \times Vs \div W$$

with Vs: Volume of solution
W: Weight of fresh soil (approximately 5 g)
T: Time of incubation.

2.3 Nitrification/denitrification model

Nitrification and denitrification processes are represented following the DNDC model proposed by Changsheng Li et al. (1992) and Li et al. (2000). In this study, we used a simplified version adapted by Zaehle and Friend (2010) initially calibrated for soil WHC >40%, that we intended here to test for 30% of WHC. This simplified version needs less boundary data but keeps a mechanistic description of the main processes. Modelled N species are expressed in amount of N, i.e. N-NH_4, N-NO_3, N-NOx and N-N_2O. To be able to represent both nitrification and denitrification processes occurring in aerobic and anaerobic sites, the soil is split into aerobic and anaerobic fractions based on an empirical relationship linking O_2 consumption to soil respiration. In aerobic microsites, nitrification takes places following eq. III.3.2:

(III.3.2) $$Nitrification = f(SWC) \times f(temp) \times f(pH) \times k_{Nit} \times (1 - anvf) \times NH_4$$

with *N-NH₄* being the stock of ammonium (in gN m^{-2}), *(1-anvf)* the aerobic fraction of the soil described thereafter in eq. III.3.21, k_{Nit} the nitrification rate (day^{-1}), *f(SWC), f(temp)* and *f(pH)* three rate modifiers representing the effect of soil water content ($m^3\ m^{-3}$), temperature (K) and pH as scalar respectively. They are described by the following equations III.3.3, III.3.4 and III.3.5:

(III.3.3) $f(SWC) = 0.0243 + 0.9975 \times SWC + 5.6358 \times SWC^2 + 17.651 \times SWC^3 + 12.904 \times SWC^4$

(III.3.4) $f(temp) = 0.0233 + 0.3094 \times temp + 0.2234 \times temp^2 + 0.1566 \times temp^3 + 0.0272 \times temp^4$

(III.3.5) $f(pH) = 1.2314 + 0.7347 \times pH + 0.0604 \times pH^2$

The $N\text{-}NH_4$ nitrified is transformed into $N\text{-}N_2O$, N-NO or $N\text{-}NO_3$ due to bacterial processes and chemonitrification following equations 6,7 and 8:

(III.3.6) $Nitrification_{N2O} = ftv \times SWC \times k_{Nitrif_{N2O}} \times Nitrification$

(III.3.7) $Nitrification_{NO} = ftv \times SWC \times k_{Nitrif_{NO}} \times Nitrification + 496950 \times e^{-1.62 \times pH} \times e^{-31494/(temp \times R)} \times Nitrification$

(III.3.8) $Nitrification_{NO3} = Nitrification - Nitrification_{NO} - Nitrification_{N2O}$

with $k_{Nitrif_{NO}}$ and $k_{Nitrif_{N2O}}$ two fixed rates (d^{-1}), *ftv* a rate modifier controlled by temperature and given in eq. III.3. 9 and *R* the ideal gas constant.

(III.3.9) $ftv = 2.72^{(34.6 - \frac{9615}{temp})}$

Then, the $N\text{-}NO_3$ produced during the nitrification process enters the denitrification module where it is reduced sequentially into $N\text{-}NO_x$, $N\text{-}N_2O$ or $N\text{-}N_2$ following eq. III.3.10 to 12:

(III.3.10) $Denitrification_{NOx} = anvf \times \left(\frac{\mu_{NO3}}{0.401} + 0.09 \times \frac{NO_3}{N_{tot}}\right) \times B$

(III.3.11) $Denitrification_{N2O} = anvf \times \left(\frac{\mu_{NOX}}{0.428} + 0.035 \times \frac{NO_X}{N_{tot}}\right) \times B$

(III.3.12) $Denitrification_{N2} = anvf \times \left(\frac{\mu_{N2O}}{0.151} + 0.079 \times \frac{N_2O}{N_{tot}}\right) \times B$

The anaerobic fraction *anvf* is described following eq. III.3.13:

(III.3.13) $anvf = 0.85 \times (1 - \frac{p\_soil_{O2}}{p\_air_{O2}})$

with p_air_{O2}, p_soil_{O2} being the partial pressure in the air and in the soil respectively. p_soil_{O2} is calculated following eq. III.3.14

(III.3.14) $\frac{\partial p\_soil_{O2}}{\partial t} = p\_soil_{O2} - \times k \times SOC \times f_{Cu}$

with *SOC* being the soil organic carbon stock (gC m^{-2}), *k* the decomposition rate, p_O2_{resp} the O_2 partial pressure related to the respiration, and f_{Cu} the effect of Cu on CO_2 emissions as define in eq. III.3.15, following (Sereni et al. 2021; eq. III.3.5):

(III.3.15) $f_{Cu\ co2} = \exp(-0.1 - 0.1 \times \log(Cu) + 0.12 \times pH)$

The relative growth rate of N-NO_3, N-NO_x and N-N_2O denitrifiers are described respectively by μ_{NO3}, μ_{NOX} , μ_{N2O} following eq. III.3.16, III.3.17 and III.3.18.

(III.3.16) $\mu_{NO3} = \frac{0.67 \times f_{denit}(temp) \times f_{denit\_NO3}(pH) \times NO_3}{NO_3 + 166}$

(III.3.17) $\mu_{NOX} = \frac{0.34 \times f_{denit}(temp) \times f_{denit\_NOX}(pH) \times NO_X}{NO_X + 166}$

(III.3.18) $\mu_{N2O} = \frac{0.34 \times f_{denit}(temp) \times f_{denit\_N2O}(pH) \times N_2O}{N_2O + 166}$

with $f_{denit}(temp)$, $f_{denit\_NO3}(pH)$, $f_{denit\_NOX}(pH)$, $f_{denit\_N2O}(pH)$ being rates modifiers depending on air temperature and soil pH described in eq. III.3.19 to III.3.22.

(III.3.19) $f_{denit}(temp) = 2^{(temp-22.5)/10}$

(III.3.20) $f_{denit\_NO3}(pH) = 1 - \frac{1}{1+e^{(4.25 \times pH)/0.5}}$

(III.3.21) $f_{denit\_NOX}(pH) = 1 - \frac{1}{1+e^{(5.25 \times pH)}}$

(III.3.22) $f_{denit\_N2O}(pH) = 1 - \frac{1}{1+e^{(6.25 \times pH)/1.5}}$

The denitrifier biomass dynamic *B* (kg m^{-2}) is described following eq. III.3.23.

(III.3.23) $\frac{\partial B}{\partial t} = (anvf \times (\mu_{NO3} + \mu_{NOX} + \mu_{N2O}) - 3.82 \times 10^{-3}) \times B$

Finally, all the gaseous forms of mineral N are emitted into the atmosphere. We wrote the adapted model in R, with a the time step of the model of 30 minutes and most of the parameters were kept to the original values of Changsheng Li et al. 1992; Li et al. 2000) except k_nit which was modified to 0.1743 instead of 0.2 to better fit the data from the control. Furthermore, the amounts of N-NH_4 fixed to the clay were reduced to 0 as the bioassay was performed in excess of N-NH_4 (see 2.2.0).

We used measures of N species at the end of preincubation period as initial values of N species for DNDC (Table III.3.1a and Fig. III.3.2.). To estimate the anaerobic volume fraction during the 3 days bio-assay, we used a C mineralization rate *k* (eq. III.3.14) determined on the basis of measurements performed on the same soil (Annabi et al. 2007) and ran DNDC for a 45 days equilibrium period. We then extracted the initial anaerobic volume fraction and partial O_2 pressure.

2.4 Statistical analysis

The dose-response curves of PNA to Cu gradient were plotted and tested with linear, quadratic or cubic functions as fitting models. Our aim was to find, if possible, a similar modelling fit function for all moisture incubation treatments. Thus, for each moisture treatment, the two best functions of fit were selected through AIC and R^2 criteria, and compared with ANOVA. After selection of a common type of functions, the permutability of the different functions parameters was tested with the Chow test (gap package which tested the regression 1 on the basis of the samples 2 and vice-versa). If the p-value exceeds its critical values, regressions cannot be considered equal (Zhao 2007)).

To estimate the effect of [Cu] and soil moisture on the different variables measured, we used nonparametric Kruskall-Wallis test. The fits between the model and the data were measured using root mean square error (RMSE, eq. III.3.24):

(III.3.24) $RMSE = \sqrt{\frac{1}{N}\sum_{i=1}^{N}(X_i - Y_i)^2}$

where *i* is the number of observations (1 to N), *X* is the predicted value and Y is the observed value. RMSE was decomposed in standard bias (eq. III.3.25), non-unity slope (eq. III.3.26) and lack of correlation (eq. III.3.27) component following Gauch et al. (2003), with $\bar{X}$ and $\bar{Y}$ the mean modelled and observed values, b the slope of the least squares regression of Y on X and r^2 the square of the correlation:

(III.3.25): $SB = (\bar{X} - \overline{Y})^2$

(III.3.26) $NU = (1 - b)^2 \times \sum \frac{x_n^2}{N}$

(III.3.27) $LC = (1 - r^2) \times \sum \frac{y_n^2}{N}$

All the analysis were done with R 3.2.3 (R Core Team, 2015).

3 RESULTS

3.1. Effect of Cu on potential nitrification activity (PNA): statistical model selection

The soil N species measured at the end of the soil pre-incubation in each soil moisture treatment were used to initialise the DNDC model (Table III.3.1). Two anomalous points leading to anomalous calculated N-NO_2 values were excluded from the experimental results because of technical problems during measurements (the C replicates in the DR and DO cases).

Table III.3.1: N species measured in the soils at the end of pre-incubation period further used to initialise the DNDC model, mean modelled N-NO_3 stocks and mean emissions of N-NH_4, N-N_2, N-N_2O, N-NOx modelled without Cu. 90 = 90 % WHC; 60= 60%WHC; DO =Dry only; DR =Dry Rewet condition during pre-incubation. A, B and C are replicates.

	Measured (µg.g soil^{-1})			Modelled (gN.m^{-2}h^{-1} for emissions, gN.m^{-2} for stocks)					
Ech	N-NH_4	N-NO_2	N-NO_3	N-NH_4 emissions	N-N_2 emissions	N-N_2O emissions	N-NOx emissions	N-NO_3 stocks	N-NO_3/N-NH_4 stocks
30_A	4.3	0.1	15.3	NA	NA	NA	NA	NA	NA
30_B	4.0	0.2	14.4						
30_C	4.5	0.2	14.3						
60_A	6.9	0.1	18.8	2.28. 10^{-10}	2.26 10^{-7}	1.3 10^{-4}	1.3. 10^{-3}	456.3	0.21
60_B	6.9	0.2	18.8						
60_C	6.7	0.2	18.7						
90_A	8.2	0.2	23.6	2.64. 10^{-11}	6.21 10^{-7}	2.7 10^{-5}	2.7 10^{-4}	509.8	0.24
90_B	12.6	0.9	24.0						
90_C	8.8	0.2	24.2						
DO_A	5.4	0.2	26.1	2.35 10^{-10}	4.3 10^{-7}	1.1 10^{-4}	1.1 10^{-3}	432.0	0.19
DO_B	5.9	0.3	29.8						
DO_C	7.4	0.9	26.4						
DR_A	3.7	0.2	28.4	2.36. 10^{-10}	3.72 10^{-7}	9.4 10^{-5}	1.1 10^{-3}	454.5	0.21
DR_B	3.4	0.2	29.8						
DR_C	5.0	0.3	29.9						

The bioassay experiments performed at the end of the soil pre-incubation allowed us to determine the rate of nitrate production as a function of soil [Cu] for each soil moisture (Fig. III.3.1). In all cases, the PNA was found to decrease with the increase in soil [Cu] but at different rates depending on the moisture treatment. Based on AIC (suppl. Table III.3.1) values, we first selected the model that better fitted the data. For 30 and 60% of WHC, a quadratic model was found to provide the better compromise between the number of parameters and the prediction capacity for incubation. For 90% WHC, no significant difference was found between the cubic and the quadratic models (ANOVA, p.v=0.07). For DR, no significant difference was found between linear and quadratic models (supplementary Tables III.3.1a and III.3.1b) whereas for DO the cubic model provided a substantially better fit than the quadratic model (AIC and adj. R2 score, suppl table III.3.1). Finally, we found that the quadratic model fitted correctly all the sets of data, allowing to be homogeneous across the moisture's incubation treatments (Fig. III.3.2b). The quadratic function was thus chosen to quantify the Cu effect on PNA also for the DO treatment.

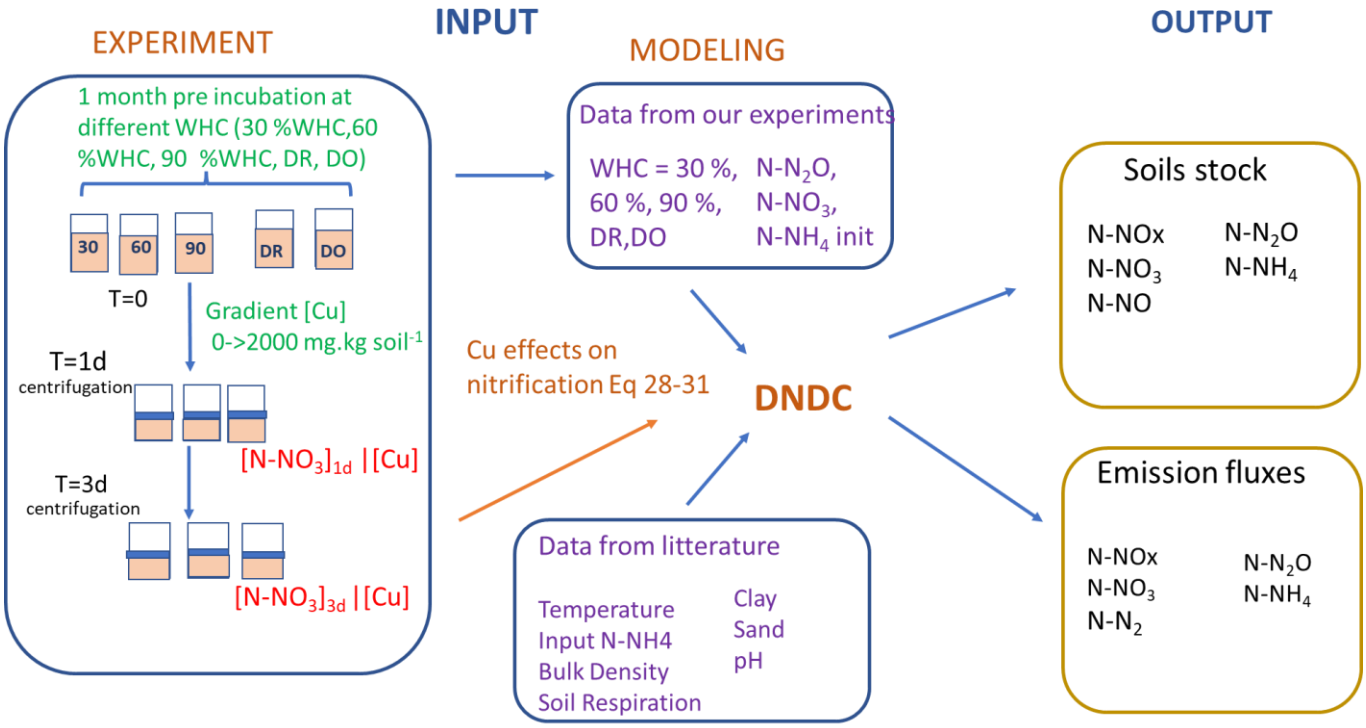

Fig. III.3.1: Schematic representation of experimental and modelling procedures. Left refers to the experimental part and center to right to the modelling part. Soils were first pre-incubated 5 weeks at different WHC. $N\text{-}NO_2$, $N\text{-}NO_3$ and $N\text{-}NH_4$ soil concentrations were then measured after this preincubation, and values were used to initialise DNDC. A bioassay was then applied on soil aliquots. Copper (Cu) was spiked at 0, 50, 100, 250, 500, 750, 1000, 2000 mg Cu.kg $soil^{-1}$ of soil to reach concentrations of 12, 62, 112, 262, 512, 762, 1012 and 2012 mg Cu.kg $soil^{-1}$ and left for incubation. After 1 and 3 days of incubation, $N\text{-}NO_3$ production was measured in the supernatant. $N\text{-}NO_3$ productions against [Cu] gradients were used to define the functions of eq. III.3.28 to III.3.31 in §3.1. Soil respiration values were extracted from the curve C_i of Fig 1 in Annabi et al. (2007).

The parameters of the 5 quadratic functions (one for each moisture treatment) were found different from each other, except between 60 and 90%WHC (p.v=0.001, Chow test). A single function was thus used to adjust PNA to soil [Cu] at 60 and 90% WHC but with different intercepts for these two WHC treatments (suppl. Table III.3.2 and Fig. III.3.2).

The final 4 quadratic equations (eq. III.3. 28 for 30%WHC, eq. III.3. 29.for 60 and 90%WHC, eq. III.3.30 for DR, and eq. III.3.31 for DO, Fig. III.3.2) were then added in the DNDC model, allowing to adjust the eq. III.3. 2 which regulates the nitrate production to soil Cu contents:

(III.3.28) $F_{Cu30} = 0.782 - 0.000451 \times Cu + 9.49 \times 10^{-8} \times Cu^2$

(III.3.29) $F_{Cu60/90} = b - 0.000342 \times Cu + 4.30 \times 10^{-8} \times Cu^2$

with b= 0.795 for 60%WHC and b= 0.0.79629 for 90 %WHC

(III.3.30) $F_{CuDR} = 0.552 - 0.000164 \times Cu + 6.09 \times 10^{-8} \times Cu^2$

(III.3.31) $F_{CuDO} = 0.625 - 0.000192 \times Cu + 2.82 \times 10^{-8} \times Cu^2$

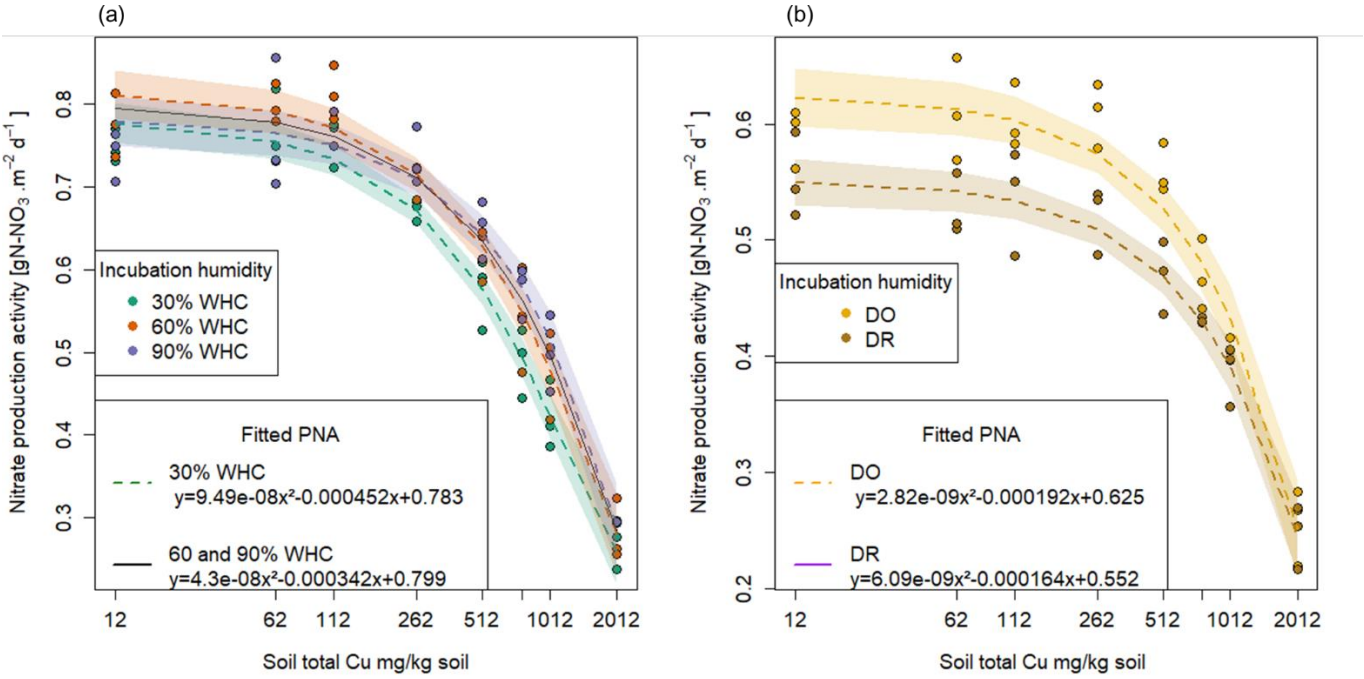

Fig. III.3.2: Fitted functions of potential nitrifying activities against soil [Cu] for each moisture incubation condition. Points are the measured nitrate production and lines the fitted quadratic function with their 95% confidence interval. (a). Constant moisture treatments: green is for 30% WHC, red for 60% WHC and purple for 90% WHC. The black line is the common fitting function used for 60 and 90% WHC incubation conditions. (b). Variable moisture treatments: brown is for Dry-rewetting (DR) and yellow for dry only (DO).

3.2. Modelling soil nitrate concentrations in Cu contaminated treatments using a DNDC-Cu model.

3.2.a. Set up of the DNDC-Cu model

The DNDC model was originally constructed to model both C and N soil cycles. The relative proportion of nitrification and denitrification processes thus depends on soil aerobic fraction determined both by soil C respiration and soil moisture (eqs. III.3.13 and III.3.14). Before any addition of Cu function in DNDC, we estimated this soil aerobic fraction, arising from C mineralisation and the aerobic fraction. Therefore, we used previous data from 366 days incubations made on the same uncontaminated soil (Annabi et al. 2007) to first fit a C mineralisation coefficient rate, k. The resulting k coefficient (k =1.234 e^{-4} $gC.m^{-2}.30min^{-1}$) was introduced in the DNDC model and forced to equilibrium (45 days) without soil Cu contamination effect. This provided us a basal aerobic volume fraction for each soil moisture through eq. III.3.13 corresponding to 0.00352 at 30%, 0.006167 at 60% (and DR/DO to which bio assays were performed at 60% WHC) and 0.02705 at 90% of the WHC and partial O_2 pressure to 211.4 hPa at 30% WHC, 210.7 hPa at 60% WHC, DR and DO and 205.4 hPa at 90% WHC. These values were then used to initiate our DNDC-Cu version. We then ran the DNDC-Cu version for a 3-day modelisation. The

constant rate of C mineralisation, k, was adjusted to take into account Cu through the eq III.3.13 and the eq III.3.28-31 adjusted N-NO_3 production rate (Fig. III.3.1) to Cu.

3.2.b. DNDC-Cu model validation

A validation of our DNDC-Cu model was made by comparing experimental data of soil measured after 1 and 3 days of incubation with model outputs. A better fit was provided for 60 and 90% of WHC which are in the range of DNDC calibration compared to 30 %WHC where the nitrate production is largely underestimated (more than twice after 3 days of incubation, Fig III.3.3.a). The regression slopes between modelled and measured soil [nitrate] for 60 and 90% WHC were respectively 0.94 and 0.91 (R2=0.99 in both cases, Fig. III.3.3a.) whereas for 30% WHC the regression slope was 1.21 (R2=0.92) (Fig. III.3.3a). For DR, the soil nitrate stocks were overestimated at 762 mgCu.kg $soil^{-1}$ soil and underestimated at 2012 mgCu.kg $soil^{-1}$ (Fig. III.3.3b) (respectively 389.7 gN.m-2 and 310.5 $gN.m^{-2}$ mean modeled nitrate against 375.3 and 290.6 $gN.m^{-2}$ mean measured nitrate) but overall modelling adequately fitted the data with a regression slope at 0.95 and R2=0.99 too.

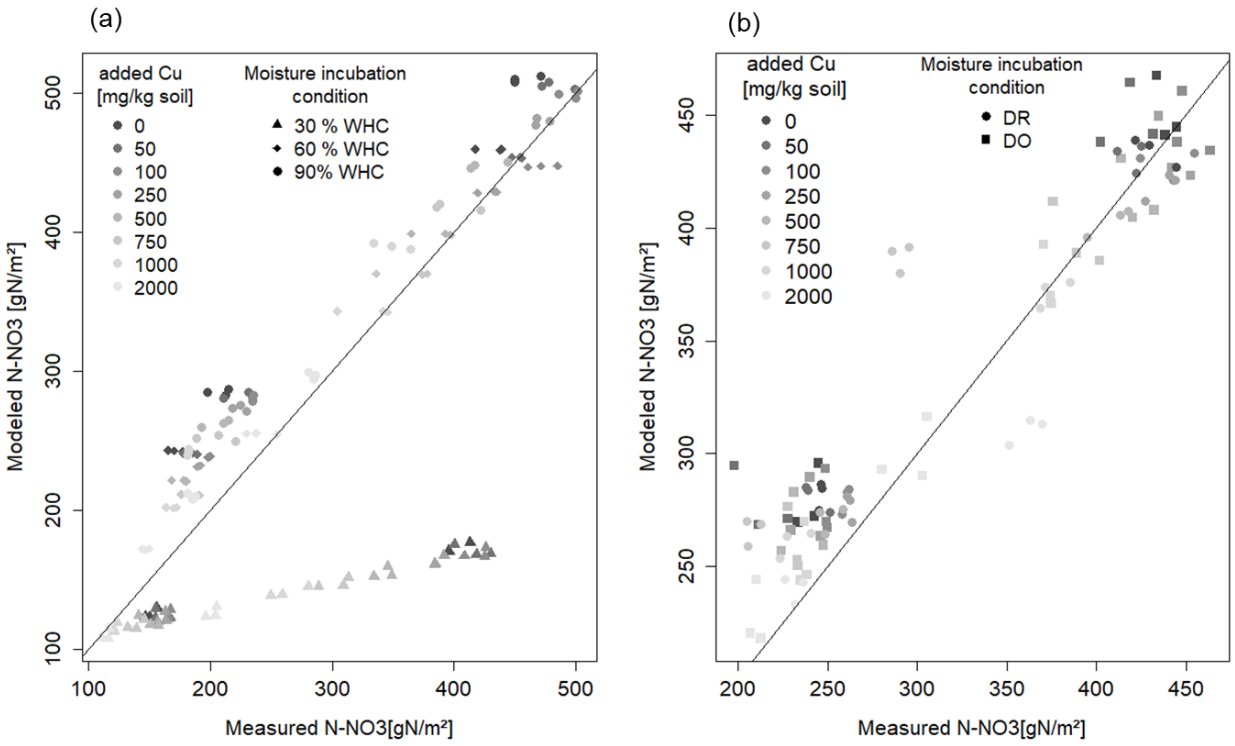

Fig III.3.3: Comparison of modeled against measured soil [nitrate] incubated in different moisture. (a) = 3 incubations under constant humidity. (b) = Dry-rewetting (DR) and Dry only (DO) conditions. For 30% WHC, Model=1.84 * Measure and R2=0.93; for 60% WHC Model=0.93 *measure. R2=0.99; for 90% WHC Model=0.90 * measure. R2=0.99 ; for Dry -rewetting (DR) model = 0.96*measure. R2=0.98; for Dry only (DO)Model=0.95*measure. R2=0.99

Considering all incubations treatments, RMSE was about 57.3 as a mean (46.4 gN-NO_3.m^{-2} standard error) for a mean soil nitrate measured at 390 gN-NO_3.m^{-2} (69 gN-NO_3.m^{-2} standard error) after 3 days of incubation. However, for the 30% WHC, RMSE was 139.9 thus 3.7 times more than for the other treatments (Suppl. Fig. III.3.1). Despite the reduction of nitrate production rate from 0.2000 to 0.1753 gN.$hour^{-1}$ (see material and methods), soil nitrate stock was still slightly overestimated in the 90% WHC as shown by the largest lack of correlation in this case compared to the 60% WHC treatment (Fig. III.3.3a, suppl. Fig. III.3.1). Lack of correlation was small for all tested moisture incubation treatments (mean $\sqrt{LC}$ = 23.0, standard error =5.4 which is roughly 1/20 of the produced nitrate in 3 days in uncontaminated treatment). Results showed that our DNDC-Cu version was able to reproduce the variability observed in Cu contaminated soils except for the 30% WHC treatment where soil nitrate stocks were largely underestimated. The following results thus focused on the use of DNDC-Cu for DR, DO, 60 and 90% of WHC treatments to predict soil N emissions.

3.3 Use of DNDC-Cu to predict N fluxes in contaminated soils.

3.3.a. Effect of soil [Cu]on soil N stocks.

The soil Cu function we included in the DNDC-Cu model modified specifically the default nitrification equation in complement to pH, soil moisture and O_2 availability (eq. III.3.2.). In the presence of low [Cu] (12-512 mgCu.kg $soil^{-1}$), the predicted N-NO_3 soil stocks were found equivalent between 60 and DO and, to a less extend, DR treatments (Suppl. Fig III.3.2). When soil [Cu] increased, soil [N-NO_3] decreased but with different rates depending on the moisture of incubations (eq. III.3.28-31). Up to 548 mgCu.kg $soil^{-1}$, we modelled the lowest N-NO_3 stocks in DR incubated soils. Above it, N-NO_3 soil stocks were the smallest for the 60% WHC treatment as a result of the sharpest decrease in N-NO_3 production due to soil [Cu]. N-NO_3 soil stock for incubation at 90% WHC were the highest for soil [Cu] below 1432 mgCu.kg $soil^{-1}$. Between 1432 and 2000 mgCu.kg $soil^{-1}$, N-NO_3 soil stocks were similar for 90% WHC, DR and DO (Suppl. Fig. III.3.2).

The decrease in the nitrification rates with the increase in soil [Cu] resulted in an increase in soil N-NH_4 stocks. Our model also predicted largest N-NH_4 stocks in the DR and DO soils than in the 60 and 90% WHC soils (Suppl. Fig.3). The variations in N-NH_4 and N-NO_3 stocks were however different across soil moistures so that at the highest [Cu], the N-NH_4 soil stocks were modelled similar between all moisture treatments whereas the N-NO_3 stocks were modelled smallest for the 60% WHC treatment. The N-NO_3/ N-NH_4 stocks ratios thus varied between soil moistures with Cu levels whereas in the absence of Cu, N-NO_3/ N-NH_4 ratios were similar among soil moisture treatments. The ratio of N-NO_3/ N-NH_4 decreased faster for 60/90% WHC than for DR/DO with an increase in soil [Cu] (suppl fig III.3.4; Table III.3.2).

Table III.3.2: Percentage of variation in soil N-NO_3 stocks, soil N-NO_3/N-NH_4 stocks, N-NH_4, N-N_2, N-NOx and N-N_2O emissions in response to soil [Cu] in the various incubation conditions for a 3-day modelisation.

a.

Moisture condition	Added Cu (mgCu.kg $soil^{-1}$)	N-NO_3 soils stocks	Emission N-NH_4	Emission N-N_2	Emission N-NOx	Emission N-N_2O	Soil stocks N-NO_3/N-NH_4
60	0	0.0	0.0	0.0	0.0	0.0	0.0
60	50	-1.3	0.3	-17.9	-3.5	-2.1	-1.5
60	100	-2.6	0.6	-24.4	-5.5	-4.1	-3.2
60	250	-6.7	1.5	-35.0	-10.5	-9.8	-8.0
60	500	-13.3	2.9	-45.6	-17.8	-19.0	-15.7
60	750	-19.5	4.3	-53.4	-24.5	-27.7	-22.8
60	1000	-25.4	5.5	-59.8	-30.6	-35.8	-29.3
60	2000	-44.5	9.7	-78.0	-50.5	-62.3	-49.4
90	0	0.0	0.0	0.0	0.0	0.0	0.0
90	50	-1.0	0.3	-16.4	-6.7	-3.1	-1.2
90	100	-2.2	0.6	-22.4	-9.4	-5.3	-2.7
90	250	-6.0	1.5	-32.3	-14.5	-11.1	-7.3
90	500	-12.1	3.0	-42.7	-20.8	-20.1	-14.7
90	750	-18.0	4.5	-50.7	-26.1	-28.4	-21.5
90	1000	-23.6	5.8	-57.4	-30.8	-36.2	-27.8
90	2000	-41.8	10.3	-76.4	-46.0	-61.6	-47.2

b.

Moisture condition	Added Cu (mgCu.kg soil^{-1})	NO_3 soil stocks	Emission NH_4	Emission N_2	Emission NOx	Emission N_2O	Stocks NO_3/NH_4
DO	0	0.0	0.0	0.0	0.0	0.0	0.0
DO	50	-0.7	0.2	-17.7	-3.2	-1.7	-0.8
DO	100	-1.5	0.3	-23.9	-4.8	-3.2	-1.8
DO	250	-3.9	0.8	-33.5	-8.4	-7.6	-4.7
DO	500	-8.1	1.7	-42.8	-13.6	-14.8	-9.6
DO	750	-12.3	2.6	-49.8	-18.4	-22.1	-14.5
DO	1000	-16.5	3.5	-55.8	-23.1	-29.3	-19.3
DO	2000	-33.3	7.0	-75.7	-41.6	-58.3	-37.7
DR	0	0.0	0.0	0.0	0.0	0.0	0.0
DR	50	-0.6	0.1	-17.6	-3.6	-1.6	-0.7
DR	100	-1.3	0.3	-23.8	-5.3	-3.1	-1.6
DR	250	-3.5	0.7	-33.3	-9.1	-7.3	-4.2
DR	500	-7.2	1.4	-42.4	-14.2	-14.3	-8.6
DR	750	-10.9	2.2	-49.1	-19.0	-21.2	-12.8
DR	1000	-14.5	2.9	-54.8	-23.5	-27.9	-16.9
DR	2000	-28.6	5.7	-73.2	-40.7	-54.1	-32.5

With the decrease in soil N-NO_3 stocks at high [Cu], we predicted a decrease in the growth of denitrifying bacteria (eq. III.3. 13). Consequently, the modelled denitrifying bacterial pool was reduced when soil [Cu] increases (Fig. III.3.4). Whatever the soil [Cu], denitrification was however modelled roughly twice larger in the soils incubated at 90% WHC than in the other treatment as this moist treatment is defined as perfect condition for denitrifying bacteria in the DNDC model (Changsheng Li et al. 1992). Soils incubated at 60% WHC were modeled with the lowest denitrifying bacterial pool. No difference between the DR and DO soils was found due to uncertainties in the modelled denitrifying bacterial pool which resulted from the different concentrations in N species used to initialize DNDC-Cu (Table III.3.1). The soil N-N_2O stocks and dissolved N-NOx being directly related to denitrifying bacteria and its followed similar trends than soil N-NO_3 stocks with a global decrease in soil stocks with an increase in soil [Cu] (table III.3.2) and larger stocks at the wetter treatment.

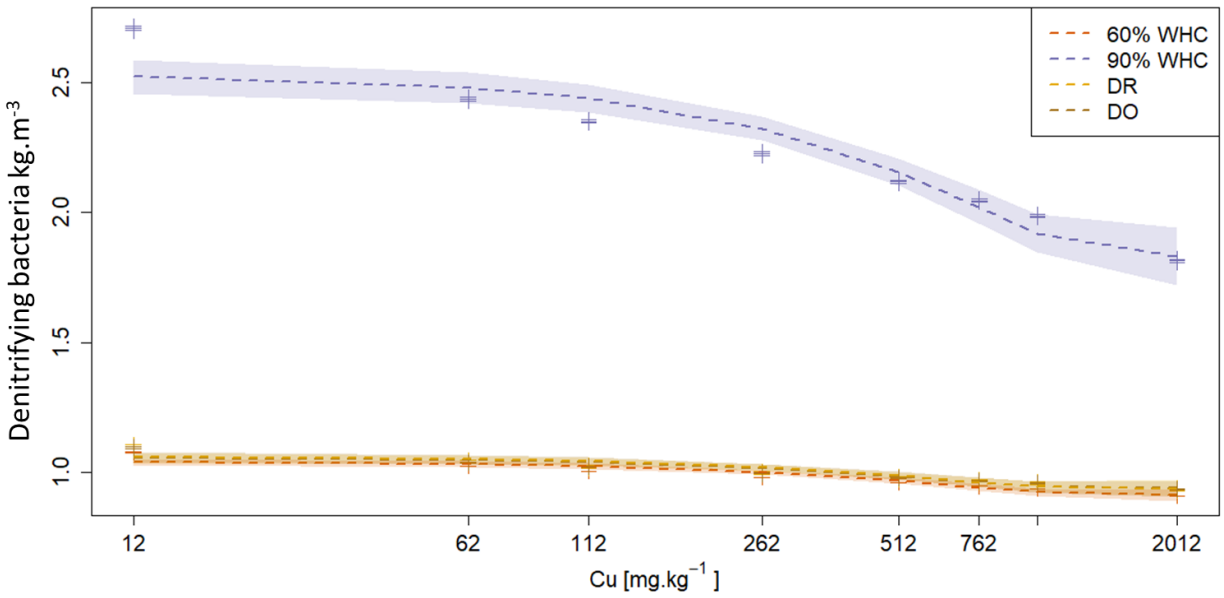

Fig III.3.4. Modelled soil denitrifying bacterial pool after 3 days ($gN.m^{-3}$ soil) for the 4 moisture treatments. Purple is for 90% WHC, red for 60% WHC, brown for dry rewetting (DR) and yellow for dry only (DO). Red, brown and yellow curves being superposed. Pools were modelled for 12, 62, 112, 262, 512, 762, 1012 and 2012 mg Cu,kg soil $^{-1}$ as represented by cross. Quadratic fits were used for representation.

3.3.b. Estimation of soil N emissions under various moistures

Large differences are predicted in the N-NH_4, N-NOx and N-N_2O fluxes between the 90% WHC soil and the 3 other soil moisture treatments (Fig. III.3.5). For instance, we modelled a decrease comparable in N-NOx emissions between DR/DO and 60-90% WHC for soil [Cu] about 112 mgCu.kg $soil^{-1}$ (2-3% respectively - Table III.3.2a and III.3.2b.) but with the increase in soil [Cu], the variation of emissions between soil moisture became larger. Hence, around 2012 mgCu.kg soil $^{-1}$ we modelled more than 50% decrease in N-NOx and 62% decrease in N-N_2O emission fluxes for soils at 60% WHC against only 40% decrease in N-NOx and 54% in N-N_2O emission for soils previously exposed to DR (Tables III.3.2a and III.3.b.). Thus, intensities of fluxes between two moisture treatments reversed with an increase in soil Cu contamination.

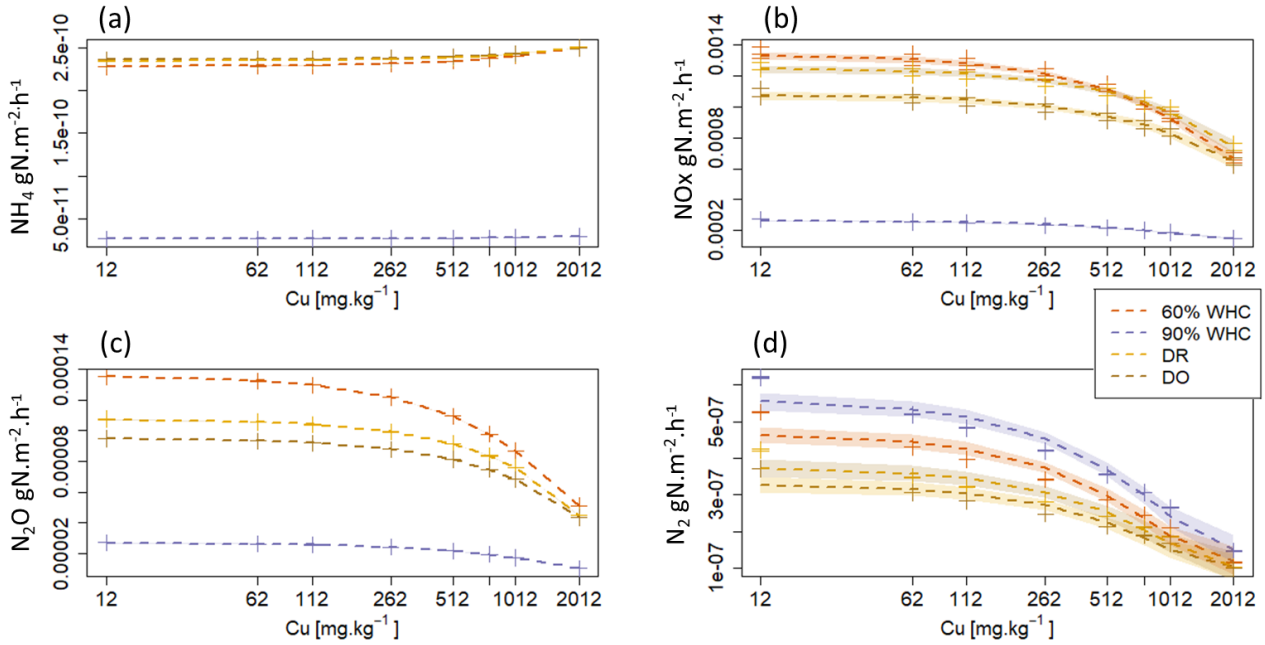

Fig III.3.5: Modelled N emission fluxes at 3 days in $gN.m^{-2}$.30min under the different moisture conditions. a.) N-NH_4 emission fluxes. b.) N-NOx emission flues c.) N-N_2O emission fluxes and d.) N-N_2 emission fluxes. Purple is for 90% WHC, red for 60% WHC, brown for dry rewetting (DR) and yellow for dry only (DO). Fluxes were modelled for 12, 62, 112, 262, 512, 762, 1012 and 2012 mg Cu.kg soil $^{-1}$ as represented by cross. Quadratic fits were used for representation.

The smallest fluxes were predicted for the wetter treatment despite higher modelled N-N_2O stocks at 90% WHC whatever [Cu]. N-NH_4 fluxes were modelled higher for the DR soils than in the 60% WHC incubated for soil Cu higher than 1774 mgCu.kg $soil^{-1}$ and smallest below. The emissions of N-NH_4 in the DO treatment were predicted to be higher than those of the DR treatment for soil Cu higher than 1290 mgCu.kg $soil^{-1}$ and smallest below (Fig. III.3.5a). In the studied range of added Cu, N-NOx fluxes predicted by the model are largest from 60%WHC to DO, DR and 90% WHC (Fig. III.3.5b.) for moderate Cu input (~ below 1380 mgCu.kg $soil^{-1}$). The decrease in N-NOx emission with the increase in soil [Cu] was however steeper for soils incubated at 60%WHC. Hence, at 2012 mgCu.kg $soil^{-1}$ N-NOx fluxes in soil incubated at 60%WHC were similar to those in the soils incubated under drought treatment (Fig. III.3.5b.)). N-N_2O fluxes had similar trends than N-NOx for moderate Cu inputs but fluxes were still largest from 60% WHC to DO, DR and 90% WHC (Fig. III.3.5.c).

The N-N_2O emissions fluxes in the presence of Cu were predicted to be 4 times smallest in the 90%WHC treatment compared to the others, whereas N-N_2 emissions were larger at this wettest treatment (Fig. III.3.5.d). The ratio of emitted N-N_2O per denitrification products (e.g N-N_2O/ N-N_2O+ N-N_2) was hence smallest in the moistest soils, which means that the largest soils N-N_2O stocks in the case of 90%WHC had more chance to be transformed rather than emitted (Fig. III.3.6).

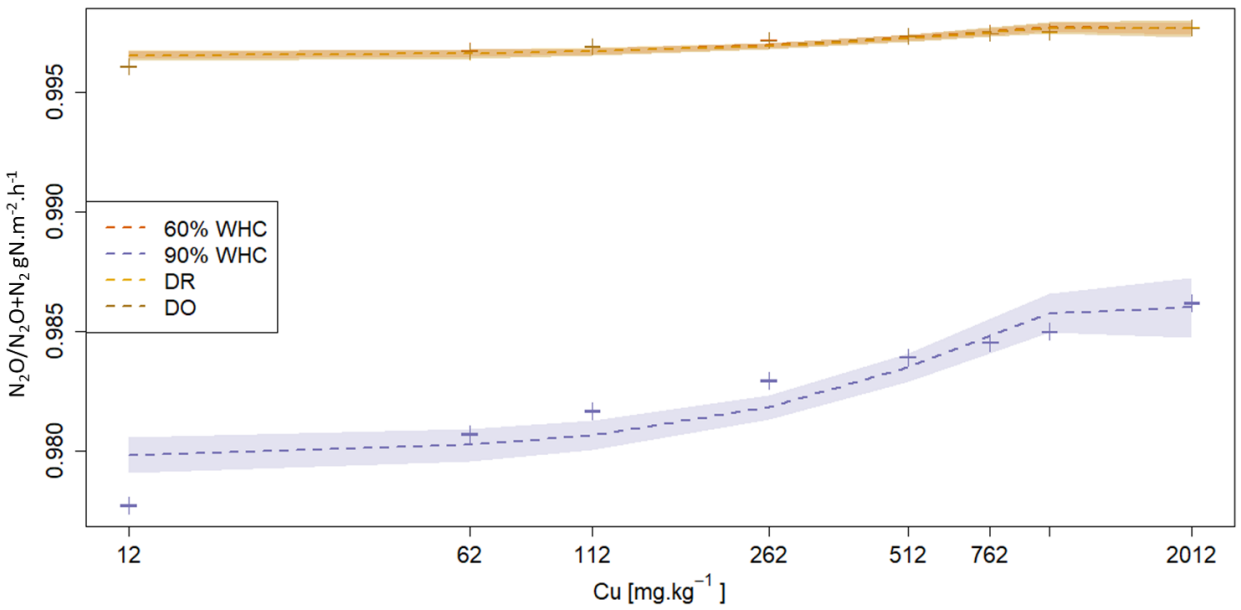

Fig. III.3.6: Proportion of N_2O emitted arising from the denitrification calculated as N_2O/N_2O+N_2 modelled fluxes in response to soil Cu concentration for the various moisture conditions. Red is for 60 % WHC, purple is for 90% WHC, yellow for the DR and brown for the DO. Red, yellow and brown curves are superposed. Fluxes were modelled for 12, 62, 112, 262, 512, 762, 1012 and 2012 mg Cu.kg soil $^{-1}$ as represented by cross. Quadratic fits were used for representation.

4 DISCUSSION

4.1. From laboratory experiment to soil N emission modelling

Thanks to our laboratory experiments, we were able to define a function modulating the soil N-NO_3 production rates in relation with soil [Cu] and depending on the soil moisture. Our results showed that soil nitrate decreases with an increase in soil [Cu].

After implementing these Cu modulating functions into the DNDC-Cu model, we were able to reproduce the observed soil nitrate stock particularly for the soils incubated at 60 and 90% of WHC. The variability around the mean due to the Cu effect was also reproduced by our DNDC-Cu version at 30% of WHC despite strong underestimation of mean soil nitrate stocks due to model moisture-limit (Changsheng Li et al. 1992). In the case of the DR and DO incubated soils, the so-called “Cu function” also accounted for the effect of drought stress. In fact, our Cu functions were defined on the basis of soil nitrate production against the whole gradient of Cu thus also considering the control without Cu. However, the (double) stress effect was also well reproduced in nitrate production.

4.2. From N-N_2O, N-N_2 and N-NOx soil stocks to emissions

In the present study, we predicted highest soil N-N_2, N-N_2O and N-NOx stocks in the moistest treatments as they are produced by the denitrifying bacteria expected to behave optimally at 90% WHC or after DR cycles (Changsheng Li et al. 1992; Homyak et al. 2017). However, N-N_2O and N-NOx emissions were modelled higher in the driest soils, whereas numerous studies (Dobbie and Smith 2003; Xiong et al. 2007; Manzoni et al. 2012) reported high measured N-N_2O emissions with high moisture. In the present version of DNDC-Cu, the soil N emissions were directly controlled by their diffusion in soil, calculated on the basis of clay and soil moisture content. The diffusion of each species would hence be 11 times smaller under 90% WHC (D_s= 0.00357) than under the 60% WHC treatment (D_s=0.0306) because the model described the diffusion as a whole and do not separated pores with or without water. Diffusion was hence slower in the water than in the air. Thus, the weighted mean diffusion was lower in the high moisture treatment. Without Cu soil nitrous stocks being roughly 1.6 times and soils N-N_2 stocks 11.1 larger under 90% WHC treatment than the other, the emission of N-N_2O were larger under driest treatment even if stocks were smaller.

Several studies also reported flushing event with dry rewetting cycles which would enhance C mineralisation, known as the Birch effect (Birch 1958; Göransson et al. 2013), hence reducing soil O_2 concentration. Moreover, soil [O_2] is closely related to the pore size distribution, being of major importance in nitrification/denitrification control (Khalil et al. 2004) with a dominating nitrification for aggregates up to 0.25cm (Kremen et al. 2005). Pore size distribution under dry/rewet events is controlled by cracking, (des)aggregation (Denef et al. 2001; Cosentino et al. 2006) or gas displacement (Kemper et al. 1985) that we weren't able to take into account in the present study. In DNDC, the calculation of denitrification rate and diffusion was based on a rough description of anaerobic zone with approximation of soil pore space distribution (Li et al. 2000; Blagodatsky et al. 2011). The soil pore space distribution approach has been demonstrated to be more generally applicable (Arah and Vinten 1995; Schurgers et al. 2006) whereas soil aggregates have been shown to control the extend of nitrification and denitrification (Kremen et al. 2005; Schlüter et al. 2018). However, if models have been proposed to take O_2 availability at the aggregate size into account in the nitrous oxide production (Leffelaar 1988; Kremen et al. 2005), they also point out the difficulty in parametrization which need a large panel of soil measurements. Moreover, they are rarely transposable at the meso-and regional scale due to high spatial variations in soil structure (Butterbach-Bahl et al. 2013). The DNDC-Cu version we used here particularly pointed out the difficulty in dealing on biogeochemistry model with physical processes, with large discrepancies between modelled soils stocks and emissions. The validation we performed focused on soil nitrates stocks and a second step to go further on would be the measure of gaseous species to ensure that emissions were also impacted by soils treatment. Moreover, we assumed here that soil [Cu] affected the C mineralisation with a decrease in soil O_2 production leading to an increase in denitrification and N-N_2O, N-NOx. Nevertheless, the present DNDC-Cu version didn't take into account the retroaction between C and N cycles. Further research would thus be required to include Cu contamination into C and N interacting cycles.

4.3. Expected ecological implications of soil Cu contamination

Based on nitrate production measurements, we modeled a decrease in denitrifying activities with an increase in soil [Cu] as a consequence of the decrease in soil nitrate stocks. However, the experiments performed here did not allow us to determine if the soil Cu contamination rather affects

nitrifying bacteria (e.g. decrease in nitrifying activity and in $N\text{-}NO_3$ production) or denitrifying bacteria (e.g. increase in denitrifying activities and $N\text{-}NO_3$ consumption). The effect of soil contamination on $N\text{-}N_2O$ production is debated because i) species involved are not clearly identified (Wrage-Mönnig et al. 2018), ii) species richness is not necessary related to soil functions (Ruyters et al. 2013) and iii) denitrifying communities could be differently sensitive than the nitrifying to soil contamination (Vásquez-Murrieta et al. 2006; Hund-Rinke and Simon 2008). Also, our modeling approach of $N\text{-}N_2O$, $N\text{-}N_2$ and N-NOx production in the contaminated context could have been more constrained with measurement of denitrification rate to assess the effect of Cu on proportion of production and consumption of $N\text{-}NO_3$

Based on our simulations, the soil Cu contamination wass expected to substantially modify the proportion of available N in soils with the increase in $N\text{-}NH_4$ stock at the expense of $N\text{-}NO_3$. $N\text{-}NH_4$ accumulation and the large expected decrease in $N\text{-}NO_3/N\text{-}NH_4$ ratio in contaminated soils (around 50% for the 60% WHC) may lead to shift in plant community structures with different preferences in N assimilation (Peacock et al. 2001; Cui and Song 2007). Therefore, Cu stress could not only have implications in microbial community patterns as a stressor, but could also induce further shifts due to N species redistributions in soils.

4.4. Climate change could substantially modify contaminated soil N emission

It is well known that climate change and rainfall patterns could substantially modify the soil N balance and its GHG emissions (Galloway et al. 2003, 2008; Butterbach-Bahl et al. 2013). Our results showed that increased Cu contamination as well might affect soil N emissions with smallest emissions of N-NOx and $N\text{-}N_2O$. These two gases are of major importance in GHG mitigation with a warming potential per mass 300 and 40 times greater than CO_2, respectively. Agricultural soils being the dominating source of $N\text{-}N_2O$ (Beauchamp 1997; Signor and Cerri 2013), even a limited decrease in their emissions could have major implication for climate. Based on our modelling, the join effect of soil moisture and [Cu] wass particularly important with larger differences in $N\text{-}N_2O$ and N-NOx emissions between rainfall patterns at high [Cu] (3.3.b.). We (Sereni et al. in press) previously/also showed that soil Cu contamination differently affect soils nitrification depending of primary soil moisture stress. Here we showed that the $N\text{-}N_2O$ and N-NOx emission variations are significantly more sensitive to the combined effect of Cu and precipitation regime than the nitrate stock. Based on these results, soil Cu inputs on moistest soils would lead to a largest decrease in soil $N\text{-}N_2O$ and N-NOx emission compared to that on driest soils, and even more than on soils submitted to abrupt and intense shifts in rainfall patterns as the DR and DO soils.

5. CONCLUSION

In the present study, we aimed at combining ecotoxicological experiments and biogeochemical modelling focusing on the effect of soil Cu contamination on soil N emission under different soil moisture treatments. Based on a 3-day bioassay measuring soil $N\text{-}NO_3$ over time, we were able to adjust the DNDC model to take into account the Cu effect on soil N emission. Experiments were performed under different moisture treatments to create a DNDC-Cu model taking account the effect of an exposure to a constant moisture (30, 60 or 90%WHC) or to a single long drought period (DO) or

several dry rewetting cycle (DR). The DNDC-Cu version we proposed was able to reproduce the observed Cu effect on soil nitrate stock with r2>0.99 and RMSE<10% for all treatments in the DNDC calibration range (>40%WHC).

We modelled a Cu effect inducing a decrease in denitrifying bacterial pool leading to an increase in $N\text{-}NH_4$ soil stocks at the expense of $N\text{-}NO_3$, $N\text{-}N_2O$ and N-NOx stocks. Emissions of $N\text{-}NH_4$ were expected to slightly increase with soil Cu contamination whereas those of $N\text{-}N_2O$ and N-NOx are expected to decrease. We also showed that the effect of soil Cu contamination was different among moisture treatment and N species. In fact, we modelled that the largest [Cu] (2012mg Cu.kg $soil^{-1}$) provoked a decrease in soil nitrate stocks from -28% in the DR case to -44% in the 60%WHC whereas $N\text{-}N_2O$ emission were expected to decrease up to 63% in the 90% WHC (-62% in the 60%WHC case, -54% in the DO case). Our results tended to show that the amount of $N\text{-}N_2O$ emitted from denitrification would decrease with an increase in soil [Cu] and from 60% WHC to DR, DO and 90% WHC, so that less $N\text{-}N_2O$ produced would be converted to $N\text{-}N_2$. This result points out two main difficulties in biogeochemical modelling: i) the difficulty to take into account hydrological dynamics (produced $N\text{-}NO_3$ and $N\text{-}NH_4$ could be expected to leach) and soil structures at different spatial scale (denitrification is estimated based on rough estimation on anaerobic soil volume which also controlled emissions rates through diffusion processes) and ii) linking soil function to microbial dynamics, in particular in this case were only the $N\text{-}NO_3$ stock was measured (without dealing between production and consumption for instance). Despite these two main points of uncertainty, the combination of incubations and of modelisation we conducted here emphasize the need to account for soil contamination when dealing with soil GHG emission modelling and climate change, as both contamination and rainfall patterns affect in a different way the soil N-NOx and $N\text{-}N_2O$ emissions.

Acknowledgments:

Parts of this study were financially supported by the French National Research Agency ANR CESA-13-0016-01 through the CEMABS project and the Labex BASC through the Connexion project. LS thanks the Ecole Normale Supérieure (ENS) for funding her PhD. The authors thank Amélie Trouvé for her help in soil data analysis, Sébastien Breuil for soil processing and Christelle Marrauld for bioassay design.

References :

Anav a., Friedlingstein P, Kidston M, et al (2013) Evaluating the Land and Ocean Components of the Global Carbon Cycle in the Cmip5 Earth System Models. J Clim 130401082723008. https://doi.org/10.1175/JCLI-D-12-00417.1

Annabi M, Houot S, Francou C, et al (2007) Soil Aggregate Stability Improvement with Urban Composts of Different Maturities. Soil Sci Soc Am J 71:413–423. https://doi.org/10.2136/sssaj2006.0161

Arah Jrm, Vinten Aja (1995) Simplified Models Of Anoxia And Denitrification In Aggregated And Simple-Structured Soils. Eur J Soil Sci. Https://Doi.Org/10.1111/J.1365-2389.1995.Tb01347.X

Bateman EJ, Baggs EM (2005) Contributions of nitrification and denitrification to N2O emissions from soils at different water-filled pore space. Biol Fertil Soils 41:379–388. https://doi.org/10.1007/s00374-005-0858-3

Beauchamp EG (1997) Nitrous oxide emission from agricultural soils. In: Canadian Journal of Soil

Science

Bech J, Poschenrieder C, Llugany M, et al (1997) Arsenic and heavy metal contamination of soil and vegetation around a copper mine in Northern Peru. Sci Total Environ. https://doi.org/10.1016/S0048-9697(97)00136-8

Birch HF (1958) The effect of soil drying on humus decomposition and nitrogen availability. Plant Soil. https://doi.org/10.1007/BF01343734

Blagodatsky S, Grote R, Kiese R, et al (2011) Modelling of microbial carbon and nitrogen turnover in soil with special emphasis on N-trace gases emission

Broos K, Warne MSJ, Heemsbergen DA, et al (2007) Soil factors controlling the toxicity of copper and zinc to microbial processes in Australian soils. Environ Toxicol Chem 26:583–590. https://doi.org/10.1897/06-302R.1

Butterbach-Bahl K, Baggs EM, Dannenmann M, et al (2013) Nitrous oxide emissions from soils: How well do we understand the processes and their controls? Philos Trans R Soc B Biol Sci 368:. https://doi.org/10.1098/rstb.2013.0122

Butterbach-Bahl K, Kahl M, Mykhayliv L, et al (2009) A European-wide inventory of soil NO emissions using the biogeochemical models DNDC/Forest-DNDC. Atmos Environ 43:1392–1402. https://doi.org/10.1016/j.atmosenv.2008.02.008

Cambier P, Michaud A, Paradelo R, et al (2019) Trace metal availability in soil horizons amended with various urban waste composts during 17 years – Monitoring and modelling. Sci Total Environ 651:2961–2974. https://doi.org/10.1016/j.scitotenv.2018.10.013

Changsheng Li, Frolking S, Frolking TA (1992) A model of nitrous oxide evolution from soil driven by rainfall events: 1. Model structure and sensitivity. J Geophys Res. https://doi.org/10.1029/92jd00509

Conrad R (1996) Soil microorganisms as controllers of atmospheric trace gases (H2, CO, CH4, OCS, N2O, and NO). Microbiol. Rev.

Cosentino D, Chenu C, Le Bissonnais Y (2006) Aggregate stability and microbial community dynamics under drying-wetting cycles in a silt loam soil. Soil Biol Biochem. https://doi.org/10.1016/j.soilbio.2005.12.022

Cui X, Song J (2007) Soil NH4+/NO3- nitrogen characteristics in primary forests and the adaptability of some coniferous species. Front. For. China

De Vleeschouwer F, Gérard L, Goormaghtigh C, et al (2007) Atmospheric lead and heavy metal pollution records from a Belgian peat bog spanning the last two millenia: Human impact on a regional to global scale. Sci Total Environ. https://doi.org/10.1016/j.scitotenv.2007.02.017

Denef K, Six J, Bossuyt H, et al (2001) Influence of dry-wet cycles on the interrelationship between aggregate, particulate organic matter, and microbial community dynamics. Soil Biol Biochem. https://doi.org/10.1016/S0038-0717(01)00076-1

Dobbie KE, Smith KA (2003) Nitrous oxide emission factors for agricultural soils in Great Britain: The impact of soil water-filled pore space and other controlling variables. Glob Chang Biol 9:204–218. https://doi.org/10.1046/j.1365-2486.2003.00563.x

Galloway Jn, Aber Jd, Erisman Jw, Et Al (2003) The Nitrogen Cascade. Bioscience 53:341. Https://Doi.Org/10.1641/0006-3568(2003)053[0341:Tnc]2.0.Co;2

Galloway JN, Townsend AR, Erisman JW, et al (2008) Transformation of the nitrogen cycle: Recent

trends, questions, and potential solutions. Science (80-.).

Gauch HG, Hwang JTG, Fick GW (2003) Model Evaluation by Comparison of Model-Based Predictions and Measured Values. In: Agronomy Journal

Giller KE, Witter E, McGrath SP (2009) Heavy metals and soil microbes. Soil Biol Biochem. https://doi.org/10.1016/j.soilbio.2009.04.026

Giltrap DL, Li C, Saggar S (2010) DNDC: A process-based model of greenhouse gas fluxes from agricultural soils. Agric Ecosyst Environ 136:292–300. https://doi.org/10.1016/j.agee.2009.06.014

Göransson H, Godbold DL, Jones DL, Rousk J (2013) Bacterial growth and respiration responses upon rewetting dry forest soils: Impact of drought-legacy. Soil Biol Biochem. https://doi.org/10.1016/j.soilbio.2012.08.031

Homyak PM, Allison SD, Huxman TE, et al (2017) Effects of Drought Manipulation on Soil Nitrogen Cycling: A Meta-Analysis. J Geophys Res Biogeosciences 122:3260–3272. https://doi.org/10.1002/2017JG004146

Hund-Rinke K, Simon M (2008) Bioavailability assessment of contaminants in soils via respiration and nitrification tests. Environ Pollut 153:468–475. https://doi.org/10.1016/j.envpol.2007.08.003

IPCC (2019) IPCC Special Report on Climage Change and Land: Chapter 4: Land Degradation. 1–112

Jones CM, Spor A, Brennan FP, et al (2014) Recently identified microbial guild mediates soil N2O sink capacity. Nat Clim Chang 4:801–805. https://doi.org/10.1038/nclimate2301

Kemper WD, Rosenau R, Nelson S (1985) Gas Displacement and Aggregate Stability of Soils. Soil Sci Soc Am J. https://doi.org/10.2136/sssaj1985.03615995004900010004x

Kesik M, Ambus P, Baritz R, et al (2005) Inventories of N2O and NO emissions from European forest soils. Biogeosciences. https://doi.org/10.5194/bg-2-353-2005

Khalil K, Mary B, Renault P (2004) Nitrous oxide production by nitrification and denitrification in soil aggregates as affected by O2 concentration. Soil Biol Biochem. https://doi.org/10.1016/j.soilbio.2004.01.004

Khan S, Cao Q, Zheng YM, et al (2008) Health risks of heavy metals in contaminated soils and food crops irrigated with wastewater in Beijing, China. Environ Pollut. https://doi.org/10.1016/j.envpol.2007.06.056

Knutti R, Sedláček J (2012) Robustness and uncertainties in the new CMIP5 climate model projections. Nat Clim Chang 3:369–373. https://doi.org/10.1038/nclimate1716

Kremen A, Bear J, Shavit U, Shaviv A (2005) Model demonstrating the potential for coupled nitrification denitrification in soil aggregates. Environ Sci Technol 39:4180–4188. https://doi.org/10.1021/es048304z

Lado LR, Hengl T, Reuter HI (2008) Heavy metals in European soils: A geostatistical analysis of the FOREGS Geochemical database. Geoderma 148:189–199. https://doi.org/10.1016/j.geoderma.2008.09.020

Leffelaar PA (1988) Dynamics of partial anaerobiosis, denitrification, and water in a soil aggregate: Simulation. Soil Sci 146:427–444. https://doi.org/10.1097/00010694-198812000-00004

Li C, Aber J, Stange F, et al (2000) A process-oriented model of N2O and NO emissions from forest soils: 1. Model development. J Geophys Res Atmos 105:4369–4384. https://doi.org/10.1029/1999JD900949

Manzoni S, Schimel JP, Porporato A (2012) Responses of soil microbial communities to water stress: Results from a meta-analysis. Ecology 93:930–938. https://doi.org/10.1890/11-0026.1

Mertens J, Wakelin SA, Broos K, et al (2010) Extent of copper tolerance and consequences for functional stability of the ammonia-oxidizing community in long-term copper-contaminated Soils. Environ Toxicol Chem 29:27–37. https://doi.org/10.1002/etc.16

Miranda KM, Espey MG, Wink DA (2001) A rapid, simple spectrophotometric method for simultaneous detection of nitrate and nitrite. Nitric Oxide - Biol Chem 5:62–71. https://doi.org/10.1006/niox.2000.0319

Moyano FE, Manzoni S, Chenu C (2013) Responses of soil heterotrophic respiration to moisture availability: An exploration of processes and models. Soil Biol Biochem 59:72–85. https://doi.org/10.1016/j.soilbio.2013.01.002

Nicholson FA, Smith SR, Alloway BJ, et al (2003) An inventory of heavy metals inputs to agricultural soils in England and Wales. Sci Total Environ 311:205–219. https://doi.org/10.1016/S0048-9697(03)00139-6

Peacock AD, Mullen MD, Ringelberg DB, et al (2001) Soil microbial community responses to dairy manure or ammonium nitrate applications. Soil Biol Biochem. https://doi.org/10.1016/S0038-0717(01)00004-9

Petersen DG, Blazewicz SJ, Firestone M, et al (2012) Abundance of microbial genes associated with nitrogen cycling as indices of biogeochemical process rates across a vegetation gradient in Alaska. Environ Microbiol 14:993–1008. https://doi.org/10.1111/j.1462-2920.2011.02679.x

Rillig MC, Ryo M, Lehmann A, et al (2019) The role of multiple global change factors in driving soil functions and microbial biodiversity. Science (80-) 366:886–890. https://doi.org/10.1126/science.aay2832

Ruyters S, Springael D, Smolders E (2013) Recovery of Soil Ammonia Oxidation After Long-Term Zinc Exposure Is Not Related to the Richness of the Bacterial Nitrifying Community. Microb Ecol 66:312–321. https://doi.org/10.1007/s00248-013-0210-7

Schlüter S, Henjes S, Zawallich J, et al (2018) Denitrification in soil aggregate analogues-effect of aggregate size and oxygen diffusion. Front Environ Sci. https://doi.org/10.3389/fenvs.2018.00017

Schurgers G, Dörsch P, Bakken L, et al (2006) Modelling soil anaerobiosis from water retention characteristics and soil respiration. Soil Biol Biochem 38:2637–2644. https://doi.org/10.1016/j.soilbio.2006.04.016

Sereni L, Guenet B, Lamy I (2021) Does Copper Contamination Affect Soil CO2 Emissions? A Literature Review. Front Environ Sci 9:29. https://doi.org/10.3389/fenvs.2021.585677

Signor D, Cerri CEP (2013) Nitrous oxide emissions in agricultural soils: a review. Pesqui Agropecuária Trop. https://doi.org/10.1590/s1983-40632013000300014

Steinnes E, Allen RO, Petersen HM, et al (1997) Evidence of large scale heavy-metal contamination of natural surface soils in Norway from long-range atmospheric transport. Sci Total Environ 205:255–266. https://doi.org/10.1016/S0048-9697(97)00209-X

Vásquez-Murrieta MS, Cruz-Mondragón C, Trujillo-Tapia N, et al (2006) Nitrous oxide production of heavy metal contaminated soil. Soil Biol Biochem. https://doi.org/10.1016/j.soilbio.2005.08.007

Vuichard N, Messina P, Luyssaert S, et al (2018) Accounting for Carbon and Nitrogen interactions in the Global Terrestrial Ecosystem Model ORCHIDEE (trunk version, rev 4999): multi-scale

evaluation of gross primary production. Geosci Model Dev Discuss. https://doi.org/10.5194/gmd-2018-261

Wrage-Mönnig N, Horn MA, Well R, et al (2018) The role of nitrifier denitrification in the production of nitrous oxide revisited. Soil Biol Biochem 123:A3–A16. https://doi.org/10.1016/j.soilbio.2018.03.020

Wuana RA, Okieimen FE (2011) Heavy Metals in Contaminated Soils: A Review of Sources, Chemistry, Risks and Best Available Strategies for Remediation. ISRN Ecol 2011:1–20. https://doi.org/10.5402/2011/402647

XIONG Z-Q, XING G-X, ZHU Z-L (2007) Nitrous Oxide and Methane Emissions as Affected by Water, Soil and Nitrogen. Pedosphere 17:146–155. https://doi.org/10.1016/s1002-0160(07)60020-4

Zaehle S, Friend A (2010) Carbon and nitrogen cycle dynamics in the O-CN land surface model: 1. Model description, site-scale evaluation, and sensitivity to parameter estimates. Global Biogeochem Cycles 24:. https://doi.org/10.1029/2009GB003521

Zandalinas SI, Fritschi FB, Mittler R (2021) Global Warming, Climate Change, and Environmental Pollution: Recipe for a Multifactorial Stress Combination Disaster. Trends Plant Sci xx:1–12. https://doi.org/10.1016/j.tplants.2021.02.011

Zechmeister-Boltenstern S, Schaufler G, Kitzler B (2007) NO, NO2, N2O, CO2 and CH4 fluxes from soils under different land use: temperature sensitivity and effects of soil moisture. Geophys Res Abstr

Zhao JH (2007) Gap: Genetic analysis package. J Stat Softw. https://doi.org/10.18637/jss.v023.i08

Suppl. Table III.3.1a Adjusted rsquared and AIC (Awaike Criteria information) values for linear, quadratic and cubic regression of PNA against added Cu during incubation for the various moisture condition. 30, 60 and 90 are for 30,60 and 90% WHC, DR for dry rewet and DO for dry only

Linear		Quadratic		Cubic		mositure
Adj.R2	AIC	Adj.R2	AIC	Adj.R2	AIC	
0.9206	-71.4824	**0.9655**	**-90.6062**	0.9645	-89.0669	30
0.9271	-72.9706	**0.9476**	**-79.9895**	0.9452	-78.0966	60
0.9348	-80.4546	0.9339	-79.2689	**0.9409**	**-81.1044**	90
0.9303	**-101.5814**	0.9276	-99.7848	0.9253	-98.1974	DR
0.9238	-89.7099	0.9202	-87.7364	**0.9514**	**-98.8169**	DO

Suppl. Table III.3.1b: p.value of ANOVA between models providing the lowest AIC (table 1a. in bold) for each moisture condition. 30, 60 and 90 are for 30, 60 and 90% WHC, DR for dry rewet and DO for dry only. For DO incubation we compare quadratic to cubic and quadratic to linear because in all other cases quadratic model were selected.

moisture condition	ANOVA	
	Compared models	p.value
30	Quadratique |cubic	0.541
60	Quadratique |cubic	0.768
90	Quadratique |cubic	0.077
DR	Linear|quadratic	0.6767
DO	Cubic|quadratic *	0.001

Suppl. table III.3.2: Fitted function for PNA evolution against soil Cu contamination. Results are given for the equations in the form of PNA =c+bCu+aCu^2 with the estimated values of a. b. c and their associated standard errors for all moisture conditions as well as adjusted r squared. The "60_90" condition represents the single model fitted both conditions further used in the DNDC chosen model.

Moisture condition	c	Std_error_c	b	Std_error_b	a	Std_error_a	Adj_r2
30	0.777	1.14E-02	-4.49E-04	3.53E-05	9.49E-08	1.74E-08	0.97
60	0.811	1.42E-02	-4.00E-04	4.40E-05	6.73E-08	2.17E-08	0.95
90	0.779	1.44E-02	-2.82E-04	4.47E-05	1.88E-08	2.21E-08	0.93
	0.795	1.21E-02	-3.41E-04	3.21E-05	4.30E-08	1.59E-08	
	Intercept shift for 90% WHC compared to 60% WHC		Std Error for intercept shift for 90% WHC compared to 60% WHC		Pv of intercept shift for 90% WHC compared to 60%WHC		
60_90	1.29 E-03		1.23 E-2		0.99		0.94
DR	0.550	9.41E-03	-1.64E-04	2.91E-05	6.09E-09	1.44E-08	0.93
DO	0.623	1.21E-02	-1.92E-04	3.75E-05	2.82E-09	1.85E-08	0.92

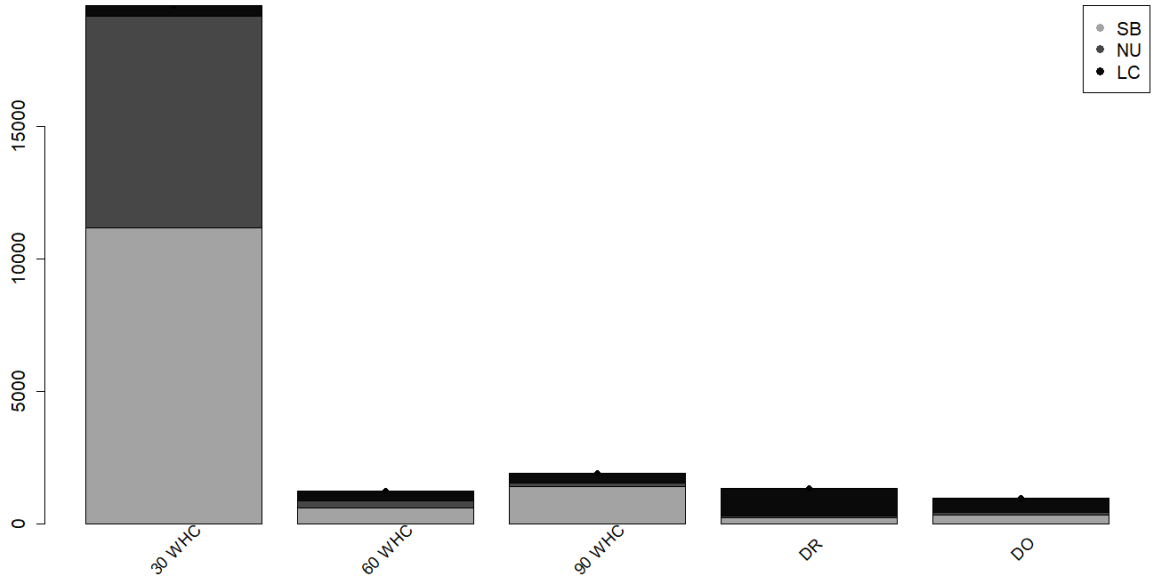

Suppl. Fig. III.3.1: Mean Standard deviation decomposition in standard bias (SB). Non-Unity slope (NU) and Lack of Correlation (LC) components for the comparison of soils N-NO_3 modelled and measured. Results are shown for the different moisture incubations conditions (30, 60 and 90% WHC, DR for dry rewet, DO for dry only)

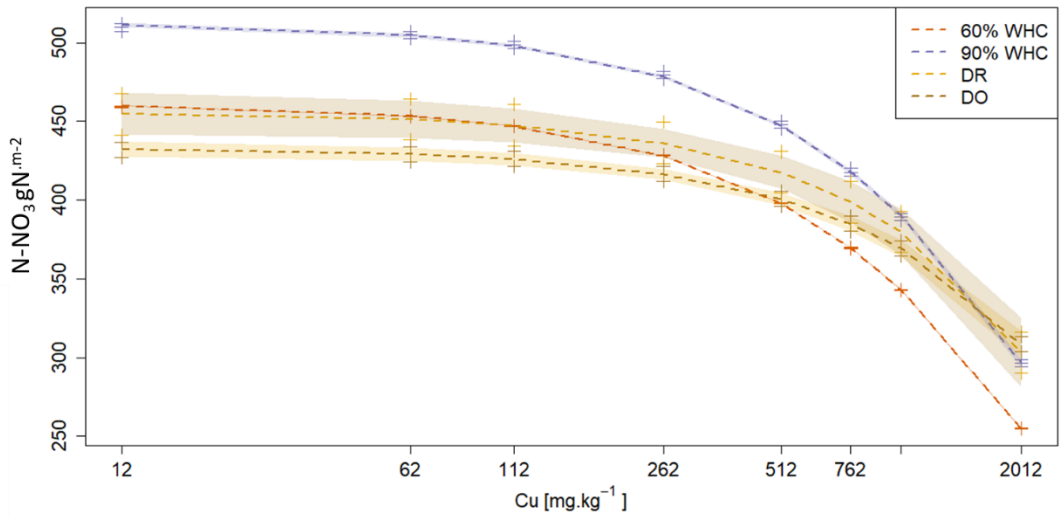

Suppl. Fig. III.3.2: Predicted soil N-NO_3 stocks (gN.m^{-2}) modelled after 3 days in the 4 tested soil moisture conditions. Purple is for 90% WHC, red for 60% WHC, brown for dry-rewetting (DR) and yellow for dry only (DO). Stocks were modelled for 12, 62, 112, 262, 512, 762, 1012 and 2012 mg Cu.kg soil $^{-1}$ as represented by cross and quadratic fit was used for representation.

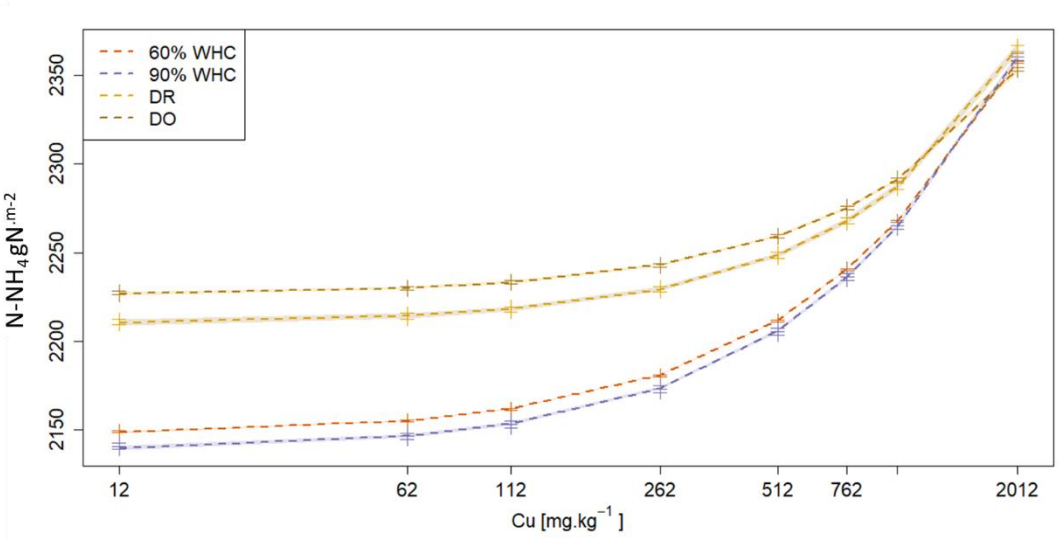

Suppl. Fig. III.3.3.: Soil N-NH4 stocks (gN.m^{-2}) modelled after 3 days in the 4 tested soil moisture conditions. Purple is for 90% WHC, red for 60% WHC, yellow for dry-rewetting (DR) and brown for dry only (DO). Stocks were modelled for 12, 62, 112, 262, 512, 762, 1012 and 2012 mg Cu.kg soil $^{-1}$ as represented by cross and quadratic fits were used for representation.

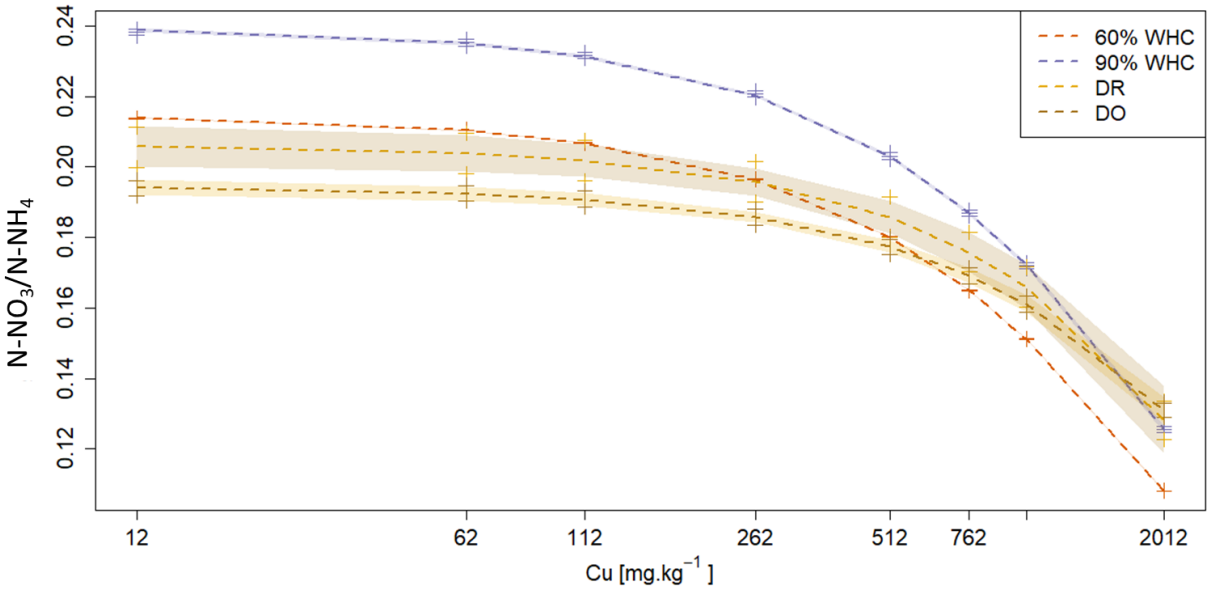

Suppl. Fig. III.3.4: $N\text{-}NO_3/N\text{-}NH_4$ soils concentration modeled after 3 days for the different moisture condition. Red is for 60 % WHC, purple is for 90% WHC, yellow for thedry-rewetting (DR) and brown for dry only (DO). Red, yellow and brown curves are superposed. Soils stocks were modelled for 12, 62, 112, 262, 512, 762, 1012 and 2012 mg Cu.kg soil $^{-1}$ as represented by cross. Quadratic fits were used for representation.

Conclusion et discussion générales :

Les deux objectifs principaux de la thèse étaient d'identifier les effets du changement climatique sur la contamination au Cu d'un sol et de définir des fonctions réponses entre cette contamination et la respiration hétérotrophe et entre cette contamination et la nitrification/dénitrification.

La contamination au Cu concerne de grandes surfaces de l'Europe et nous avons pu montrer que les différentes formes de Cu (disponible, sous forme de Cu en solution et biodisponible sous forme de Cu libre) n'étaient pas localisées aux mêmes endroits suggérant que les risques ne peuvent être déduits simplement des teneurs totales. Nos résultats suggèrent également que le changement climatique et les variations abruptes de précipitations peuvent affecter la partition du Cu entre les différentes phases du sol. En effet, d'une part de plus fortes précipitations sont attendues dans certaines zones où une grande proportion du Cu est susceptible de passer dans la solution du sol, de sorte que du Cu peut être exporté. D'autre part, nous avons pu montrer que l'alternance des cycles de dessiccation et d'humectation avait pour effet une diminution de la quantité de Cu en solution.

Une différence notable des deux études (II.1.B et II.2.B) reste néanmoins la détermination des quantités de Cu en solution. Dans un cas la propension du Cu à passer en solution s'est faite via l'analyse théorique des coefficients de distribution à l'équilibre entre le Cu total et le Cu en solution. Dans l'autre cas, il s'agit de mesures expérimentales du Cu en solution à la suite de préincubations à humidités puis d'ajouts de Cu. Le premier cas ne considère donc pas la quantité de Cu totale, qu'elle soit due au fond géochimique ou aux apports (atmosphériques, agricoles, industriels…), tandis que dans le second cas les mesures peuvent avoir été effectuées avant que l'équilibre ne soit atteint. La résultante en termes d'estimation des exports de Cu est donc incertaine pour les zones présentant de faibles coefficients de dissociation, une augmentation globale des précipitations, et une augmentation des intensités couplée à des périodes d'assèchement. Par ailleurs, en prenant l'activité nitrifiante potentielle comme end-point, nous avons pu montrer qu'un stress hydrique préliminaire affectait la réponse au stress secondaire de contamination. En effet, l'inhibition de l'activité nitrifiante des sols ayant été exposés à de fortes humidités se fait pour des concentrations en Cu supérieures à celle des sols ayant été exposés à des humidités faibles. De plus, pour des concentrations faibles en Cu, les sols étant restés à humidité constante présentent des activités nitrifiantes supérieures (2 fois) à ceux ayant subi un stress d'humectation-dessiccation, et l'activité nitrifiante potentielle des premiers serait même stimulée à de faibles concentrations de Cu ajouté. En revanche aux fortes concentrations en Cu (1000 $mgCu.kg^{-1}$) les activités nitrifiantes sont similaires entre les sols, quel que soit leur historique d'incubation visant à mimer des différences de pluviométrie. Qu'il s'agisse de la mobilité ou de la toxicité, les effets de la contamination dépendraient donc à la fois du climat global moyen de la zone mais aussi des conditions physico-chimiques plus ponctuelles au moment de l'apport.

La comparaison des modélisations de Rh des modèles de surface continentale à des bases d'observations de Rh au regard de la concentration en Cu a pu confirmer l'intérêt de prendre en compte la contamination dans ces modèles. En effet, dans plus de la moitié des cas analysés, le Cu

était un prédicteur significatif des résidus de modèle, et ce, avec un effet d'ordre comparable à celui de l'argile voire de la température. Les fonctions de réponse pour la respiration hétérotrophe et pour la nitrification/dénitrification déterminées montrent qu'une contamination faible au Cu (de l'ordre des doses agronomiques) augmente les émissions de gaz à effet de serre (CO_2, N_2O, NOx), hors condition de dessiccation-humectation préalable alors qu'une contamination plus forte les diminue. Néanmoins, nos résultats suggèrent que cette diminution passe par une diminution des bactéries du sol. Les microbes étant supposés à l'origine des pools de carbone les plus stables, les stocks de carbone du sol diminueraient donc, augmentant alors la disponibilité et la toxicité de métaux comme le Cu. De telles rétroactions ont pu être montrées par Aponte et al., (2021) sur des sites à proximité d'industries et contaminés en Cu et arsenic dans lesquels les activités enzymatiques diminuaient dans les sites contaminés, cette diminution étant corrélée avec une diminution en carbone organique. Ici, nous avons établi des fonctions réponses permettant de prendre en compte l'effet d'une contamination du sol dans les modèles d'émissions de carbone et d'azote des sols. L'incorporation de ces fonctions dans les modèles de surface continentale pourraient permettre d'estimer les effets de la concentration en Cu sur l'évolution des stocks de carbone du sol comme suggéré par Aponte et al., (2021). Il resterait pour cela à améliorer les fonctions réponses que nous avons établies en prenant en compte les rétroactions entre le cycle de l'azote et du carbone et en intégrant l'effet du Cu sur les plantes.

D'autre part, en milieu agricole, la contamination peut se faire à travers des apports en pesticides ou fongicides minéraux ou à travers l'apport de fertilisants organiques. Les contaminations sont ainsi apportées avec des matières diverses, et souvent de la matière organique. Certains modèles permettent de prendre en compte ces différents paramètres pédologiques pour estimer les concentrations en éléments traces métalliques, ions majeurs, pH ou quantité de C dissous dans la solution ou dans le sol, mais n'intègrent pas d'effet des éléments traces sur les processus biologiques (Bonten et al., 2011). D'autres modèles permettent de prendre en compte l'apport de matière organique des fertilisants dans l'estimation des minéralisations de carbone ou d'azote, mais pas le transfert de contaminants ni leurs effets sur les processus de minéralisation du carbone ou de l'azote (Cagnarini et al., 2021). Deux améliorations notables pourraient donc être i) l'intégration de l'effet de la contamination des sols sur les fonctions biologiques dans ces modèles prédictifs de partition des éléments ; ii) parfaire les simulations d'apports de fertilisants agricoles qui se concentrent surtout sur l'évolution des matières organiques exogènes (stockage du carbone dans le sol, stimulations des minéralisations du carbone ou de l'azote) par la prise en compte de la contamination des sols et de son effet sur les émissions de gaz à effet de serre.

En outre, la prise en compte de la contamination des sols dans les modèles de surface continentale nécessite de considérer la contamination actuelle des sols, mais aussi son évolution potentielle. En effet, les simulations de changements de pratiques agricoles ou localisation des différentes cultures à la suite du changement climatique ne prennent actuellement pas en compte les flux de contaminants associés aux pratiques agricoles malgré leur grande variabilité. Dans ce contexte, la réalisation d'un modèle complet nécessiterait de prendre en compte les effets de la contamination i) sur les émissions de carbone et d'azote des sols (les interactions entre ces deux cycles), ii) sur leurs retombées sur les stocks de carbone et iii) la spéciation d'éléments tout en intégrant les effets des conditions climatiques sur les processus biologiques ainsi que sur les transferts de contaminants et sur leurs effets. Dans la mesure où les effets de la contamination (disponibilité, toxicité) dépendent

également des autres stress subis, une prise en compte plus fine des conditions climatiques générales mais aussi de leurs variabilités et modifications ponctuelles (stress) serait également à envisager. Néanmoins, une des difficultés majeures reste l'interpolation de fonctions de stress générales aux grandes échelles des modèles de surface continentale, et par exemple la définition de stress climatique pour chaque type de climat.

References

Adler, R. F., Gu, G., Sapiano, M., Wang, J. J., and Huffman, G. J. (2017). Global Precipitation: Means, Variations and Trends During the Satellite Era (1979–2014). *Surv. Geophys.* 38, 679–699. doi:10.1007/s10712-017-9416-4.

Allison, F. E., Sherman, M. S., and Pinck, L. A. (1949). Maintenance of soil organic matter: I. Inorganic soil colloid as a factor in retention of carbon during formation of humus. *Soil Sci.* 68, 463–478. doi:10.1097/00010694-194912000-00005.

Aponte, H., Mondaca, P., Santander, C., Meier, S., Paolini, J., Butler, B., et al. (2021). Enzyme activities and microbial functional diversity in metal(loid) contaminated soils near to a copper smelter. *Sci. Total Environ.* 779. doi:10.1016/j.scitotenv.2021.146423.

Arneth, A., Sitch, S., Bondeau, A., Butterbach-Bahl, K., Foster, P., Gedney, N., et al. (2010). From biota to chemistry and climate: Towards a comprehensive description of trace gas exchange between the biosphere and atmosphere. *Biogeosciences* 7, 121–149. doi:10.5194/bg-7-121-2010.

Augustsson, A., Filipsson, M., Öberg, T., and Bergbäck, B. (2011). Climate change - An uncertainty factor in risk analysis of contaminated land. *Sci. Total Environ.* 409, 4693–4700. doi:10.1016/j.scitotenv.2011.07.051.

Bååth, E. (1989). Effects of heavy metals in soil on microbial processes and populations (a review). *Water. Air. Soil Pollut.* 47, 335–379. doi:10.1007/BF00279331.

Ballabio, C., Panagos, P., Lugato, E., Huang, J. H., Orgiazzi, A., Jones, A., et al. (2018). Copper distribution in European topsoils: An assessment based on LUCAS soil survey. *Sci. Total Environ.* 636, 282–298. doi:10.1016/j.scitotenv.2018.04.268.

Beddington, J. R., and May, R. M. (1977). Harvesting natural populations in a randomly fluctuating environment. *Science (80-.).* 197, 463–465. doi:10.1126/science.197.4302.463.

Birch, H. F. (1958). The effect of soil drying on humus decomposition and nitrogen availability. *Plant Soil* 10, 9–31. doi:10.1007/BF01343734.

Bitton, G., Henis, Y., and Lahav, N. (1976). Influence of clay minerals, humic acid and bacterial capsular polysaccharide on the survival of Klebsiella aerogenes exposed to drying and heating in soils. *Plant Soil* 45, 65–74. doi:10.1007/BF00011129.

Blanck, H. (2002). A critical review of procedures and approaches used for assessing pollution-induced community tolerance (PICT) in biotic communities. *Hum. Ecol. Risk Assess.* 8, 1003–1034. doi:10.1080/1080-700291905792.

Bonten, L. T. C., Groenenberg, J. E., Meesenburg, H., and De Vries, W. (2011). Using advanced surface complexation models for modelling soil chemistry under forests: Solling forest, Germany. *Environ. Pollut.* 159, 2831–2839. doi:10.1016/j.envpol.2011.05.002.

Brynhildsen, L., and Rosswall, T. (1997). Effects of metals on the microbial mineralization of organic acids. *Water. Air. Soil Pollut.* 94, 45–57. doi:10.1023/A:1026423202978.

Cagnarini, C., Lofts, S., D'Acqui, L. P., Mayer, J., Grüter, R., Tandy, S., et al. (2021). Modelling of long-term Zn, Cu, Cd and Pb dynamics from soils fertilised with organic amendments. *SOIL* 7, 107–123. doi:10.5194/soil-7-107-2021.

Campbell, E. E., and Paustian, K. (2015). Current developments in soil organic matter modeling and

the expansion of model applications: A review. *Environ. Res. Lett.* 10. doi:10.1088/1748-9326/10/12/123004.

Christensen, J. H., and Christensen, O. B. (2003). Severe summertime flooding in Europe. *Nature* 421, 805–806. doi:10.1038/421805a.

Ciais, P., Sabine, C., Bala, G., Bopp, L., Brovkin, V., Canadell, J., et al. (2013). "Carbon and other biogeochemical cycles," in *Climate Change 2013 the Physical Science Basis: Working Group I Contribution to the Fifth Assessment Report of the Intergovernmental Panel on Climate Change*, ed. V. B. and P. M. M. Stocker, T.F., D. Qin, G.-K. Plattner, M. Tignor, S.K. Allen, J., Boschung, A. Nauels, Y. Xia (. Cambridge University Press, Cambridge, United Kingdom and New York, NY, USA.), 465–570. doi:10.1017/CBO9781107415324.015.

Csonka, L. N. (1989). Physiological and genetic responses of bacteria to osmotic stress. *Microbiol. Rev.* 53, 121–147. doi:10.1128/mmbr.53.1.121-147.1989.

Davidson, E. A., and Janssens, I. A. (2006). Temperature sensitivity of soil carbon decomposition and feedbacks to climate change. *Nature* 440, 165–173. doi:10.1038/nature04514.

Davidson, E. A., Keller, M., Erickson, H. E., Verchot, L. V., and Veldkamp, E. (2000). Testing a conceptual model of soil emissions of nitrous and nitric oxides. *Bioscience* 50, 667–680. doi:10.1641/0006-3568(2000)050[0667:TACMOS]2.0.CO;2.

Denef, K., Six, J., Bossuyt, H., Frey, S. D., Elliott, E. T., Merckx, R., et al. (2001a). Influence of dry-wet cycles on the interrelationship between aggregate, particulate organic matter, and microbial community dynamics. *Soil Biol. Biochem.* doi:10.1016/S0038-0717(01)00076-1.

Denef, K., Six, J., Paustian, K., and Merckx, R. (2001b). Importance of macroaggregate dynamics in controlling soil carbon stabilization: Short-term effects of physical disturbance induced by dry-wet cycles. *Soil Biol. Biochem.* 33, 2145–2153. doi:10.1016/S0038-0717(01)00153-5.

Diaz-Ravina, M., Baath, E., and Frostegard, A. (1994). Multiple heavy metal tolerance of soil bacterial communities and its measurement by a thymidine incorporation technique. *Appl. Environ. Microbiol.* 60, 2238–2247. doi:10.1128/aem.60.7.2238-2247.1994.

Duggin, J. A., Voigt, G. K., and Bormann, F. H. (1991). Autotrophic and heterotrophic nitrification in response to clear-cutting northern hardwood forest. *Soil Biol. Biochem.* 23, 779–787. doi:10.1016/0038-0717(91)90149-E.

FAO (2015). Fao stat. Available at: https://www.fao.org/family-farming/detail/fr/c/357469/ [Accessed October 16, 2021].

FAO (2020). FAO stat. Available at: https://www.fao.org/sustainability/news/detail/en/c/1274219/ [Accessed October 16, 2021].

Fernández-Calviño, D., and Bååth, E. (2016). Interaction between pH and Cu toxicity on fungal and bacterial performance in soil. *Soil Biol. Biochem.* 96, 20–29. doi:10.1016/j.soilbio.2016.01.010.

Friedlingstein, P., Bopp, L., Ciais, P., Dufresne, J. L., Fairhead, L., LeTreut, H., et al. (2001). Positive feedback between future climate change and the carbon cycle. *Geophys. Res. Lett.* 28, 1543–1546. doi:10.1029/2000GL012015.

Han, F. X., Banin, A., and Triplett, G. B. (2001). Redistribution of heavy metals in arid-zone soils under a wetting-drying cycle soil moisture regime. *Soil Sci.* 166, 18–28. doi:10.1097/00010694-200101000-00005.

Harris, R. F. (2015). "Effect of water potential on microbial growth and activity," in *Water Potential Relations in Soil Microbiology*, 23–95. doi:10.2136/sssaspecpub9.c2.

Hashimoto, S., Carvalhais, N., Ito, A., Migliavacca, M., Nishina, K., and Reichstein, M. (2015). Global spatiotemporal distribution of soil respiration modeled using a global database. *Biogeosciences* 12, 4121–4132. doi:10.5194/bg-12-4121-2015.

Hayes, M. H. B., and Clapp, C. E. (2001). Humic substances: Considerations of compositions, aspects of structure, and environmental influences. *Soil Sci.* 166, 723–737. doi:10.1097/00010694-200111000-00002.

Henin, S., and Dupuis, M. (1945). Essai de bilan de la matière organique du sol. *Ann. Agron.* 11, 17–29.

Holtan-Hartwig, L., Bechmann, M., Risnes Høyås, T., Linjordet, R., and Reier Bakken, L. (2002). Heavy metals tolerance of soil denitrifying communities: N2O dynamics. *Soil Biol. Biochem.* 34, 1181–1190. doi:10.1016/S0038-0717(02)00055-X.

Hong, S., Candelone, J. P., Soutif, M., and Boutron, C. F. (1996). A reconstruction of changes in copper production and copper emissions to the atmosphere during the past 7000 years. *Sci. Total Environ.* doi:10.1016/0048-9697(96)05171-6.

Huang, B., Li, Z., Huang, J., Guo, L., Nie, X., Wang, Y., et al. (2014). Adsorption characteristics of Cu and Zn onto various size fractions of aggregates from red paddy soil. *J. Hazard. Mater.* doi:10.1016/j.jhazmat.2013.10.074.

Hueso, S., García, C., and Hernández, T. (2012). Severe drought conditions modify the microbial community structure, size and activity in amended and unamended soils. *Soil Biol. Biochem.* 50, 167–173. doi:10.1016/j.soilbio.2012.03.026.

Ipcc, T. (2013). Carbon and Other Biogeochemical Cycles.

Jackson, T. A. (1998). "The Biogeochemical and Ecological Significance of Interactions between Colloidal Minerals and Trace Elements," in *Environmental Interactions of Clays*, 93–205. doi:10.1007/978-3-662-03651-8_5.

Jenny, H. (1941). *Factors of Soil Formation. A System of Quantitative Pedology, Soil Science.*

Joos, F., Roth, R., Fuglestvedt, J. S., Peters, G. P., Enting, I. G., Von Bloh, W., et al. (2013). Carbon dioxide and climate impulse response functions for the computation of greenhouse gas metrics: A multi-model analysis. *Atmos. Chem. Phys.* 13, 2793–2825. doi:10.5194/acp-13-2793-2013.

Khalil, K., Mary, B., and Renault, P. (2004a). Nitrous oxide production by nitrification and denitrification in soil aggregates as affected by O2 concentration. *Soil Biol. Biochem.* doi:10.1016/j.soilbio.2004.01.004.

Khalil, K., Mary, B., and Renault, P. (2004b). Nitrous oxide production by nitrification and denitrification in soil aggregates as affected by O2 concentration. *Soil Biol. Biochem.* 36, 687–699. doi:10.1016/j.soilbio.2004.01.004.

Killham, K., and Firestone, M. K. (1984). Salt stress control of intracellular solutes in streptomycetes indigenous to saline soils. *Appl. Environ. Microbiol.* 47, 301–306. doi:10.1128/aem.47.2.301-306.1984.

Kleber, M., Sollins, P., and Sutton, R. (2007). A conceptual model of organo-mineral interactions in soils: Self-assembly of organic molecular fragments into zonal structures on mineral surfaces. *Biogeochemistry* 85, 9–24. doi:10.1007/s10533-007-9103-5.

Kremen, A., Bear, J., Shavit, U., and Shaviv, A. (2005). Model demonstrating the potential for coupled nitrification denitrification in soil aggregates. *Environ. Sci. Technol.* 39, 4180–4188. doi:10.1021/es048304z.

Lawrence, D. M., Oleson, K. W., Flanner, M. G., Thornton, P. E., Swenson, S. C., Lawrence, P. J., et al. (2011). Parameterization improvements and functional and structural advances in Version 4 of the Community Land Model. *J. Adv. Model. Earth Syst.* 3. doi:10.1029/2011ms000045.

Li, J., Wang, J. T., Hu, H. W., Ma, Y. B., Zhang, L. M., and He, J. Z. (2016). Copper pollution decreases the resistance of soil microbial community to subsequent dry-rewetting disturbance. *J. Environ. Sci. (China)*. doi:10.1016/j.jes.2015.10.009.

Luo, Y., Ahlström, A., Allison, S. D., Batjes, N. H., Brovkin, V., Carvalhais, N., et al. (2016). Toward more realistic projections of soil carbon dynamics by Earth system models. in *Global Biogeochemical Cycles*, 40–56. doi:10.1002/2015GB005239.

Luo, Z., Wang, G., and Wang, E. (2019). Global subsoil organic carbon turnover times dominantly controlled by soil properties rather than climate. *Nat. Commun.* 10. doi:10.1038/s41467-019-11597-9.

Lützow, M. V., Kögel-Knabner, I., Ekschmitt, K., Matzner, E., Guggenberger, G., Marschner, B., et al. (2006). Stabilization of organic matter in temperate soils: Mechanisms and their relevance under different soil conditions - A review. *Eur. J. Soil Sci.* 57, 426–445. doi:10.1111/j.1365-2389.2006.00809.x.

Ma, Y., Lombi, E., Nolan, A. L., and McLaughlin, M. J. (2006). Short-term natural attenuation of copper in soils: Effects of time, temperature, and soil characteristics. *Environ. Toxicol. Chem.* 25, 652–658. doi:10.1897/04-601R.1.

Maliszewska, W., Dec, S., Wierzbicka, H., and Woźniakowska, A. (1985). The influence of various heavy metal compounds on the development and activity of soil micro-organisms. *Environ. Pollution. Ser. A, Ecol. Biol.* 37, 195–215. doi:10.1016/0143-1471(85)90041-8.

Manceau, A., and Matynia, A. (2010). The nature of Cu bonding to natural organic matter. *Geochim. Cosmochim. Acta* 74, 2556–2580. doi:10.1016/j.gca.2010.01.027.

Manzoni, S., Schimel, J. P., and Porporato, A. (2012). Responses of soil microbial communities to water stress: Results from a meta-analysis. *Ecology* 93, 930–938. doi:10.1890/11-0026.1.

Martin, J. P., Ervin, J. O., and Shepherd, R. A. (1966). Decomposition of the Iron, Aluminum, Zinc, and Copper Salts or Complexes of Some Microbial and Plant Polysaccharides in Soil. *Soil Sci. Soc. Am. J.* 30, 196–200. doi:10.2136/sssaj1966.03615995003000020017x.

Martin, J. P., and Haider, K. (2015). "Influence of Mineral Colloids on Turnover Rates of Soil Organic Carbon," in, 283–304. doi:10.2136/sssaspecpub17.c9.

Moreno, J. L., Bastida, F., Ros, M., Hernandez, T., and Garcia, C. (2009). Soil organic carbon buffers heavy metal contamination on semiarid soils: Effects of different metal threshold levels on soil microbial activity. *Eur. J. Soil Biol.* 45, 220–228. doi:10.1016/j.ejsobi.2009.02.004.

Noyes, P. D., McElwee, M. K., Miller, H. D., Clark, B. W., Van Tiem, L. A., Walcott, K. C., et al. (2009). The toxicology of climate change: Environmental contaminants in a warming world. *Environ. Int.* 35, 971–986. doi:10.1016/j.envint.2009.02.006.

Oades, J. M. (1984). Soil organic matter and structural stability: mechanisms and implications for management. *Plant Soil* 76, 319–337. doi:10.1007/BF02205590.

Odum, E. P. (1985). Trends Expected in Stressed Ecosystems. *Bioscience* 35, 419–422. doi:10.2307/1310021.

Odum, E. P., Finn, J. T., and Franz, E. H. (1979). Perturbation Theory and the Subsidy-Stress Gradient. *Bioscience* 29, 349–352. doi:10.2307/1307690.

Oechel, W. C., Vourlitis, G. L., Hastings, S. J., Zuluete, R. C., Maxman, L., and Kane, D. (2000). Acclimation of ecosystem CO2 exchange in the Alaskan Arctic in response to decadal climate warming. *Nature* 406, 978–981. doi:10.1038/35023137.

Oorts, K., Ghesquiere, U., Swinnen, K., and Smolders, E. (2006). Soil properties affecting the toxicity of CuCl2 and NiCl 2 for soil microbial processes in freshly spiked soils. *Environ. Toxicol. Chem.* 25, 836–844. doi:10.1897/04-672R.1.

Or, D., Smets, B. F., Wraith, J. M., Dechesne, A., and Friedman, S. P. (2007). Physical constraints affecting bacterial habitats and activity in unsaturated porous media - a review. *Adv. Water Resour.* 30, 1505–1527. doi:10.1016/j.advwatres.2006.05.025.

Otkin, J. A., Svoboda, M., Hunt, E. D., Ford, T. W., Anderson, M. C., Hain, C., et al. (2018). Flash droughts: A review and assessment of the challenges imposed by rapid-onset droughts in the United States. *Bull. Am. Meteorol. Soc.* 99, 911–919. doi:10.1175/BAMS-D-17-0149.1.

Pancholy, S. K., Rice, E. L., and Turner, J. A. (1975). Soil Factors Preventing Revegetation of a Denuded Area Near an Abandoned Zinc Smelter in Oklahoma. *J. Appl. Ecol.* 12, 337. doi:10.2307/2401736.

Parton, W. J., Schimel, D. S., Cole, C. V., and Ojima, D. S. (1987). Analysis of Factors Controlling Soil Organic Matter Levels in Great Plains Grasslands. *Soil Sci. Soc. Am. J.* 51, 1173–1179. doi:10.2136/sssaj1987.03615995005100050015x.

Paul, E. A. (2015). "Soil Microbiology, Ecology, and Biochemistry," in *Soil Microbiology, Ecology and Biochemistry*, 1–14. doi:10.1016/b978-0-12-415955-6.00001-3.

Pietrzyk, S., and Tora, B. (2018). Trends in global copper mining - A review. in *IOP Conference Series: Materials Science and Engineering* doi:10.1088/1757-899X/427/1/012002.

Prather, M. J., Holmes, C. D., and Hsu, J. (2012). Reactive greenhouse gas scenarios: Systematic exploration of uncertainties and the role of atmospheric chemistry. *Geophys. Res. Lett.* 39. doi:10.1029/2012GL051440.

Raynaud, X., and Nunan, N. (2014). Spatial ecology of bacteria at the microscale in soil. *PLoS One* 9. doi:10.1371/journal.pone.0087217.

Reed, S. T., and Florida, a (1996). Chapter 26 Copper and Zinc. 703–722.

Ruosteenoja, K., Markkanen, T., Venäläinen, A., Räisänen, P., and Peltola, H. (2018). Seasonal soil moisture and drought occurrence in Europe in CMIP5 projections for the 21st century. *Clim. Dyn.* 50, 1177–1192. doi:10.1007/s00382-017-3671-4.

Sánchez-García, C., Doerr, S. H., and Urbanek, E. (2020). The effect of water repellency on the short-term release of CO2 upon soil wetting. *Geoderma* 375, 114481. doi:10.1016/j.geoderma.2020.114481.

Sangiumsak, N., and Punrattanasin, P. (2014). Adsorption behavior of heavy metals on various soils. *Polish J. Environ. Stud.* 23, 853–865.

Schimel, J. (2013). Soil carbon: Microbes and global carbon. *Nat. Clim. Chang.* 3, 867–868. doi:10.1038/nclimate2015.

Schimel, J. P. (2018). Life in Dry Soils: Effects of Drought on Soil Microbial Communities and Processes. *Annu. Rev. Ecol. Evol. Syst.* 49, 409–432. doi:10.1146/annurev-ecolsys-110617-062614.

Schimel, J. P., Firestone, M. K., and Killham, K. S. (1984). Identification of Heterotrophic Nitrification

in a Sierran Forest Soil. *Appl. Environ. Microbiol.* 48, 802–806. doi:10.1128/aem.48.4.802-806.1984.

Schlesinger, W. H., and Andrews, J. A. (2000). Soil respiration and the global carbon cycle. *Biogeochemistry* 48, 7–20. doi:10.1023/A:1006247623877.

Schlesinger, W. H., and Bernhardt, E. S. (2013). *Biogeochemistry: An Analysis of Global Change*.

Sébastien Sauvé, Murray B., M., Wendell A., N., and William H., H. (1997). Copper Solubility and Speciation of In Situ Contaminated Soils: Effects of Copper Level, pH and Organic Matter. *Water. Air. Soil Pollut.* 100, 133–149.

Six, J., Elliott, E. T., and Paustian, K. (2000). Soil Structure and Soil Organic Matter II. A Normalized Stability Index and the Effect of Mineralogy. *Soil Sci. Soc. Am. J.* 64, 1042–1049. doi:10.2136/sssaj2000.6431042x.

Smorkalov, I. A., and Vorobeichik, E. L. (2011). Soil respiration of forest ecosystems in gradients of environmental pollution by emissions from copper smelters. *Russ. J. Ecol.* 42, 464–470. doi:10.1134/S1067413611060166.

Soler-Rovira, P., Fernández-Calviño, D., Arias-Estévez, M., Plaza, C., and Polo, A. (2013). Respiration parameters determined by the ISO-17155 method as potential indicators of copper pollution in vineyard soils after long-term fungicide treatment. *Sci. Total Environ.* 447, 25–31. doi:10.1016/j.scitotenv.2012.12.077.

Sparks, D. L. (2003). *Environmental Soil Chemistry: Second Edition*. doi:10.1016/B978-0-12-656446-4.X5000-2.

Stotzky, G. (1966). Influence of clay minerals on microorganisms. 3. Effect of particle size, cation exchange capacity, and surface area on bacteria. *Can. J. Microbiol.* 12, 1235–1246. doi:10.1139/m66-165.

Temminghoff, E. J. M., Van Der Zee, S. E. A. T. M., and De Haan, F. A. M. (1997). Copper mobility in a copper-contaminated sandy soil as affected by pH and solid and dissolved organic matter. *Environ. Sci. Technol.* 31, 1109–1115. doi:10.1021/es9606236.

Thornton, I., and Webb, J. S. (1980). "Trace Elements in Soils and Plants," in *Food Chains and Human Nutrition* doi:10.1007/978-94-011-7336-0_12.

Tobor-Kapłon, M. A., Bloem, J., and De Ruiter, P. C. (2006). Functional stability of microbial communities from long-term stressed soils to additional disturbance. *Environ. Toxicol. Chem.* doi:10.1897/05-398R1.1.

Tóth, G., Hermann, T., Szatmári, G., and Pásztor, L. (2016). Maps of heavy metals in the soils of the European Union and proposed priority areas for detailed assessment. *Sci. Total Environ.* 565, 1054–1062. doi:10.1016/j.scitotenv.2016.05.115.

Violante, A., Huang, P. M., and Gadd, G. M. (2007a). *Biophysico-Chemical Processes of Heavy Metals and Metalloids in Soil Environments*. doi:10.1002/9780470175484.

Violante, A., Krishnamurti, G. S. R., and Pigna, M. (2007b). "Factors Affecting the Sorption-Desorption of Trace Elements in Soil Environments," in *Biophysico-Chemical Processes of Heavy Metals and Metalloids in Soil Environments*, 169–213. doi:10.1002/9780470175484.ch5.

Violante, A., Ricciardella, M., Pigna, M., and Capasso, R. (2005). "Effects of Organic Ligands on the Adsorption of Trace Elements onto Metal Oxides and Organo-Mineral Complexes," in *Biogeochemistry of Trace Elements in the Rhizosphere*, 157–182. doi:10.1016/B978-044451997-9/50007-6.

Walworth, J. L. (1992). Soil Drying and Rewetting, or Freezing and Thawing, Affects Soil Solution Composition. *Soil Sci. Soc. Am. J.* 56, 433–437. doi:10.2136/sssaj1992.03615995005600020015x.

Wang, J., Bao, Q., Zeng, N., Liu, Y., Wu, G., and Ji, D. (2013). Earth System Model FGOALS-s2: Coupling a dynamic global vegetation and terrestrial carbon model with the physical climate system model. *Adv. Atmos. Sci.* 30, 1549–1559. doi:10.1007/s00376-013-2169-1.

Wang, Q. Y., Liu, J. S., Wang, Y., and Yu, H. W. (2015). Accumulations of copper in apple orchard soils: distribution and availability in soil aggregate fractions. *J. Soils Sediments*. doi:10.1007/s11368-015-1065-y.

West, T. S., Coombs, T. L., Society, R., and Sciences, B. (1981). Soil as the Source of Trace Elements [and Discussion]. *Philos. Trans. R. Soc. Lond. B. Biol. Sci.* 294, 19–39. Available at: http://www.jstor.org/stable/2395553.

Wieder, W. R., Bonan, G. B., and Allison, S. D. (2013). Global soil carbon projections are improved by modelling microbial processes. *Nat. Clim. Chang.* 3, 909–912. doi:10.1038/nclimate1951.

Wolf, I., and Russow, R. (2000). Different pathways of formation of N2O, N2 and NO in black earth soil. *Soil Biol. Biochem.* 32, 229–239. doi:10.1016/S0038-0717(99)00151-0.

Wood, J. M. (2015). Bacterial responses to osmotic challenges. *J. Gen. Physiol.* 145, 381–388. doi:10.1085/jgp.201411296.

Xing, S., Zhao, M., and Ma, Z. (2011). Removal of heavy metal ions from aqueous solution using red loess as an adsorbent. *J. Environ. Sci.* 23, 1497–1502. doi:10.1016/S1001-0742(10)60581-5.

Xu, J., Wei, Q., Yu, Y., Peng, S., and Yang, S. (2013). Influence of water management on the mobility and fate of copper in rice field soil. *J. Soils Sediments* 13, 1180–1188. doi:10.1007/s11368-013-0716-0.

Zheng, S., and Zhang, M. (2011). Effect of moisture regime on the redistribution of heavy metals in paddy soil. *J. Environ. Sci.* 23, 434–443. doi:10.1016/S1001-0742(10)60428-7.

université PARIS-SACLAY

ÉCOLE DOCTORALE
Agriculture, alimentation, biologie, environnement, santé (ABIES)

Titre : Effets d'une contamination diffuse des sols sur leurs émissions de gaz à effet de serre : cas du cuivre pour la prise en compte d'une contamination dans les modèles de surface continentale et l'évolution des risques en contexte de changement climatique

Mots clés : changement climatique, respiration hétérotrophe, écotoxicologie, cycles du carbone et de l'azote, modélisation, échelle globale et régionale

Résumé : Dans le contexte du changement climatique la compréhension des facteurs modulant les émissions de gaz à effet de serre (GES) (CO_2, N_2O, Nox...) des sols est essentielle. Parmi ceux-ci, les facteurs pédo-climatiques sont majoritairement étudiés. La contamination des sols n'est en revanche pas considérée malgré les grandes surfaces déjà concernées. Pourtant, il est connu qu'une contamination peut affecter les activités des organismes des sols à l'origine des émissions de GES mais la résultante sur les émissions à l'échelle globale reste peu renseignée. Pour répondre à cette question, nous avons étudié le cuivre (Cu) du fait de ses nombreuses utilisations agricoles et de sa réactivité vis-à-vis des constituants du sol et avons travaillé selon deux axes : i) associer, à l'échelle continentale, une contamination des sols en Cu à ses différentes formes et à leur risque pour l'environnement ; ii) intégrer des fonctions réponses au Cu pour les. émissions de GES liées aux cycles de C et N dans les modèles de surfaces continentales. Une première partie étudiant la (bio)disponibilité du Cu à l'échelle de l'Europe et les effets d'un double stress (humidité et contamination) sur la nitrification des sols a pu montrer que les conditions pédo-climatiques historiques, présentes et futures influençaient l'ampleur de l'impact d'une contamination. Dans la deuxième partie nous avons confirmé la nécessité de prendre la contamination en compte dans les estimations de flux de GES des sols par les modèles de surface continentales. Nous avons établi des fonctions reliant la concentration en Cu des sols à leurs émissions de CO_2 puis à leurs émissions d'espèces azotées en re-paramétrant le modèle biogéochimique DNDC en un nouveau modèle DNDC-Cu. Ce modèle DNDC-Cu a ensuite été utilisé pour estimer les émissions azotées de sols contaminés sous diférentes humidités du sol.

Title: Effect of diffuse soil contamination on its greenhouse gases emission: example of Cu in the land surface model and evolution of risks in the context of climate change

Keywords: climate change, heterotrophic respiration, ecotoxicology, regional and global scale, C and N cycles, modeling

Abstract : In the context of climate change, it is essential to understand the factors modulating greenhouse gas (GHG) emissions from soils (CO2, N2O, NOx...). Among these, pedo-climatic factors are mainly studied. However, soil contamination is not considered despite the large surface areas already concerned. However, it is known that contamination can affect the activities of soil organisms at the origin of the greenhouse gases emissions, but the result on global emissions remains poorly understood. To answer this question, we studied copper (Cu) because of its numerous uses for instance in agriculture and its reactivity with soil constituents and worked along two axes: i) to associate at the continental scale a Cu contamination of soils with the different forms of Cu and their risk for the environment; ii) to integrate response functions to Cu for GHG emissions related to C and N cycles in land surface models. A first part studying the (bio)availability of Cu at the European scale and the effects of a double stress (moisture and contamination) on soil nitrification showed that historical, present and future soil-climatic conditions influence the magnitude of the impact of a contamination. In the second part, we confirmed the need to take contamination into account in the estimation of soil GHG fluxes by land surface models to estimate soil heterotrophic respiration. We established functions relating soil Cu concentration to soil CO2 emissions and soil N species emissions for different soil moisture and re-parameterized the DNDC biogeochemical model into a DNDC-Cu version. Then, we used our DNDC-Cu to estimate N species emissions for contaminated soils under different soil moistures.

Maison du doctorat de l'Université Paris-Saclay
2ème étage aile ouest, Ecole normale supérieure Paris-Saclay
4 avenue des Sciences,
91190 Gif sur Yvette, France